An Investigation into the Physiological Role of Annexin A11

Luxmi Fatimathas

A thesis submitted to University College London for the degree of Doctor of Philosophy

September 2009

Division of Cell Biology
UCL Institute of Ophthalmology
11-43 Bath Street
London
EC1V 9EL

Declaration

I, Luxmi Fatimathas, confirm that the work presented in this thesis is my own. Where information has been derived from other sources, I confirm that this has been indicated in the thesis.

Luxmi Fatimathas

Abstract

The calcium-dependent phospholipid-binding protein annexin A11 was discovered over 25 years ago, however little is known about its function. This thesis supports a role for annexin A11 in the cell cycle and suggests an association with the microtubule network. Recent studies have implicated annexin A11 in the autoimmune disease sarcoidosis, which is further investigated in this study.

A single nucleotide polymorphism within annexin A11 (R230C) was identified as a highly associated susceptibility locus for sarcoidosis. Over-expression of annexin $A11^{WT}$ and annexin $A11^{R230C}$ showed no difference in their distribution. Stimulation with ionomycin, which induces a rise in intracellular calcium, resulted in the translocation of both variants to the plasma membrane and nuclear envelope with approximately the same time course. The calcium-dependent translocation of annexin A11 is therefore unaffected by the R230C mutation. In this one aspect there appears to be no difference between the two variants, however much still remains to be investigated such as the potential extracellular roles of these variants and their function in immune cells.

Much of the work in this thesis has focused on elucidating the function of wild type annexin A11, particularly during the cell cycle. During mitosis the distribution of annexin A11 is highly dynamic and localises to the mitotic spindle at metaphase and anaphase, as well as the midbody at cytokinesis. The use of methanol fixation highlighted the co-localisation of annexin A11 with the microtubule network throughout mitosis, as well as at interphase. Furthermore annexin A11 was shown to concentrate at the centrosome, again during both mitosis and interphase. Several centrosomal proteins also localise to the midbody and are key regulators of mitotic progression, supporting a similar role for annexin A11. Furthermore the centrosomal localisation of annexin A11 may serve as an ideal docking site from which it can be easily targeted throughout the cell.

This study highlights the novel localisation of annexin A11 to the centrosome and the microtubule network. Furthermore these findings contribute to a growing picture for the role of annexin A11 in the cell cycle, particularly with regards to its use of the microtubule network – a feature which may also have a role in interphase cells.

For Amma and Appa
Thank you for everything

Acknowledgements

I would like to start by thanking my supervisor Prof. Stephen Moss for giving me the opportunity to pursue a PhD in his lab and for the guidance he has given me over the past three years. This PhD would not have been possible without the support of my PhD programme at the LMCB and funding provided by the MRC. I would also like to thank my thesis committee; Prof Karl Matter, Dr Paul Kellam and Dr Adolfo Saiardi, for their continued encouragement and reassurance.

The daily work of this PhD has been made infinitely easier through the efforts of Steven Griffiths, Claire Cox and Aida, who have kept the lab running smoothly over the past few years. There are so many people at the Institute who have all made my time here such great fun. So a lot of thank yous go to; Ian 'Dr Evil' White, Emily Eden for being my favourite B.F.G, Veronika, James 'n' Katy, my steadfast crossword buddy Rush, Marcin, Hideki and Emily Steed for being the smiliest person I know.

A huge thanks goes to Becca, my super post doc. Thank you for teaching me everything I know about molecular biology, for never making me feel stupid even when I didn't have a clue (!) and for always being so supportive, both in and out of the lab. Matt, my darling work hubby, thank you for your inexhaustible enthusiasm for science and for being my verbal sparring partner!

I wouldn't have been able to get through this PhD were it not for my lab and office. Jenny and Jay, I'm so glad you both chose to join the Institute, you've not only made my time at the Institute more fun but have made all our LMCB trips something to be cherished. Thanks to Mark 'Bourbon' Evans for being the ever reliable voice of reason and Adam for being a God. Ah-Lai, you've seen me through so many ups and downs, you've always seen the best in me and been there to lend a patient ear – thank you so much.

Thanks also to all you Mullers out there, both past and present. Hari, Christina, Aaron and Megan – you've all made lunch a real laugh and provided much appreciated banter. A special thanks to Bhatia; from clueless undergrads to hopefully not so clueless postgrads, you've always been my constant friend. Thanks for never being too busy to be bugged and enduring my often nonsensical air filling! To Shweta, my unwarranted target for all things insulting and sarcastic - that you faithfully endure that deserves thanks enough! Thank you for your many shoulder-leaning, rock-being services and thanks to both you and Anand for making Cambridge an ever relaxing sanctuary amidst a crazy three years – I am most grateful.

I would also like to thank Shazeen for being truly understanding and for our many corridor chats!

And to Rugina for always being honest but supportive and making sure I stayed on track. I am also endlessly appreciative to Michelle, Nicola and Saj for keeping me relatively sane and reminding me of life outside of the lab.

Lastly I want to thank my Appa for setting the foundations of my education from day one, without which I never would have made it this far. Thanks also to my Amma for your unwavering support and for giving me the strength and courage to follow this road.

Contents

List of Figures

List of Tables

List of Abbreviations

5’ UTR	5’ untranslated region
a.a	Amino acid
A11	Annexin A11
A431	human epidermoid carcinoma
AAA	ATPases associated with diverse cellular activities
AIP1	ALG2 Interacting Protein 1
ALG2	Apoptosis Linked Gene 2
Alix	ALG2 Interacting Protein X
ALLN	N-acetyl-leucyl-leucyl-norleucinal
AM	Acetoxylmethyl
AMD	Age-related macular degeneration
AMP-PNP	Adenylyl-imidodiphosphate
ANX	Annexin
APS	Anti-phospholipid syndrome
AurA	Aurora A kinase
β_2-GPI	β_2-glycoprotein I
BFA	Brefeldin A
BRB80	Brinkleys buffer 80
BSA	Bovine serum albumin
BTNL2	Butyrophilin-like 2
CADTK	Calcium dependent tyrosine kinase
CAP-50	Calcyclin associated protein-50
CCV	Clathrin-coated vesicle
CD	Cluster of differentiation
Cdc14	Cell division cycle 14
Cdk1	Cyclin dependent kinase 1
Cep55	Centrosomal protein 55kDa
CFTR	Cystic fibrosis conductance regulator protein channel
CHMP4B	Chromatin modifying protein 4B
CHO1	Chinese Hamster Ovary 1
COP	Coat Protein Complex
Ct	C terminal
DMEM	Dubeccos minimal essential media
DSP	Dithiodipropionic acid di(N-hydroxysuccinimide ester)
DTT	Dithiothreitol
EGF	Epidermal growth factor
EGFR	Epidermal growth factor receptor
EGTA	Ethylene glycol tetraacetic acid
ERK	Extracellular signal regulated kinase
ESCRT I	Endosomal Sorting Complex Required for Transport I
F-actin	Filamentous actin
FCS	Foetal calf serum

FIP	Family of rab11 interacting proteins
FPR	Formyl peptide receptor
GCP2/3	γ tubulin complex proteins 2/3
GFP	Green fluorescent protein
GST	Glutathione S transferase
GTPase	Guanosine triphosphatase
HDAC6	Histone deacetylase 6
HeLa	human cervix adenocarcinoma
HEPES	4-(2-hydroxyethyl)-1-piperazineethanesulfonic acid
HLA	Human leucocyte antigen
IFNα	Interferon-α
IFNγ	Interferon-γ
IgG	Immunoglobulin G
IL-2	Interleukin-2 (IL-2)
IL-2R	Interleukin-2 receptor
INCENP	Inner centromere protein
IPTG	Isopropyl β-D-1-thiogalactopyranoside
kDa	Kilodaltons
KIF	Kinesin family
LAP2	lamin- and chromatin-binding nuclear protein 2
LB	Lurias Broth
LDL	low density lipoprotein
MAP	Microtubule-associated protein
MAPK M	Mitogen activated protein kinase
MHC	Major histocompatibility complex
MKLP1	Mitotic kinesin-like protein
MTOC	Microtubule organising centre
MVB	Multivesicular body
Mya	Million years ago
NE	Nuclear envelope
Nt	N terminal
Nuf	Nuclear-fallout protein
NuMA	Nuclear mitotic apparatus protein
OD	Optical density
PBS	Phosphate buffered saline
PC	Phosphatidylcholine
PCM	Pericentriolar material
PCR	Polymerase chain reaction
PDGF-BB	Platelet derived growth factor BB
PDGF-R	Platelet derived growth factor receptor
PEF	Penta EF Hand
PFA	Paraformaldehyde
PG	Phosphatidylglycerol
PIP	Phosphatidylinositol phosphate

PKC	Protein kinase C
Plk1	Polo-like kinase 1
PM	Plasma membrane
PMA	Phorbol 12-myristate 13-acetate
PS	Phosphatidylserine
PtdIns4,5P_2	Phosphatidylinositol-4,5-bisphosphate
PVDF	Polyvinylidene fluoride
PVR	Proliferative vitreoretinopathy
Rab6-KIFL	Rab6 binding kinesin-like protein
RPE	Retinal pigment epithelial
SAK	Staphylokinase
Sar	Secretion-associated and ras-related protein
SDS PAGE	Sodium dodecyl sulfate polyacrylamide gel electrophoresis
Sec	Secretory pathway
Sirt 2	Silent mating type information regulation 2
siRNA	Small interfering RNA
SLE	Systemic lupus erythrematosus
SNARE	SNAP (Soluble NSF Attachment Protein) receptor
SNP	Single nucleotide polymorphism
Src	Sarcoma
STOP	Stable tubule-only polypeptide
TAE	Tris acetate ethylenediaminetetraacetic acid
TBS	Tris buffered saline
TEMED	Tetramethylethylenediamine
TGN	Trans golgi network
TNFα	Tumour necrosis factor α
TRPV	Transient receptor like potential vanalloid
Tsg101	Tumor susceptibility gene 101
v-SNARE	vesicular-SNAP (Soluble NSF Attachment Protein) receptor
v-Src	viral-Sarcoma
WT	Wild type
γTuRC	γ tubulin ring complex
zf MKLP1	Zebrafish mitotic kinesin-like protein
Zen-4	Zygotic lethal enclosure abnormal 4

Chapter One:
Introduction

1. Introduction

1.1 The Annexin Family

The annexins are a family of calcium-dependent phospholipid-binding proteins, which are present in all eukaryotes but have not yet been described in prokaryotes. They were first discovered in the 1970s and 80s and were named at the time according to their biochemical properties, for example annexin A7 was originally named synexin [1] and annexin A1 named lipocortin [2]. They remained a disparate set of proteins for some years, until sequence homology and unique domain structures were identified, resulting in the term annexins being coined in 1990.

1.1.1 Annexin Nomenclature and Molecular Phylogeny

Formal classification of the annexins in 1990 led to the current alphabetical nomenclature [3], with vertebrate annexins classified as the A family, invertebrate annexins the B family, fungal and mold annexins as C, plant annexins as D and protist annexins as E. This illustrates the highly conserved nature of the annexins through evolution. The oldest members are the protist annexins, originating approximately 1,200 Mya, followed by the divergence of the plant annexins, fungal, invertebrate and lastly vertebrate annexins [4] (Figure 1).

There are 12 mammalian annexins (ANXA1-ANXA11, ANXA13), usually with corresponding orthologues within the vertebrate family. However it should be noted that some annexins have been lost or duplicated in certain species like fish [5]. The duplication of annexin genes is also seen in humans, exemplified by annexin A6. This annexin was first thought to have emerged by the tandem duplication and fusion of a distinct annexin [6]. However subsequent sequence analysis showed the two halves of annexin A6 to be most similar to annexin A5 and annexin A10, supporting the idea of chromosomal duplication of these regions resulting in the formation of annexin A6 [7].

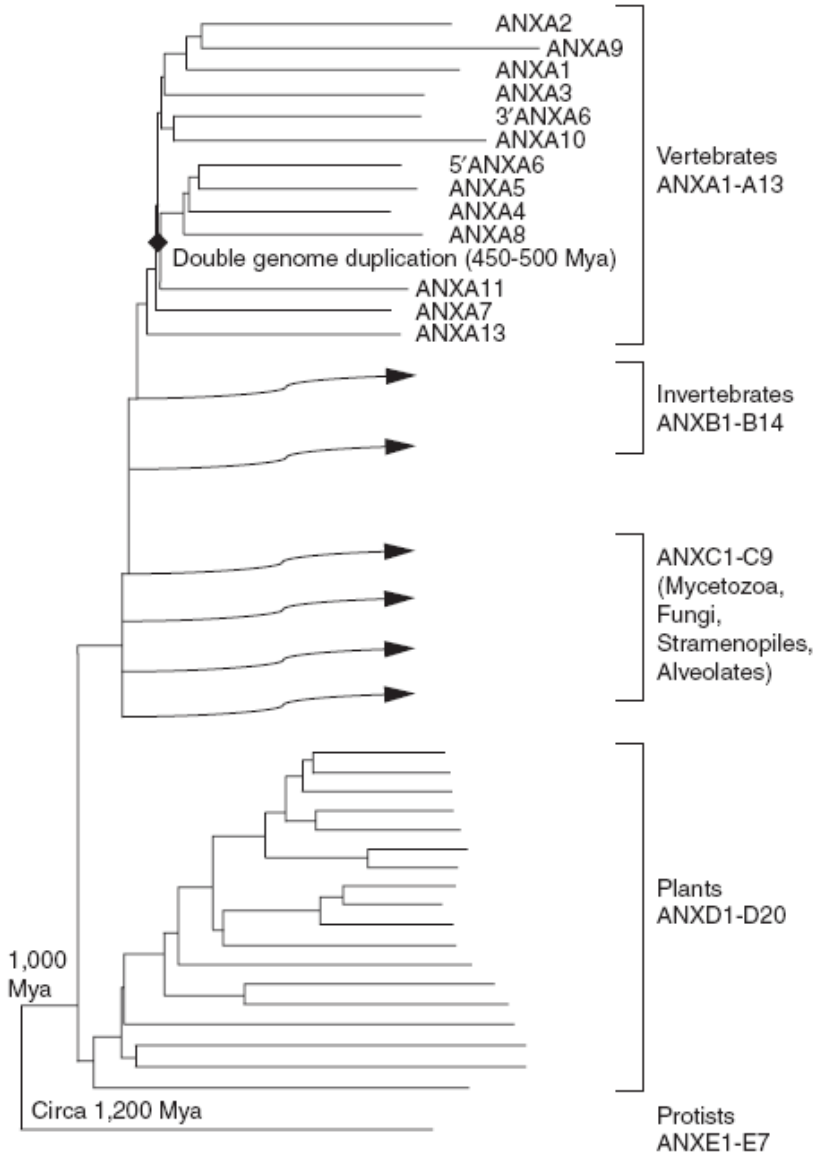

Figure 1 Phylogenetic Tree of the Annexins

Taken from [5]. The annexins originated approximately 1200 Mya (million years ago). The first annexins to diverge from the ancient protist annexins (ANXE) were the plant annexins (ANXD). These annexins were followed by the evolution of the fungal (ANXC), the invertebrate (ANXB) and finally the vertebrate (ANXA) annexins. The largest of these groups are the plant annexins with currently 20 known members, followed by the invertebrate, the vertebrate, the fungal and lastly the protist annexins. The vertebrate family currently consist of 12 annexins, named annexin A1 – A11 and annexin A13. Annexin A12 has yet to be ascribed.

Vertebrate annexins best exemplify the stereotypical annexin structure. This comprises a unique N terminal domain, followed by a C terminal domain containing four highly conserved regions called annexin repeats, or eight in the case of annexin A6 [8], which can bind calcium. The plant annexins (annexin Ds) tend to lack the N terminal domains as well as functional calcium binding sites in two of the four annexin repeats [9]. The annexin

C family members, which range from species as simple as the unicellular protozoan *Giardia lamblia* to the more complex multicellular fungus *Neurospora crassa,* do contain variable N terminal domains. As yet amongst these more primitive annexins, no clear front runner has been identified as a putative ancestor to the annexin A family members. It is however known, from gene structure analysis, that annexin A11 is the common ancestor to all but two of the vertebrate annexins, preceded in evolution only by annexin A13 and annexin A7.

1.1.2 Annexin Structure

The annexins are composed of two domains; the conserved C terminal domain, often referred to as the annexin core and the divergent N terminal effector domain or head.

Annexin Core Domain

This domain contains the highly conserved annexin repeats, of which there are usually four, of about 70 amino acids in length. Each repeat contains the 17 amino acid consensus sequence, referred to as the endonexin fold. Though primary sequence homology of this domain between the different annexins ranges only between 45-55%, the secondary and tertiary structures are almost superimposable, as shown through x-ray crystallography [5]. The first annexin core domain to be crystallised was that of human annexin A5 [10].

This study showed that each repeat was folded into five alpha helices that are wound into a right handed super helix (Figure 2). The five helices, designated A to E, are arranged such that A and B, and D and E form two parallel helix-loop-helix structures. Helix C is situated perpendicular to these two structures and connects the C terminus of helix B to the N terminus of helix D [11]. The annexin core itself is formed into a planar, cyclic structure, giving it a slightly curved form with the convex side believed to be the membrane binding surface and the concave side facing the cytoplasm. The convex side was shown to house unique calcium binding sites [12], different to the type I calcium binding sites of EF hand proteins.

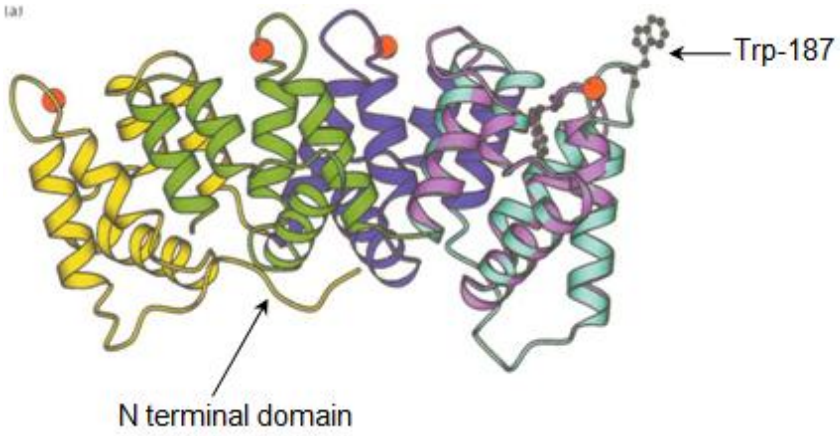

Figure 2 Ribbon Drawing of the Crystal Structure of Human Annexin A5

Taken from [13]. The crystal structure of annexin A5 depicted here is representative of all vertebrate annexins. The N terminal domain (shown here as unstructured) lies along the concave side of the protein. The C terminal core comprises four annexin repeats, shown in yellow (1st repeat), dark blue (2nd repeat), violet/cyan (3rd repeat) and green (4th repeat). The structure of the 3rd repeat in low calcium conditions is depicted in violet. High calcium conditions cause a structural change in this repeat, depicted in cyan, such that a tryptophan residue is exposed. This conformational change is unique to annexin A5, as most other annexins do not show a significant conformational change upon binding calcium. Calcium (shown in red) binds to the exposed loops of the annexin repeats.

Crystallisation of other annexins led to further characterisation of these calcium binding sites, which are divided into high affinity type II sites, made of a 'GxGT-[38 residues]-D/E' motif and low affinity type III sites [11]. These calcium binding sites are formed by loops from different parts of the core domain converging and have different structures in addition to their different affinities. Type II sites localise to the loop between helix A and helix B, a region commonly known as the endonexin fold, whereas type III sites are located to the loop between helix D and helix E. The sites themselves interact with calcium ions via three or two peptide oxygen groups, for type II and III sites respectively, and a bidentate carboxylate head group.

The number and precise location of calcium binding sites between the annexins varies, for example annexin A1 was shown to have six calcium binding sites [11], but annexin A5 only five [12]. More dramatically annexin A9 has lost the calcium binding sites in all four of its annexin repeats [5]. These structural differences account for variation in calcium affinity between family members and so also affect phospholipid binding.

The ability of the annexins to bind membranes is generally regulated by calcium and occurs via the convex side of the protein. In the presence of calcium, annexin A2 has been shown using cryoelectron microscopy to assemble at lipid bilayers [14]. Further

investigation demonstrated that annexin A2 is capable of binding phospholipid membranes in both a calcium dependent and calcium independent manner [15]. Binding to these membranes is facilitated by slight changes in conformation, as illustrated by annexin A5 which alters the position of the annexin repeats such that the calcium binding sites become coplanar with the membrane [16]. This coplanar arrangement usually induces only subtle changes in conformation, except in the case of annexin A6 whose two halves undergo approximately 90° rotations to reach this configuration [17].

Annexin N Terminal Head

The N terminal domain shows the greatest variability amongst the annexins and can vary in length from less than 20 amino acids, for example in annexin A3 with 13 residues and annexin A5 with 16 residues, to just over 200 amino acids for annexin A11. Unlike the annexin core which has been crystallised for several of the annexins, much less is known about the tertiary structure of the N terminal head. A few crystal structures have been compiled for the shorter annexins, including annexin A1 [18], annexin A3 [19] and A5 [16]. In these cases where the N terminal domains are relatively short, they tend to extend along the inner, concave surface of the protein and often have hydrophobic interactions with this surface.

This is true of annexin A5, whose N terminal domain is buried between the first and fourth annexin repeats to which it is anchored [16]. The 3D conformation of the N terminus is suggested to exert functional effects on the annexin core, as in the case of annexin A3. A tryptophan residue within the N terminus of annexin A3 is known to interact with the first, second and fourth annexin repeats via hydrogen bonds and Van der Waals interactions. The side chain of this residue points into a hinge region between the annexin repeats and it is suggested that this positioning could alter the flexibility of the protein and so affect its calcium and phospholipid binding properties [19].

The longer the N terminal head, the more complex the interactions appear to become, as illustrated by annexin A1, which though short in comparison to annexin A11, is more than twice the length of annexin A5. The crystal structure of annexin A1 in the absence of calcium revealed the ability of the N terminus to form an alpha helix containing both polar and non-polar regions. This amphipathic helix substituted for helix D within the third annexin repeat, which under these conditions was unwound and protruded out from the

protein surface. In the presence of calcium the N terminus was more exposed and not packaged into the annexin core. Given that this domain is known to bind S100A11, it is possible that this interaction is facilitated by the conformational change induced in the N terminus in the presence of calcium [18].

Although the N terminal heads of the longer annexins have not been crystallised, much has been written about their functions, as they are known to contain a range of domains and binding sites which lend these annexins to more complex regulation (Figure 3). As mentioned above, annexin A1 can bind the S100 protein S100A11, this is a characteristic of several of the annexins including annexin A11 which binds S100A6 [20] and annexin A2 which binds S100A10 [21], both via their N terminal domains.

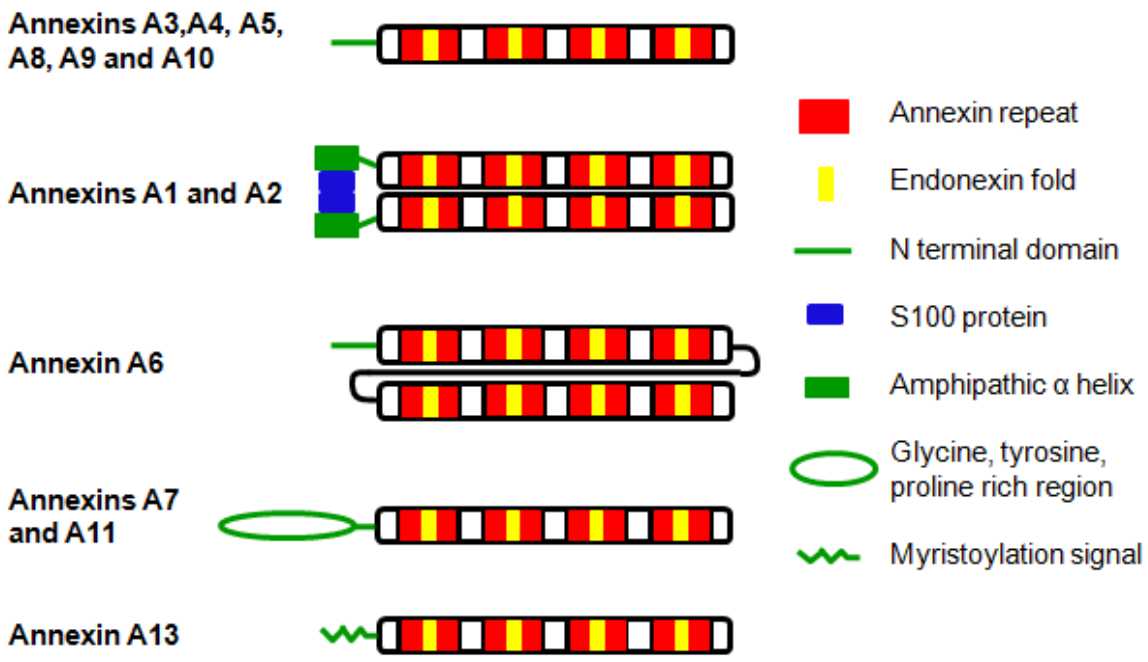

Figure 3 Schematic of Vertebrate Annexin N and C Terminal Domains

The vertebrate annexins show a high degree of homology in their C terminal cores, each containing four annexin repeats, with the exception of annexin A6 which contains eight. The N terminal domains however are more variable between the annexins and contain a variety of different sub-domains. Annexins A1 and A2 contain amphipathic alpha helices in their N terminal domains which facilitate binding to S100 proteins, allowing the formation of heterotetramers of two annexin proteins and two S100 proteins. Annexins A7 and A11 contain glycine, tyrosine and proline rich N terminal domains, with annexin A11 having the longest N terminal domain of all the vertebrate annexins. Annexin A13 is unique in containing a myristoylation signal in its N terminal domain.

The N terminal domains are also targets for phosphorylation by several kinases, including

protein kinase C which phosphorylates annexin A2 [22] and the EGF receptor kinase which targets annexin A1 [23]. Such events can result in functional consequences and in the case of annexin A1 its phosphorylation on tyrosine residues is implicated in late stage inward vesiculation of multivesicular bodies [24], whereas phosphorylation on serine residues is essential for translocation to the plasma membrane [25].

Proteases, as well kinases, target the N terminal domains and several of the annexins contain sequences marking them out for proteolysis [26], adding another layer of enzymatic regulation. In addition to these motifs, are signals for nuclear localisation [27], myristoylation [28] and transglutaminase crosslinking [29].

1.1.3 Annexin Interacting Proteins

S100 Proteins

S100 proteins are a group of low molecular weight proteins belonging to the superfamily of EF hand proteins. The EF hand motif comprises a helix-loop-helix motif which binds calcium with a high affinity. S100 proteins contain two of these motifs connected by a hinge region and are capable of forming both hetero- and homodimers. These proteins are present only within vertebrate lineages. Their functions are diverse and include modulating both actin and microtubule networks, promoting cell survival and proliferation, calcium homeostasis and mediating muscle contraction (reviewed in [30]). The functions of these proteins are highly intertwined with those of the annexins, which they are known to bind.

Annexin A2 binds S100A10 via its N terminal domain [21], in a heterotetrameric complex of two annexin A2 molecules and two S100A10 molecules [31]. This interaction is unique amongst the annexin-S100 complexes, as S100A10 does not contain functional calcium binding sites. Therefore its interaction with annexin A2 is calcium independent and is instead dependent on the interaction of hydrophobic side chains of both proteins and post-translational modifications of annexin A2, such as N-acetylation [32].

This complex has been shown to interact with several membrane ion channels such as TRPV5 and TRPV6 (transient receptor like potential vanalloid type 5 and 6 channels) and is suggested to regulate their distribution and functionality [33]. Similarly this complex

interacts with the CFTR (cystic fibrosis conductance regulator protein channel) channel and is also implicated in regulating its channel currents [34]. In addition, the annexin A2-S100A10 complex plays a role in membrane trafficking, for example in exocytosis of secretory vesicles [35] and polarised vesicular transport [36]. It is also implicated in junctional formation, in both the formation of adherens junctions [37] and the reassembly of tight junctions following breakdown [38].

The binding of annexin A1 to S100A11 is thought to lead to heterotetramer formation in a similar manner to that of the annexin A2-S100A10 complex, although this has never been formally proven. This interaction is also mediated by the annexin N terminal domain, however it is calcium dependent [39]. S100A11 has also been shown to interact with annexin A6 [40], though the functional role of this interaction is currently unknown. Although little is also known about the function of the annexin A1-S100A11 complex, it has been speculated to have a role at the plasma membrane in epidermal keratinocyte differentiation [41] and has been shown to diminish phospholipid vesicle aggregation *in vitro* [42].

Other annexin S100 interactions include those of annexin A11 with S100A6, discussed in Section 1.2.8 and annexin A6 with both S100A1 and S100B. Unlike the interactions discussed so far, the interaction of annexin A6 with S100 proteins occurs via both its N terminal domain and its C terminal core [43]. It also forms a heterotetramer with S100 proteins and this formation appears to block the ability of S100A1 and S100B to inhibit intermediate filament formation.

Cytoskeletal Proteins

Several annexins are known to bind cytoskeletal components, in particular actin. These include annexin A1 [44], A2 [45], A5 [46] and A6 [47]. The best characterised of these interactions is that of annexin A2 with F-actin. Annexin A2 induces actin microfilament bundling *in vitro* [45] in a calcium dependent manner and binds F-actin via its C terminal domain [48]. Tyrosine phosphorylation of annexin A2 modulates its effects on the actin cytoskeleton and has been shown to regulate actin branching [49] and the formation of insulin-induced actin domes [50]. Annexin A2 is located at the interface between phosphatidylinositol-4,5-bisphosphate (PtdIns4,5P_2) enriched membranes and F-actin,

where it is involved in membrane-associated actin assembly [51,52]. The annexin A2-actin interaction is involved in physiological processes such as membrane ruffling and protrusion [53], and is also implicated in pathophysiological processes such as wound healing [54] and tumour invasion [55,56].

Annexin A1, like annexin A2 [55], is suggested as a potential drug target for anti-cancer therapies due to its actin binding properties [57,58]. In the presence of calcium annexin A1 induces actin microfilament bundling *in vitro* [59]. It has also been shown to bind the actin regulator profilin, in a calcium independent manner [60], though the physiological role of this interaction is not yet known. The interaction of annexin A6 and actin is believed to play a role in the contractile tissues of the heart [61] and smooth muscle [47]. In cardiac muscle annexin A6 co-purified with the sarcolemma and bound actin in a calcium dependent manner. This interaction is hypothesised to stabilise the sarcolemma during contraction. In smooth muscle cells annexin A6 relocalised to the plasmalemma in response to elevated calcium levels and co-precipitated with actomyosin. This interaction is suggested to be important in smooth muscle contraction. Plasma membrane targeting of annexin A6 has also been shown to stimulate F-actin accumulation at the plasma membrane. This is suggested to be a mechanism by which plasma membrane targeted annexin A6 diminishes store-operated calcium entry into the cell [62]. An interaction between annexin A5 and actin has also been shown, however the function of the annexin A5-actin interaction is less clear. It is known to be calcium dependent and is suggested to be specific to gamma actin [46].

Other Ligands

A wide range of other proteins have been reported to interact with annexins. Annexin A6 binds the GTPase (guanosine triphosphatase) activating protein p120 [63]. p120GAP is involved in inactivating the small Ras family of GTPases, which are known to have a key role in oncogenesis. Annexin A6 was shown to directly bind the calcium dependent lipid binding domain (known as the C2 domain) of p120GAP *in vitro*. The binding site for p120GAP within annexin A6 was later mapped to the linker region between the two lobes of annexin A6 [64]. Annexin A6 is suggested to regulate Ras activity via its ability to target p120GAP to the plasma membrane in a calcium dependent manner [65].

The use of recombinant annexin A7 has identified the penta EF hand protein sorcin as a calcium-dependent interactor [66]. This interaction occurs between the N terminal domain of annexin A7 [66] and the N terminal domain of sorcin [67]. Annexin A7 was shown to enhance the binding of sorcin to phospholipid membranes, as tested using purified chromaffin granules. The physiological function of this interaction is unknown, however it may be involved in membrane dynamics as sorcin binding of annexin A7 has been shown to inhibit annexin A7 stimulated aggregation of chromaffin granules [66]. Annexin A11 interacts with the penta EF hand protein ALG2 (Apoptosis Linked Gene 2), which belongs to the group I PEF family, as opposed to the group II PEF family of which sorcin is a member [68]. Annexin A11 has also been shown to interact with the motor protein CHO1 (Chinese Hamster Ovary 1). These interactions are discussed further in 1.2.8 Annexin A11 Interacting Proteins.

In addition to the various protein interactions of the annexins, several of the annexins are known to bind ribonucleic acids (RNA). Annexin A2 specifically binds polyguanosine residues in the presence of calcium *in vitro* [69]. The investigation of annexin A2 ribonucleoprotein complexes led to the identification of *c-myc* mRNA as a direct binding target of annexin A2. The overexpression of annexin A2 resulted in the up-regulation of c-myc protein. It is therefore suggested that this interaction, through the regulation of *c-myc* translation, could modulate cellular transformation. Annexin A1 also has been shown to bind RNA as well as DNA [70] and in complex with S100A6 to anneal to and unwind double stranded DNA [71].

1.1.4 Annexins in Membrane Trafficking

The annexins are known to bind membranes in a calcium dependent manner, however several of the annexins can bind membrane phospholipids in the absence of calcium. A fraction of the annexin A1 protein population identified in human placenta, was shown to bind membranes without the need for calcium [72]. Further analysis of this isolated pool of protein demonstrated that it can be phosphorylated by the EGF receptor kinase. Subsequently a calcium independent membrane binding pool of annexin A1 has been detected in association with the plasma membrane and in isolated multivesicular bodies [23]. The ability of this pool of annexin A1 to bind membranes independently of the presence of calcium, was found to be dependent on its phosphorylation state.

Phosphorylation by the EGF receptor kinase resulted in the loss of its calcium independent membrane binding properties. A pool of calcium independent membrane binding annexin A5 has also been detected, in cultured chick embryo fibroblasts [73]. Although these annexins do not require calcium to bind membranes, the calcium dependent phospholipid binding properties of the annexins still dominate their functionality.

Annexins in Exocytosis

The role of annexins in exocytosis began with initial observations of the membrane aggregation properties of annexin A7 [1]. Annexin A7 was shown to aggregate isolated adrenal chromaffin granules in the presence of calcium *in vitro*. Electron microscopy showed individual granules in close apposition to each other. However fusion of these granules was only stimulated upon the addition of low concentrations of arachidonic acid, suggesting that annexin A7 mediates the contact between membranes but does not initiate fusion [74]. Annexin A2 has similarly been shown to promote chromaffin granule aggregation *in vitro* in the presence of calcium [75], with fusion again only occurring upon addition of arachidonic acid. Furthermore, studies in permeabilised adrenal chromaffin cells demonstrated that the gradual failure of secretory activity due to the loss of intracellular proteins was partially inhibited in the presence of purified annexin A2 [76]. The rescue of calcium stimulated secretory activity was lost when annexin A2 antibodies were added [76] and appears to be dependent on the phosphorylation state of annexin A2 [77]. Inhibition of protein kinase C (PKC) in these cells prevents the reconstitution of secretion by purified annexin A2. However the addition of PKC-prephosphorylated annexin A2 over-rides the inhibition of PKC, restoring secretory function. Taken together these studies support a phosphorylation dependent role for annexin A2 in exocytosis.

Studies *in vivo* in different cell lines however have produced conflicting results for a universal role of annexin A2 in exocytosis. The up-regulation of annexin A2 protein levels or the down-regulation of annexin A2 function in adrenal pheochromocytoma cells, has shown no effect on calcium dependent dopamine release [78]. A mutant clone of this cell line is known to express higher levels of annexin A2 and is rich in small cytoplasmic vesicular structures called enlargeosomes. Annexin A2 was shown to localise to the surface of these structures and following siRNA-mediated depletion of annexin A2 enlargeosome exocytosis was significantly decreased [79]. siRNA-mediated depletion of the annexin A2-S100A10 complex in endothelial cells, decreased the calcium dependent

secretion of von Willebrand factor, but not tissue plasminogen activator [35]. Therefore the role of annexin A2 in exocytosis is cell type specific and moreover is highly dependent on the specific secretory granule pathway examined. However one must also question the significance of these studies in cell lines, given that the annexin A2 knock out mouse is essentially normal.

Annexin A13b has also been implicated in exocytosis in canine polarised epithelial cells. Permeabilised cells showed deficient membrane trafficking from the trans-Golgi network (TGN) to the apical membrane in the presence of antibodies targeting annexin A13b, though trafficking to the basolateral membrane was not affected [80]. The myristoylation of annexin A13b stimulates this apical transport [81], as does the myristoylation of annexin A13a. However annexin A13a in addition to stimulating apical transport, inhibits basolateral transport from the TGN, exhibiting a dual role in both positively and negatively regulating exocytosis [82].

The mechanistic workings of the annexins in exocytosis is not well understood and warrants further investigation, particularly with regard to how these proteins would fit into the well-established SNARE model (reviewed in [83]). This is especially of interest given the work carried out on synaptotagmins - a family of membrane trafficking proteins characteristically containing two C2 domains, responsible for calcium dependent lipid binding. Like the annexins, they have also been shown to aggregate chromaffin granules *in vitro* and promote fusion upon addition of arachidonic acid [84]. They have now been shown to enhance the calcium- and SNARE-dependent fusion of membranes *in vitro* [85].

Annexins in Endocytosis

The main annexins implicated in endocytosis are annexins A1, A2 and A6, all of which localise to endosomes [23,86,87]. Annexin A1 is associated with multivesicular bodies (MVBs) containing internalised epidermal growth factor (EGF) receptors and EGF receptor kinase [23]. Following EGF stimulation, the EGF receptor is internalised and sorted to early endosomes for recycling or degradation. During this process they are processed in MVBs prior to targeting to recycling endosomes or the lysosome. MVBs, as the name implies, contain multiple internal vesicles in which cargo is stored. These vesicles are formed through inward vesiculation. The role of annexin A1 in this process was examined in a mouse lung fibroblast cell line derived from the annexin A1 knock out mouse [24].

EGF stimulation increased inward vesiculation of EGF receptor containing MVBs and this effect was abolished in annexin A1 knock out cells. This effect was then rescued upon expression of wildtype annexin A1 in knock out cells. However no rescue was achieved when an EGF phosphorylation mutant of annexin A1 was expressed. Therefore annexin A1 appears to enhance inward vesiculation, in a phosphorylation dependent manner.

Annexin A2 is also implicated in the biogenesis of MVBs, specifically in the budding of MVBs from the early endosome [88]. Labelled EGF was used to follow endosomal trafficking in annexin A2 depleted cells. In these cells EGF was not rapidly degraded as in control cells, but accumulated in early endosomes. Similarly, labelled dextran which in control cells trafficked from early to late endosomes, was only detected in the early endosomes of annexin A2 depleted cells. Electron microscopy of knock down cells showed that regions of multivesiculation were present, suggesting inward vesiculation was viable. However these regions were often incorporated within the early endosomes. Therefore annexin A2 appears to play an important role in early to late endosome trafficking via its regulation of the endocytosis-mediated formation of MVBs. The phosphorylation state of annexin A2 has since been found to be important in early to late endosome trafficking [89]. Isolated early endosomes were shown to contain tyrosine phosphorylated annexin A2. Furthermore N terminal tyrosine phosphorylation mutants of annexin A2 demonstrated that phosphorylation at tyrosine 23 was required for efficient endosome binding. Phosphomimetic and non-phosphorylable forms of annexin A2 were expressed in annexin A2 depleted cells. The block in early to late endosome transport observed in knock down cells, was rescued by the expression of the phosphomimetic mutant but not the non-phosphorylable mutant. So as in the case of annexin A1, the phosphorylation state of annexin A2 regulates its endocytic function.

The roles suggested here for annexins A1 and A2 focus on the early stages of the endocytic pathway. Annexin A6 however has been implicated in both the early and late stages of endocytosis. Annexin A6 has been shown to bind β-spectrin [90], a protein capable of binding lipid membranes and the actin cytoskeleton. *In vitro* budding assays have shown the addition of recombinant annexin A6 to promote budding, associated with the loss of β-spectrin from membranes. The ability of annexin A6 to bind membranes in this assay was inhibited by the addition of the recombinant annexin A6 binding domain of β-spectrin. *In vivo* budding was inhibited by the cysteine protease inhibitor N-acetyl-leucyl-

leucyl-norleucinal (ALLN), resulting in a delay but not complete inhibition in the uptake of low density lipoprotein (LDL). Clathrin-coated vesicle (CCV) budding of ALLN treated membranes was shown to occur *in vitro* without the need for annexin A6. Taken together these experiments suggest that annexin A6 is involved in ALLN-sensitive, CCV budding from the plasma membrane. This is likely to be mediated through the annexin A6 dependent activation of a cysteine protease, resulting in the separation of the clathrin lattice from the spectrin membrane cytoskeleton [91]. This specificity of annexin A6 for a subset of CCV budding provides a possible explanation for the efficient endocytosis seen in A431 cells, which do not express annexin A6 and do not show enhanced endocytosis upon annexin A6 over-expression [92].

More recent work has focused on the role of annexin A6 in the later stages of endocytosis, in particular MVB and lysosome fusion. Annexin A6 localises to late endosomal and prelysosomal compartments as shown by immunofluorescence and electron microscopy [93]. Trafficking of low density lipoprotein (LDL) through the endocytic pathway has shown that annexin A6 is associated with LDL vesicles throughout the endocytic pathway, even at late stages [94]. Subcellular fractionation also detected annexin A6 throughout the endocytic pathway, with higher amounts in late endosomal fractions. In addition, microinjection of an N terminal deletion mutant of annexin A6 resulted in the accumulation of LDL in large endosomal compartments and a delay in its degradation, suggesting a block in late endosome to lysosome trafficking [95]. Collectively these studies suggest a role for annexin A6 in modulating late endosome to lysosome trafficking. However it should be noted that the annexin A6 knock out mouse is generally considered normal, therefore the role for annexin A6 in this trafficking pathway is likely to be non-essential.

In vitro data supporting the role of the annexins in endocytosis is now being substantiated *in vivo*, through the use of knock out mouse cell lines as well as siRNA depletion and over-expression in transformed cell lines. As yet no specific molecular mechanism has been uncovered for the annexins in endocytosis. However a model has been put forward for the annexin A1-S100A11 tetramer in membrane aggregation [96], which may also be applicable to the conformationally similar annexin A2-S100A10 tetramer. In this model the annexin A1-S100A11 heterotetramer is suggested to stabilise membrane interactions in order to allow endocytosis to proceed. In response to calcium binding a conformational change may occur to expose the N terminal domain, allowing it to either bind another

membrane surface directly or via the formation of a heterotetramer with S100A11. Annexin A1 phosphorylation is involved in MVB inward vesiculation [24] and in the context of this model N terminal phosphorylation could make annexin A1 more susceptible to proteolysis. Resulting cleavage could destabilise the heterotetramer and aid in the completion of vesicle fission.

1.1.4 Annexins in Membrane Organisation

Annexins have been shown to organise the lipid composition of membranes both *in vitro* and *in vivo*. Much of the initial evidence for this originated from scanning force microscopy of *in vitro* systems. Annexin A2, as part of a heterotetramer with S100A10, was shown to bind to artificial lipid bilayers made of phosphatidylcholine (PC) and phosphatidylserine (PS) in the presence of calcium. Furthermore this binding resulted in the redistribution of PS microdomains, such that they were significantly depleted in the vicinity of annexin A2 protein clusters [97]. Similarly annexin A4 binding to PC and phosphatidylglycerol (PG) membranes *in vitro* was shown to redistribute PG to sites where annexin A4 was bound, as shown using a fluorescently labelled PG derivative [98]. *In vivo* work has shown annexin A2, in complex with its binding partner S100A10, to colocalise with phosphatidylinositol-4,5-bisphosphate (PtdIns4,5P_2) at F-actin enriched sites of the plasma membrane. *In vitro* liposome co-pelleting assays demonstrated a direct interaction between PtdIns4,5P_2 and the annexin A2-S100A10 complex, with an affinity similar to that of a known PtdIns4,5P_2-binding pleckstrin homology domain [52]. In this instance it is believed that the induction of PtdIns4,5P_2 accumulations at the plasma membrane induces the recruitment of annexin A2 to these sites, which then facilitates the reorganisation of the actin cytoskeleton. However *in vitro* studies have shown that annexin A2 itself can stimulate the accumulation of discrete patches of PtdIns4,5P_2, as shown by imaging of fluorescently labelled annexin A2 and PtdIns4,5P_2 [99]. This did not occur in the presence of annexin A2 PtdIns4,5P_2-binding mutants. Therefore *in vivo* and *in vitro* evidence has yet to reach a consensus on whether annexin A2 determines lipid organisation within the plasma membrane or whether the localisation of annexin A2 is simply a consequence of established lipid domains.

Annexin A6 is also implicated in membrane organisation in smooth muscle cells. Upon contraction annexin A6 has been shown to relocalise from the cytoplasm to the

sarcolemmal membrane. In the presence of calcium annexin A6 was shown to be in a complex with actomyosin and cholesterol- and sphingomyelin-enriched sarcolemmal membrane fractions, which are known to be associated with caveolae. *In vitro* reconstitution experiments using these purified constituents resulted in the formation of a structured precipitate, similar to that formed from *in vivo* preparations [47]. Taken together annexin A6 is suggested to have a role in regulating the sarcolemmal membrane upon contraction. Annexin A2 is also implicated in organising the sarcolemmal membrane of smooth muscle cells, as it has been demonstrated to promote the aggregation of lipid raft microdomains in these cells in a calcium dependent manner [100]. The contraction induced association of annexin A2 with the sarcolemmal membrane was shown to be lost upon proteolytic cleavage of annexin A2 [101]. This degradation was significantly blocked upon treatment with a calpain inhibitor. It is therefore believed that calpain may regulate annexin A2 binding to lipid rafts, providing a means by which the signalling events triggered by these lipid raft associations can be terminated.

1.1.5 Annexins and Ion Channels

The first annexin demonstrating an effect on ion flow was annexin A6 [102], in an *in vitro* system of reconstituted sarcoplasmic reticulum membranes. Annexin A6 was shown to increase the frequency of opening and the open time of the calcium release channel. In this system annexin A6 was added to the luminal side of the lipid bilayer, however *in vivo* annexin A6 is predominantly exposed to the cytosolic face of the membrane. *In vivo* studies in neuronal cultures have since shown annexin A6 to regulate ion channels via the cytoplasmic surface of the membrane [103]. The interaction of annexin A6 with the phospholipid membrane was disrupted via the intracellular perfusion of anti annexin A6 antibodies. This resulted in an increase in the magnitude of calcium currents in spinal cord neurons and of potassium currents in both spinal cord and dorsal root ganglion neurons. Conversely the over-expression of plasma membrane targeted annexin A6 has been shown to decrease store-operated calcium entry [62]. *In vitro* studies have now shown that annexin A6 exhibits ion channel properties in the absence of other proteins, as demonstrated by electrophysiological experiments in an artificial membrane system [8]. Therefore the effects on calcium currents observed in the previous studies, may not be due to the modulation of calcium channels by annexin A6, but by annexin A6 itself acting as a calcium channel.

Stronger evidence for the annexins themselves acting as ion channels followed on from the crystal structure analysis of annexin A5. Annexin A5 comprises a central pore region lined with polar residues [16] (Figure 4). Evidence for calcium channel activity came from calcium imaging experiments and electrophysiological recordings. Imaging of the calcium fluorophore Fura-2 in liposomes across which a calcium gradient had been established [104], showed that the addition of annexin A5 caused an influx of calcium which did not occur upon application of the N terminal deletion mutant. Patch clamp experiments on liposomes further demonstrated the requirement of specific residues within annexin A5 [105]. The mutation of a key glutamic acid residue within the channel pore resulted in decreased conductance for calcium and increased conductance for sodium and potassium, as shown by single channel recordings. Mutational analysis has also led to the hypothesis that certain glutamic acid residues determine the conductance of the channel by regulating its diameter [106]. Although there is a substantial amount of data supporting the *in vitro* function of annexin A5 as a calcium ion channel, this has yet to be definitively proven *in vivo*.

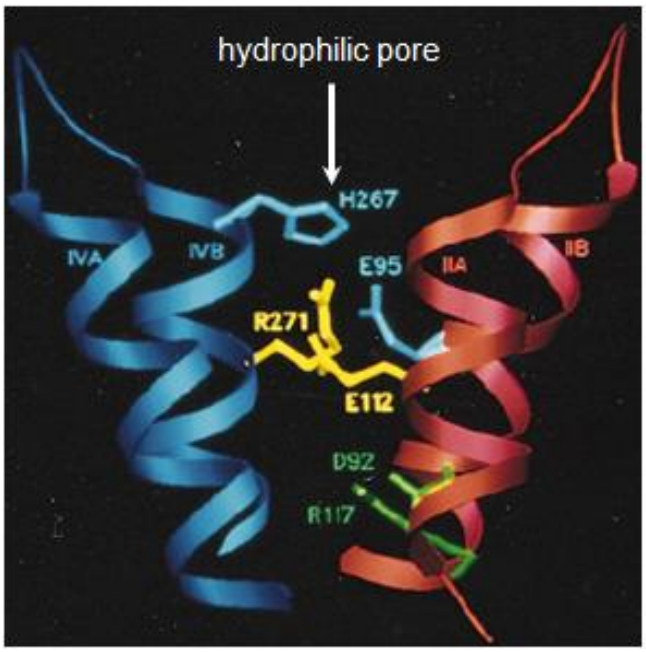

Figure 4 Crystal Structure of the Annexin A5 Pore

The ion channel properties of annexin A5 are thought to arise from its ability to form a hydrophilic pore from four alpha helices (depicted here in blue and red). Two salt bridges (shown in blue and yellow) which extend into the pore have been shown via mutational analysis to be necessary for the voltage sensing ability of the ion channel. Taken from [13].

A more convincing case has been put forward for the role of the annexins as modulators of ion channel activity, with particular regard to annexin A2 and its interaction with S100A10. Disruption of this interaction through the injection of a truncated annexin A2 peptide encoding the S100A10 binding site, resulted in a gradual decrease in the amplitude of chloride channel currents in vascular endothelial cells [107]. S100A10 itself is implicated in promoting the expression of several ion channels through regulating their translocation to the plasma membrane. This is mediated through direct interactions with the channels, as exemplified by the binding of S100A10 to the sensory neuron-specific sodium channel [108], the widely expressed potassium channel TASK-1 [109] and the neuronally expressed sodium channel ASIC1a [110]. Although S100A10 alone is able to direct the targeted expression of ion channels, its interaction with annexin A2 has also been shown to be necessary in certain circumstances. S100A10 binds the epithelial calcium channels TRPV5 and TRPV6. Both annexin A2 and S100A10 have been shown to be in complex with TRPV5 and to colocalise with TRPV5 and TRPV6. Moreover, siRNA-mediated depletion of annexin A2 results in diminished TRPV5 and TRPV6 calcium currents, highlighting the importance of annexin A2 in this complex [33]. In this context annexin A2 may regulate the trafficking of ion channels to the cell surface, as S100A10 does and in addition may be involved in tethering the channels to the plasma membrane given the membrane and cytoskeletal binding properties of this annexin.

1.1.6 Extracellular Roles of the Annexins

The annexins are not known to contain signals targeting them for secretion into the extracellular milieu, nevertheless studies have shown several of the annexins to be involved in extracellular events. Particular importance has been placed on annexin A2 in plasmin production (discussed in 1.1.7 Annexins in Disease), annexin A1 in inflammation and annexin A5 in cell death and blood clotting.

Annexin A5 binds phosphatidylserine (PS), which in dying cells is flipped to the outer leaflet of the lipid bilayer. It is this characteristic which has led to the use of annexin A5 as a marker of dying or dead cells, not only *in vitro* but also *in vivo* in patients (reviewed in [111]). Upon binding of PS annexin A5 self-associates to form a trimer, resulting in the formation of a membrane bound lattice [112]. This binding requires calcium and is

enhanced in the presence of zinc [113], at levels which occur naturally in the extracellular environment such as circulating blood where annexin A5 and also annexin A4 have been detected [114].

Autoantibodies against annexin A5 in the circulating blood of pregnant women have been correlated with a tendency towards miscarriage [115]. It is hypothesised that these antibodies disrupt the anti-coagulant properties of the annexin A5 lattice on the surface of placental synctiotrophoblasts, resulting in increased clotting and subsequent miscarriage [116]. The anti-coagulant activity of annexin A5 has also been shown to act directly on platelets. Binding of annexin A5 to activated platelets, via exposed PS on the platelet membrane, prevented the binding of the pro-coagulant Factor Xa which is necessary for the formation of the prothrombinase complex [117]. It is therefore suggested that annexin A5 can inhibit coagulation through the disruption of activation complexes on the platelet cell surface, thus preventing the formation of thrombin.

The extracellular function of annexin A1 also targets cells of the circulatory system, specifically of the innate immune system. *In vitro* and *in vivo* studies have shown that after the translocation of annexin A1 to the cell surface of leukocytes following adhesion to endothelial cells, a small proportion of this pool of annexin A1 is proteolytically cleaved and released into the extracellular environment in its truncated inactive form [118]. Neutralising antibodies against the cell surface-attached form of annexin A1 enhanced extravasation in a mouse model, supporting the role of annexin A1 in the inhibition of leukocyte transmigration. The mechanism by which annexin A1 exerts these effects has since been investigated *in vitro*. Annexin A1 has been shown to inhibit leukocyte adhesion through the binding of the formyl peptide receptor (FPR) family which activates downstream ERK (Extracellular Signal-regulated Kinase) cascades [119]. Neutralising antibodies against annexin A1 prevented this decrease in adhesion. In further support of this, leukocytes from the annexin A1 knockout mouse demonstrate an increased ability to transmigrate [120]. The function of annexin A1 in this process is of particular significance as glucocorticoid treatment has been shown to inhibit leukocyte adhesion and delay transmigration whilst also up-regulating annexin A1 expression in these cells [121]. Annexin A1 is therefore believed to be a key regulator of the anti-inflammatory effects of glucocorticoid treatment not only in the innate immune system, but also the adaptive immune system (reviewed in [122]).

1.1.7 Annexins in Disease

The annexins have been implicated in a range of pathological conditions, although to date no annexin has been found to be the root cause of a disease. Nevertheless the annexins are proving to be important markers and targets in a range of disease pathologies including cancer, diabetes and autoimmune disease.

Cancer

In terms of the prognostic value of the annexins in disease, there is much emphasis on annexin expression in cancer progression. Tissue microarray analysis has shown several annexins to be down-regulated in prostate cancer [123]. Annexin A1 in particular has been verified as down-regulated in both patient samples [124] and a prostate cancer cell line [125]. Further investigation into prostate cancer has highlighted a potential mechanistic role for annexin A7 in cancer pathology. Annexin A7 was shown to be down-regulated [126] in prostate cancer, with enhanced loss of expression in metastatic tissue samples compared to primary prostate tumour samples. A similar trend was observed in breast cancer samples [127]. A loss of heterozygosity was detected in regions of the chromosome flanking the annexin A7 gene locus in both prostate cancer [126] and breast cancer samples [128]. Furthermore the annexin A7 heterozygous knockout mouse is prone to tumour development [129]. Collectively these studies suggest annexin A7 may act as a tumour suppressor gene.

In terms of harnessing the annexins as therapeutic targets in cancer, annexin A2 has been the focus of several studies. Immunohistochemical analysis has shown the expression of annexin A2 in ductal epithelia from invasive breast cancer tissues, which was absent in normal or non-invasive breast cancer tissues [130]. The up-regulation of annexin A2 expression is suggested to affect the invasive nature of cancer cells, as shown through the comparison of metastatic and non-metastatic breast cancer cell lines [130]. In line with data collected from ductal tissue samples, annexin A2 expression was absent in the non-invasive cell line and present in the invasive cell line. Annexin A2 is a known receptor for tissue plasminogen and tissue type plasminogen activator and so promotes the conversion of plasminogen to plasmin [131]. The cells of the invasive breast cancer cell line were able to carry out this function, however cells of the non-invasive cancer cell line were not [130].

This provides a possible mechanism by which annexin A2 regulates cancer cell invasion, as plasmin can degrade the extracellular matrix, so aiding migratory behaviour. This is supported by the detection of increased mRNA and protein levels of annexin A2 in migrating cells relative to stationary cells [54]. Annexin A2 may also contribute to tumour cell invasiveness by increasing motility through its known interactions with F-actin [51,53]. This is supported by investigations into anti-cancer drug treatment strategies targeting this protein, namely the use of the steroidal lactone withaferin A [55].

Withaferin A treatment of invasive cancer cells showed a marked decrease in migration, suggested to be due to the effects on annexin A2 and its ability to regulate the actin cytoskeleton [55]. *In vitro* studies showed withaferin A could bind annexin A2 and promote annexin A2 dependent F-actin bundling, which was also observed *in vivo*. This effect was shown to be annexin A2 dependent, as cells with low endogenous levels of annexin A2 were more resistant to this effect and cells over-expressing annexin A2 were more sensitive to this effect. Therefore annexin A2 represents a potential therapeutic target in the treatment of cancer through restricting its spread.

Diabetes

In addition to its affects on the cytoskeleton, annexin A2 promotes plasmin production as previously mentioned [131]. Although this has implications in cancer pathology, it is especially significant in diabetes. Annexin A2 has been implicated in the pathology of both type I and type II diabetes, due to its role in vascular endothelial biology and hypercoagulation which occurs in both forms of diabetes. The production of plasmin, which dissolves blood clots so preventing excessive coagulation, is reduced in high glucose and insulin conditions. This reduction was partially prevented upon addition of annexin A2 [132]. The addition of annexin A2 via injection in a mouse model of diabetes also decreased the effects of diabetic nephropathy and again it is suggested to be due to the anti-coagulation properties of annexin A2 [133]. The inability of endogenous annexin A2 to exert these anti-coagulant effects in diabetes is suggested to be due to its glycation in high glucose and high insulin conditions [134]. Annexin A2 may also contribute to disease pathology through its phosphorylation. Insulin-dependent tyrosine phosphorylation of annexin A2 is known to result in changes in the actin cytoskeleton [50]. This remodelling significantly alters the cell morphology, such that actin domes are formed, and also diminishes cell adhesion. This may result in as yet undetermined effects *in vivo* in the

context of diabetes.

Autoimmune Diseases

The role of the annexins in autoimmune disease is less clear than that of diabetes and cancer. However autoantibodies against the annexins have been detected in many autoimmune diseases. Anti-phospholipid syndrome (APS), an autoimmune diease characterised by increased thrombosis, has in particular been associated with annexin A2. Alongside the major autoantibody present in APS against β_2-glycoprotein I (β_2-GPI), autoantibodies against annexin A2 have also been detected in APS patient sera [135]. *In vitro* binding assays have shown annexin A2 to bind β_2-GPI and the over-expression of annexin A2 in endothelial cells was shown to enhance β_2-GPI binding to the plasma membrane. Taken together this supports a role for annexin A2 as a receptor for β_2-GPI [45]. This model in which β_2-GPI binds to endothelial cells via annexin A2 is suggested to activate these cells, so promoting the formation of pro-coagulant complexes on their surfaces and therefore thrombi. Autoantibody production in APS is also suggested to promote coagulation by disrupting the cell surface distribution of annexin A5 and subsequently inhibiting its anti-coagulant activities [136]. Autoantibodies against annexin A11 have also been detected in APS and in several other autoimmune diseases, as discussed in 1.2 Annexin A11, specifically in 1.2.10 The Immune System and 1.2.11 Disease.

1.2 Annexin A11

The initial identification of annexin A11 is most likely to have come from early studies on a ‘synexin-like’ protein. This 56kDa calcium binding protein was first discovered in adrenal medulla and liver tissue in 1983 [137]. It was shown to have characteristics similar to that of synexin, in that it enhanced the aggregation of chromaffin granules and phosphatidylserine liposomes. However protease treatments of these two proteins showed them to have different sensitivities and peptide maps. Several years later, a ‘synexin-like’ protein was also found in human blood platelets [138] with the suggestion that it may belong to a newly identified family of proteins, called annexins.

In 1992 the primary structure of annexin A11 was elucidated, following its purification from rabbit lung as a “calcyclin associated protein” [139]. It was then named CAP-50, calcyclin

associated protein-50, but following protease digestion was shown to belong to the annexin family. It exhibited properties common to annexin family members, including the inhibition of phospholipase A_2 and calcium dependent binding of anionic phospholipids – in this case phosphatidylserine, phosphotidylinositol, phosphatidylethanolamine and phosphatidic acid.

1.2.1 Primary Structure

Annexin A11, known as CAP-50 when it was first classified as an annexin in 1992 [139], was purified from bovine lung [140] for further characterisation. In this study it was identified as a unique annexin, distinct from synexin (now reclassified as annexin A7) to which it is closely related. Primary structure analysis of partial amino acid sequences showed bovine lung CAP-50 to have 91% homology with rabbit lung CAP-50, which was first highlighted as being an annexin, but only 63% homology with human synexin. Further sequence analysis was carried out after cloning of CAP-50 cDNA from bovine chondrocytes [141] and from a rabbit lung cDNA library [142].

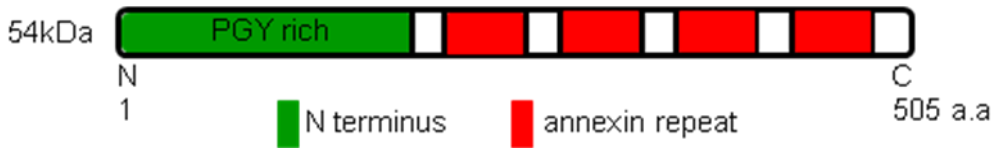

Figure 5 Schematic of Annexin A11 Protein Showing N Terminal and C Terminal Domains

Annexin A11 is a 54kDa protein of 505 amino acids. It comprises a C terminal core and an N terminal head. The C terminal core contains four highly conserved sub-domains called annexin repeats, with calcium binding properties. The long N terminal head is proline (P), glycine (G) and tyrosine (Y) rich.

Results from both studies showed annexin A11 to be a 505 amino acid protein of 54kDa. On SDS PAGE, annexin A11 runs at 55 to 56kDa, most likely due to its proline rich content which can restrain the conformation of denatured proteins. The C terminus was shown to contain four highly conserved annexin repeats with an overall 50% homology with other vertebrate annexin C termini [142]. The N terminus of annexin A11 is the longest of all the annexins and is rich in proline, glycine and tyrosine residues (Figure 5). It shows little homology with the N termini of the rest of the annexins, other than annexin A7, confirming the identification of CAP-50 as a new annexin family member [139].

1.2.2 Isoforms

The continued study of bovine annexin A11, one of the first species in which annexin A11 was identified, uncovered the existence of two isoforms; annexin A11-A and A11-B [143]. These isoforms differ in their N termini due to alternative splicing of exons 3a and 3b. Northern blot analysis however could not detect the annexin A11-B transcript, indicating very low expression levels. Moreover this splice variant is not expressed in mice or humans [144], nor is its peptide sequence conserved in nine other investigated species.

There are three annexin A11 isoforms which have been identified in humans [144], one of which is also present in mice (Figure 6). However these isoforms result from alternative mRNA splicing of exons 1a, b and c in the 5' UTR (untranslated region) of annexin A11 and therefore are also of uncertain functional importance.

1.2.3 Tertiary Structure

Although the primary and secondary structures of annexin A11 have now been well characterised, little is known of its tertiary structure as the protein has not yet been crystallised. However the tertiary structure of its C terminal domain in high calcium conditions has been predicted using x-ray crystallography data obtained from annexin A1 and A5 [145]. As with other annexins the calcium binding sites appear to be located along the convex surface of the molecule, whilst the N terminus is exposed to the cytosol, on the concave side of the molecule. Calcium binding is predicted to alter the exposure of several tyrosine residues in the N terminal domain, which may affect functionality.

1.2.4 Gene Structure

Annexins A7, A11 and A13 are believed to have evolved from a common vertebrate ancestor, about 700 Mya [144], with annexin A11 being the last of the three to diverge from this ancestor. Analysis of the core domain of annexin A11, which contains the four annexin repeats, showed identical intron and exon splice patterns to all the annexins, with the exceptions of annexin A7 and A13. This suggests annexin A11 is the paralogous ancestor of the other nine vertebrate annexins.

The human annexin A11 gene is located on chromosome 10 (Chr10q23) and contains

fifteen exons. Exon 1 is untranslated and is followed by intron 1, which comprises almost half of the gene, then exons 2 to 5 which encode the N terminus, and lastly exons 6 to 15 which encode the C terminus. The untranslated exon 1 can be subdivided into exons 1a, b and c, combinations of which produce the 5' UTR splice variants of annexin A11; isoform a encoding 1a, isoform b encoding 1a and 1c and isoform c encoding 1a, 1b and 1c (Figure 6).

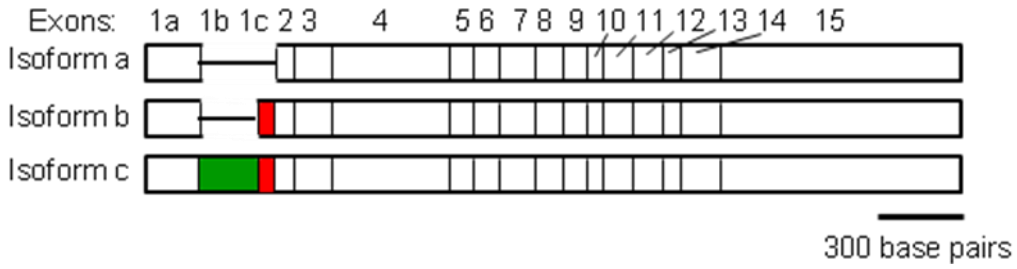

Figure 6 Human Annexin A11 mRNA Transcript Splice Variants

The annexin A11 mRNA transcript is encoded by 2,486 base pairs arranged from exons 1 to 15. Exons 2 to 15 are translated into protein, whereas exon 1 encodes the untranslated 5' UTR. Exon 1 is subdivided in exons 1a, 1b (green) and 1c (red), which are alternatively spliced into three annexin A11 isoforms. Isoform c contains exons 1a, 1b and 1c, whereas isoform b lacks exon 1b and isoform a lacks both exons 1b and 1c.

1.2.5 Tissue and Cellular Distribution

Annexin A11 is expressed in a wide range of tissues including spleen, heart, lung and testis [140] (Figure 7). At the subcellular level annexin A11 expression has been examined in several cell lines. It was initially shown to be predominantly nuclear, but excluded from the nucleoli in rat 3YI embryonic fibroblasts [140]. This has since also been shown in chicken embryonic fibroblasts [146], as well as transformed cell lines including human epidermoid carcinoma (A431) [147] and human cervix adenocarcinoma (HeLa) [146]. However, further investigation has shown this expression pattern to be dependent on several factors.

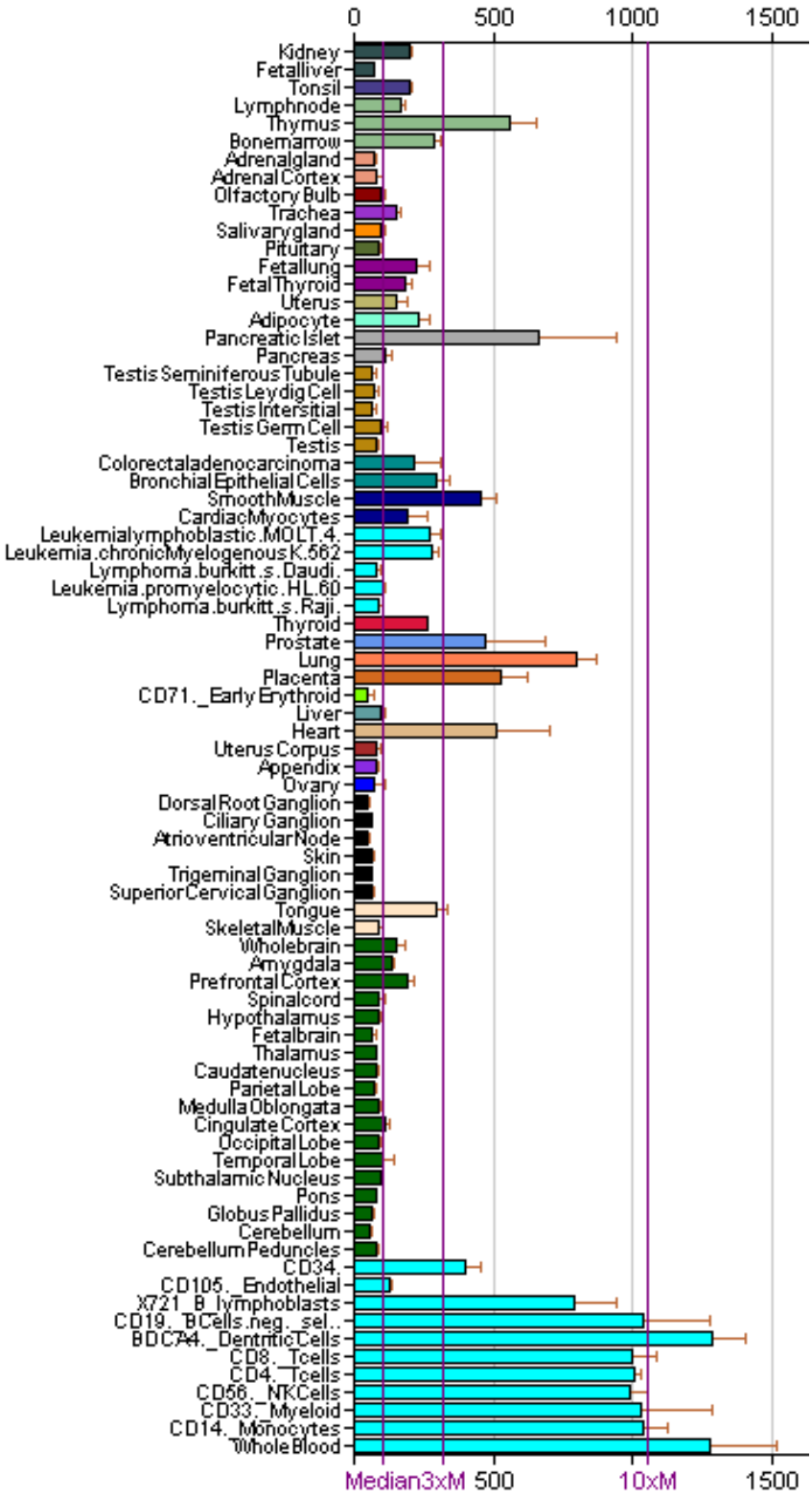

Figure 7 Tissue Distribution of Annexin A11 mRNA

Annexin A11 is expressed at different levels in a wide range of tissues, with high expression patterns detected in thymus, lung and smooth muscle and low expression patterns in testis, adrenal glands and brain. Image produced by [148].

Annexin A11 expression is differentially regulated during tissue development. Immunostaining of adult rat tissues shows mainly cytoplasmic staining with weak staining in the nucleus. The opposite was observed in rat embryonic tissues. However, nuclear staining is not a hallmark of embryonic tissue, as endodermal cells were shown to lack nuclear staining throughout development [149]. The general difference in nuclear staining, between adult tissue comprising mainly post mitotic cells and embryonic tissue, suggests a role for annexin A11 in the regulation of cell proliferation.

In cultured cells, cell-cell contact also affects the subcellular distribution of annexin A11. Nuclear staining is present in both subconfluent and confluent cells. However, in confluent cells there is also strong staining for annexin A11 at the plasma membrane along cell-cell contacts. In subconfluent cells staining outside the nucleus is restricted to vesicles in the cytoplasm, similar to that seen in cells at the boundary of a confluent monolayer. These annexin A11 positive vesicular structures are closely apposed to the microtubule network [146]. Annexin A11 may therefore have some involvement in vesicular trafficking along these networks.

Another major regulator of annexin A11 distribution is calcium. In A431 cells a rise in intracellular calcium causes a partial relocalisation of annexin A11 to the nuclear envelope. This sensitivity to calcium is determined by the C terminal domain. However the specificity of the response towards the nuclear envelope appears to be determined by the N terminus [146]. This correlates with earlier work suggesting that the N terminus of annexin A11 contains its nuclear localisation signal [27].

Given that the expression of annexin A11 is widespread in a range of tissues and cell types, it is likely to be involved in basic cellular processes fundamental to all cells. In addition, as its distribution is affected by several factors, it may have a variety of roles dependent on both the intra- and intercellular environment.

1.2.6 The Cell Cycle

It is known that as the cell cycle progresses the distribution of annexin A11 changes [150]. In interphase cells of cultured cell lines, as previously mentioned, it is mainly nuclear with some cytoplasmic staining. However as prophase progresses it partially translocates to the

degenerating nuclear envelope. By metaphase annexin A11 is present along mitotic spindles and at anaphase it begins to concentrate along the central spindle. At telophase annexin A11 begins to accumulate at the midbody, as well as the reforming nuclear envelope [147]. At cytokinesis it is concentrated at the midbody in two parallel disc structures [146]. The presence of annexin A11 at both the degenerating and reforming nuclear envelope, as well as its co-localisation at these times with the nuclear protein LAP2, confirmed its association with microtubule-induced nuclear folds [147]. This suggests a possible role of annexin A11 in regulating nuclear envelope degeneration and regeneration.

The function of annexin A11 at the midbody has been further investigated, with respect to membrane trafficking. It has previously been noted that annexin A11 positive vesicles appear bound to the microtubule network [146]. It has also been shown that Brefeldin A (BFA), an inhibitor of vesicle trafficking, delays the completion of cytokinesis [151]. In A431 cells this results in binucleate cells. However annexin A11 accumulation at the midbody was BFA-insensitive, suggesting that the presence of annexin A11 at the midbody is independent of BFA-sensitive vesicular trafficking. Therefore the contribution of annexin A11 to cytokinesis may not relate to membrane expansion but to a more specific role at the point of abscission.

The importance of annexin A11 in abscission at cytokinesis has been further highlighted by siRNA-mediated depletion, which results in the absence of a midbody and as a consequence abortive cytokinesis. Daughter cells furrow normally, but are unable to sever the cytoplasmic bridge connecting them, leading to apoptosis [150]. Cytokinetic defects also are seen with the loss or mutation of other constituents of the midbody matrix, such as the mammalian motor protein CHO1.

1.2.7 Phosphorylation and Proteolysis

Annexin A11 is known to be phosphorylated by both serine/threonine kinases and tyrosine kinases. *In vitro* kinase assays have shown increased tyrosine phosphorylation of annexin A11 by PDGF-R (platelet derived growth factor receptor), Src kinase, EGF-R (epidermal growth factor receptor) and CADTK (calcium dependent tyrosine kinase) [152]. Increased tyrosine phosphorylation of annexin A11 has also been shown in cultured smooth muscle

cells in response to treatment with PDGF-BB (platelet derived growth factor BB) [152].

In addition to being a tyrosine kinase substrate, *in vitro* kinase assays have shown that MAPK (mitogen activated protein kinase) phosphorylates annexin A11 on serine and threonine residues [153]. This was observed in rat embryonic fibroblasts transformed with the viral oncogene v-src. An increase in serine and threonine phosphorylation of annexin A11 was detected in the v-src transformed cells when compared to untransformed control cells [153]. This is due to the activation of downstream serine and threonine kinases by v-src, in particular MAPK which was shown to be constituitively activated in v-src transformed cells. This increase in phosphorylation altered the mobility of annexin A11 in SDS PAGE and appeared to mark out the cytoplasmic pool of annexin A11, as shown by subcellular fractionation.

Annexin A11 has therefore been shown to respond to physiological phosphorylation signals and to be phosphorylated by several important kinases. Though the functional significance of these modifications is as yet unknown, initial findings suggest a role in regulating the localisation of annexin A11 [153].

With regard to proteolysis, annexin A11 has been shown to be degraded by intrinsic proteases in rat lung homogenates into four smaller polypeptides of 42, 47, 49 and 52kDa, in the absence of calcium [26]. In the presence of calcium this degradation was limited to a single break down product of 52kDa. It is suggested that the N terminus of annexin A11 makes this annexin more prone to degradation as it houses a strong PEST signal. PEST signals are sequences rich in proline (P), glutamate (E), serine (S) and threonine (T), which are associated with rapidly degraded proteins. Its degradation however is not attributed to the lysosomal pathway as it is does not contain a KFERQ-like motif, which is associated with lysosomal targeting and is present in several other annexins.

1.2.8 Interacting Proteins

ALG2

Apoptosis Linked Gene 2 (ALG2) is a 22kDa calcium binding, penta EF hand protein with homologs in *Drosophila melangoaster*, *Caenorhabditis elegans*, *Dictyostelium discoideum*

and plants [154]. This family of proteins contain five EF hand motifs in their C termini and have N termini rich in glycine and hydrophobic residues.

ALG2 was first identified in a screen for genes involved in apoptosis, using a 'death trap' assay in mouse T-cell hybridoma cells [155]. This showed that the knockdown of ALG2 results in increased resistance to apoptosis induced by T-cell receptor stimulation, staurosporine, and the glucocorticoid dexamethasone. In contrast the over-expression of ALG2 in mouse fibroblasts resulted in enhanced sensitivity to apoptosis induced by a combination of the phorbol ester PMA and the calcium ionophore ionomycin. The function of ALG2 in apoptosis is thought to be downstream of the caspases or caspase independent, as these enzymes were normally activated in response to cell death-inducing stimuli in ALG2 depleted cells.

ALG2 is known to interact with several proteins, most notably with Alix/AIP1 (ALG2 Interacting Protein X/ALG2 Interacting Protein 1) in a calcium dependent manner, via a 33 amino acid stretch within the proline rich C terminus of Alix [156]. Alix has been shown to play a vital role in the cell cycle via its interaction with the ESCRT I (Endosomal Sorting Complex Required for Transport I) machinery through its binding to Cep55 and CHMP4b [157-159]. The ESCRT machinery has been implicated in the final stages of the cell cycle at abscission, during which time it is thought ESCRT I recruits ESCRT III to serve as the executer of membrane fission between the two daughter cells [158]. Tsg101 is part of the ESCRT I complex involved in this process and is known to interact directly with ALG2 in a calcium dependent manner [158,160].

The interaction between ALG2 and annexin A11 was first shown by a yeast two-hybrid screen and then verified by expression of recombinant proteins and *in vitro* interaction assays [68]. This interaction was also proven to be calcium dependent and has since been demonstrated *in vivo*, via the immunoprecipitation of annexin A11 [personal communication, Dr Hideki Shibata, University of Nagoya, Japan]. Both proteins have a cytoplasmic and nuclear distribution. Following stimulation with the calcium ionophore ionomycin, they have been shown to partially co-localise - not only with each other but also with the COP II component Sec31A [personal communication, Dr Hideki Shibata]. Using recombinant proteins, a direct interaction has been shown between ALG2 and Sec31A [161].

Although the functional significance of the interaction of ALG2 with these various proteins has not yet been clearly elucidated, a picture is emerging for a role of ALG2 in membrane trafficking.

S100A6

S100A6, also known as calcyclin, belongs to the S100 family of calcium binding proteins, all of which comprise two EF hand motifs. It was first identified in Ehrlich ascites tumour cells and found to exist as a non-covalent dimer. Several protein interactions involving S100A6 have been shown *in vitro* but have yet to be confirmed *in vivo* [162]. Some of these interactions include the annexins, namely annexins A2, A6 and A11 [139,163] – all shown initially via calcyclin affinity chromatography.

Annexin A11 was originally discovered via its calcium dependent interaction with S100A6 and was so named CAP-50, calcyclin associated protein-50 [139]. It was later shown, via the expression of recombinant proteins, that S100A6 binds the N terminal domain of annexin A11 *in vitro* [20]. The possibility of this interaction occurring *in vivo* was previously thought to be limited, as they do not co-localise in resting interphase cells. During this time annexin A11 remains in the cytoplasm and nucleoplasm and S100A6 at the nuclear envelope [147]. However, a rise in calcium provides an opportunity for them to interact, as annexin A11 translocates to the nuclear envelope, a process which naturally occurs at prophase [147]. Annexin A11 has since also been shown to co-localise with S100A6 in proliferating cells of the mouse embryonic testis, both in the cytoplasm and nucleus [164].

S100A6, like annexin A11, is cell cycle regulated. Its peak expression occurs between G1 and S phase in smooth muscle cells [165]. In addition, its expression is known to be up-regulated in several types of cancer, including that of the bile duct [166,167], the pancreas [167] and leukocytes [139]. Given these properties it is possible that the S100A6-annexin A11 complex may function to regulate the cell cycle.

CHO1

CHO1 belongs to the kinesin-6 family of plus end directed motor proteins, previously known as the MKLP1 (Mitotic Kinesin-like Protein-1) family [168], which also includes

pavarotti in *Drosophila melanogaster* [169], zen-4 in *Caenorhabditis elegans* [170] and MKLP-1 and 2 in humans [171]. CHO1 is known to interact with annexin A11 at cytokinesis, as shown by the immunoprecipitation of endogenous annexin A11 from synchronised human epidermoid cells [146].

The kinesin-6 family in particular has been strongly implicated in cell cycle regulation. Pavarotti in *D.melanogaster* has been to shown to be important in oogenesis, where it localises to ring canals – the equivalent of the midbody structure of the mammalian cleavage furrow. The expression of pavarotti mutants in nuclear localisation or ATP binding, leads to sterile ovaries [172]. Zen-4 in *C.elegans* localises to the mitotic spindle and the midbody matrix. When depleted in embryos, embryogenesis proceeds temporarily without completion of cytokinesis, leading to multinucleate cells. The end result is embryonic lethal [170]. zfMKLP1 in *D.rerio* also localises to the mitotic spindle and the midbody matrix. The expression of dominant negative zfMKLP1 in early embryos resulted in the failure of cytokinesis and multinucleated blastomeres [173].

This family of proteins is equally important in humans. MKLP2 localises to the central spindle and the cleavage furrow on either side of the midbody. Depletion of MKLP2 results in the mislocalisation of important cell cycle regulators, including INCENP, Cdc14, Aurora B kinase and Plk1 [174,175]. The resulting failure in cytokinesis [175] is a phenotype also seen with the depletion of MKLP1. However the defect caused by MKLP1 depletion takes effect at a slightly earlier time point in daughter cell separation, whereby furrow ingression fails to complete. In cells depleted of MKLP2 furrow ingression does complete, resulting in the formation of intercellular bridges. In both cases abscission does not occur and the furrow or intercellular bridge regresses, forming binucleate cells [176].

Given the established roles for kinesin-6 family members in the cell cycle, it is not surprising to find that disruption of CHO1, either by mutation, antibody blockade or knock down [177,178,178] perturbs cytokinesis, preventing furrow ingression completion and producing binucleate cells. The function of CHO1 during the cell cycle relates to its ability to bind components of the cytoskeleton. It has been shown to cross link anti-parallel microtubules *in vitro* [171], akin to the overlapping microtubules found at the spindle midzone where CHO1 is known to localise [178]. It also binds F-actin and antibody blockade of this F-actin binding domain results in incomplete cytokinesis and formation of

multinucleate cells [177]. Though much is known about the role of CHO1 in the cell cycle, there is still little understanding of what role CHO1 may play in interphase cells.

1.2.9 Phosphoinositides

Annexin A11 like all other annexins is capable of binding phospholipids. As previously mentioned annexin A11 distribution is regulated during mitosis. It has also been noted that several phosphoinositides are temporally and spatially regulated during the cell cycle [179]. Phosphatidylinositol-4,5-bisphosphate (PtdIns4,5P_2) in particular accumulates at the cleavage furrow. Preventing PtdIns4,5P_2 accumulation at the furrow inhibits the completion of cytokinesis resulting in multinucleated cells [180]. Furthermore PtdIns4,5P_2 hydrolysis at the furrow has been shown to be necessary for the completion of cytokinesis [181]. PtdIns4,5P_2 has also been proposed to be important in maintaining the tight association between the plasma membrane and the midbody during the final stages of cytokinesis [182]. Annexin A11 is suggested to interact with a range of specific phosphoinositides, as detected via an *in vitro* PIP (phosphatidylinositol phosphate) strip assay [146]. In the presence of calcium, this assay demonstrated the ability of annexin A11 to strongly bind phosphatidylinositol, phosphatidylinositol-3-phosphate, phosphatidylinositol-4-phosphate, phosphatidylinositol-5-phosphate, phosphatidylinositol-3,4-bisphosphate, phosphatidylinositol-3,5-bisphosphate and also to a lesser extent phosphatidylinositol-4,5-bisphosphate (PtdIns4,5P_2) [146]. The ability to associate with PtdIns4,5P_2 may be of particular relevance at cytokinesis.

The binding of annexin A11 to phospholipids has been shown to be phosphorylation dependent, with phosphorylated annexin A11 having a reduced affinity for phosphatidylserine (PS) binding in v-src transformed rat embryonic fibroblasts [153]. Annexin A11 is not only phosphorylated on serine/threonine residues in response to v-src, but also on tyrosine residues in response to platelet-derived growth factor (PDGF). The effect of tyrosine phosphorylation on phospholipid binding is however unknown.

1.2.10 The Immune System

Several groups have identified annexin A11 expression in cells of the immune system, such as macrophages [183,184], neutrophils [185] and T cells [186]. Annexin A11 is also

highly expressed in dendritic cells and monocytes (Figure 7). In neutrophils, it has been found to translocate from the cytosol to granule membranes *in vitro* [185] and to localise to periphagosomal regions during phagocytosis [187]. It is therefore speculated that annexin A11 may affect neutrophil mediated immune responses by regulating phagocytosis. A role in phagocytosis is also implied in macrophages, where annexin A11 has been shown to localise to phagosomes, using subcellular fractionation before and after phagocytosis stimulation [188].

The importance of annexin A11 in normal immune responses is highlighted by the fact that autoantibodies against this protein have been identified in several autoimmune diseases, where the balance between self and non-self immune responses is disrupted. Autoimmune diseases identified with this characteristic include systemic lupus erythematosus (SLE), rheumatoid arthritis, Sjorgens syndrome, Raynauds disease and polymyisitis [189]. Several of these diseases, such as Sjorgens syndrome, rheumatioid arthritis and SLE are more prevalent in women. Changing oestrogen levels are believed to affect the immune response and it has been shown that annexin A11 mRNA levels are increased in oestrogen pre-treated macrophages, following withdrawal of this hormone [190].

1.2.11 Disease

The significance of annexin A11 in disease pathology is unclear. However, as described above, annexin A11 is suggested to have a role in the immune system and possibly in a number of autoimmune diseases. In addition to this, the involvement of annexin A11 has been alluded to in retinal diseases such as age-related macular degeneration (AMD) [191] and proliferative vitreoretinopathy (PVR) [192]. This is due to its detection in Drusen, a collection of extracellular aggregates within the retina, as well as its expression in dedifferentiated, cultured human retinal pigment epithelial (RPE) cells.

One of the most notable suggestions for the involvement of annexin A11 in disease is in sarcoidosis. Sarcoidosis is a systemic immune disorder with a phenotype of epithelioid granulomas, which result in the accumulation of lesions affecting many organs, such as the lungs, kidney, skin and eyes. A recent genome-wide study of a set of German patients and control subjects, identified a single nucleotide polymorphism (SNP) in annexin A11 as the most highly associated susceptibility locus [193]. Further investigation of annexin A11

in control subjects demonstrated that annexin A11 mRNA was expressed in a range of immune cells and was strikingly decreased in activated CD8 and CD19 positive cells compared to their resting counterparts. The cause and mechanism of this disease is not well understood and it may be that annexin A11 has a role in its initiation. It is speculated that it may be through an effect on apoptosis or perhaps through altering the fine balance of signalling between immune cells like CD8 and CD19 lymphocytes.

More recent work has also uncovered a role for annexin A11 in ovarian cancer. Annexin A11 was found to be differentially expressed in ovarian cancer cell lines that were either sensitive or resistant to the anti-cancer drug, cisplatin. This was detected through antibody microarrays and confirmed through immunoblotting, as well as immunohistochemistry of tissue samples [194]. Autoantibodies against annexin A11 have also been shown to be significantly raised in primary ovarian cancer patients, with a smaller proportion of patients with recurrent tumours also showing raised levels [195]. This appeared to be specific to ovarian cancer as no significant difference was detected in patients with colon, breast, pancreatic and prostate cancer or diabetes. Further work demonstrated that the knock down of annexin A11 negatively regulated the proliferation of ovarian cancer cell lines and conferred resistance to cisplatin [196]. This collection of studies strongly suggests a role for annexin A11 in ovarian cancer pathology.

1.2.12 Membrane Fusion

Annexin A11 has been shown to be present in the outer acrosomal membrane of spermatozoa in the presence of calcium, suggesting a possible involvement in the acrosomal reaction. During this reaction the acrosomal membrane fuses with the plasma membrane and releases acrosomal enzymes, allowing penetration of the ova by the spermatozoa [197].

Annexin A11 is also speculated to be involved in membrane fusion events in pancreatic β cells. Annexin A11 was shown by immunofluorescence to be present in the cytoplasm of pancreatic endocrine cells and in the pancreatic β cell line MIN6. Electronmicroscopy of MIN6 cells revealed annexin A11 to be in insulin granules. Furthermore treatment of these cells with anti-annexin A11 antibodies inhibited calcium and GTP-γS induced insulin secretion [198].

1.2.13 Therapy

Annexin A11 has been investigated as a possible therapeutic tool, whereby it is fused to staphylokinase (SAK), a fibrin-selective thrombolytic protein. By exploiting the phosphatidylserine (PS) binding ability of annexin A11 it has been suggested that this fusion protein could be used to resolve blood clots, as activated platelets expose PS in their membranes [199].

1.3 Thesis Aims

Annexin A11 was first identified over 25 years ago, however not much is known about its physiological activity within the cell. In more recent years functional associations have been suggested with the cell cycle [150] and the autoimmune diseased state [193].

This thesis aims to investigate the role of annexin A11 in sarcoidosis, a granuloma associated autoimmune disease. The role of annexin A11 in the cell cycle shall also be further elucidated, both with regards to its distribution and to its function at cytokinesis with the motor protein MKLP1/CHO1. In addition to published links within the aforementioned fields, the cellular distribution of annexin A11 shall be characterised with the view to uncovering previously unknown localisations to better understand its role during both mitosis and interphase.

Chapter Two:
Materials and Methods

2. Materials and Methods

2.1 Cell Culture

HeLa (human cervix adenocarcinoma), A431 (human epidermoid carcinoma), ARPE19 (human retinal pigment epithelium) and CaCo-2 (human colorectal adenocarinoma) cells were cultured in DMEM (Dulbeccos minimal essential media, Gibco) with 10% heat-inactivated FCS, 100IU/ml penicillin, 100μg/ml streptomycin and 292μg/ml L-glutamine and incubated at 37°C with 5% CO_2.

2.2 Cell Synchronisation

Cells were plated at 30% confluency. The next day cells were incubated in media containing 5mM thymidine (Sigma) to cause cell cycle arrest in early S phase. This was carried out overnight for 16h. Cells were then washed in PBS three times and released into media containing 100ng/ml nocodazole for 7h, resulting in a prometaphase block. Alternatively, unsynchronised cells were incubated overnight in 100μM monastrol, producing a prometaphase block. Prometaphase arrested cells were then washed in PBS three times and released into fresh media. Cells were fixed and permeabilised at 0, 15, 30, 45 and 60min post release, using 4% paraformaldehyde (PFA) for 10min at room temperature or -20˚C methanol for 5min.

2.3 Polymerase Chain Reactions

PCR primers used were designed using online resources [200,201] (see table 1).

Primer	Orientation	Species	Sequence	Use
A11 R230C F	Forward	Human	GACTGCCTGGGGAGTTGCTCC AACAAGCAGCGG	Annexin A11 Mutagenesis (production of R230C mutant)
A11 R230C R	Reverse	Human	GCTGCTTGTTGGAGCAACTCC CCAGGCAGTC	Annexin A11 Mutagenesis (production of R230C mutant)
A11 R230C Seq	Forward	Human	CCCAGTTTGGAAGCCGAGGC	Annexin A11 Sequencing of R230C site
A11 cDNA F	Forward	Human	GGGCCATGGG TATGAGCTAC CCTGGCTATC C	Annexin A11 cDNA amplification
A11 cDNA R	Reverse	Human	CCCGGATCCT GGTCATTGCC ACCACAGATC TTCAG	Annexin A11 cDNA amplification

Table 1 Primers Used for PCR Reactions

PCR reactions were performed using Platinum Pfx (Invitrogen) with dNTP mixes (Bioline) in a Mastercycler Gradient (Eppendorf). PCR products were analysed by electrophoresis using ethidium bromide-containing agarose gels (0.8% in TAE buffer, National Diagnostics) and imaged using a Syngene Transilluminator. The DNA was gel extracted using a QIAquick Gel Extraction Kit (QIAGEN).

2.4 Plasmid Construction

The purified PCR products were cloned into TOPO vectors using a TOPO cloning kit (Invitrogen). The constructs were then digested using the appropriate restriction endonuclease (New England Biolabs) and ligated into the necessary vector using T4 DNA ligase (New England Biolabs) (see table 2).

Plasmid	Vector	Insert	Cloning Kit (Invitrogen)
GST-A11	pGEX-4T-2 (Amersham)	Human annexin A11 full length coding sequence	TOPO TA Cloning Kit *
A11-GFP	pEGFP-N1 (Clontech)	Human annexin A11 full length coding sequence	TOPO TA Cloning Kit *
A11-Nt-GFP	pEGFP-N1 (Clontech)	Human annexin A11 N terminal	TOPO TA Cloning Kit *
A11-Ct-GFP	pEGFP-C3 (Clontech)	Human annexin A11 C terminal	TOPO TA Cloning Kit *
A11-R230C-GFP	pEGFP-C3 (Clontech)	Human annexin A11 full length coding sequence with R230C mutation	Stratagene Quikchange II Site-Directed Mutagenesis Kit
A11-Ct-R230C-GFP	pEGFP-C3 (Clontech)	Human annexin A11 C terminal with R230C mutation	Stratagene Quikchange II Site-Directed Mutagenesis Kit

Table 2 Plasmids, Vectors and Inserts Used

* Made by Dr Alejandra Tomas

2.5 Site Directed Mutagenesis

Site directed mutagenesis was carried out in plasmids containing the desired gene insert. Single amino acid changes were made using two oligonucleotide primers which were complimentary to the target gene, but were designed to contain the appropriate mutation in the middle of the primer. PCR reactions were carried out using 125ng of each primer, 50ng of the plasmid containing the gene insert, dNTP mix and Platinum Pfx (Invitrogen) in a 50µl volume. The PCR reaction was performed for 18 cycles of 30s at 95˚C (to separate

template strands), 1min at 55˚C (to anneal the primers) and finally 4min at 68˚C (to extend from the primers). The reaction was then cooled to 4˚C and digested at 37˚C for 1h with 1µl Dpn1 to remove the parental methylated and hemimethylated DNA. 15µl of this reaction was transformed into competent XL-1 Blue *E.coli*.

2.6 Plasmid Amplification

Plasmids were transformed into chemically competent bacteria and grown overnight in LB broth (Fisher Scientific) with the appropriate selective antibiotic (50µg/ml kanamycin or ampicillin) at 37°C in a shaking incubator. Plasmids were then purified using QIAGEN Plasmid Mini, Midi or Maxi kits, depending on the volume of culture grown. 0.75ml of bacterial culture was kept aside to which 0.25ml of glycerol was added to make a glycerol stock, stored at -80°C.

DNA concentrations of the purified plasmids were determined using absorbance readings measured by a BioPhotometer (Eppendorf).

2.7 Transient Transfections

Cells were plated at 50% confluency on 35mm glass bottomed microwell dishes (MatTek) in DMEM containing 10% heat-inactivated FCS without antibiotics. Following an overnight incubation at 37°C with 5% CO_2 the cells were transfected. Cells were transfected with 3µg of plasmid DNA using 9µl of TransIt LT1 transfection reagent (Mirus). 9µl of TransIt LT1 transfection reagent (Mirus) was incubated with DMEM containing 10% heat-inactivated FCS without antibiotics, for 15min at room temperature. 3µg of plasmid DNA was then added to this solution and incubated for a further 30min at room temperature. The volume of DMEM used in the transfection complex was such that the total volume reached 100µl.

2.8 Immunofluorescence Analysis and Fluorescence Probes

Cells were fixed using 4% paraformaldehyde (PFA) for 20min at room temperature and then permeabilised for 10min at room temperature with 0.2% Triton in PBS. Alternatively cells were fixed using pre-chilled methanol for 5min at -20˚C and then rehydrated at room

temperature by incubating three times with PBS for 15min. Next cells were put into blocking solution of 1% BSA in PBS, for 30min at room temperature.

Cells were then incubated with primary antibody (see table 3) made up in 1% BSA in PBS (Sigma) overnight at 4˚C. Following three washes with PBS the cells were incubated with secondary antibody made up in 1% BSA in PBS for 1h at room temperature (see table 3). Cells in 35mm glass bottomed microwell dishes were then mounted with Vectashield mounting medium (VectorShield Laboratories).

Primary Antibody	**Target**	**Species**	**Source**	**Dilution**
L-19	Annexin A11	Goat anti human	Santa Cruz Biotech	1/50
MKLP1	MKLP1	Rabbit anti human	Santa Cruz Biotech	1/100
Alpha Tubulin	α-tubulin	Mouse anti human	Zymed	1/50
PLK1	P1k1	Rabbit anti mouse	Abcam	1/1000
INCENP	INCENP	Rabbit anti human	Abcam	1/1000
Aurora B	Aurora B	Rabbit anti human	Abcam	1/1000
HH7	Annexin A2	Rabbit anti human	*	1/60
N-19	Annexin A7	Goat anti human	Santa Cruz Biotech	1/100
Pericentrin	Pericentrin A and B	Rabbit anti mouse	Abcam	1/1000
γ tubulin	γ tubulin	Rabbit anti human	*[2]	1/1000
Secondary Antibody	**Target**	**Species**	**Source**	**Dilution**
Anti goat Alexa 488		Donkey	Molecular Probes	1/500
Anti rabbit Alexa 647		Donkey	Molecular Probes	1/500
Anti mouse Alexa 555		Donkey	Molecular Probes	1/500

Table 3 Primary and Secondary Antibodies Used for Immunofluorescence

* Kind gift from Gift from Prof Volke Gerke, Westfalische Wilhelms-Universitat Munster, Germany
*[2] Kind gift from Prof Karl Matter, Institute of Ophthalmology, UCL

Cells were visualised using an inverted Leica TCS SP2 AOBS confocal microscope using a 63x oil/water immersion lense. Images were analysed and processed using Leica Confocal Software Version 2.6.1 and Zeiss LSM Image Browser Version 4.2.0.121.

2.9 Live Confocal Imaging and Calcium Imaging

Cells were transfected with the appropriate construct and incubated overnight at 37°C with 5% CO_2 in DMEM containing 10% heat-inactivated FCS without antibiotics. Cells were then washed once in DMEM without phenol red (Invitrogen) and imaged in DMEM without phenol red at 37°C on an inverted Leica TCS SP2 AOBS confocal microscope.

For calcium imaging, following a single wash in DMEM without phenol red, cells were incubated with 5µM Fura Red AM in DMEM without phenol red for 30min at 30°C and then 30min 37°C. Cells were washed three times in DMEM without phenol red and imaged in DMEM without phenol red. Images were analysed and processed using Leica Confocal Software Version 2.6.1 and Zeiss LSM Image Browser Version 4.2.0.121.

2.10 Polyacrylamide Gel Electrophoresis

Gels for SDS-PAGE were made using Acrylamide/Bis-Acrylamide (Sigma), Tris-HCl and 10% SDS and were polymerised using TEMED (Sigma) and 10% APS. 10% acrylamide was used in the resolving gel and 4% in the stacking gel. Samples were boiled in SDS-PAGE buffer before loading. The gels were run at 80V for the first 5min and then at 150V until the molecular weight ladder (BenchMark protein ladder, Invitrogen) had run the entire length of the gel.

The gels were transferred onto Hybond PVDF Transfer membrane (Amersham) for 45min at 150mA per gel for Western blotting.

2.11 Western Blotting

Following transfer of the proteins to PVDF, membranes were blocked with 8% milk for 1h. Primary antibody also made up in 8% milk was then added and incubated overnight at 4°C on an orbital shaker (see table 3). The membranes were washed three times in PBS + 0.05% Tween for 10min each. Secondary HRP conjugated antibody made up in 8% milk was then added and incubated at room temperature on an orbital shaker for 1h (see table 4). Following three PBS washes for 10min each, membranes were imaged using the ECL Western blotting detection system (GE Healthcare).

For Western blotting against phosphotyrosine-containing proteins, membranes were blocked with 5% BSA in TBS for 1h. Primary antibody also made up in 5% BSA in TBS was then added and incubated overnight at 4°C on an orbital shaker (see table 3). The membranes were washed 3 three times in TBS + 0.05% Tween for 10min each. Secondary HRP conjugated antibody made up in 5% BSA in TBS was then added and incubated at room temperature on an orbital shaker for 1h (see table 4). Following three TBS washes for 10min each, membranes were imaged as above.

Primary Antibody	Target	Species	Source	Dilution
L-19	Annexin A11	Goat anti human	Santa Cruz Biotech	1/200
MKLP1	MKLP1	Rabbit anti human	Santa Cruz Biotech	1/100
Alpha Tubulin	α-tubulin	Mouse anti human	Zymed	1/1000
HH7	Annexin A2	Mouse anti human	*	1/60
ALG-2	ALG-2	Rabbit anti mouse	*[2]	1/500
4G10	phosphotyrosine	Mouse anti human	Millipore (Upstate Biotechonology)	1/1000
EGFR	EGF receptor	Sheep anti human	Fitzgerald Industries International	1/2000
Secondary Antibody	**Target**	**Species**	**Source**	**Dilution**
HRP Goat anti rabbit	Rabbit	Goat	Dako	1/2000
HRP Rabbit anti goat	Goat	Rabbit	Dako	1/2000
HRP Goat anti mouse	Mouse	Goat	Dako	1/2000
HRP Donkey anti sheep	Sheep	Donkey	Dako	1/2000

Table 4 Primary and Secondary Antibodies Used for Western Blotting

* Kind gift from Prof Volker Gerke, Westfalische Wilhelms-Universitat Munster, Germany

*[2] Kind gift from Dr Hideki Shibata, Nagoya University, Japan

2.12 Production of GST Fusion Proteins

Plasmids encoding the GST fusion proteins were transformed into BL21 bacteria and grown overnight in LB broth (Fisher Scienific) with the appropriate selective antibiotic (50μg/ml kanamycin or ampicillin) at 37°C in a shaking incubator. The initial starter culture of 20ml LB broth was then expanded to 200ml and grown until the OD, measured using a BioPhotometer (Eppendorf), was 0.8. The culture was then cooled to 27°C in a shaking incubator for 1h, after which recombinant protein expression was induced with 1mM IPTG

(Invitrogen). Cultures were grown for another 4h at 27°C.

The cultures were centrifuged at 5000rpm for 15min at 4°C. To obtain the protein, the pellets were resuspended in 20ml of cold resuspension buffer (1% Triton X-100, 1mg/ml lysozyme, protease inhibitors (Sigma) in PBS). 1mM EDTA was included in the buffer when obtaining annexin A11 GST fusions, in order to chelate the calcium to prevent annexin binding to cell membranes. The resuspended solution was then thoroughly vortexed and sonicated six times for 10s each. The solutions were centrifuged at 10000rpm for 15 min at 4°C. The supernatants were aliquoted and frozen at -80°C for later use.

2.13 GST Fusion Protein Pulldown Assays

GST fusion proteins were first bound to glutathione beads (Sigma). A 1.5ml aliquot of previously purified GST fusion protein was incubated with 200μl of 50% glutathione bead slurry for 2h at 4°C on a rotator. The slurry was made up in lysis buffer containing protease inhibitors (Sigma), which from this point onwards lacked calcium chelators in order to facilitate any possible annexin A11 interactions. Lysis buffer was composed of 10mM HEPES, 142.5mM potassium chloride, 0.2% NP40, 100μM $CaCl_2$, 2.5mM sodium pyrophosphate, 1mM β glycerol phosphate and 1mM sodium orthovanadate. The beads, now bound to the GST fusion protein, were spun down at 9000rpm at 4°C for 3min. The pellet was washed three times in 1ml PBS + 0.03% Tween (Sigma) with protease inhibitors. To perform the pulldown the pellet was then incubated with whole cell lysate (from ~$6x10^6$ cells) containing protease inhibitors for 2h at 4°C on a rotator. The beads were spun down and supernatants kept. The beads were washed with lysis buffer containing protease inhibitors three times. Both the pellet and the supernatants were boiled with SDS-PAGE buffer, containing DTT (Sigma) for reduction. The samples were frozen at -20°C and stored for later use in SDS-PAGE.

2.14 Immunoprecipitation

In order to immunoprecipitate specific proteins from whole cell lysates, Protein G Sepharose beads (Sigma) were first bound to the appropriate antibody. This was done by incubating 30μl of 50% bead slurry, made up in lysis buffer, with 1μg of the required

antibody, overnight at 4°C on a rotator. Lysis buffer was composed of 10mM HEPES, 142.5mM potassium chloride, 0.2% NP40, 100μM $CaCl_2$, 2.5mM sodium pyrophosphate, 1mM β glycerol phosphate and 1mM sodium orthovanadate. The following day cells were lysed (in lysis buffer containing protease inhibitors, Sigma) and incubated with preclearing beads (30μl of 50% bead slurry) on ice for 30min. The cell lysates were spun down at 9000rpm for 5min at 4°C. The previously antibody bound beads were also spun down and washed with lysis buffer. The supernatants from the centrifuged cell lysates were added to the antibody bound beads and incubated for 2h on a rotator at 4°C.

Following incubation, the reactions were spun down at 9000rpm at 4°C for 3min. The supernatants were kept and boiled for 10min with an equal amount of SDS-PAGE buffer, containing DTT for reduction. The pellets were washed with lysis buffer containing protease inhibitors (Sigma) four times and then resuspended in 60μl SDS PAGE buffer, containing DTT for reduction and boiled for 10min. Samples were stored at -20°C for later use.

2.15 DSP Treatment

In order to stabilise weak protein-protein interactions prior to immunoprecipitation experiments, cells were treated with DSP (dithiodipropionic acid di(N-hydroxysuccinimide ester)) (Sigma), which couples molecules containing primary amines by the formation of amine bonds. Plated cells were washed thoroughly with PBS three times to remove any amines present in the media. Cells were then incubated in a crosslinking solution (50mM triethanolamine, 1.25M sucrose, 10mM $CaCl_2$) containing 1mM DSP at room temperature for 30min. This solution was removed and the cells washed once in blocking solution (50mM triethanolamine, 1.25M sucrose, 10mM $CaCl_2$, 250mM ethanolamine). Cells were then incubated in fresh blocking solution, twice, for 15min each time. Next the cells were washed three times in PBS and harvested by scraping the cells off and then centrifugation. The cell pellet was resuspended in lysis buffer containing protease inhibitors, sonicated for 30s and centrifuged at 13,000rpm to remove any debris. The supernatant was removed and subjected to immunoprecipitation.

2.16 RNA Interference and Transfection of siRNA

Commercially available annexin A11 siRNA was obtained (Dharmacon) and resuspended as per the instructions provided to a concentration of 20μM. Aliquots were stored at -20°C.

Cells were plated at 30% confluency on 35mm glass bottomed microwell dishes (MatTek) in DMEM containing 10% heat-inactivated FCS without antibiotics. Following an overnight incubation at 37°C with 5% CO_2 the cells were transfected. For each dish, 8μl of 20μM annexin A11 siRNA was incubated with 152μl of OptiMEM 1 medium (Gibco) and 5μl of Oligofectamine (Invitrogen) was incubated with 35μl of OptiMEM 1 medium. After a 15min incubation at room temperature the two solutions were mixed and left for a further 30min incubation at room temperature. The final solution was then added drop wise to the cells and left to incubate overnight. Cells were then transfected again a day later, with a second dose of siRNA in the same way. Control cells were treated in the same way but transfected with 20μM mammalian All Star negative control siRNA (Qiagen).

Cells were either fixed and permeabilised for staining and microscopy or lysed and boiled for 10min in a heating block with an equal volume of 2X SDS PAGE buffer for SDS PAGE.

2.17 Silver Staining of Polyacrylamide Gels

SDS PAGE gels were first fixed for 30min in 50% methanol/10% acetic acid solution and then in 5% methanol/7% acetic acid for another 30min. They were then rinsed twice in water for 15min each. The gels were sensitised for 1min in sodium thiosulphate (20mg/100ml), rinsed twice in water for 2min each and then incubated in 0.2% $AgNO_3$/1mM formaldehyde. Gels were washed again in water for 1min and then developed in 6% Na_2CO_3/6mM formaldehyde. This reaction was stopped with 2.3M citric acid.

2.18 Microtubule Co-sedimentation Assay

Cells were harvested and lysed using a cell scraper in Brinkleys Buffer (BRB80; 80mM PIPES, 1mM $MgCl_2$) containing protease inhibitors and 0.2% Triton X-100. Cells were then clarified by centrifugation at 165000g for 20min at 4˚C. The resulting supernatant was incubated at 33˚C with 2mM GTP, 2mM $MgCl_2$ and 20μM taxol for 30min. Control supernatants were incubated without taxol. 1.5mM AMP-PNP was then added and the

supernatants incubated for a further 20min at 33˚C. The samples were then spun through an equal volume of a 15% sucrose cushion at 165000g for 20min at 25˚C. The pellets were resuspended in 2X SDS PAGE buffer and boiled for 10min. The supernatants were collected and mixed with a greater volume of -20˚C acetone and centrifuged at 13,000rpm for 2min. The resulting supernatants were discarded and the pellets resuspended in 2X SDS PAGE buffer and boiled for 10min.

2.19 RNA Isolation and cDNA Production

Cells at 100% confluency in a T25 flask were washed twice with PBS. RNA was then isolated using the RNeasy kit (Qiagen). Following treatment of the cells in buffer RLT, as described in the Qiagen RNeasy kit protocol, cells were passed through a QIAshredder (Qiagen), before continuing with the RNeasy kit protocol. The isolated RNA was then DNase treated using amplification grade deoxyribonuclease I (Invitrogen), according to the manufacturers instructions. The resulting DNA-free RNA was reverse transcribed using the Roche Transcriptor High Fidelity cDNA Synthesis Sample Kit (Roche), according to the manufacturers instructions.

Chapter Three:
Study of the Annexin A11 Sarcoidosis Associated Mutant

3. Results: Study of the Annexin A11 Sarcoidosis Associated Mutant

Sarcoidosis is a multisystem immune disorder, which results in the formation of epitheloid granulomas throughout the body, particularly affecting the lungs, eyes and skin. It was first identified in 1869 by Jonathan Hutchinson and later named by Carl Boeck, both of whom initially recognised the dermatological symptoms of the disease [202].

The immune systems of affected individuals show a delayed hypersensitivity response to skin tests, as well as a reduced number of lymphocytes in circulating blood. In contrast patients show an increase in CD3 and CD4 positive T cells in the lungs. Activated T cells from sarcoid lungs also overexpress several receptors, including interleukin-2 receptor (IL-2R), and produce increased amounts of cytokines, including interleukin-2 (IL-2) [203] and interferon-γ (IFNγ) [204]. Moreover interferon-α (IFNα) induced production of IFNγ and IL-2 has been reported to stimulate the development of sarcoidosis [205].

Monocytes and macrophages are also heavily involved in the formation of sarcoid granulomas [206]. Alveolar macrophages secrete a range of cytokines, including tumour necrosis factor α (TNFα) which is a current target for therapy, as increased production of TNFα has been associated with sarcoidosis [207]. In particular alveolar macrophages from sarcoidosis patients secrete interleukin-15, which has been shown to bind IL-2R and induce T cell proliferation [208].

Given the complex nature of the immune pathways involved and the interplay between different immune cell types, understanding the aetiology of sarcoidosis has proven difficult. However a working hypothesis of granuloma formation has emerged, whereby formation is initiated by antigen presentation to macrophages. Initially a phagosome is unable to form, resulting in ‘frustrated phagocytosis’. Once the phagosome does form the antigen is processed via the MHC class II (major histocompatibility complex class II) pathway, where it is degraded in lysosomes and presented on the cell surface by MHC class II proteins to T cells (Figure 8). CD4 positive T cells specific to this antigen proliferate and accumulate at the site of inflammation. If the initial immune response is too strong then eosinophils and neutrophils may also be recruited here. At this point the cocktail of cytokines present

determine the lifespan of the granuloma [209].

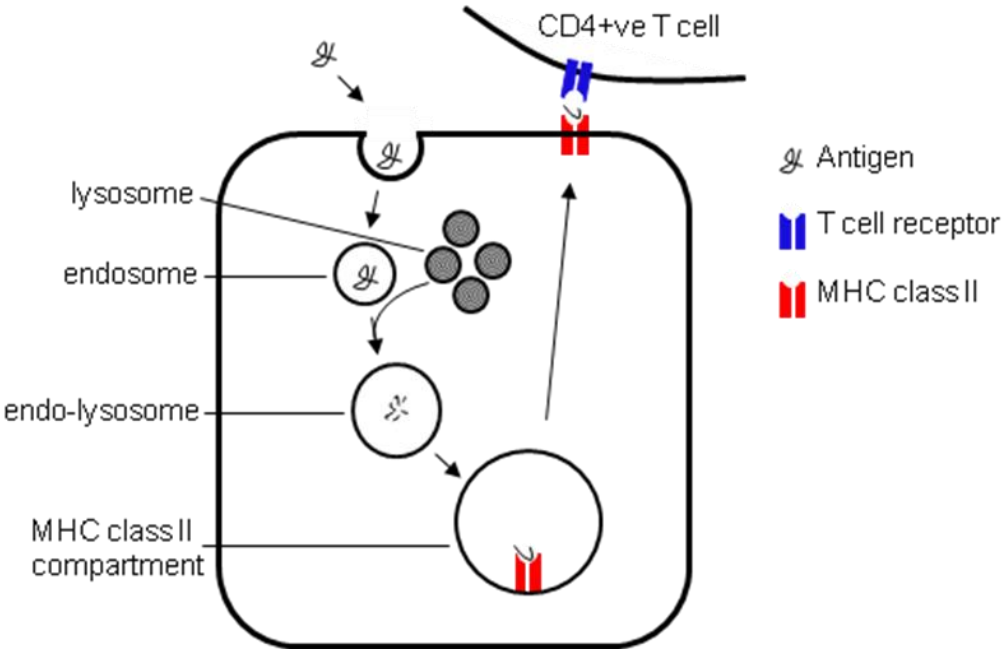

Figure 8 MHC Class II Pathway

In the MHC class II pathway, once an antigen is phagocytosed by a macrophage, the endosomes containing the engulfed antigen fuse with lysosomes. Acid proteases within the endo-lysosomes degrade the antigen into short peptides. The endo-lysosomes then fuse with the MHC class II compartment, where the peptides are loaded onto MHC class II molecules. Vesicles containing peptide loaded MHC class II molecules are trafficked to and fuse with the plasma membrane. The cell is then able to present the processed antigen to CD4 positive T cells.

The initiating antigen in this process is unknown, though viral and bacterial involvement have been speculated [210]. A better picture is however emerging for the genetic factors linked to susceptibility to sarcoidosis. Familial linkage studies, where regions containing alleles more commonly shared between affected family members were sought, uncovered the butyrophilin-like 2 (BTNL2) gene. BTNL2 lies within the MHC class II region and is a member of the B7 receptor family. It is thought to act as a costimulatory molecule for T cell activation.

The SNP in BTNL2 causes a premature stop codon, producing a truncated protein with functional deficits, as it can no longer localise to membranes. Truncation of another B7 family member, B7-1, in mice produced a proinflammatory effect. Therefore the BTNL2 truncation may act in a similar manner, favouring pathological immune responses, as seen in sarcoidosis [211]. However the BTNL2 gene lies close to the human leukocyte antigen

DRB1 (HLA-DRB1) gene and shows a high likelihood (high linkage disequilibrium) of being inherited together with HLA-DBR1 [212]. Therefore it may be the HLA class II genes, like HLA-DRB1, that increase susceptibility to sarcoidosis.

Several HLA genes have been implicated in association studies, with the suggestion that these mutant HLA proteins present antigen to T cells in a manner that induces a pathological immune response. These include both HLA class I genes, such as HLA-B7 and B8, as well as HLA class II genes which are known to be upregulated on alveolar macrophages from sarcoidosis patients [212]. Thus far the focus on susceptibility genes has been restricted to MHC proteins. However a recent study has identified a non-MHC protein, namely annexin A11.

The identification of annexin A11 was the result of a genome wide association study, using 500 control and disease presenting individuals from a German population in order to find novel genetic markers for sarcoidosis. Several disease associated single nucleotide polymorphisms (SNPs) were found, including those in HLA loci and the BTNL2 gene, confirming previous work. Excluding these known areas of association, an individual SNP within the annexin A11 gene produced the highest association signal, alongside five other neighbouring SNPs within this haplotype that were also strongly associated with sarcoidosis [193]. Two alleles for annexin A11 were identified with differing rates of homo- and heterozygosity among controls and sarcoidosis patients. The distribution of the sarcoidosis associated SNP within these different alleles is as yet unknown.

The non-synonymous SNP in annexin A11 results in the switch of a basic arginine to a polar cysteine, within the highly conserved region of the first annexin repeat in the C terminus. This SNP had previously been detected in a bioinformatic analysis of the human genome for non-synonymous mutations and was noted as an SNP likely to have a deleterious effect [213]. Immunohistochemistry of control and sarcoidosis patient lung tissue showed no difference in annexin A11 expression; expression being nuclear in epithelial and mononuclear cells and within cilia of bronchial epithelial cells. Annexin A11 mRNA was found to be expressed in CD4, CD8, CD14 and CD19 positive immune cells. Interestingly in control individuals annexin A11 mRNA expression was significantly reduced in active CD8 and CD19 positive cells compared to those at rest [193]. Whether this would also be true of the SNP variant is unknown.

The mechanism of action of annexin A11 in sarcoidosis is as yet unidentified. However a role in regulating apoptosis has been speculated and may have significance as a means of granuloma resolution [155]. In this context, annexin A11 is known to bind calcyclin and ALG-2, both of which are implicated in regulating apoptosis in caspase dependent and independent pathways, respectively [155,214].

3.1 Characterisation of the Annexin A11 Single Nucleotide Polymorphism

The single nucleotide polymorphism in annexin A11 which is associated with sarcoidosis was found in a genome wide study of a German population [155]. This study identified a substitution mutation, in exon 6 of the human annexin A11 gene, of a cytosine to a thymine (Figure 9B). This altered the codon from a basic arginine to a polar cysteine, at residue 230. The R230C mutation is in the C terminal domain of annexin A11, within the first 14 residues of the first annexin repeat (Figure 9A). Analysis of the protein sequence of annexin A11 in both vertebrates and invertebrates shows a high degree of homology in the regions flanking the mutated site, between species as distant as humans and zebrafish (Figure 9C). The annexin repeats are important domains required for the calcium binding properties of the annexins. A mutation in this region could therefore have significant functional consequences. In order to investigate this, first the distribution of the annexin $A11^{R230C}$ was examined.

Figure 9 Annexin A11 Sarcoidosis Associated Single Nucleotide Polymorphism

(A) Full length wild type human annexin A11 protein sequence. N terminal domain residues (grey box). Annexin repeats (bold). The sarcoidosis associated SNP results in a change in a single amino acid (red box) **(B)** Schematic of annexin A11, showing the mutation (arrow) lies within the first annexin repeat. Shown below is the nucleotide sequence of the human wildtype and sarcoidosis associated SNP (red box) and flanking regions. **(C)** Evolutionary conservation of the amino acids surrounding the SNP affected amino acid (red box) in a range of different species. Residues conserved between all six species shown (bold).

This required the expression of GFP tagged annexin $A11^{WT}$ and annexin $A11^{R230C}$ constructs in human cell lines. The main cell lines used in this study, A431 and HeLa, were first genotyped to determine which form of annexin A11 they endogenously expressed. The exon in which the mutation arises is small, less than 90 base pairs long, which would make designing effective primers for genotyping difficult. Therefore an alternative approach was taken. This involved isolating the RNA from the cell lines and reverse transcribing them into cDNA. The resulting cDNA represents the total expressed genes of the cell line and was used as a template to specifically amplify the annexin A11 gene, using primers designed against the start and end of the gene. This produced a 1512 base pair product visualised on an ethidium bromide agarose gel. This product is also seen in the positive control lane where the template used was a cDNA clone of annexin A11 (from Gene Services). No product was seen in the negative control lane, where no template was added, proving that there was no contamination of the samples during the experiment with extraneous DNA (Figure 10A). The annexin A11 cDNA products from the cell lines were extracted from the agarose gel, isolated and then subjected to sequencing. The results showed that both cell lines expressed the wild type (R230) form of annexin A11.

The A431 cell line was then used to express GFP tagged constructs of full length, N terminal domain and C terminal domain annexin A11. Cells were transfected by liposome delivery of the plasmid DNA and incubated overnight. The cells were then fixed in 4% PFA and imaged on a confocal microscope. Full length annexin A11 showed a nuclear and cytoplasmic distribution (Figure 10B), in line with previous reports of endogenous expression patterns of annexin A11 in transformed cell lines [146,147]. Annexin A11-C-terminal-GFP was predominantly cytoplasmic and mostly excluded from the nucleus, whereas annexin A11-N-terminal-GFP was predominantly nuclear with weak cytoplasmic staining (Figure 10B). This also confirms previous reports showing that the N terminal domain is responsible for nuclear targeting and the C terminal domain, lacking this targeting signal, is excluded from this region [27,146].

The annexin A11-GFP and annexin A11-C-terminal-GFP constructs were mutagenised using primers designed against the SNP site, which incorporated the mutation and flanking regions 15 base pairs either side of the mutation site. The mutant constructs were expressed in A431 cells and showed no difference in distribution to their wild type counterparts. Annexin A11-R230C-GFP was both nuclear and cytoplasmic, as is annexin

A11-GFP and annexin A11-C-terminal-R230C-GFP was predominantly cytoplasmic with weak nuclear staining, as is annexin A11-C-terminal-GFP (Figure 10B). Therefore the sarcoidosis associated SNP does not affect the localisation of annexin A11 in unstimulated A431 cells.

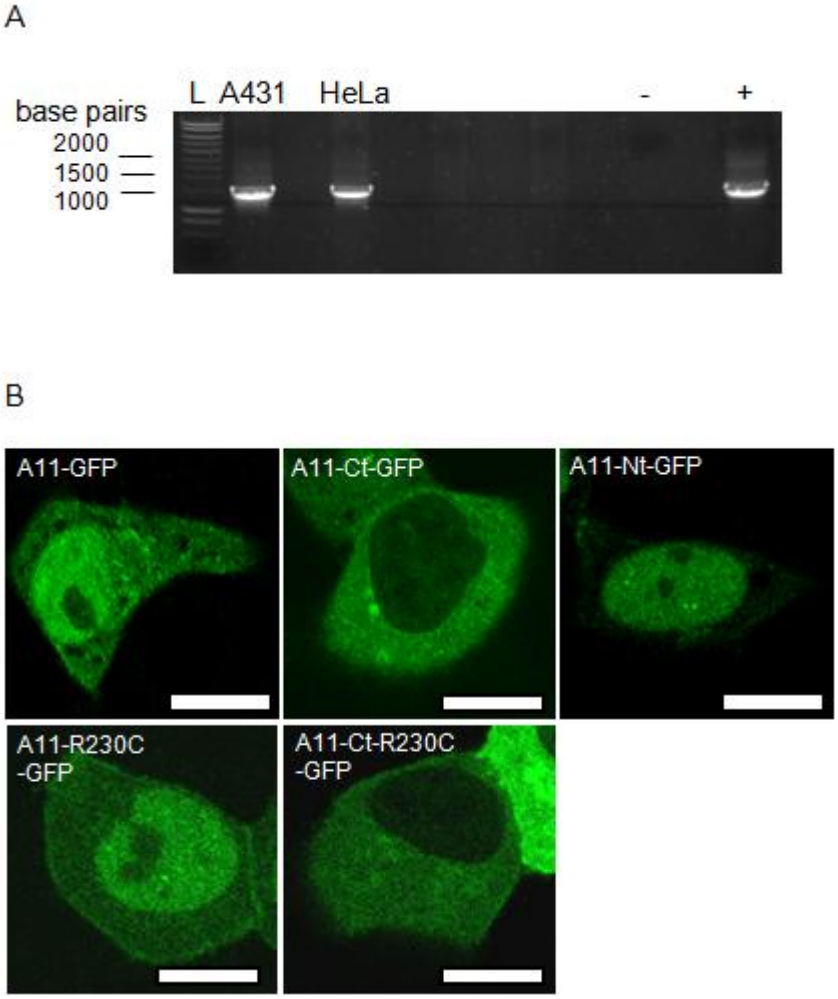

Figure 10 Overexpresion of GFP Tagged Annexin A11^{WT} and Annexin A11^{R230C}

(**A)** Agarose gel of amplified annexin A11 cDNA, obtained by reverse transcription of RNA isolated from HeLa and A431 cell lines. Negative control lane contains a reaction with no template included. Positive control lane contains a reaction with the annexin A11 cDNA clone (Gene Services). DNA ladder (L). **(B)** Expression of annexin A11-GFP, annexin A11-Ct-GFP, annexin A11-Nt-GFP, annexin A11-R230C-GFP and annexin A11-Ct-R230C-GFP in A431 cells transfected with 3µg of plasmid DNA and incubated overnight, prior to fixation in PFA. (Scale Bars 10µm)

3.2 The Response of Annexin A11^{WT} and Annexin A11^{R230C} to Changes in Intracellular Calcium

The SNP in annexin A11 lies within its C terminal domain. The resulting change in amino acid from a basic arginine to a polar cysteine could alter the C terminal domain structure in a manner that could affect its calcium binding properties, particularly as this mutation lies within an annexin repeat. The effects of elevated calcium levels on the localisation of GFP tagged annexin A11^{WT} and annexin A11^{R230C} constructs were tested by stimulating cells with ionomycin or EGF (epidermal growth factor).

A431 cells were transfected with plasmid DNA and incubated overnight. The cells were then transferred into media lacking phenol red and foetal calf serum (FCS), to decrease background fluorescence, and which was HEPES buffered to prevent large changes in pH during imaging. Cells were imaged for 5min, on an inverted confocal microscope with an incubator set at 37ºC, before treatment with either ionomycin or EGF. In both cases the treatment was applied in media equal in volume to that already in the culture dish, so minimising the effects of bolus administration. Images were taken every 9 – 12s.

3.2.1 The Response of Annexin A11^{WT} and Annexin A11^{R230C} to Ionomycin

Ionomycin is an ionophore which raises intracellular calcium levels and was used to stimulate transfected A431 cells. The addition of 1µM ionomycin to A431 cells expressing annexin A11-GFP caused a relocalisation of the tagged protein (Figure 11). Prior to treatment annexin A11-GFP was diffuse in the nucleus and cytoplasm. Following treatment it first relocalised to the plasma membrane, depleting cytosolic GFP fluorescence whilst remaining constant in the nucleoplasm. Annexin A11-GFP was then lost from the nucleoplasm as it relocalised to the nuclear envelope. This process took place within 10min. Line scans were taken across the length of the cell, at a point crossing both the plasma membrane and the nuclear envelope. Prior to treatment, line scan analysis showed no discrete localisation of annexin A11-GFP to membranes. However following ionomycin treatment, line scans showed peaks of membrane enrichment; outer peaks representing the plasma membrane (PM) and inner peaks representing the nuclear envelope (NE) (Figure 11). A similar pattern of relocalisation was observed for stimulated A431 cells expressing annexin A11-R230C-GFP (Figure 12).

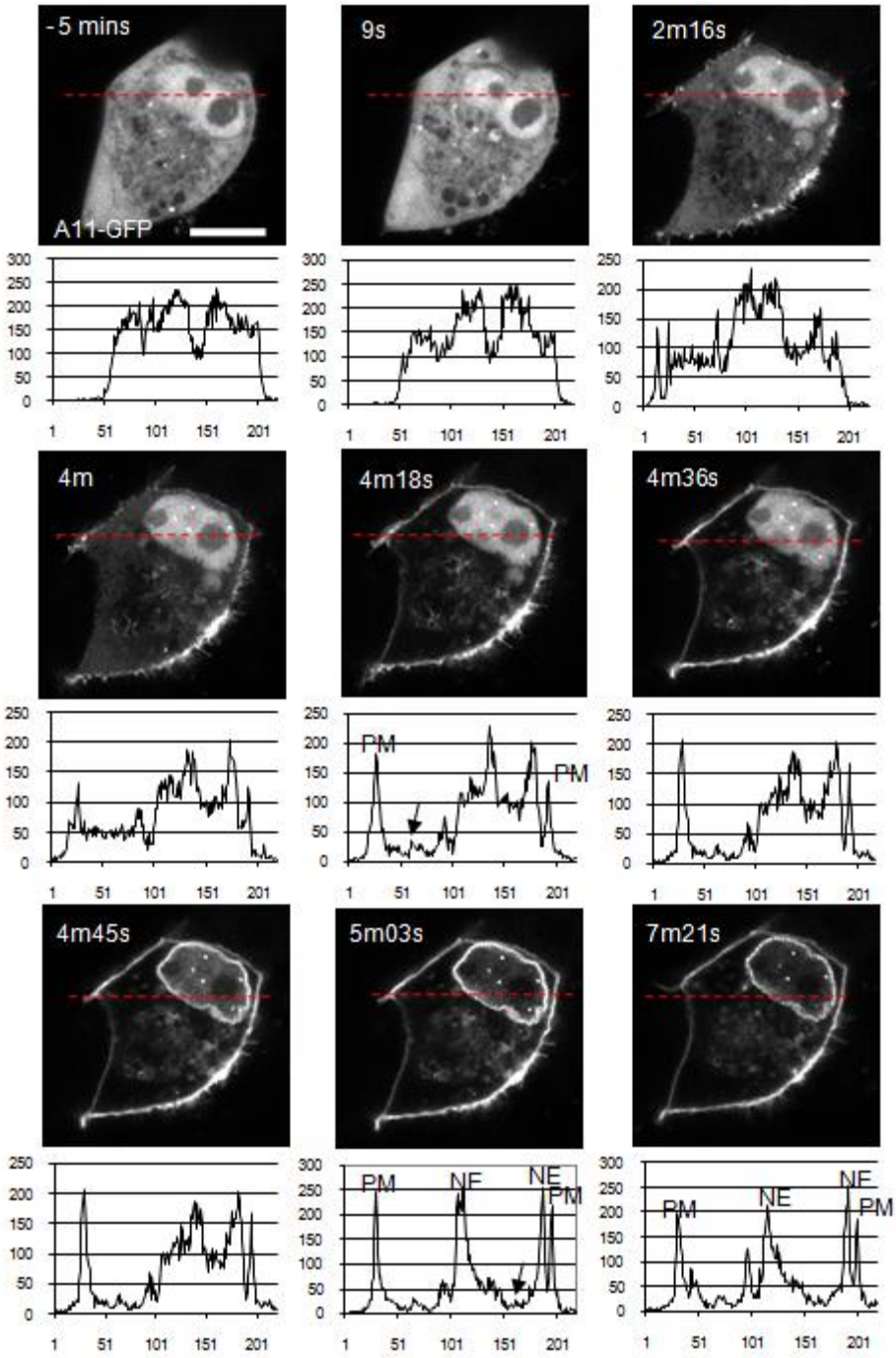

Figure 11 Annexin A11^{WT} Response to Ionomycin

Real time imaging of annexin A11-GFP expressed in A431 cells transfected with 3µg of plasmid DNA and incubated overnight. Cells were imaged in DMEM without phenol red and treated with 1µM ionomycin. Time pre and post treatment noted. Line scans taken through the cell (red) and plotted in graphs below images; gray scale (y axis), position along line in pixels (x axis), plasma membrane (PM), nuclear envelope (NE), maximal cyto- or nucleoplasmic depletion (arrow) (Scale Bars 10µm)

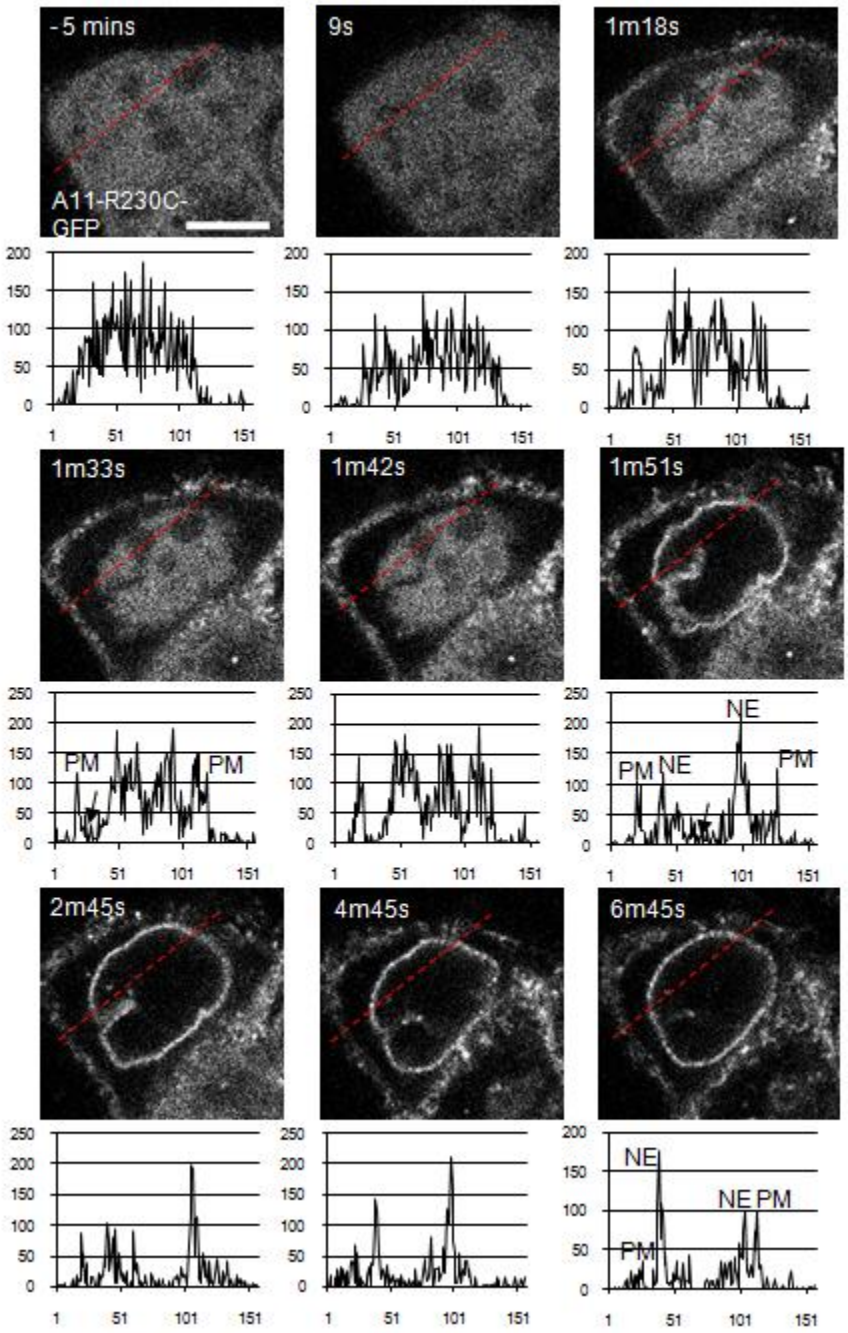

Figure 12 Annexin A11^{R230C} Response to Ionomycin

Real time imaging of annexin A11-R230C-GFP expressed in A431 cells transfected with 3µg of plasmid DNA and incubated overnight. Cells were imaged in DMEM without phenol red and treated with 1µM ionomycin. Time pre and post treatment noted. Line scans taken through the cell (red) and plotted in graphs below images; gray scale (y axis), position along line in pixels (x axis), plasma membrane (PM), nuclear envelope (NE), maximal cyto- or nucleoplasmic depletion (arrow) (Scale Bars 10µm)

The time taken for both annexin A11-GFP and annexin A11-R230C-GFP to relocalise to the plasma membrane and the nuclear envelope was quantified. The time taken to relocalise to either compartment was defined as the maximal enrichment achieved during the time course of the experiment i.e. the point at which no more GFP tagged protein is lost from the cytoplasm to the plasma membrane or the nucleoplasm to the nuclear envelope. This is illustrated by line scans showing clear peaks for membrane enrichment alongside troughs of maximally depleted cytoplasm or nucleoplasm. In the example shown for annexin A11-GFP maximal plasma membrane accumulation is achieved at 4min 18s post stimulation, where the two plasma membrane peaks are clearly defined and the trough representing cytoplasmic depletion drops no further (Figure 11). In the example shown for annexin A11-R230C-GFP this occurs at 1min 33s post stimulation (Figure 12). Maximal nuclear envelope accumulation for the annexin A11-GFP expressing cell shown occurs at 5min 3s (Figure 11). Again there are two clear peaks representing nuclear envelope localisation and a trough between these peaks representing nucleoplasmic depletion, which drops no further beyond this time point. Maximal nuclear envelope accumulation for the annexin A11-R230C-GFP expressing cell shown occurs at 1min 51s (Figure 12). The time taken for annexin A11-GFP and annexin A11-R230C-GFP to relocalise to the plasma membrane and nuclear envelope was quantified in 36 cells each. On average the time taken for A11-GFP to relocalise to the plasma membrane in response to ionomycin was 458s (+/- 70s) and for A11-R230C-GFP it was 516s (+/- 74s). On average the time taken for A11-GFP to relocalise to the nuclear envelope in response to ionomycin was 483s (+/- 76s) and for A11-R230C-GFP it was 533s (+/- 75s). There was no significant difference between the wild type and mutant GFP tagged proteins in the time taken to relocalise to the plasma membrane ($P=0.089$) or the nuclear envelope ($P=0.155$), as determined by a two tailed student t-test (Figure 13).

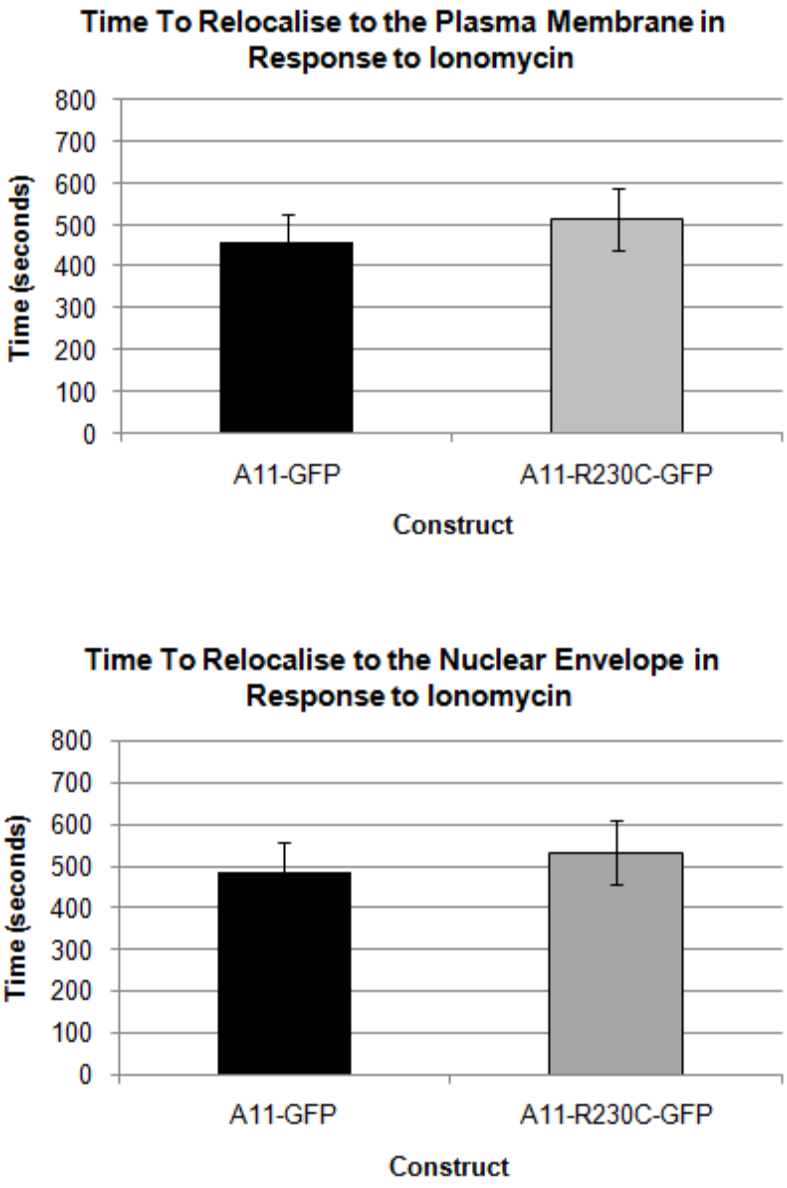

Figure 13 Annexin A11^{WT} and Annexin A11^{R230C} Respond to Ionomycin in a Similar Manner

Bar charts of the average time taken for Annexin A11-GFP and Annexin A11-R230C-GFP, expressed in A431 cells, to relocalise to the plasma membrane (P=0.089) and nuclear envelope (P=0.155) in response to 1µM ionomycin . Errors bars represent standard errors of the mean from three experiments with n = 36 cells for each construct.

The effect of ionomycin stimulation on annexin A11-C-terminal-GFP and annexin A11-C-terminal-R230C-GFP was then examined. Initial experiments did not show any relocalisation of either wild type or mutant GFP tagged proteins in response to 1µM ionomycin. Both mutant and wild type proteins remained excluded from the nucleus, diffuse within the cytoplasm and without any membranous accumulation (Figure 14). In

order to confirm that the cells were responding to the ionomycin, calcium imaging was carried out. Following transfection and overnight incubation, cells were loaded with 5µM Fura Red AM (acetoxylmethyl) in order to visualise intracellular calcium levels. Fura Red AM is a fluorescent indicator of calcium levels, in which a decrease in fluorescence corresponds to an increase in calcium. Fura Red AM was loaded onto the cells in media lacking FCS, to prevent cleavage of the AM group by esterases before the calcium indicator could enter the cell. The cells were first loaded for 30min at 30ºC, to decrease compartmentalisation within the cell, and then 30min at 37ºC. Cells were subsequently imaged in media lacking phenol red and FCS. Both the GFP and Fura Red signals were imaged.

Annexin A11 C-terminal-GFP, annexin A11 C-terminal-R230C-GFP and GFP alone all showed a lack of relocalisation upon ionomycin treatment (Figure 14). The cells were responsive to ionomycin, as an increase in intracellular calcium was detected by a decrease in the Fura Red signal. This decrease in Fura Red fluorescence was quantified for individual GFP expressing cells (graphs in Figure 14). The Fura Red signal dropped an average of 4.6 gray scale units (n=9) in 1 minute post-ionomycin stimulation, compared to an average increase of 1.1 gray scale units (n=9) in 5min of imaging pre-stimulation. Therefore annexin A11-C-terminal-GFP and annexin A11 C-terminal-R230C-GFP do not relocalise to the plasma membrane or nuclear envelope in response to an ionomycin-stimulated increase in intracellular calcium in A431 cells.

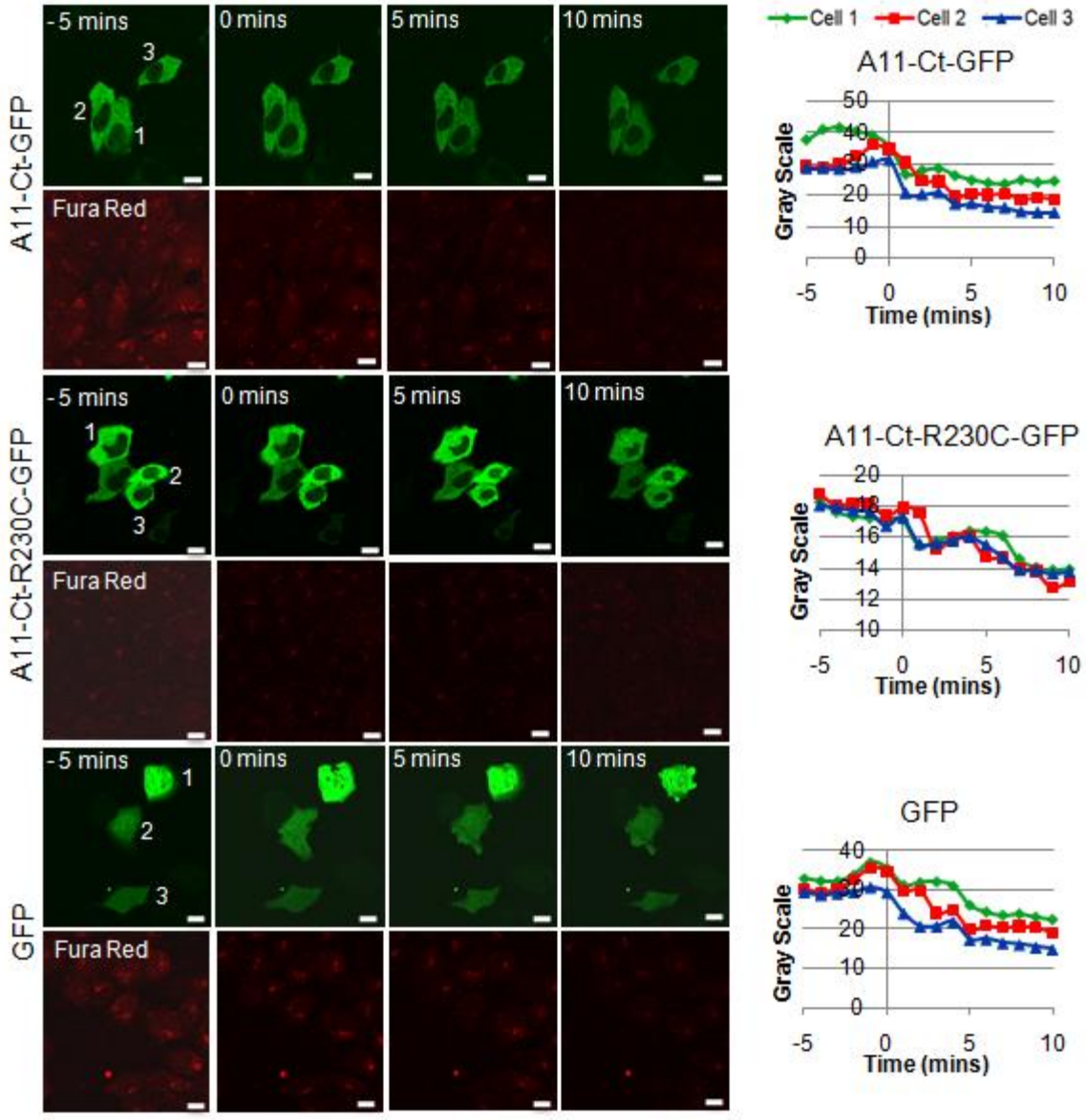

Figure 14 Annexin A11^{WT} and Annexin A11^{R230C} Respond to Ionomycin in a Similar Manner

Real time imaging of annexin A11-Ct-GFP, annexin A11-Ct-R230C-GFP and GFP expressed in A431 cells transfected with 3 µg of plasmid DNA and incubated overnight. Prior to imaging cells were loaded with Fura Red AM in DMEM without phenol red for 30min at 30°C and then 30min at 37°C. Cells were then imaged in DMEM without phenol red and with treated with 1µM ionomycin. GFP construct (green), Fura Red (red). Graphs of Fura Red fluorescence correspond to the cells (1-3) shown in the images. Time pre- and post-treatment noted. (Scale Bars 10µm)

3.2.2 The Response of Annexin A11^{WT} and Annexin A11^{R230C} to Epidermal Growth Factor (EGF)

Ionomycin is capable of eliciting rapid, large and sustained increases in calcium within the cell, however it is a non-physiological reagent. EGF is a well characterised physiological agonist, which also elicits a rapid rise in intracellular calcium levels via the EGF receptor. The A431 cell line is particularly responsive to EGF as it expresses elevated levels of the EGF receptor on its plasma membrane [215]. The addition of 100ng/ml of human EGF to A431 cells expressing annexin A11-GFP, annexin A11-R230C-GFP, annexin A11-C-terminal-GFP, annexin A11-C-terminal-R230C-GFP and GFP alone, did not elicit a relocalisation of the proteins during the 10 minute time frame imaged post stimulation (Figure 15A). Annexin A11-GFP and annexin A11-R230C-GFP remained diffuse within the cytoplasm and nucleoplasm. Annexin A11-C-terminal-GFP and annexin A11-C-terminal-R230C-GFP remained excluded from the nucleus and diffuse throughout the cytoplasm. None of the GFP tagged annexin A11 proteins or GFP alone showed membranous accumulations upon EGF treatment.

In order to verify that the cells were responsive to EGF, the cells were lysed in SDS-PAGE buffer immediately after the experiment and the samples subjected to SDS-PAGE. Control samples of transfected, imaged, but unstimulated A431 cells were also prepared. Western blotting for the EGF receptor showed that the receptor was expressed by these cells (Figure 15B). Furthermore a phosphotyrosine blot showed an increase in the strength of a protein band at 170kDa in stimulated cells but not unstimulated cells (Figure 15B). This band size corresponds to the phosphorylated EGF receptor, which upon binding of EGF autophosphorylates. Therefore the stimulated A431 cells imaged are responsive to EGF, though no relocalisation was observed of the GFP tagged annexin A11 proteins expressed.

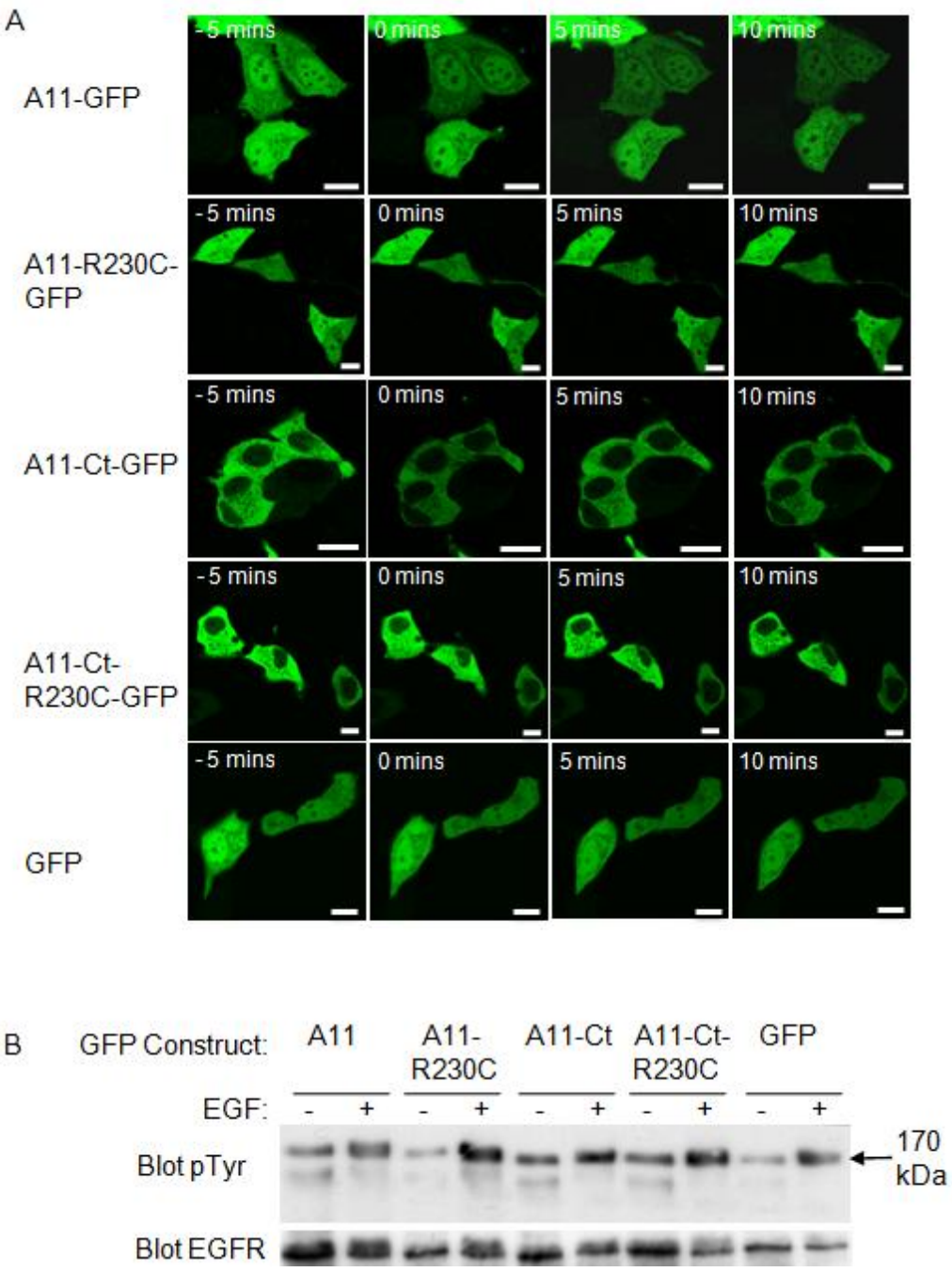

Figure 15 Annexin A11^{WT} and Annexin A11^{R230C} Do Not Relocalise in Response to EGF Treatment

(A) Real time imaging of annexin A11-GFP, annexin A11-R230C-GFP, annexin A11-Ct-GFP, annexin A11-Ct-R230C-GFP and GFP expressed in A431 cells transfected with 3µg of plasmid DNA and incubated overnight. Cells were imaged in DMEM without phenol red and with treated with 100ng/ml of EGF (human epidermal growth factor). Time pre and post treatment noted. (Scale Bars 10µm) **(B)** Following imaging of the transfected cells, the cells were lysed in boiling SDS-PAGE buffer and subjected to SDS-PAGE and Western blotting. EGF receptor was blotted for using a polyclonal sheep anti-EGFR antibody (1/2000 dilution) and phosphorylated proteins using a monoclonal mouse anti-phosphotyrosine antibody (1/1000 dilution). Band corresponding to the size of the phosphorylated EGF receptor shown in the phosphotyrosine blot (arrow).

3.3 Discussion

A recent study, in a German population, identified a single nucleotide polymorphism in annexin A11 as the most highly associated susceptibility locus for the autoimmune disorder sarcoidosis [193]. Until this study the association of annexin A11 with autoimmune diseases, such as systemic lupus erythrematosus, rheumatoid arthritis and Raynauds disease, was limited to the detection of autoantibodies [216]. Given the ubiquitous expression of many annexins, including annexin A11, it is not surprising that it, along with other annexins [217,218] have been detected in sera from patients with autoimmune diseases. Therefore the finding of a mutation in annexin A11 which could potentially predispose an individual to the development of sarcoidosis is significant.

The mutation (R230C) is not present in endogenous annexin A11 of A431 cells. Following confirmation of the normal annexin A11 genotype in this cell line, we went on to characterise annexin $A11^{R230C}$ through over-expression experiments. As the mutation arises in the C-terminal domain of annexin A11, GFP tagged constructs of both full length and C-terminal domain annexin A11 were expressed. No difference was seen in the localisation of GFP tagged $annexin^{WT}$ or annexin $A11^{R230C}$ in resting A431 cells. This suggested that under unstimulated conditions annexin $A11^{R230C}$ can localise normally and so possibly function in the same way as annexin $A11^{WT}$. This led us on to investigate the effect of calcium on annexin $A11^{WT}$ and annexin $A11^{R230C}$.

Initial experiments in A431 cells over-expressing GFP tagged annexin A11, were carried out using ionomycin. Ionomycin is a potent calcium ionophore that produces large, irreversible rises in intracellular calcium levels. This resulted in the relocalisation of GFP tagged annexin $A11^{WT}$ first to the plasma membrane and then the nuclear envelope. The lag between these two relocalisations is most likely due to the strong calcium buffering capability of the nucleus [219]. This redistribution to the plasma membrane and nuclear envelope confirms previous reports of GFP tagged annexin $A11^{WT}$ relocalising to these domains in ionomycin-stimulated cells. This was shown to occur both in the presence and absence of extracellular calcium [147]. The relocalisation to the nuclear envelope has also been demonstrated in ionomycin-stimulated cells endogenously expressing annexin A11 [147], however a plasma membrane relocalisation was not observed, highlighting a difference between endogenous expression and over-expression of GFP tagged annexin

$A11^{WT}$.

The localisation of endogenously expressed annexins to the nuclear envelope in response to ionomycin is also known to occur with annexins A4 and A5 [220], which under resting conditions have both a nuclear and cytoplasmic distribution. This has been observed in human foetal lung fibroblasts, as well as human foreskin fibroblasts which are suggested to also show some weak plasma membrane relocalisation [221]. Although all the annexins have lipid membrane binding capabilities, they do not all relocalise to the plasma membrane and nuclear envelope in response to ionomycin. Annexin A2, which under resting conditions is diffuse in the cytoplasm, takes on a granular appearance in response to ionomycin [221]. Annexin A6 which is excluded from the nucleus in resting cells, has been suggested to redistribute throughout the plasma membrane in human foetal lung fibroblasts [221] but to relocalise to secretory granules and early endosomes in T lymphocyte cells [222] – thus highlighting cell type specific differences.

With regards to over-expression studies, GFP tagged annexin A7 which has both a nuclear and cytoplasmic distribution, has also been shown to relocalise in response to ionomycin [223]. This relocalisation mimics that of GFP tagged annexin $A11^{WT}$, as the protein first localises to the plasma membrane and then the nuclear envelope. This is unsurprising given the high homology between annexin A7 and annexin A11, annexin A7 being the most closely related vertebrate annexin to annexin A11. It is interesting to note that the annexins which show a similar response to annexin A11 when cells are stimulated with ionomycin, share more homology with annexin A11 than those which show a different response. Within the vertebrate annexins, sequence homology to annexin A11 can be ranked from most homologous to least as follows; annexin A7, annexin A4, annexin A6, annexin A5, annexin A8, annexin A3, annexin A13, annexin A1, annexin A2, annexin A10, and annexin A9. In the annexins examined thus far, annexin A7 shows the most similarity to annexin A11 in its response to ionomycin, followed by annexins A4, A5 and A6 which show partial similarity and lastly annexin A2 which shows no similarity in relocalisation. Therefore, aside from the affinity of the annexins for phospholipids, similar targeting sequences may also be involved in their binding to specific domains in response to a rise in intracellular calcium.

The arginine residue which is mutated in annexin $A11^{R230C}$ is however conserved in all

vertebrate annexins and so is unlikely to be part of a specific targeting sequence. This is illustrated by the mutation of this residue in annexin A11, demonstrating no effect on the relocalisation of GFP tagged annexin $A11^{R230C}$ in response to ionomycin. That is to say the cytoplasmic pool of GFP tagged annexin $A11^{R230C}$ also translocated to the plasma membrane and the nuclear pool of GFP tagged annexin $A11^{R230C}$ to the nuclear envelope. Furthermore this occurred with approximately the same time course as its wild type counterpart. It is however still possible that a subtle difference in the time taken to relocalise to these membranous compartments may occur, but only be detectable using a far greater number of cells.

It should be noted that the GFP tagged C-terminal domain constructs showed no significant relocalisation upon ionomycin treatment for either annexin $A11^{WT}$ or annexin $A11^{R230C}$. This is in contrast to previous reports carried out in the same cell line, showing a relocalisation to large vesicular structures within the cell [147]. This difference may be attributed to a difference in the passage number of the cell line, which may affect its responsiveness to calcium. The cells imaged in this study were nevertheless responsive to ionomycin treatment, as demonstrated by a drop in Fura Red fluorescence representing a rise in intracellular calcium levels. The C-terminal domain of annexin A11 is responsible for its calcium-binding properties. Taken together it is likely that although the GFP tagged C-terminal domains of annexin A11 are calcium sensitive, without the N-terminal domain prolonged attachment to the plasma or nuclear membrane is not possible. However it should be taken into consideration that the live images were taken every 9 seconds and it is therefore theoretically possible that the membranous accumulations were not captured at the time points imaged. This could also be true for the live imaging of both GFP tagged full length and C-terminal domain annexin $A11^{WT}$ and annexin $A11^{R230C}$, in response to EGF (epidermal growth factor).

In all four cases no relocalisation of the fluorescently labelled annexin A11 was observed in response to EGF, although the cells themselves appeared to be responsive to EGF. This was confirmed through Western blotting for phosphotyrosine-containing proteins immediately after the experiments were performed. In cells treated with EGF, a phosphotyrosine band corresponding in size to the phosphorylated EGF receptor is enhanced. It is therefore possible that the rise in intracellular calcium in response to EGF is too transient and/or too small to stimulate the membranous relocalisation of annexin

A11. This has been shown to be true for the calcium-induced relocalisation of endogenous annexin A4. Relocalisation occurred in response to ionomycin but not to more transient calcium waves induced by agonists such as bradykinin [220]. Calcium levels are sustained upon treatment with ionomycin, whereas the rise in EGF-stimulated calcium levels has been shown to return to basal levels after 30s to one minute [224]. Furthermore, EGF stimulation of A431 cells is known to increase calcium levels to between 400nM and 700nM, whereas ionomycin raises levels into the low micromolar range. Taken together the lack of response of annexin A11 to EGF, as well as the delay in response to ionomycin, suggests annexin A11 is not particularly sensitive to calcium, which is in line with other studies [225]. The delayed response to ionomycin may be due to other essential calcium-dependent events preceeding relocalisation, such as protein-protein interactions with known binding partners such as ALG-2 [68] or tyrosine phosphorylation of annexin A11 which is known to occur in response to ionomycin [147]. Therefore future studies should involve the testing of different calcium agonists, which elicit changes in calcium levels to different degrees and durations. In addition it would be interesting to mutate the known phosphorylation sites of annexin A11, which lie within the last three annexin repeats of the C-terminal domain [226], to assess whether this affects the response of annexin $A11^{WT}$ and annexin $A11^{R230C}$ to these calcium agonists.

Although no functional difference could be detected in response to calcium between annexin $A11^{WT}$ and annexin $A11^{R230C}$, structural analysis suggests that the R230C mutation may yet exert a functional effect on annexin A11. The tertiary structures of several of the annexins have been elucidated, though not that of annexin A11. Of the known crystal structures, the two annexins with the highest degree of homology to annexin A11 are annexin A8, showing 53% sequence identity and 71% sequence similarity, and annexin A5, showing 53% sequence identity and 73% sequence similarity. The arginine at residue 230 in annexin A11 is conserved between annexins A5 and A8. Furthermore annexin A11 contains six cysteine residues (Figure 16A), two of which are conserved in annexin A8 and one of which is conserved in annexin A5 (Figure 16B). This is of importance as the mutation in annexin A11 which is associated with sarcoidosis, results in a switch from an arginine to a cysteine, and cysteine residues are able to covalently bind to each other through the formation of disulphide bridges.

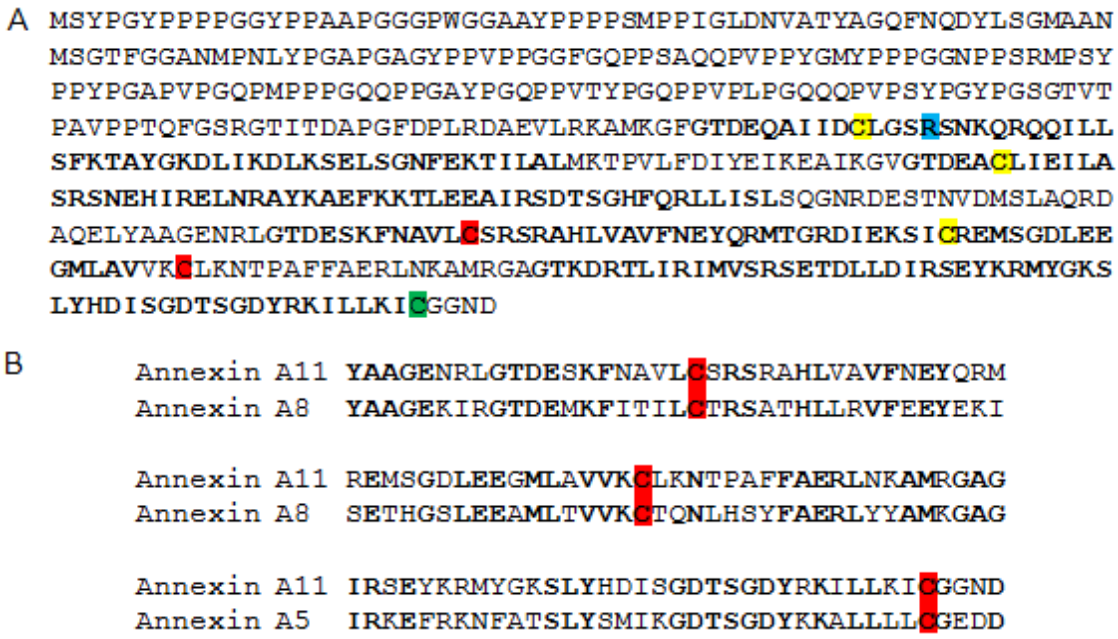

Figure 16 Annexin A11 Amino Acid Sequence

(A) Annexin A11 contains six cysteine residues, two of which are conserved in annexin A8 (red box), one of which is conserved in annexin A5 (green box) and the remaining three which are not conserved in either annexins A5 or A8 (yellow box). Annexin repeats (bold). Residue 230 (blue) **(B)** Annexin A11 sequences aligned against annexin A8 and annexin A5. Conserved residues (bold). Conserved cysteines (bold, red box).

Crystal structure analysis shows that in both annexin A8 and annexin A5 the conserved arginine at residue 230 lies near the start of an alpha helix (Figure 17A, B). In the case of annexin A8, the conserved cysteine residues (C206 and C250) are not in the vicinity of this arginine (Figure 17A). However in annexin A5 the conserved cysteine residue (C316) lies opposite this arginine, with the arginine pointing away from the cysteine (Figure 17B). Upon mutation of this arginine to a cysteine it is possible that a new conformation could arise in which the two cysteine residues are facing each other. If close enough together, this could facilitate the formation of a disulphide bridge between the sulphydryl groups of the cysteine residues and may therefore affect the alpha helical structure of this annexin repeat. This may be more likely to occur between cysteine 230 and the nearby cysteine 226, which is unfortunately not conserved in annexin A5 or A8 and so was not modelled in the crystal structures presented here.

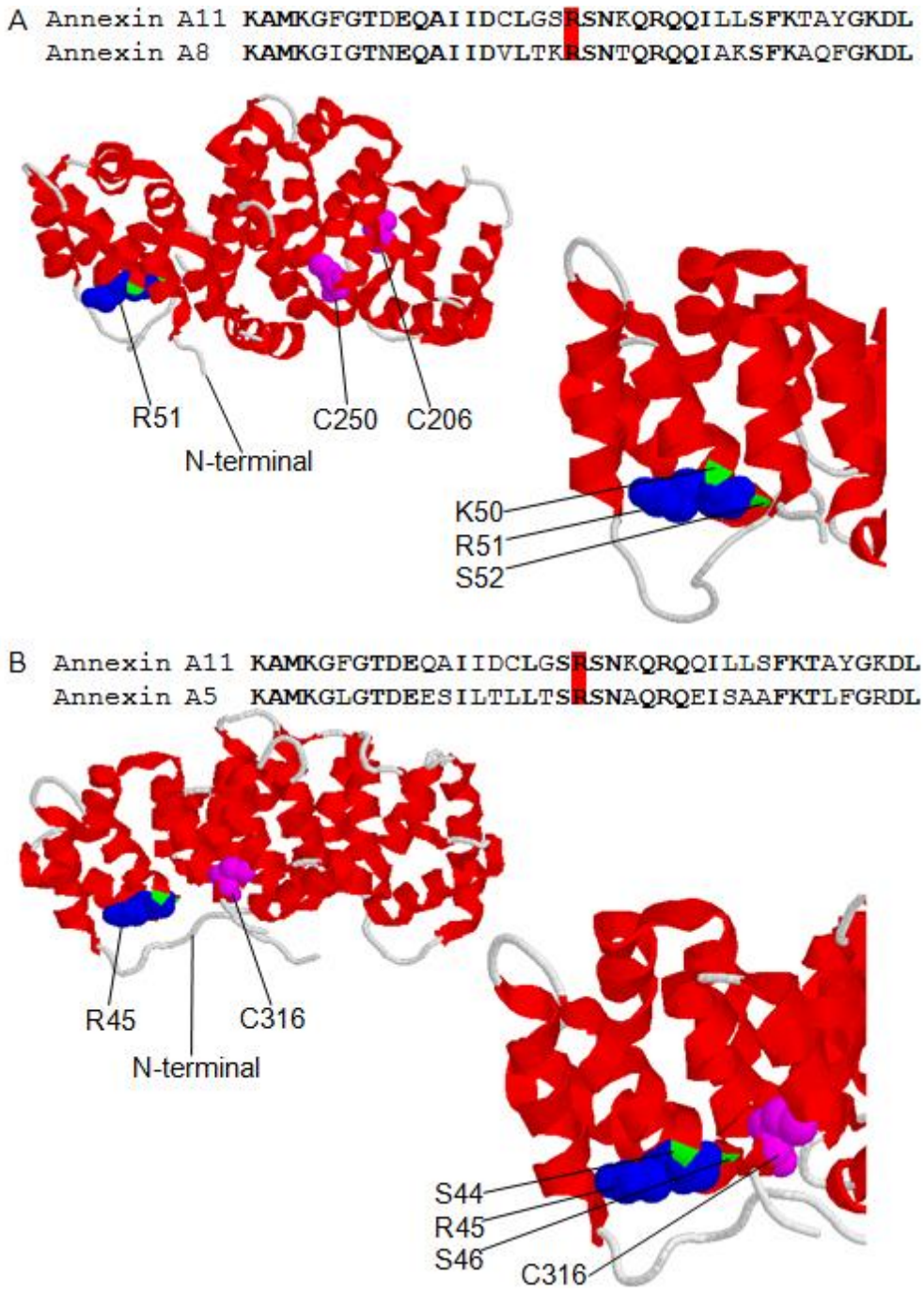

Figure 17 Crystal Structure Analysis of Annexin A8 and A5

The crystal structures of annexin A8 **(A)** and annexin A5 **(B)** were modelled in RasMol (Version 2.6). The arginine which is mutated in annexin A11^{R230C} is conserved between annexin A5 and A8 and is depicted in the crystal structures in blue. Residues either side of the arginine are shown in green. Cysteine residues which are conserved between annexin A11 and annexin A5 or annexin A8 are shown in magenta. The crystal structure of annexin A8 depicted, highlights conserved residues R50, S51, C206 and C250 and unconserved R44. The crystal structure of annexin A5 depicted, highlights conserved residues S44, R45, S46 and C316. The residues highlighted in annexin A5 and A8 are within the first annexin repeat, shown in the corresponding amino acid codes which have been aligned against annexin A11 - conserved residues (bold), mutation associated arginine (red box).

Disulphide bridge formation would only be possible in the endoplasmic reticulum or the extracellular environment, where a sufficiently oxidising milieu is present. Interestingly, annexin A11 has been shown to be secreted by activated neutrophils [227], although it does not contain a recognised secretion signal. This is in common with other annexins, such as annexins A1 and A2, which are also known to be secreted and lack known secretion signals [228,229]. Therefore under certain conditions annexin A11 may indeed be secreted. Furthermore autoantibodies against annexin A11 have been detected in several autoimmune diseases [216], suggesting that annexin A11 is released into the extracellular environment at some point, whether through secretion or perhaps following cell death. In sarcoidosis therefore, the presence of annexin $A11^{R230C}$ extracellularly may be of equal or greater importance than any intracellular role it plays. Conformational changes that could arise intracellularly may involve the N-terminal domain. Structural analysis of annexin A5 shows that the conserved arginine, which is mutated in annexin $A11^{R230C}$, lies in close proximity to the N-terminus (Figure 17B). This residue may therefore be involved in interactions with the N-terminus, and a switch from a basic arginine to a polar cysteine may disrupt or alter such interactions.

The speculations inferred from the crystal structures of annexins A5 and A8 provide some insight into how the tertiary structure of annexin A11 may be affected and also contribute to the predictive model of annexin A11 (produced by [230]). This model depicts the positions of cysteine residues within annexin A11 relative to the arginine at residue 230 (Figure 18A). Annexin A11 is strikingly rich in cysteines, relative to the other vertebrate annexins, and contains a total of six cysteines (Figure 18A). Mutation of residue 230 from an arginine to a cysteine is not predicted to grossly affect the 3D structure of annexin A11 (Figure 18B), though slight changes in the angles of the helices and loops cannot be ruled out. In annexin $A11^{R230C}$ the cysteine at residue 230 is in closest proximity to the cysteine at residue 226. However their sulphur head groups appear to be positioned away from each other, making disulphide bridge formation sterically difficult. As this is a predictive model this does not categorically rule out the suggestion made previously, from analysis of the crystal structure of annexin A5, that intramolecular disulphide bridges could form. However this model does not favour this scenario. A more likely outcome of intermolecular disulphide bridge formation is still possible, as the additional cysteine residue in annexin $A11^{R230C}$ may be better placed to interact with any of the six or seven other cysteines within annexin $A11^{WT}$ or annexin $A11^{R230C}$ molecules that are in close enough proximity.

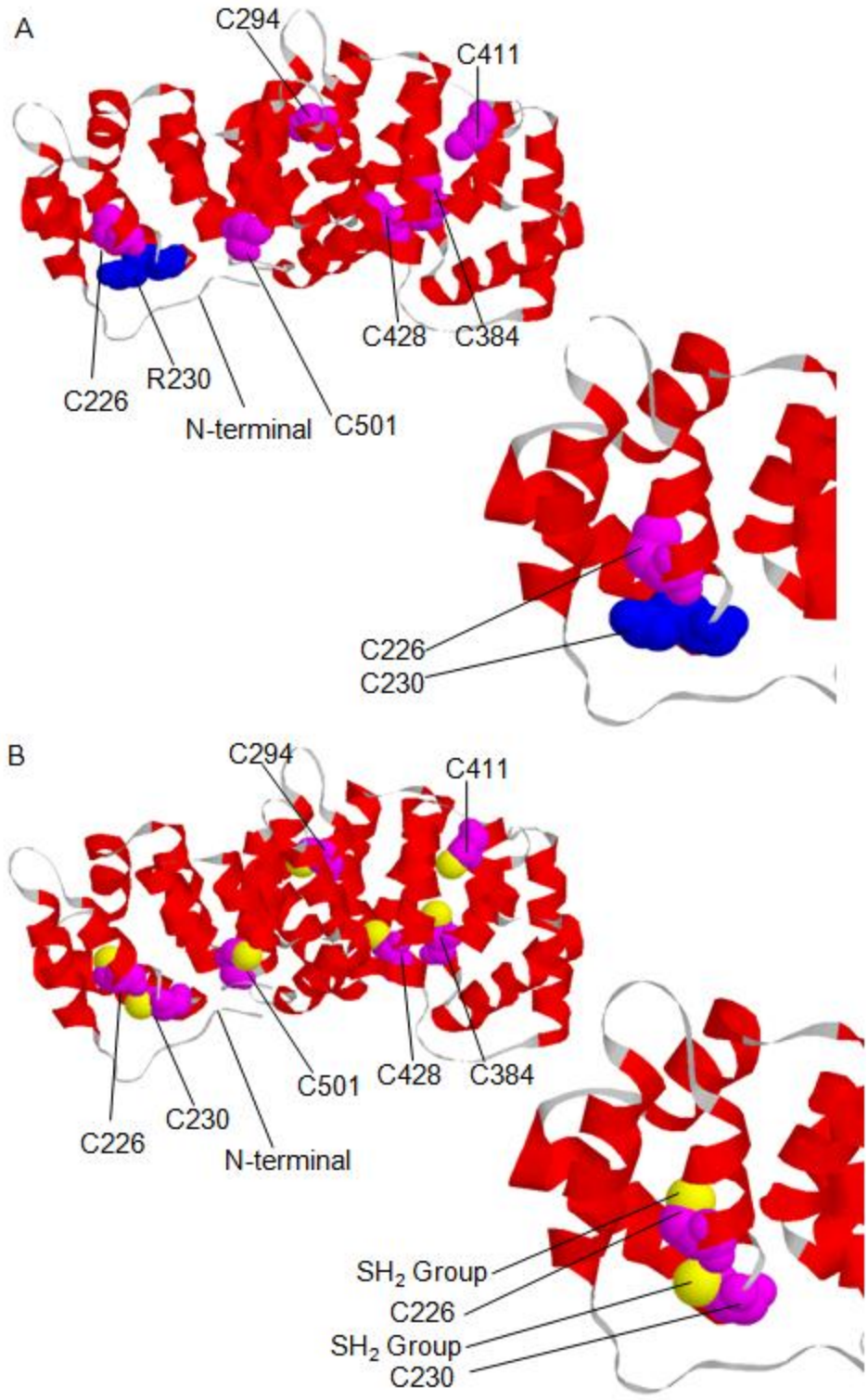

Figure 18 Predictive Model of Annexin A11^{WT} and Annexin A11^{R230C}

The models of annexin A11^{WT} **(A)** and annexin A11^{R230C} **(B)** were calculated (EMBL) and modelled in RasMol (Version 2.6). The arginine at residue 230 in annexin A11^{WT} is highlighted in blue. Cysteine residues are highlighted in magenta. In annexin A11^{R230C} the sulphydyrl groups of these residues are depicted in yellow.

If structural changes do occur in annexin A11^{R230C}, it is not clear whether these would be sufficient to result in functional effects. It is possible that although the mutation identified in annexin A11 is strongly associated with sarcoidosis, susceptibility to the disease and cellular dysfunction requires the complete haplotype to be present. This includes five other non-coding single nucleotide polymorphisms surrounding the R230C mutation, which were also validated as being strongly associated with sarcoidosis [193]. There are a large number of other SNPs within annexin A11, with 414 results listed on the NCBI SNP search, however only the R230C mutation has been linked to disease, with the remaining SNPs having no known function.

Future studies into annexin A11^{R230C} should focus on the role of this mutation in cell types more relevant to the disease, such as cells of the immune system. For example macrophages and monocytes which form part of the granulomas themselves [206], CD4 positive T cells which increase in number in the lungs of sarcoid patients [231] and CD8 positive T cells and CD19 positive B cells which strongly down-regulate expression of annexin A11 upon activation [193], suggesting a particular role for this protein in these cells. It may also be of importance to examine the role of annexin A11^{WT} and annexin A11^{R230C} in cells and tissues of the organs most affected by sarcoidosis, such as the lungs and skin.

Chapter Four:
Study of Annexin A11 and the Motor Protein CHO1 During Mitosis

4. Results: Study of Annexin A11 and the Motor Protein CHO1 During Mitosis

CHO1 is a plus end directed motor protein with orthologues in both vertebrates, such as pavarotti in *Drosophila melanogaster* [169] and invertebrates, such as zen-4 in *Caenorhabditis elegans* [170]. These proteins all belong to the kinesin-6 family and are known to interact with proteins involved in the cell cycle, such as the polo-like kinase Plk1 [232], the Aurora kinase AIR-2 [233] and the Rho GAP cyk-4 [234]. CHO1 was initially identified in Chinese Hamster Ovary cells by the immunisation of mice with CHO mitotic spindle components. One of the monoclonal antibodies produced bound to the spindles and midbodies in cultured mammalian cells [235]. This antibody, cho1, recognised the subsequently named protein CHO1.

CHO1 is a 105kDa protein consisting of three domains; an N-terminal motor domain, an alpha helical coiled-coil stalk domain and a C-terminal tail domain (Figure 19) [236]. It is capable of cross-linking anti-parallel microtubules *in vitro* [171]. CHO1 contains both ATP-dependent and ATP-independent microtubule binding sites within its motor domain. Furthermore, the N terminal domain co-sediments with taxol-stabilised microtubules [237]. CHO1 also contains an F-actin interacting domain within its tail, making it unique amongst kinesin-6 family members. It is the alternatively spliced exon 18 which is responsible for this domain in CHO1 and results in a 100 amino acid stretch within its tail domain which is absent in full length human MKLP1 [177].

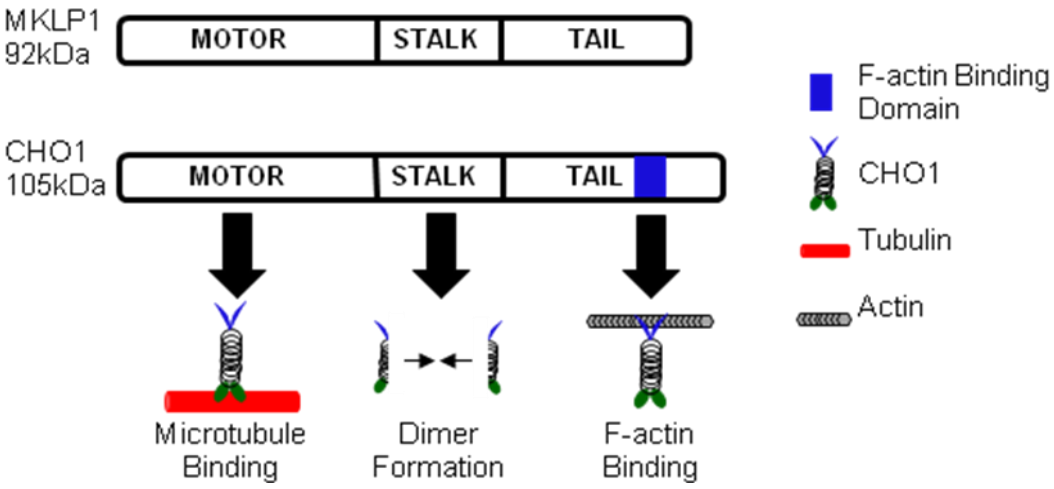

Figure 19 MKLP1/CHO1 Structure and Function

Both MKLP1 and CHO1 comprise three domains; a motor domain which binds microtubules, a stalk domain which dimerises the protein and a tail domain. CHO1 differs from MKLP1 in its tail domain, due to the alternative splicing of exon 18 of the MKLP1 gene. The translation of this exon in CHO1 provides CHO1 with an F-actin binding domain. This property makes CHO1 unique amongst this family of kinesins.

Mutation of the ATP-binding site in the motor domain of CHO1, or antibody blockade of the F-actin interacting domain, both disrupt cytokinesis [177,178]. In both cases furrow ingression is initiated but separation of the daughter cells fails, resulting in the two cells fusing back together to form binucleates. This phenotype also occurs in cells depleted of CHO1 using siRNA, with the additional loss of the midbody matrix [238].

It has been shown that the dynamic expression patterns of both CHO1 and annexin A11 during the cell cycle are strikingly similar [146]. Both localise to the nucleus of interphase cells, then to the spindle poles, spindle midzone and finally midbody as the cell cycle progresses (Figure 20). CHO1 also shows a high degree of co-localisation from anaphase onwards with other proteins that target to the midbody. These include INCENP (Inner Centromere Protein) [239] which is part of the chromosomal passenger complex and Plk1 (Polo-like kinase 1) [232]. CHO1 does not appear to interact with INCENP, but does bind Plk1 [232].

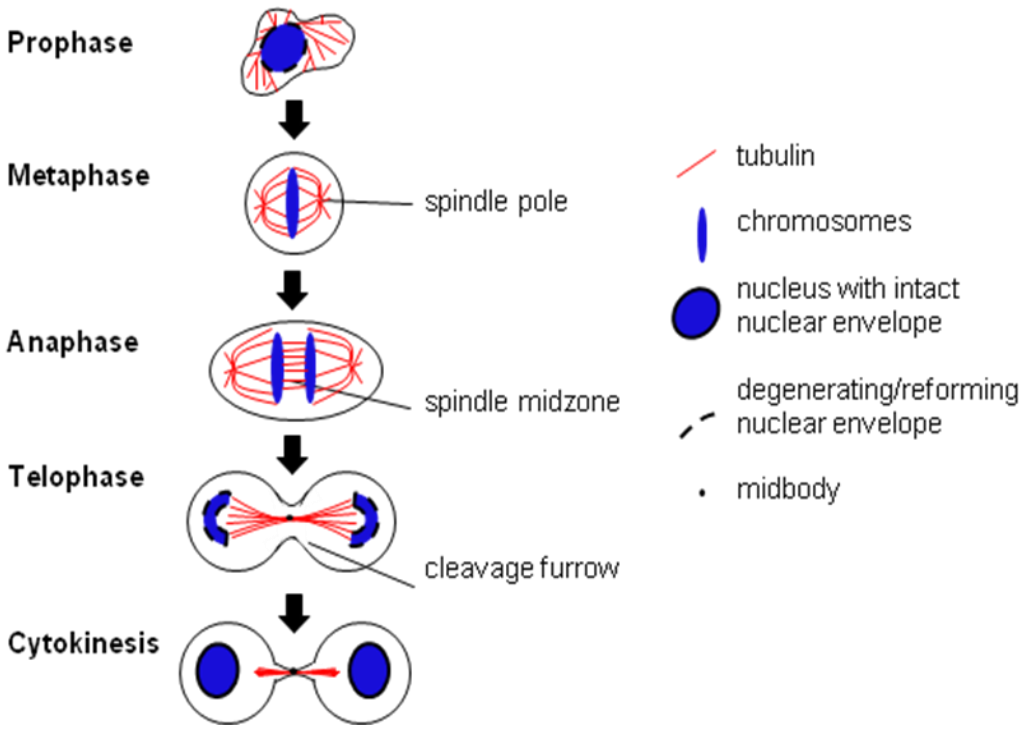

Figure 20 Cell Cycle Progression

Mitosis begins with prophase, where the nuclear envelope of the cell degenerates and the DNA contained within the nucleus begins to condense into chromosomes. At metaphase the microtubule network reassembles to form the mitotic spindle, emanating from the spindle poles towards the cell equator. The chromosomes line up at the cell equator and attach to the plus ends of the spindle microtubules. At anaphase, as the spindle elongates, the sister chromatids are pulled apart. As the cell progresses from anaphase to telophase the spindle midzone becomes compacted into the forming cleavage furrow. At the centre of this furrow resides the protein dense midbody matrix. At cytokinesis, karyokinesis completes and the nuclear envelope regenerates. The furrow continues to regress until membrane abscission occurs resulting in the separation of the two daughter cells.

The strong co-localisation of CHO1 and annexin A11 throughout the cell cycle was further investigated. Immunoprecipitation of annexin A11 uncovered an interaction with CHO1, specifically at cytokinesis [146]. It is thought that this interaction could facilitate the completion of cytokinesis, following actomyosin ring disassembly and central spindle separation – a point at which it is suggested that the plasma membrane would need to be tightly bound to midbody microtubules [150,177]. CHO1 alone, which binds microtubules, is unlikely to fulfil this role as there is no evidence of it being able to also bind the plasma membrane. It has however been suggested that annexin A11, with its ability to bind phospholipids *and* the midbody matrix via CHO1, could facilitate this association [146,150].

4.1 Annexin A11 Distribution During the Cell Cycle in PFA Fixed Cells

The distribution of annexin A11 in cells at interphase has been characterised in a variety of cell lines [140,146,147,149,150], where it has been shown to have both a nuclear and cytoplasmic distribution. In addition, it localises to the cell membrane in confluent monolayers of epithelial cells [146].

During the cell cycle however this distribution changes significantly [150]. Immunofluorescence analysis in both transformed A431 cells (Figure 25) and non-transformed, spontaneously immortalised ARPE19 cells (Figure 21) confirms this pattern. Annexin A11 localisation was followed during the cell cycle by using confocal immunofluorescence microscopy of PFA fixed cells. DNA and α tubulin staining were used to determine the position of cells within the cell cycle.

At prophase annexin A11 localises to the degenerating nuclear envelope (Figure 25). At metaphase annexin A11 can be found diffusely distributed throughout the cytoplasm (Figure 25) or additionally localised to the cell membrane with a slight accumulation at the spindle poles (Figure 21). Both of these localisations were observed in all three of the cell lines investigated (HeLa, A431, ARPE19), without an apparent preference for either state. These different distributions may therefore reflect two separate phases during metaphase, for example early and late. At anaphase annexin A11 is consistently localised to the spindle midzone. Upon closer inspection it appears to cap the plus ends of central spindle microtubules (Figure 26). By telophase and cytokinesis it concentrates at the midbody, a protein dense structure located in the middle of the cleavage furrow. This midbody localisation is consistent in several cell lines (Figure 22A-C). However, this was not observed for other annexins (Figure 22D and E), namely annexin A2 and annexin A7 - annexin A7 being the most closely related to annexin A11.

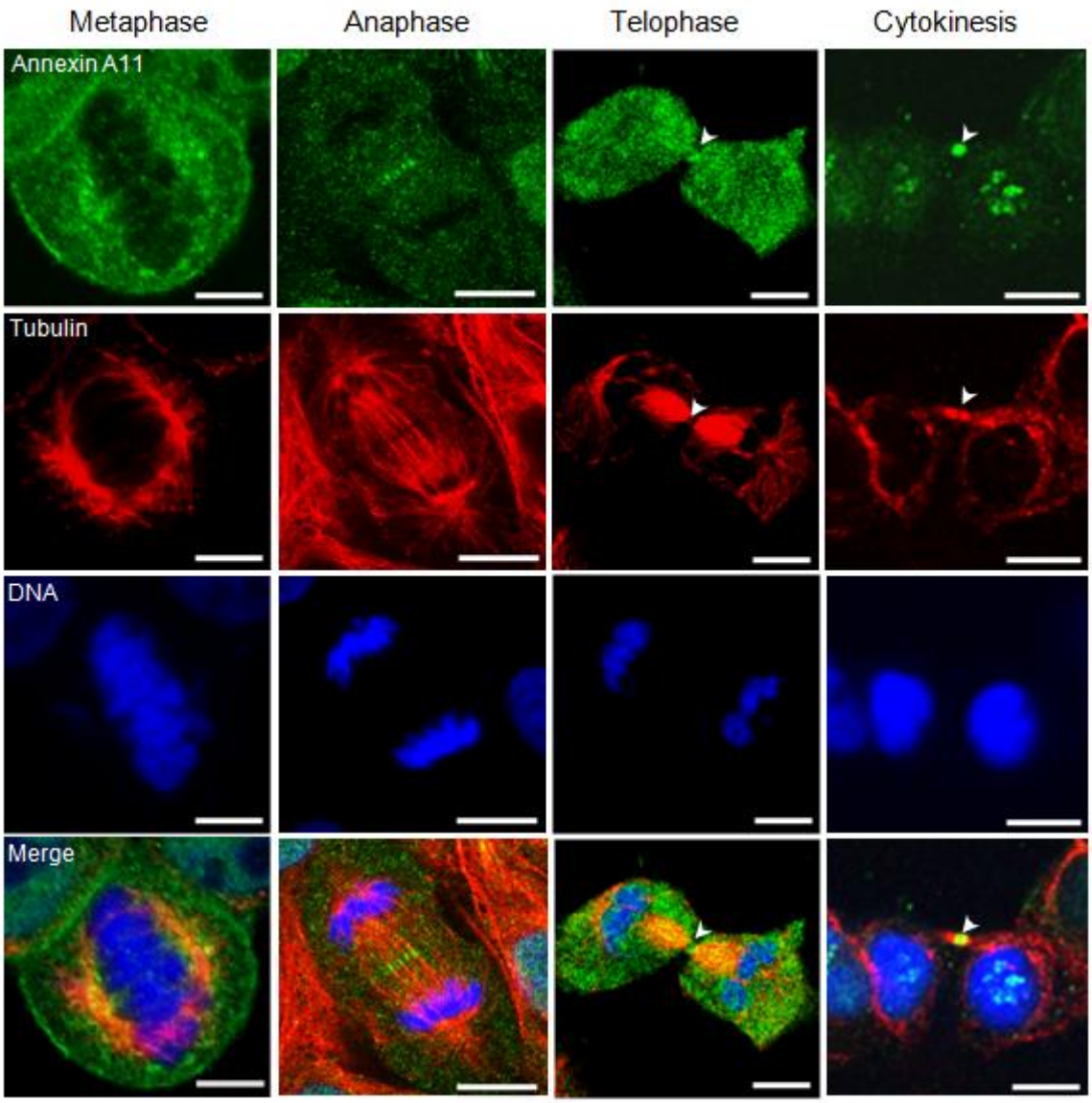

Figure 21 Annexin A11 Localisation During the Cell Cycle in ARPE19 Cells

ARPE19 cells were fixed in 4% PFA and stained for annexin A11 using a polyclonal goat anti-annexin A11 antibody (1/50 dilution), tubulin using a monoclonal mouse anti-alpha tubulin antibody (1/100 dilution) and DNA using DAPI (1/500 dilution). Location of midbody (arrowhead). (Scale Bars 10µm)

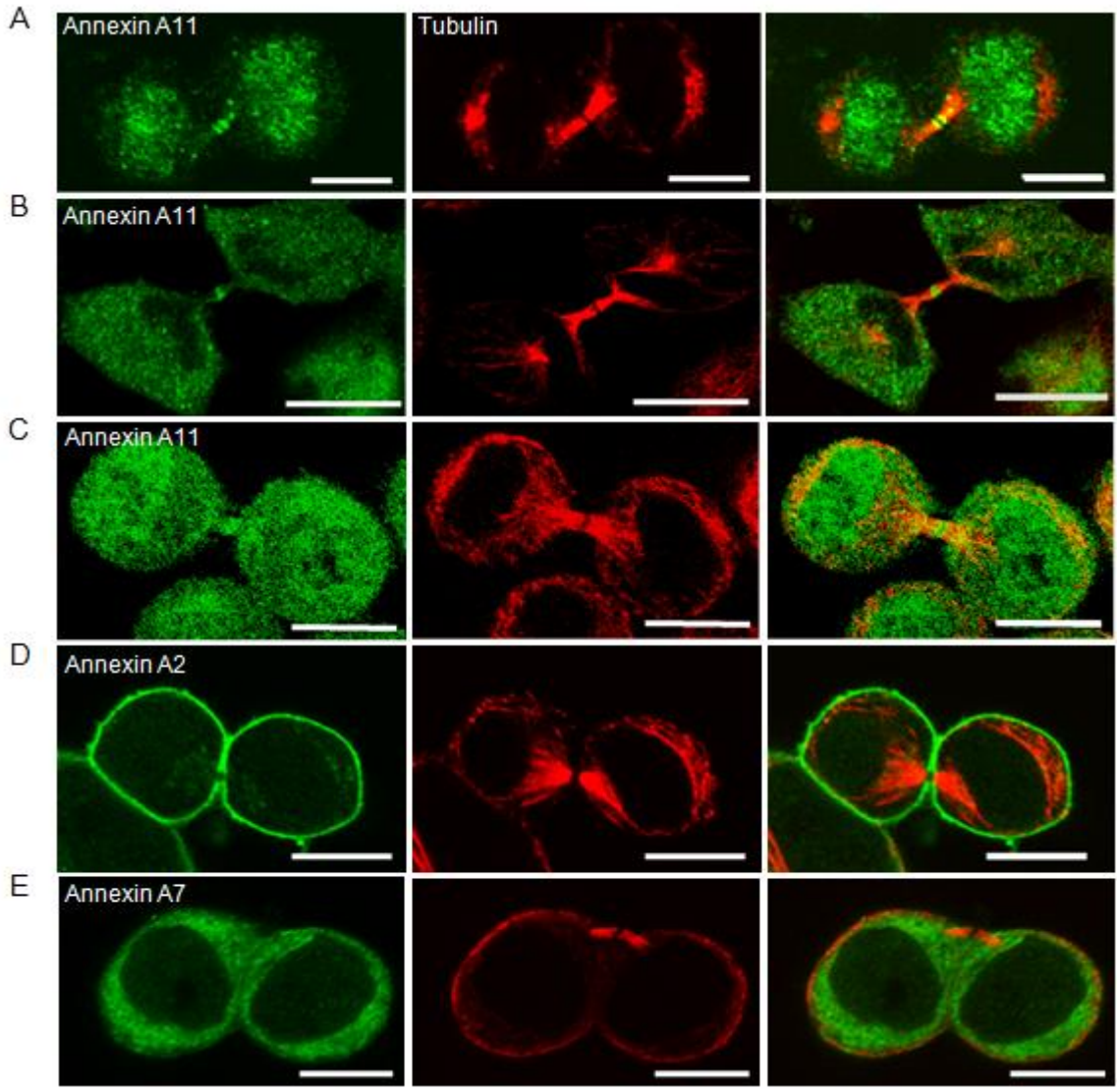

Figure 22 Annexin A11 Localises to the Midbody in Several Cell Lines

Annexin A11 is present at the midbody during cytokinesis in **(A)** A431, **(B)** ARPE19 and **(C)** HeLa cells. **(D)** Annexin A2 in A431 cells is not present at the midbody. **(E)** Annexin A7 in HeLa cells is not present at the midbody. All cells were fixed in 4% PFA. Cells were stained for tubulin using a monoclonal mouse anti-alpha tubulin antibody (1/100 dilution) and either annexin A11 using a polyclonal goat anti-annexin A11 antibody (1/50 dilution), or annexin A2 using a polyclonal rabbit anti-annexin A2 antibody (1/60 dilution) or annexin A7 using a polyclonal goat anti-annexin A7 antibody (1/50 dilution). (Scale Bars 10µm)

The intracellular targetting of the different domains of annexin A11 to the midbody was investigated through the overexpression of GFP tagged annexin A11 constructs in A431 cells. Both full length annexin A11 and its truncated forms, comprising either the C terminal or N terminal domains, localised to the midbody (Figure 23A-C). GFP alone when expressed at low levels did not localise to the midbody (Figure 23D). This was further illustrated graphically by taking line scans through the length of the cleavage furrow, in order to detect the GFP and tubulin signals in this particular region. In all four cases the tubulin signal is seen to drop at the point where the midbody is localised (Figure 24A–D). In the cases of GFP tagged full length annexin A11 and its truncated forms (Figure 24A-C), this drop in tubulin signal is concurrent with a peak in GFP signal. This peak in GFP signal was not seen with the low expression of GFP alone. However increased expression of GFP did result in targeting to the midbody (Figure 23E and 24E). Therefore expression to sufficient levels of the GFP tag alone can result in midbody targeting.

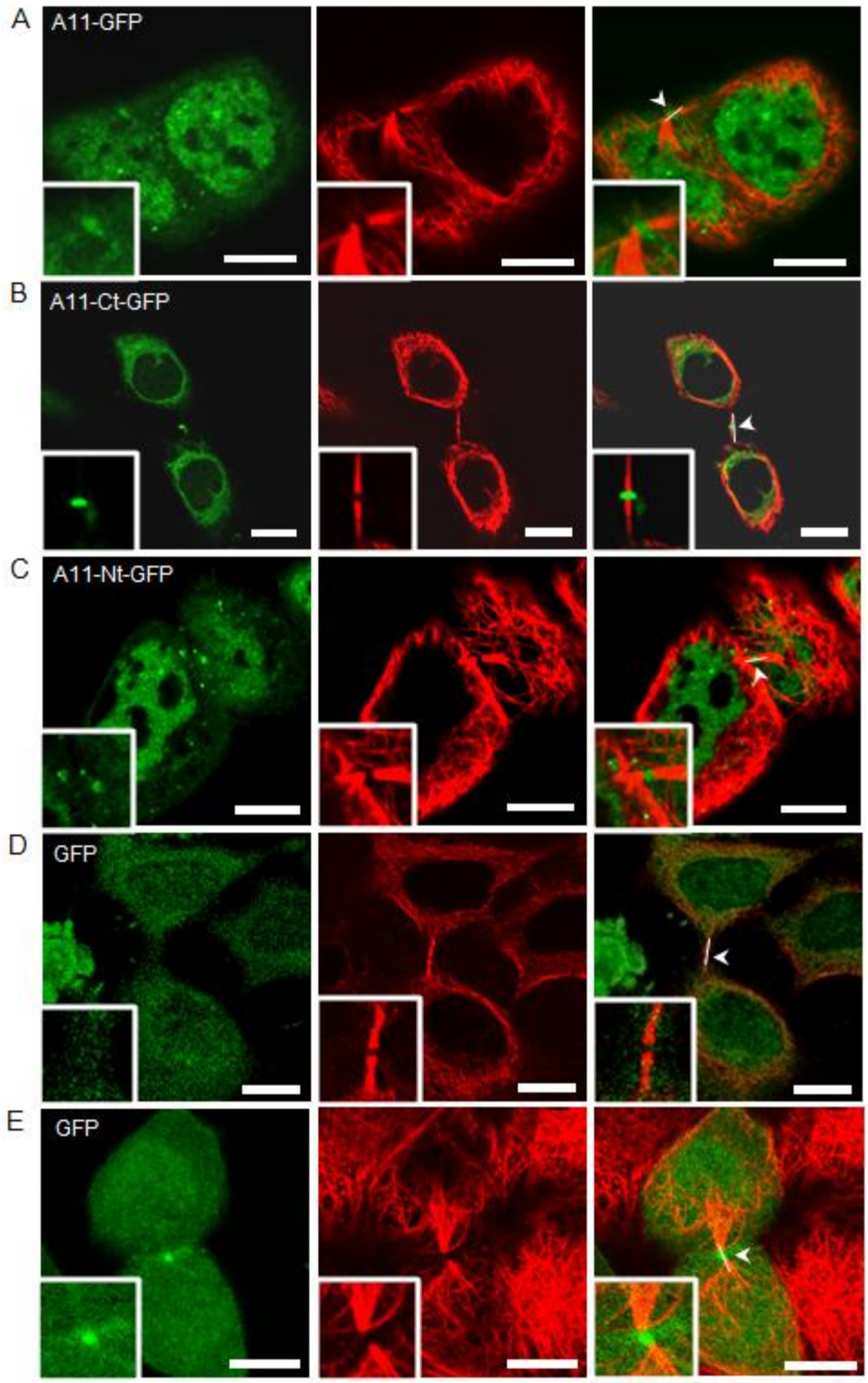

Figure 23 Localisation of Annexin A11-GFP Constructs in A431 Cells at Cytokinesis

Expression of **(A)** A11-GFP, **(B)** A11-C-terminal-GFP, **(C)** A11-N-terminal-GFP and **(D, E)** GFP in A431 cells. Cells were transfected with 3µg of plasmid DNA and incubated overnight, prior to fixation in 4% PFA. Cells were stained for tubulin using a monoclonal mouse anti-alpha tubulin antibody (1/100 dilution). Arrows point to midbodies. White lines denote where line scans were taken (See Figure 24) (Scale Bars 10µm)

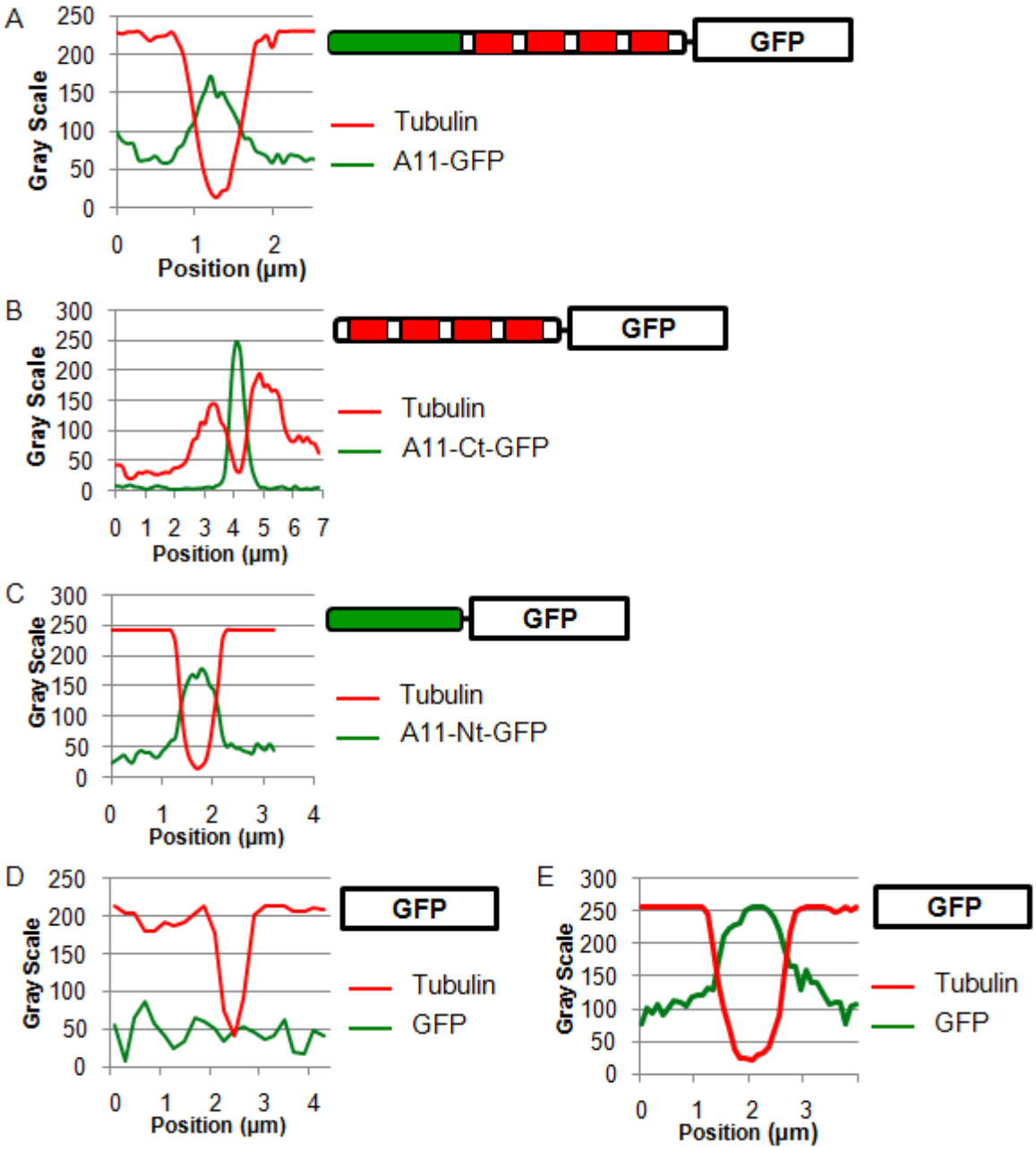

Figure 24 Line Scans of the Localisation of Annexin A11-GFP Constructs in A431 Cells at Cytokinesis

Graphs corresponding to line scans in Figure 23 (white line in merges of Figure 23 (A) – (E)) taken through the midbody (arrow head in merges of Figure 23 (A) – (E)) of A431 cells at cytokinesis expressing **(A)** A11-GFP, **(B)** A11-C-terminal-GFP, **(C)** A11-N-terminal-GFP and **(D, E)** GFP. Cells were transfected with 3µg of plasmid DNA and incubated overnight, prior to fixation in 4% PFA. Cells were then stained for tubulin using a polyclonal mouse anti-tubulin antibody (1/100 dilution).

4.2 Annexin A11 and MKLP1/CHO1 Distribution during the Cell Cycle in PFA Fixed Cells

CHO1 is a plus end directed motor protein, belonging to the MKLP1 (mitotic kinesin like protein 1) family of mitotic kinesins. In humans both CHO1 and MKLP1 are co-expressed. CHO1 is a splice variant of MKLP1 containing an additional 100 base pairs in its C terminal domain, derived from the alternative splicing of exon 18 which is not expressed in the truncated MKLP1 variant. This domain is responsible for the additional ability of CHO1 to bind F-actin, unlike MKLP1. Current commercially available antibodies are not able to distinguish between the two isoforms. Therefore both MKLP1 and CHO1 have been immunostained, without any differentiation between the two isoforms.

Previous work has shown that CHO1 co-localises with annexin A11 consistently throughout the cell cycle [150]. Immunostaining using an anti-MKLP1 antibody and an anti-annexin A11 antibody in PFA fixed A431 cells, shows that annexin A11 and MKLP1/CHO1 co-localise at several points during the cell cycle. Annexin A11 and MKLP1/CHO1 co-localise at the degenerating nuclear envelope at prophase, at the spindle midzone at anaphase and at the midbody at telophase and cytokinesis (Figure 25). At anaphase, unsurprisingly for a plus end directed motor protein, MKLP1 appears to specifically cap the plus ends of the midzone microtubules, where annexin A11 also accumulates (Figure 26). At metaphase MKLP1/CHO1 is consistently diffuse throughout the cytoplasm, whilst annexin A11 can be found diffusely distributed in the cytoplasm (Figure 25) *or* also partially localised to the spindle poles (Figure 21). In either instance the localisation of annexin A11 at metaphase does not appear to co-localise with MKLP1/CHO1.

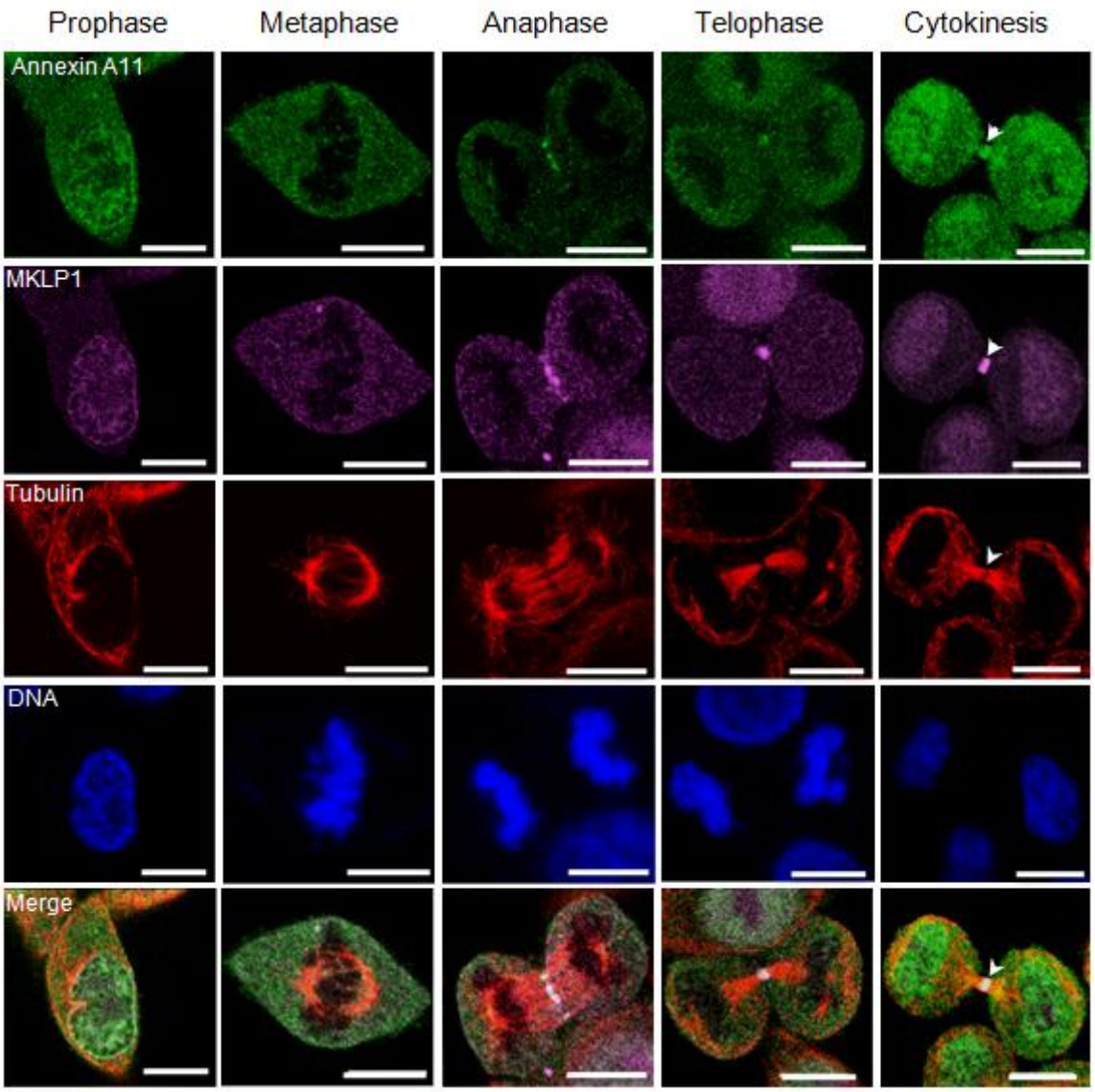

Figure 25 Annexin A11 and MKLP1 Co-localise During the Cell Cycle in A431 Cells Fixed Using PFA

Cells were fixed in 4% PFA and stained for annexin A11 using a polyclonal goat anti-annexin A11 antibody (1/50 dilution), tubulin using a monoclonal mouse anti-alpha tubulin antibody (1/100 dilution), MKLP1 using a polyclonal rabbit anti-MKLP1 antibody (1/100 dilution) and DNA using DAPI (1/500 dilution). (Scale Bars 10µm)

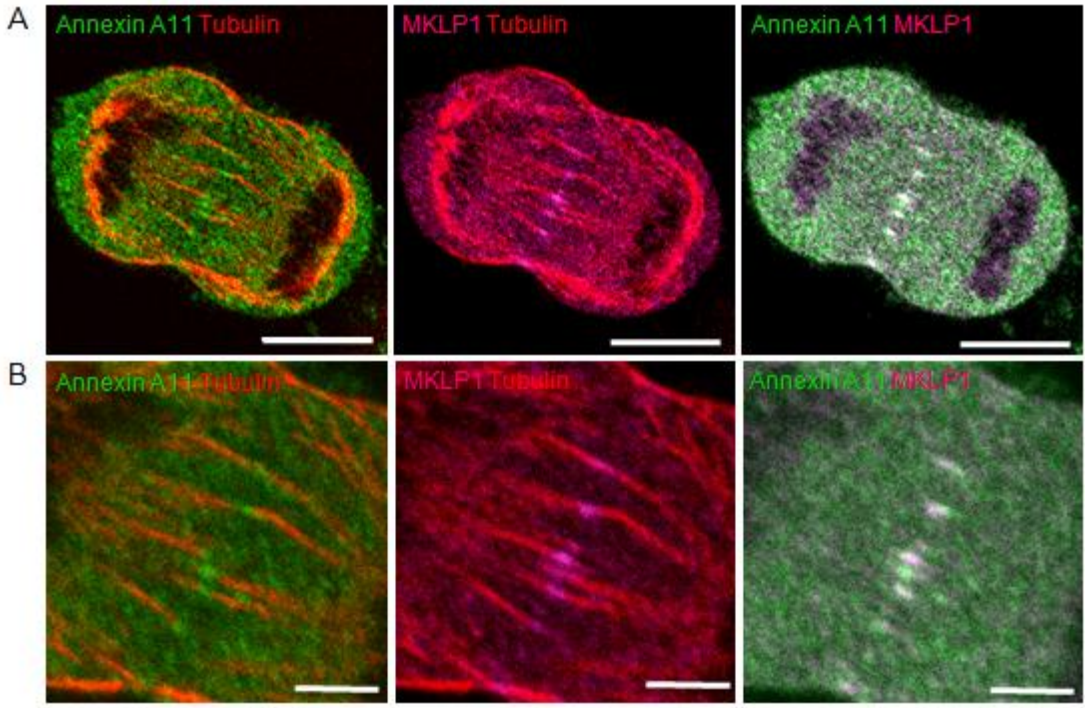

Figure 26 Annexin A11 and MKLP1 Co-localise at Anaphase at Microtubule Plus Ends In HeLa Cells Fixed Using PFA

(A) HeLa cell at anaphase (Scale Bar 10µm) **(B)** HeLa cell at anaphase magnified (Scale Bar 3µm). HeLa cells were fixed in 4% PFA and stained for annexin A11 using a polyclonal goat anti-annexin A11 antibody (1/50 dilution), tubulin using a monoclonal mouse anti-alpha tubulin antibody (1/100 dilution), MKLP1 using a polyclonal rabbit anti-MKLP1 antibody (1/100 dilution) and DNA using DAPI (1/500 dilution).

4.3 Annexin A11 and MKLP1/CHO1 Distribution during the Cell Cycle in Methanol Fixed Cells

The distribution of annexin A11 and MKLP1/CHO1 has only been examined in PFA fixed cells. However it is well known that methanol fixation can produce different staining patterns, in particular with regard to tubulin and tubulin associated proteins. PFA fixation works by cross-linking proteins, whereas methanol fixation works by dehydrating the cell and simultaneously denaturing the proteins. PFA fixation at room temperature occurs at a slower rate than methanol fixation at -20°C, resulting in increased levels of microtubule depolymerisation caused by the dynamic instability of the tubulin filaments. This is due to the dramatic decrease in GTP levels once the cell is permeabilised, which affects not only the immunostaining of microtubules but also of proteins bound to microtubules, such as MKLP1/CHO1.

Methanol fixation revealed an enhanced staining pattern for both annexin A11 and MKLP1/CHO1 during the cell cycle, which was consistent at all stages of mitosis imaged (Figure 27). This is most strikingly seen at metaphase, when both annexin A11 and MKLP1/CHO1 invariably co-localise to the entire length of the mitotic spindle, including the spindle poles. At anaphase annexin A11 localises to the spindle midzone and also the length of the midzone microtubules. MKLP1/CHO1 however is restricted to the spindle midzone alone, where it co-localises with annexin A11. At telophase and cytokinesis, both proteins co-localise strongly to the midbody. However whilst MKLP1/CHO1 is restricted to this structure, annexin A11 is present throughout the cleavage furrow in a manner that appears coincident with the microtubules.

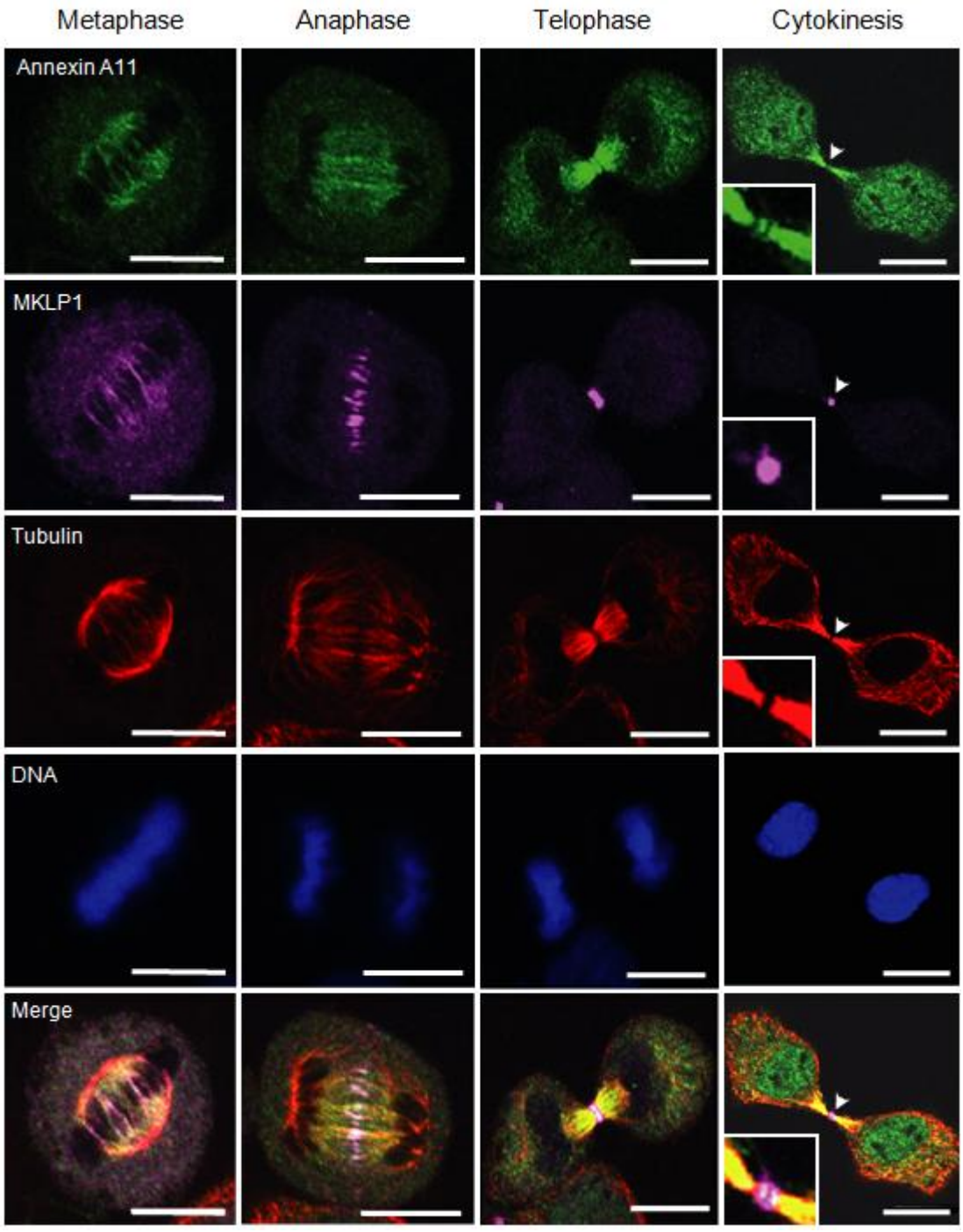

Figure 27 Annexin A11 and MKLP1 Co-localise during the Cell Cycle in HeLa Cells Fixed Using Methanol

HeLa cells were fixed in methanol and stained for annexin A11 using a polyclonal goat anti-annexin A11 antibody (1/50 dilution), tubulin using a monoclonal mouse anti-alpha tubulin antibody (1/100 dilution), MKLP1 using a polyclonal rabbit anti-MKLP1 antibody (1/100 dilution) and DNA using DAPI (1/500 dilution). (Scale Bars 10µm)

4.4 Annexin A11 and CHO1 Interaction

Given the strong colocalisation of annexin A11 and MKLP1/CHO1, alongside previous data suggesting an interaction [150], immunoprecipitations and GST pulldowns were conducted to determine whether A11 and CHO1 interact. As the interaction between these two proteins was thought to occur at cytokinesis, cells were first subjected to synchronisation. Two main methods were utilised; monastrol and thymidine-nocodazole.

Monastrol is a cell permeable, 1,4-dihydropyrimidine-based compound which inhibits Eg5 kinesin by binding to its motor domain [240]. Eg5 kinesin is a minus-end directed motor protein which binds microtubules and plays a role in assembling the mitotic spindle. Inhibition of this kinesin by monsatrol prevents centrosome separation, resulting in the production of mono-astral spindles (Figure 28A).

Thymidine is a pyrimidine deoxynucleoside which inhibits DNA synthesis, resulting in an S phase block. Following thymidine treatment the next stage of synchronisation involved arresting the cells at prometaphase. The carbamate, nocodazole, achieves this by binding β tubulin subunits to prevent tubulin polymerisation. Cells are therefore unable to pass the spindle assembly checkpoint. Recovery from nocodazole treatment is rapid, so following several PBS washes fully formed mitotic spindles can be seen after the cells were fixed (Figure 28B).

Following release from prometaphase arrest, both methods produced similar levels of synchronisation, with cells enriched at cytokinesis after about 1 hour (Figure 28C). However the thymidine-nocodazole method was chosen, as this is both a less expensive and more specific method of synchronisation. Although monastrol is not known to inhibit other kinesins [241], it may inhibit other proteins due to the high concentrations it must be used at, so producing unknown non-specific effects.

Cytokinesis-enriched cell lysates were used to perform immunoprecipitations and annexin A11-GST pull-downs. Annexin A11-GST was purified from bacteria following IPTG induction over several hours, as described in Materials and Methods 2.12 (Figure 29A). The GST fused annexin A11 was then purified from the bacterial lysate using glutathione beads, with which synchronised cell lysates were incubated. However it was not possible to detect MKLP1/CHO1 in annexin A11-GST pull-downs (Figure 29B).

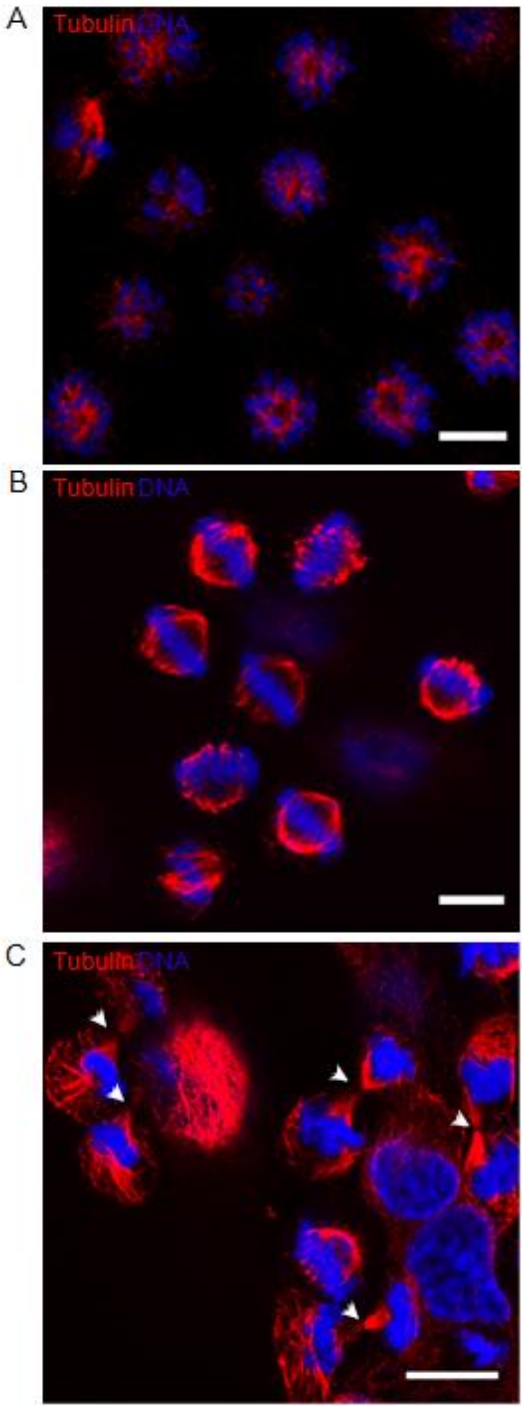

Figure 28 Synchronisation of HeLa Cells Using Thymidine, Nocodazole and Monastrol

HeLa cells cultured in media containing **(A)** 100µM monastrol for 16h or **(B)** 5mM thymidine overnight, followed by 100 ng/ml nocodazole for 7h. Both treatments result in a prometaphase block in the majority of cells. **(C)** 1h post release into normal media (DMEM, 10% FCS and antibiotics) from treatment in (B). Cells at cytokinesis marked by their cleavage furrows (arrowheads). All cells were fixed in 4% PFA and then stained for tubulin using a monoclonal mouse anti-alpha tubulin antibody (1/100 dilution) and DNA using DAPI (1/500 dilution). (Scale Bars 10µm)

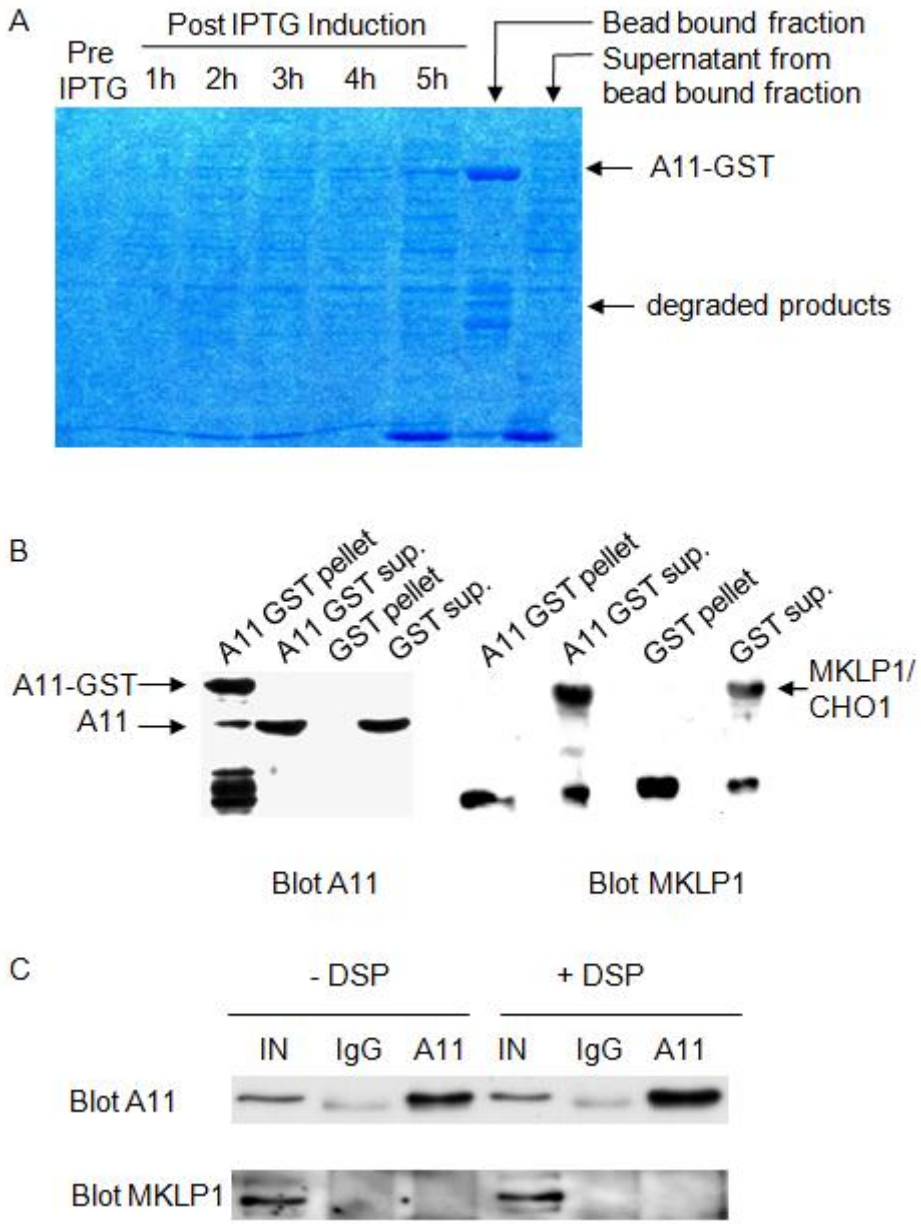

Figure 29 Annexin A11 and CHO1 Cannot Be Shown to Interact

(A) Coumassie stain of an SDS-PAGE gel containing annexin A11-GST production samples from bacterial lysates of BL21 *E.coli* transformed with plasmid DNA encoding annexin A11-GST. **(B)** Western blots of an annexin A11-GST pull-down using HeLa whole cell lysates from cells synchronised at cytokinesis, in the presence of 200µM calcium. Annexin A11 was blotted for using a polyclonal goat anti-annexin A11 antibody (1/200 dilution) and MKLP1 using a polyclonal goat anti-MKLP1 antibody (1/200 dilution) made up in 8% milk **(C)** Western blots of an annexin A11 immunoprecipitation using A431 whole cell lysates from cells synchronised at cytokinesis and treated with or without DSP. 1µg of polyclonal goat anti-annexin A11 antibody was used for immunoprecipitation of annexin A11. Annexin A11 was blotted for using a monoclonal mouse anti-annexin A11 antibody (1/1000 dilution) and MKLP1 using a polyclonal goat anti-MKLP1 antibody (1/200 dilution). IN (whole cell lysate input).

As an alternative strategy, annexin A11 immunoprecipitations were carried out in order to avoid the use of GST tagged annexin A11, which may disrupt interactions by altering tertiary structures. Initial immunoprecipitations from cytokinesis-enriched cell lysates also failed to pull down detectable MKLP1/CHO1 (Figure 29C). In order to strengthen a possibly weak interaction, immunoprecipitations were repeated using the chemical cross-linker DSP. DSP creates disulphide bridges between cysteines of interacting proteins. CHO1 however was also not pulled down with annexin A11 using this technique (Figure 29C).

Despite the apparent absence of CHO1 in these pulldown experiments, other proteins were pulled down upon annexin A11 immunoprecipitation, in both unsynchronised and synchronised cells (Figure 30A). In unsynchronised cells a protein band at approximately 37kDa was present and in synchronised cells two bands at approximately 37kDa and 65kDa were present. In all three cases these bands did not appear in the control IgG immunoprecipitates and they appeared stronger upon DSP treatment. However as these bands could be the result of non-specific antibody binding, as opposed to genuine protein-protein interactions with annexin A11, a known interaction was tested – that of annexin A11 and ALG2. In this case the immunoprecipitation of annexin A11, from cells stimulated with 1µM ionomycin for 10min and then treated with DSP, was able to verify this interaction (Figure 30B).

Given these findings supporting the experimental procedure used, the lack of any apparent interaction between annexin A11 and CHO1 may be due to its transient nature i.e. it may only occur during a small window of cytokinesis which was not captured. In addition, the original experiments demonstrating this interaction used a polyclonal antibody raised specifically against the CHO1 isoform [150]. However these experiments used a polyclonal antibody raised against a peptide mapping the N terminus of MKLP1. Although this suggests that the antibody would detect both MKLP1 and CHO1, one cannot be certain that the epitopes used for antibody production are accessible when the protein is embedded into the midbody or bound to annexin A11.

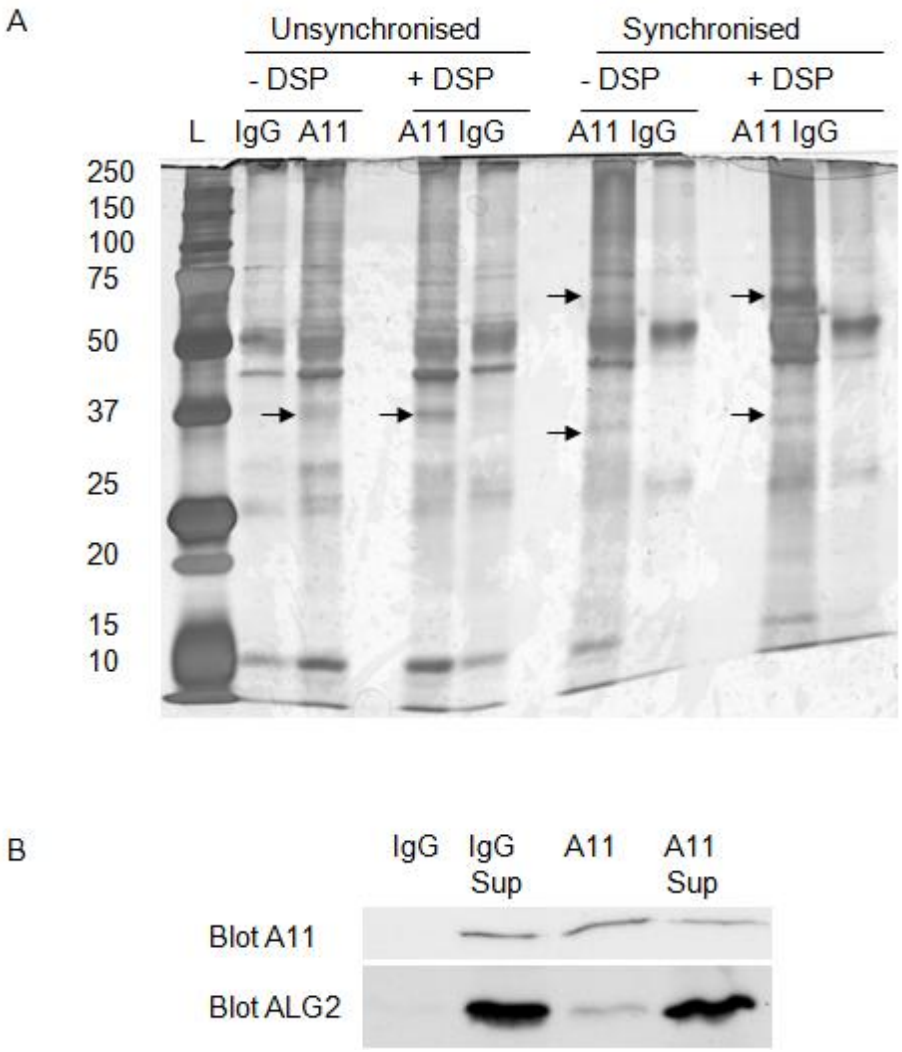

Figure 30 Annexin A11 Immunoprecipitations Pull Down Other Protein Interactors

(A) Silver stain of an SDS PAGE gel containing samples from an annexin A11 immunoprecipitation using HeLa whole cell lysates from unsynchronised cells or cells synchronised at cytokinesis, treated with or without DSP. 1µg of polyclonal goat anti-annexin A11 antibody was used for the immunoprecipitation of annexin A11. Arrows point to protein bands present in annexin A11 lanes that are absent in IgG control lanes. **(B)** Western blot of annexin A11 immunoprecipitation in A431 cells incubated in media containing 1µM ionomycin for 10min and treated with DSP. 1µg of polyclonal goat anti-annexin A11 antibody was used for the immunoprecipitation of annexin A11. Annexin A11 was blotted for using a polyclonal goat anti-annexin A11 antibody (1/200 dilution) and ALG2 using a polyclonal rabbit anti-ALG2 antibody (1/1000 dilution).

4.5 Discussion

The cell cycle distribution of annexin A11 has previously been described in tumour cells [150] and this study has confirmed these findings in several cell lines of both a transformed and a spontaneously immortalised nature. Initial experiments were conducted in cells fixed using PFA and under these conditions the metaphase localisation of annexin A11 was inconsistent. Annexin A11 either remained diffuse in the cytoplasm or showed some enrichment at the spindle poles of the mitotic apparatus. Consistency was achieved for all other stages of mitosis, where annexin A11 was detected at the degenerating nuclear envelope at prophase, the spindle midzone at anaphase and the midbody at telophase and cytokinesis.

At prophase, in PFA fixed cells, annexin A11 was shown to co-localise at the degenerating nuclear envelope with the motor protein MKLP1. The localisation of annexin A11 to this region confirms previous studies of the cell cycle [150]. Furthermore, localisation to the nuclear envelope has also been shown to occur in interphase cells, in response to a rise in intracellular calcium [147]. Such a rise in intracellular calcium is known to occur in both the cytoplasm surrounding the nucleus and in the nucleus itself just prior to nuclear envelope breakdown at prophase, as demonstrated in syncytial *Drosophila* embryos [242]. During prophase, nuclear envelope breakdown is achieved through the employment of the microtubule network [243]. Other motor proteins, such as the dynein-dynactin complex, have also been shown to localise to the nuclear envelope at prophase [244]. This complex is suggested to stabilise the plus ends of microtubules growing towards the nuclear envelope [245]. Taken together a model was suggested whereby this motor complex stabilises microtubules growing towards the nuclear envelope, facilitates attachment of plus ends to the envelope and subsequently pulls apart the nuclear envelope through tension created via the microtubules and the movement of dynein towards the forming spindle poles [243,245]. The novel localisation of MKLP1 to the nuclear envelope may also regulate this process, as MKLP1 can bind microtubules [171]. It should be noted that immunofluorescence analysis of MKLP1 utilises an antibody which detects both MKLP1 and CHO1. An interaction between CHO1 and annexin A11 has previously been shown to occur at cytokinesis [150]. It is therefore possible that the targeting of annexin A11 to the degenerating nuclear envelope may act as an anchor for CHO1. This would reinforce the interaction between the nuclear envelope and microtubular network at a time when this

interaction is critical to the onset of karyokinesis.

At anaphase, in PFA fixed cells, annexin A11 co-localises with MKLP1 at the spindle midzone. Closer inspection showed that the midzone accumulation was specific to the plus ends of the overlapping microtubules. Annexin A11 co-localises at these points with the motor protein MKLP1, which may facilitate its attachment to the microtubule plus ends as MKLP1 has been shown *in vitro* to cross-link anti-parallel microtubules [171] and its splice variant CHO1 has been shown to interact with annexin A11 [150]. The localisation of MKLP1 to the plus ends of the spindle midzone microtubules corroborates previous studies [246,247] and fits with the functional data presented. *In vitro* assays using the *C.elegans* homologue of MKLP1, ZEN-4, demonstrated the ability of this protein to induce microtubule gliding in a phosphorylation-dependent manner [246]. This ability was diminished upon phosphorylation of a threonine residue within the motor domain of ZEN-4, by cyclin-dependent kinase 1 (Cdk1). In human cells, Cdk1 is suggested to temporally regulate the microtubule-dependent association of MKLP1 to the spindle midzone at anaphase. Phosphorylation of MKLP1 is said to prevent the precocious bundling of anti-parallel microtubules at metaphase, which would result in inefficient chromosome segregation if a kinetochore microtubule from one pole was inadvertently bundled to microtubules emanating from the opposite pole. This was confirmed through the over-expression of non-phosphorylable MKLP1, which resulted in segregation defects [246]. At anaphase however, the bundling of anti-parallel microtubules by MKLP1 is beneficial as it is helps maintain the cleavage furrow [170] and assemble the contractile ring [169], both of which are necessary for the successful completion of cytokinesis.

The localisation of annexin A11 to this same region suggests that it may also have a role in this process. It is not yet known whether the spindle midzone microtubules directly bind the overlying plasma membrane, though signalling between these two regions is known to be essential for cleavage furrow ingression [248]. Furrow initiation has been shown to be regulated by stable astral microtubules which contact the cell cortex [249]. It is hypothesised that MKLP1 can then traffic along these microtubules and induce the accumulation of the centralspindlin complex, resulting in contraction of the cell cortex [250]. Following initiation of this process, annexin A11 may participate in the stabilisation of potential spindle midzone-plasma membrane interactions, through its ability to bind phospholipids [146].

MKLP1 and annexin A11 also co-localise at telophase in PFA fixed cells, at a protein dense structure called the midbody. MKLP1 has previously been identified as a component of the midbody [235,251]. A proteomic study of the midbody also identified annexins A5, A6 and A7 as midbody components, although these localisations were not corroborated via immunofluorescence [251]. Previous studies of annexin A11 and the MKLP1 splice variant CHO1, have shown that these two proteins not only co-localise at cytokinesis at the midbody, but also interact at this point [150]. This interaction is speculated to help maintain a tight association between the midbody and the plasma membrane, during a time when significant forces are being exerted at the cleavage furrow. Maintenance of this association is thought to be required for the successful completion of cytokinesis [238]. CHO1 alone cannot bind the plasma membrane but annexin A11 can, therefore helping to bridge the gap between the midbody and the plasma membrane.

This interaction was not confirmed in this study, however an antibody specific to CHO1 was not available. It is therefore likely that without enrichment of this particular variant of MKLP1 an interaction cannot readily be detected or that the epitopes detected using this antibody are not longer detectable once CHO1 is embedded at the midbody. One method used for the detection of this interaction was the immunoprecipitation of annexin A11, from both non-syncrhonised and synchronised cell lysates. Silver staining of SDS-PAGE gels with these samples uncovered the presence of annexin A11-interacting proteins, which differed between non-synchronised and synchronised cell lysates, suggesting that annexin A11 interacts with different proteins during the cell cycle. Mass spectrometry of these proteins would be beneficial in understanding the mechanism by which annexin A11 regulates the cell cycle at cytokinesis. We also attempted to determine which domain of annexin A11 was responsible for midbody targeting through the over-expression of GFP-tagged annexin A11 constructs. However as GFP alone targeted to the midbody this was not resolved using this method. Future studies will require the over-expression of annexin A11 labelled with a smaller tag that is less likely to target to the midbody itself.

Further immunofluorescence studies of annexin A11 and MKLP1 during the cell cycle were carried out using methanol fixation. Both PFA and methanol fixation can result in denaturation of cellular protein, but function through two different mechanisms. PFA fixation acts through the cross-linking of proteins, via the reaction of formaldehyde with

amino groups. This reaction results in the production of methylol groups, which can go on to form methylene bridges between polypeptides [252]. Extensive cross-linking allows the cellular architecture to be maintained. This process is slower than that of methanol fixation, which involves solubilisation of lipid membranes, dehydration of the cell and precipitation of the proteins. This method of fixation is known to better preserve microtubule integrity, as it acts faster allowing less time for microtubule depolymerisation which can result in the loss of associated proteins. What was most striking about the localisations of both annexin A11 and MKLP1 upon methanol fixation, was the consistent localisation of both proteins along the length of the mitotic spindle at metaphase. From anaphase through to cytokinesis the localisation of MKLP1 in methanol fixed cells was the same as that seen in PFA fixed cells. However annexin A11 showed a more widespread distribution; along the length of the spindle midzone at anaphase and throughout the cleavage furrow at telophase and cytokinesis. The fact that this is not seen with MKLP1 supports the notion that this is not merely an artefact of methanol fixation, particularly as MKLP1 is known to bind microtubules [171]. The distribution of annexin reflects an enhanced association of annexin A11 with the microtubule network and suggests that annexin A11 may be trafficked along the mitotic spindle throughout mitosis. It is already known that treatment of cells with Brefeldin A, which disrupts trafficking through the Golgi [253] via the inhibition of Sec7 domain-containing ARF guanine nucleotide exchange factors [254], does not prevent the accumulation of annexin A11 at the midbody [150]. It would therefore be of interest to observe the localisation of annexin A11 upon disruption of the microtubular network at different points of the cell cycle, in order to determine if this would affect midbody targeting.

Another avenue for investigation concerns the phosphorylation state of annexin A11. Phosphorylation of midbody proteins is known to be important for their targeting to this domain. For example serine phoshphorylation of MKLP1 by Aurora B kinase is required for its retention at the midbody and subsequent completion of cytokinesis [247]. Similarly targeting of Inner Centromere Protein (INCENP) to the cleavage furrow requires serine phosphorylation by polo-like kinase 3 (Plk3) [255]. Annexin A11 has also been shown to be phosphorylated during cytokinesis, however on tyrosine residues [146]. In a separate phosphoproteomic study several tyrosine phosphorylation sites within annexin A11 were identified in lung cancer cell lines [226]. These three tyrosine phosphorylation sites all lie within the C terminal domain of annexin A11 (Figure 31A), specifically within annexin

repeats II, III and IV (Figure 31B).

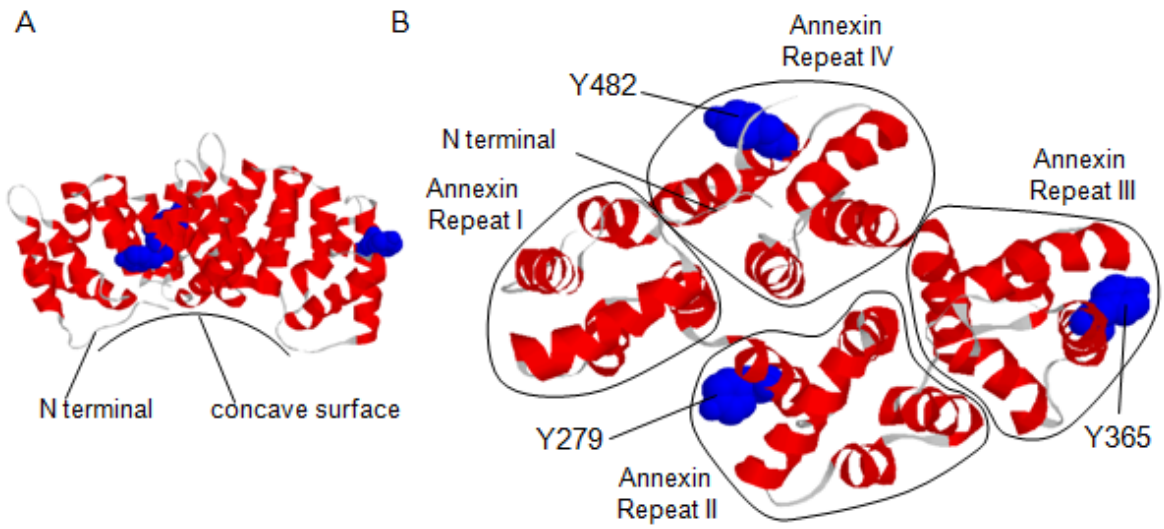

Figure 31 Predicitve Model of Annexin A11 Highlighting Known Tyrosine Phosphorylation Sites

Predictive models of annexin A11 were calculated (EMBL) and modelled in RasMol (Version 2.6). **(A)** Side view of annexin A11 with the known tyrosine phosphorylation sites (identified in [226]) highlighted in blue. **(B)** View of annexin A11 from its concave surface, with the three known tyrosine phosphorylation sites (Y279, Y365, Y482) highlighted in blue. Each of these sites lies within an annexin repeat (outlined in black).

Tyrosine phosphorylation is of particular interest as it has been shown that tyrosine phosphorylated proteins are delivered to the midbody via Rab11 GTPase positive vesicles. Furthermore it was shown that down-regulation of tyrosine phosphorylation through the inhibition of Src family kinases results in a decrease of tyrosine phosphorylated proteins at the midbody and a failure to complete cytokinesis [256]. Interestingly cytokinesis fails due to the inability of the daughter cells to abscise from each other. This results in the cells remaining connected by a long intercellular bridge of membrane – as has also been observed upon knock down of annexin A11 [150], although the midbody is also lost in the latter instance.

The role for tyrosine de-phosphorylation at the midbody is less clear. Studies were carried out on the tyrosine phosphatase, PTP-BL, which like annexin A11 targets to the midbody [257]. Over-expression of PTP-BL resulted in a failure in cytokinesis, though in this case the daughter cells fused back together to form multi-nucleated cells. However over-expression of wildtype or phosphatase inactive PTP-BL produced the same cytokinetic

defect, suggesting that the tyrosine phosphatase activity of PTP-BL is not directly involved in the regulation of cytokinesis. Conversely, investigations into the tyrosine phosphatase PTP-PEST have shown that PTP-PEST$^{-/-}$ fibroblast populations have an increased number of cells at cytokinesis, suggestive of a block at this stage [258]. These cells also showed increased tyrosine phosphorylation of PSTPIP (proline, serine, threonine phosphatase interacting protein). PSTPIP is known to be a substrate of PTP-PEST and to localise to the actin ring at the cleavage furrow of cytokinetic mammalian cells [259]. The over-expression of PTP-PEST in yeast has been shown to inhibit cell cleavage at cytokinesis [259].

Taken together these studies illustrate the importance of tyrosine phosphorylation at cytokinesis and demonstrate that a fine balance between phosphorylation and de-phosphorylation must be maintained in order for successful completion of this process. Therefore it would be of interest to investigate the effects of mutagenesis on the known tyrosine phosphorylation sites within annexin A11. This would shed light on whether tyrosine phosphorylation is required for the various cell cycle localisations of annexin A11 and whether this regulates not only cytokinesis, but the entire process of mitosis.

Chapter Five:
Study of Annexin A11 and Tubulin

5. Results: Study of Annexin A11 and Tubulin

Tubulin monomers are the basic building blocks of the microtubule network, which gives a cell its structure, provides a framework for intracellular traffic, coordinates the cell cycle and carries out a host of other complex processes. The microtubule network is one of three major polymer systems, the others being intermediate filaments and actin, which together compose the cytoskeleton. Early insights into the structure of the microtubule cytoskeleton were carried out using naturally occurring drugs that target its individual components [260]. This led to the discovery that microtubules are made of heterodimers of alpha and beta subunits and polymerise by harnessing GTP hydrolysis at the beta tubulin subunit [261]. These heterodimers go on to form linear protofilaments, which collectively form hollow, cylindrical tubes, 25 nm in diameter i.e. microtubules [262] (Figure 32).

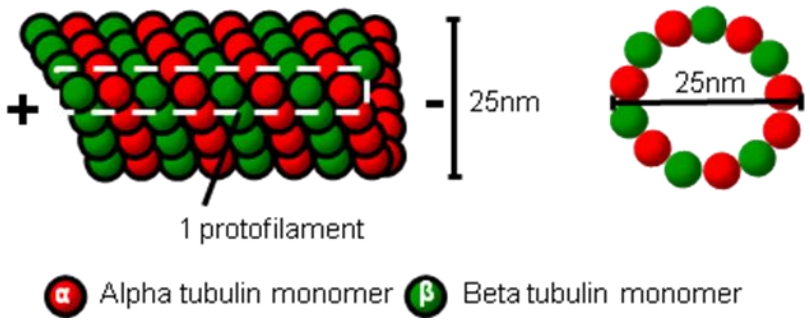

Figure 32 Microtubule Structure

Alpha and beta tubulin monomers form the basis of the microtubule network. Monomers combine to form heterodimers, which polymerise to form protofilaments. The protofilaments comprise the tubular structures known as microtubules. These hollow structures are 25 nm in diameter and vary in length.

Microtubules are polar structures with a minus end, located at the MTOC (microtubule organising centre) in centrosomally organised microtubule networks, and a plus end located distally, emanating out towards the cell cortex. The alpha and beta tubulin subunits are exposed at the minus and plus ends respectively. This polar structure sets the stage for a process termed ‘microtubule treadmilling’, whereby tubulin subunits are lost from the minus end and gained at the plus end. In steady state conditions, where the length of the microtubule does not change, the process of extension at the plus end equals that of retraction at the minus end. This process is dependent on a phenomenon called ‘dynamic instability’, where microtubule ends switch between phases of polymerisation and

depolymerisation in a stochastic manner. Polymerisation involves the binding of GTP bound tubulin subunits, which upon GTP hydrolysis become GDP-bound tubulin subunits that are subsequently released from the polymer [263,264] (Figure 33).

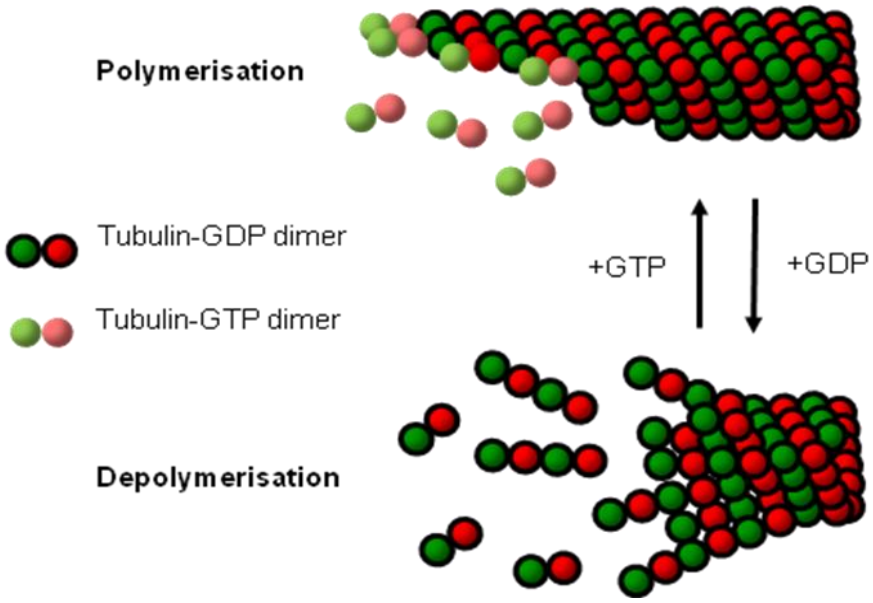

Figure 33 Microtubule Polymerisation

Microtubules are highly dynamic structures and their rates of polymerisation and depolymerisation are highly dependent on GTP levels within the cell. Tubulin heterodimers, made of a beta and alpha subunits, bind GTP. In this form they promote addition to the plus end of a microtubule resulting in polymerisation. Hydrolysis of the bound GTP causes the release of a single phosphate group, leaving behind GDP bound tubulin heterodimers. In this form their association with the microtubule is inherently unstable and results in depolymerisation. The balance between these two states determines whether the microtubule is growing or shrinking.

Microtubule stability depends not only on the rate of GTP hydrolysis and the amount of monomeric tubulin available, but also on microtubule stabilising proteins, such as the well known MAPs (microtubule associated proteins) and a variety of other proteins ranging from the Ras GTPase, Ran [265] to the STOP (stable tubule-only polypeptide) protein [266]. At the opposite end of microtubule stabilisation is microtubule severing, originally characterised by the action of the AAA ATPase (ATPases Associated with diverse cellular Activities) katanin [267], which was later shown to be the major component responsible for mitotic microtubule severing [267,268].

Several naturally occurring substances and synthetic chemicals are known to destabilise the microtubule network and have been used experimentally to better understand the

function of these structures. One such substance is nocodazole, a synthetic carbamate with reversible effects on the microtubule network. Nocodazole has been shown to bind the beta subunit of tubulin at two sites [269]. This interaction sequesters the free tubulin dimers and prevents their incorporation into microtubules, so inhibiting any further polymerisation. This results in the eventual net depolymerisation of the microtubule network due to inherent dynamic instability. Colchicine, a naturally occurring alkaloid, stimulates microtubule depolymerisation in the same manner and competes with nocodazole for binding to beta tubulin subunits [270]. Nocodazole and colchicine both preferentially bind to free tubulin unlike the microtubule polymerising drug taxol. Taxol, also known as paclitaxel, is a naturally occurring diterpene which preferentially binds microtubules through its interaction with beta tubulin subunits [271]. Taxol promotes microtubule polymerisation both *in vitro* [272] and *in vivo* [273] and its effects are prevented by colchicine co-treatment.

The use of these drugs has shed light on the role of the microtubule network in a vast array of cellular processes which occur both during interphase and during mitosis, when the microtubule network is particularly dynamic. However, these drugs target beta tubulin and therefore preodominantly affect the alpha-beta tubulin protofilaments. Although these are the two major tubulin subunits, of which there are several subtypes, it should be noted that several additional tubulin genes have been discovered. These include gamma, delta, epsilon, zeta and eta. Only alpha, beta and gamma are present in all eukaryotes, whilst the remaining forms are often organism specific [274]. An additional layer of functional variation is imposed by the post-translational modification of tubulin.

There are four well characterised post translational modifications [275]. Firstly tubulin acetylation, associated with stable microtubules, involves the addition of an acetyl group to lysine residue 40 on alpha tubulin. Deacetylation is carried out by HDAC6 (histone deacetylase 6) and SIRT2 (silent mating type information regulation 2), however the acetylating enzyme is still unknown. Alpha tubulin is also the target of detyrosination, whereby the C terminal tyrosine residue is cleaved. This residue can be added back by tubulin tyrosine ligase. Detyrosinated microtubules show a preference for binding kinesin 1 motors, which could help specify cargo trafficking along certain routes. Lastly polyglutamylation and polyglycation occur on both alpha and beta tubulin and involve the addition of glutamate or glycine residues respectively to their C termini. These

polymodifications have been suggested to support microtubule severing by katanin. Therefore subtle differences in tubulin structure can exert distinct effects on the interactions of the microtubule network with its binding proteins. This can result in downstream effects on all manner of cellular processes, including cell morphology and cargo transport.

5.1 Annexin A11 and Tubulin Co-localisation

Annexin A11 is distributed in both the nucleus and cytoplasm of several cultured cell lines, including HeLa and A431 cells [146,147,150]. However during the cell cycle annexin A11 relocalises to discrete structures (Figure 25). This includes the nuclear envelope at prophase, the mitotic spindle at metaphase and anaphase, and the midbody at cytokinesis. It was observed that the distribution of annexin A11, as determined by immunofluorescence of fixed cells, was enhanced in methanol fixed cells relative to PFA fixed cells. Methanol fixation better preserves the integrity of the microtubules. Under these conditions annexin A11 co-localises strongly with tubulin of the mitotic spindle, in particular the midzone, kinetochore microtubules and later with tubulin of the cleavage furrow (Figure 27). To determine whether annexin A11 co-localised with tubulin in cells at interphase, HeLa cells were fixed in methanol, annexin A11 and tubulin were stained for and the cells imaged on an inverted confocal microscope. The distribution of annexin A11 was both nuclear and cytoplasmic. The cytoplasmic staining was punctate in appearance and upon closer inspection a number of puncta localised along microtubule tracks (Figure 34A).

In order to determine whether the co-localisation of annexin A11 and tubulin at interphase signifies an interaction between these two proteins, microtubule co-sedimentation was performed. HeLa cells were harvested and lysed in Brinkley's buffer, which is optimal for microtubule preservation, either in the presence of 200µM calcium or 1mM EGTA. Cell lysates were incubated with or without taxol. Taxol is a taxane family drug, which stabilises microtubules through binding the beta monomer of tubulin. Lysates were incubated with 2mM GTP to compensate for the decrease in GTP levels upon cell lysis, which is a key factor in microtubule depolymerisation rates. In addition to GTP, 1.5mM AMP-PNP (non-hydrolysable ATP) was added which is known to promote the association of microtubule binding proteins, such as MAPs to microtubules. The samples were spun through a

sucrose cushion to separate soluble and insoluble fractions of tubulin i.e. tubulin subunits and microtubule filaments, respectively. Pellets (insoluble fraction) and supernatants (soluble fraction) were then subjected to SDS-PAGE. Western blotting for tubulin and actin, showed that in the absence of taxol neither tubulin nor actin pelleted, but in the presence of taxol tubulin did pellet but actin still remained in the supernatants. This confirms that without taxol microtubules depolymerised during the course of the experiment resulting in all the cellular tubulin concentrating in the soluble fraction (Figure 34B). This was true both in the presence of calcium or EGTA. Western blotting for annexin A11 showed that in the presence or absence of taxol, with calcium or with EGTA, annexin A11 resided in the soluble fractions and could not be detected in the insoluble fractions. Therefore annexin A11 does not appear to co-sediment with tubulin.

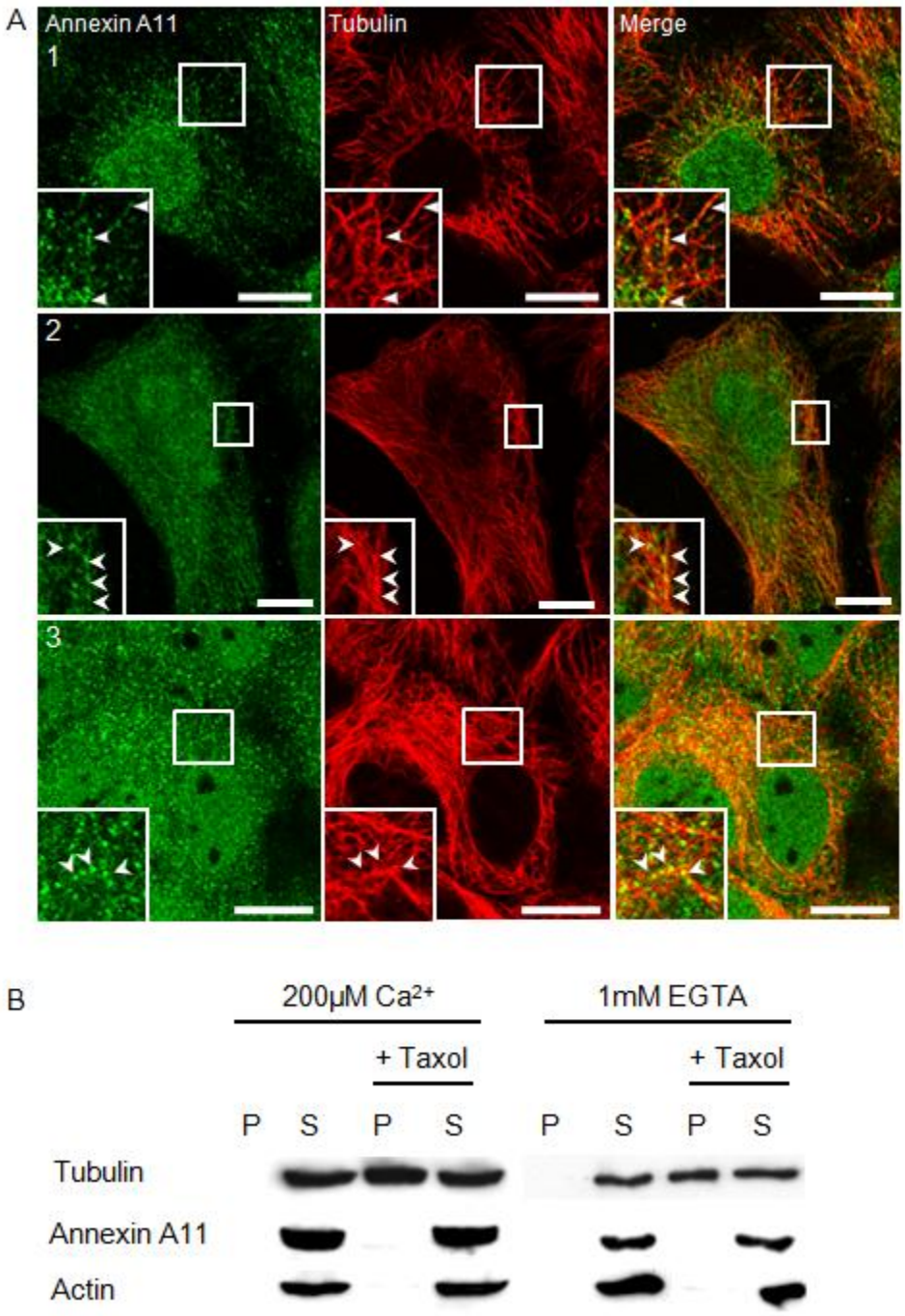

Figure 34 Annexin A11 Punctae Localise Along Microtubules

(A) HeLa cells were fixed in methanol and stained for annexin A11 using a polyclonal goat anti-annexin A11 antibody (1/50 dilution) and tubulin using a monoclonal mouse anti-alpha tubulin antibody (1/100 dilution). Three representative cells are shown (1-3). Insets show annexin A11 puncta along microtubules (arrowheads). (Scale bars 10μm) **(B)** HeLa cell lysates were subjected to microtubule cosedimentation (as detailed in Materials and Methods 2.18). Resulting pellets and supernatants were subjected to SDS-PAGE and Western blotting. Annexin A11 was detected using a polyclonal goat anti-annexin A11 antibody (1/200 dilution), tubulin using a monoclonal mouse anti-alpha tubulin antibody (1/1000 dilution) and actin using a monoclonal mouse anti-beta actin antibody (1/5000 dilution).

5.2 Annexin A11 Knock Down and Overexpression: Effect on the Microtubule Network

Although annexin A11 does not appear to co-sediment with tubulin, its co-localisation with tubulin as detected by immunofluorescence of fixed cells, suggests it may yet be involved with the microtubule network. In order to further investigate this annexin A11 was knocked down in A431, HeLa and CaCo-2 cells using RNA interference. Cells were plated at 30% confluency and transfected the following day with a pool of four different siRNA constructs targeting four different regions of the annexin A11 gene. Cells were treated with a second dose of siRNA three days after plating. Cells were lysed for SDS PAGE analysis on days 2, 3 and 6. Western blotting for annexin A11 and tubulin showed significant knockdown of annexin A11 in cells treated with annexin A11 siRNA compared to control cells treated with negative control siRNA (Figure 35A). On average by day 6 annexin A11 levels had dropped by 95% in A431 cells, 82% in HeLa cells and 89% in CaCo-2 cells (Figure 35B). The knockdown was also observed via immunofluorescence. On day 6 cells were PFA fixed and stained for annexin A11 and alpha tubulin. In siRNA treated cells, expanses of cells were seen with highly diminished levels of annexin A11 staining, compared to control cells where annexin A11 staining was strongly present in all cells. In annexin A11 siRNA treated cells the microtubules appeared unchanged in comparison to control cells. A dense network of tubulin filaments was present in both cases, as illustrated in A431 (Figure 36) and CaCo-2 cells (Figure 37).

The effect of over-expression of annexin A11 on the microtubule network was also investigated. A431 cells were transfected with GFP tagged annexin A11 constructs and incubated overnight. Cells were then methanol fixed and stained for alpha tubulin. The mirotubular network appeared unchanged in cells overexpressing annexin A11-GFP, annexin A11-R230C-GFP, annexin A11 N-terminal-GFP, annexin A11-C-terminal-GFP, annexin A11-C-terminal-R230C-GFP and GFP alone when compared to neighbouring untransfected cells (Figure 38).

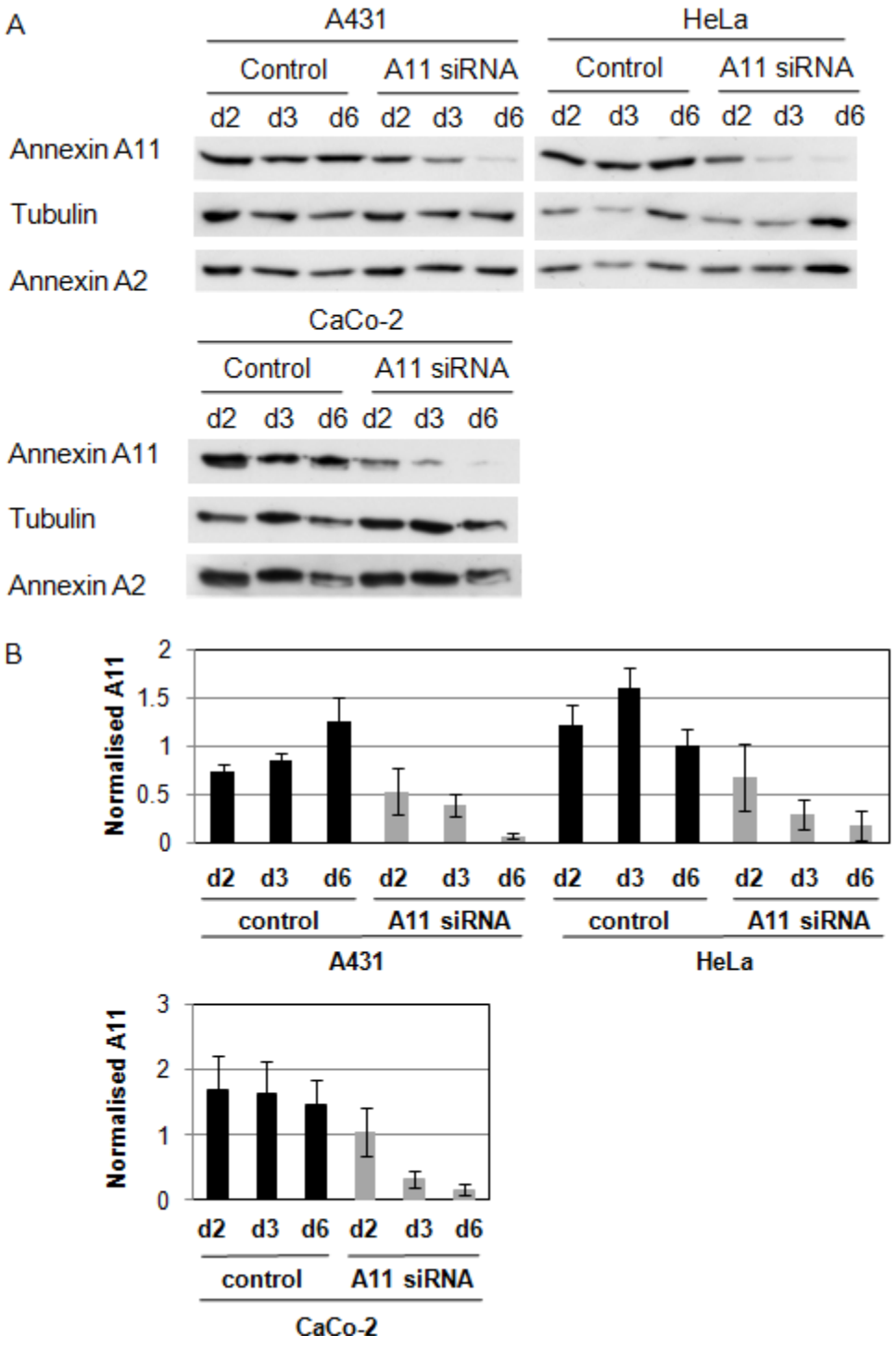

Figure 35 Annexin A11 Knock Down in Several Cell Lines Using RNA Interference

(A) Western blot of whole cell lysates from A431, HeLa and CaCo-2 cells treated with 20µM annexin A11 siRNA or 20µM scrambled control siRNA for 2, 3 and 6 days, with two treatments administered on day 1 and day 3. Annexin A11 was blotted for using a polyclonal goat anti-annexin A11 antibody (1/200 dilution) and tubulin using a monoclonal mouse anti-alpha tubulin antibody (1/1000 dilution) **(B)** Graphs of average annexin A11 protein levels normalised to tubulin in siRNA and control treated A431, HeLa and CaCo-2 cells, n=3 for each cell line.

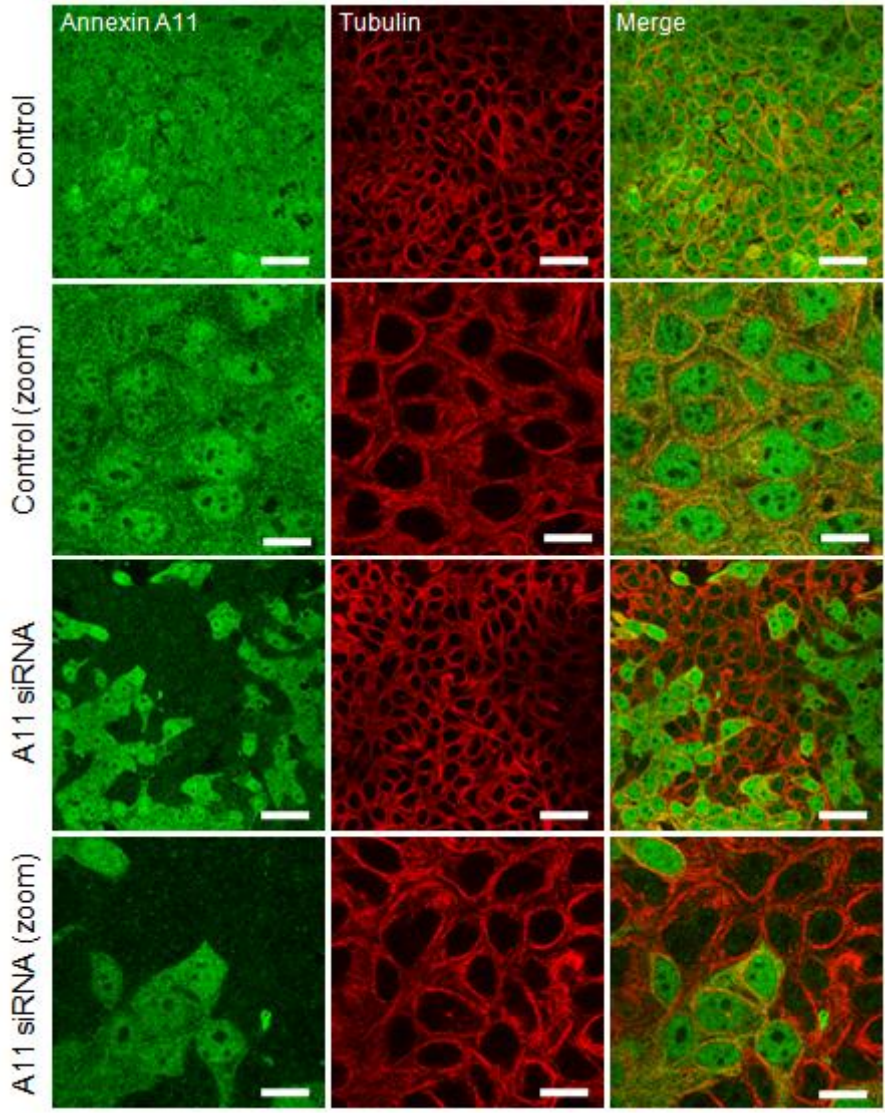

Figure 36 Annexin A11 Knock Down in A431 Cells Using RNA Interference

A431 cells were treated with 20µM annexin A11 siRNA or 20µM scrambled control siRNA for 6 days, with two treatments administered on day 1 and day 3. Cells were then PFA fixed on day 6 and stained for annexin A11 using a polyclonal goat anti-annexin A11 antibody (1/50 dilution) and tubulin using a monoclonal mouse anti-alpha tubulin antibody (1/100 dilution). (Scale bars 50µm, zoom 20µm)

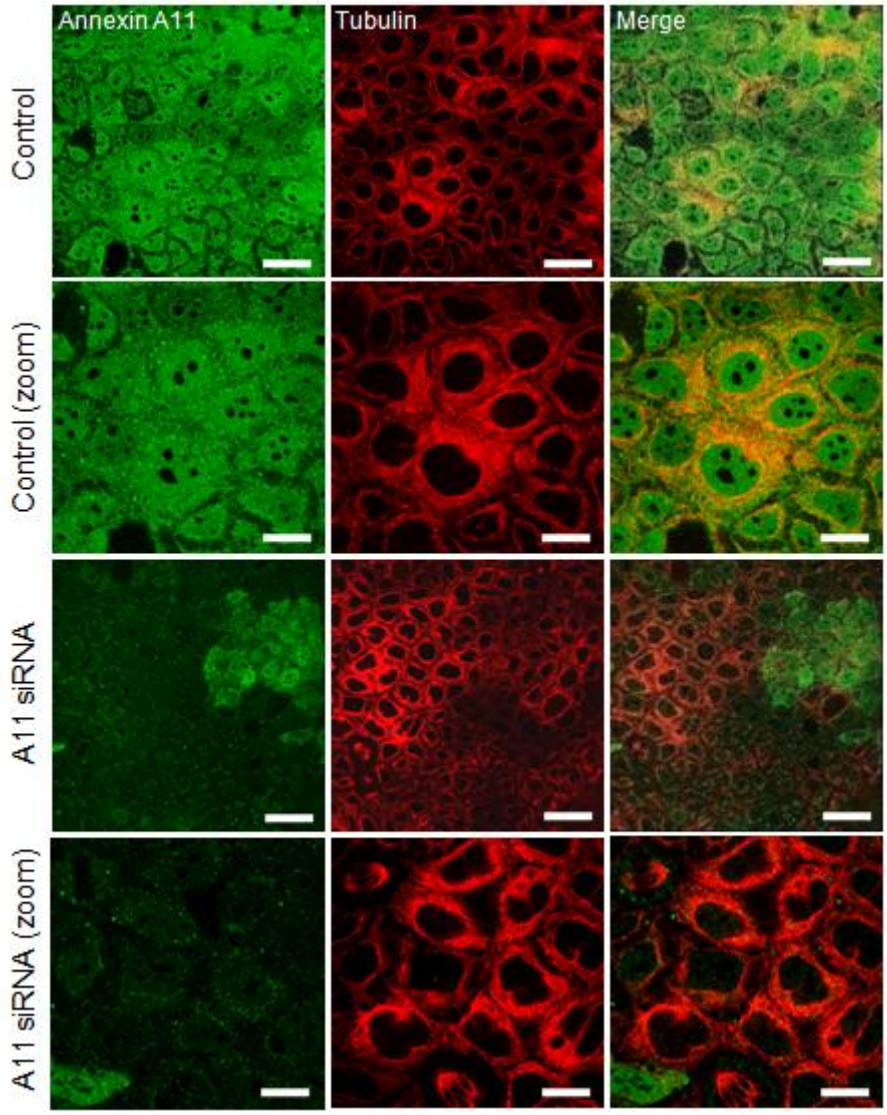

Figure 37 Annexin A11 Knock Down in CaCo-2 Cells Using RNA Interference

CaCo-2 cells were treated with 20µM annexin A11 siRNA or 20µM scrambled control siRNA for 6 days, with two treatments administered on day 1 and day 3. Cells were then PFA fixed on day 6 and stained for annexin A11 using a polyclonal goat anti-annexin A11 antibody (1/50 dilution) and tubulin using a monoclonal mouse anti-alpha tubulin antibody (1/100 dilution). (Scale bars 50µm, zoom 20µm)

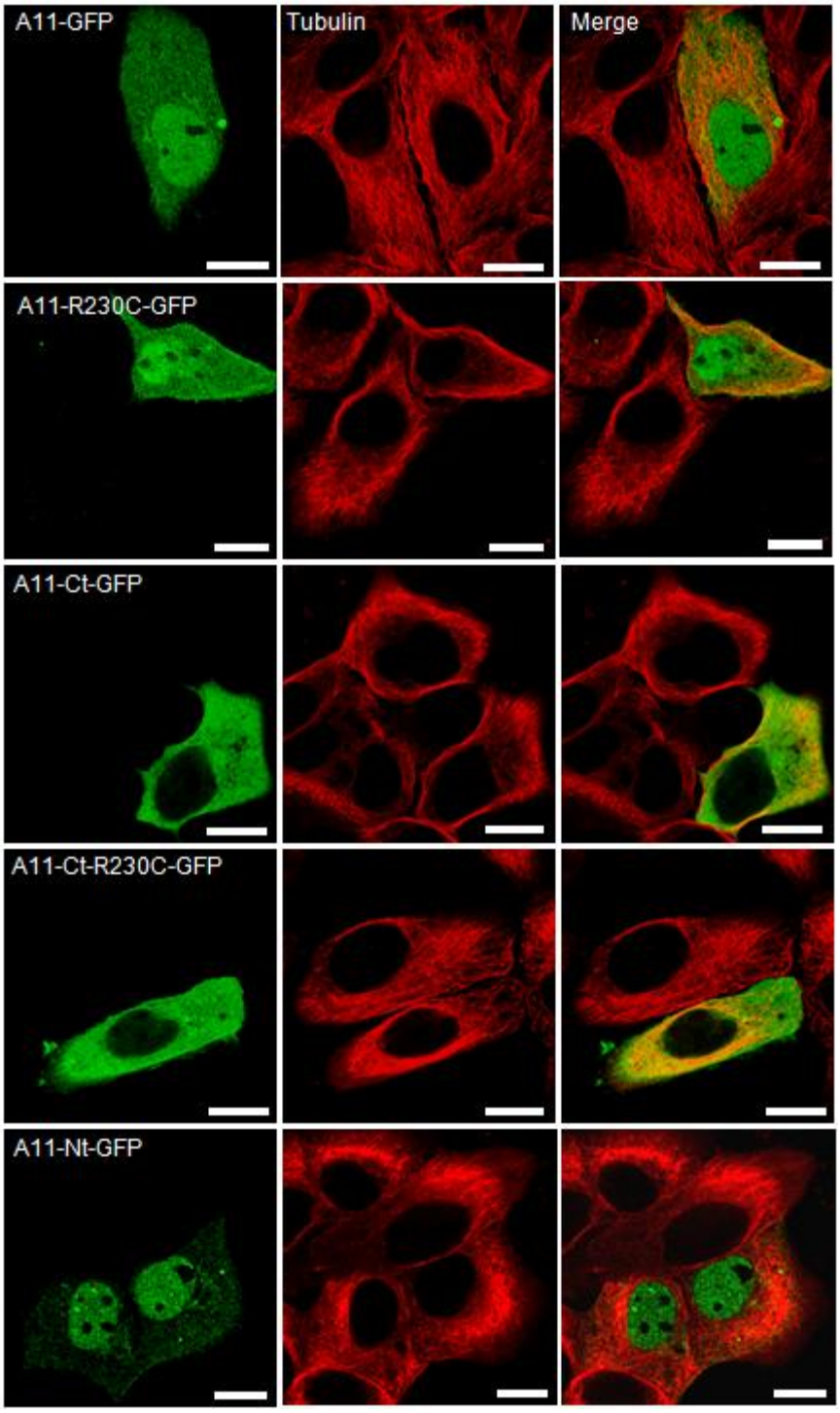

Figure 38 Overexpression of Annexin A11-GFP Constructs in A431 Cells Does Not Affect the Gross Morphology of the Microtubule Network

A431 cells were fixed in methanol and then stained for annexin A11 using a polyclonal goat anti-annexin A11 antibody (1/50 dilution) and tubulin using a monoclonal mouse anti-alpha tubulin antibody (1/100 dilution). (Scale Bars 10µm)

5.3 Annexin A11 Localisation Upon Tubulin Depolymerisation

The knockdown or overexpression of annexin A11 had no detectable effect on the microtubule network. Therefore the inverse relationship was investigated next, in which the effect of disrupting the microtubule network on the distribution of annexin A11 was examined. HeLa cells were incubated for 3 hours in 100ng/ml nocodazole. Nocadazole binds to the beta subunits of tubulin and prevents their dimerisation with beta subunits, this result in the net depolymerisation of tubulin. Following treatment with nocodazole, the cells were fixed in methanol, stained for alpha tubulin and annexin A11, and imaged on an inverted confocal microscope. Remnants of nocodazole resistant microtubule structures were present, particularly in perinuclear regions. Annexin A11 was diffuse in the cytoplasm and nucleus, but interestingly also showed discrete accumulations in perinuclear regions along the nocodazole resistant microtubules (Figure 39). The co-localisation of annexin A11 and tubulin therefore appeared to be enhanced when cells were treated with nocodazole, compared to untreated cells with intact microtubule networks.

This data suggests that whilst the integrity of the microtubule network is not dependent on annexin A11, annexin A11 localisation requires intact microtubules.

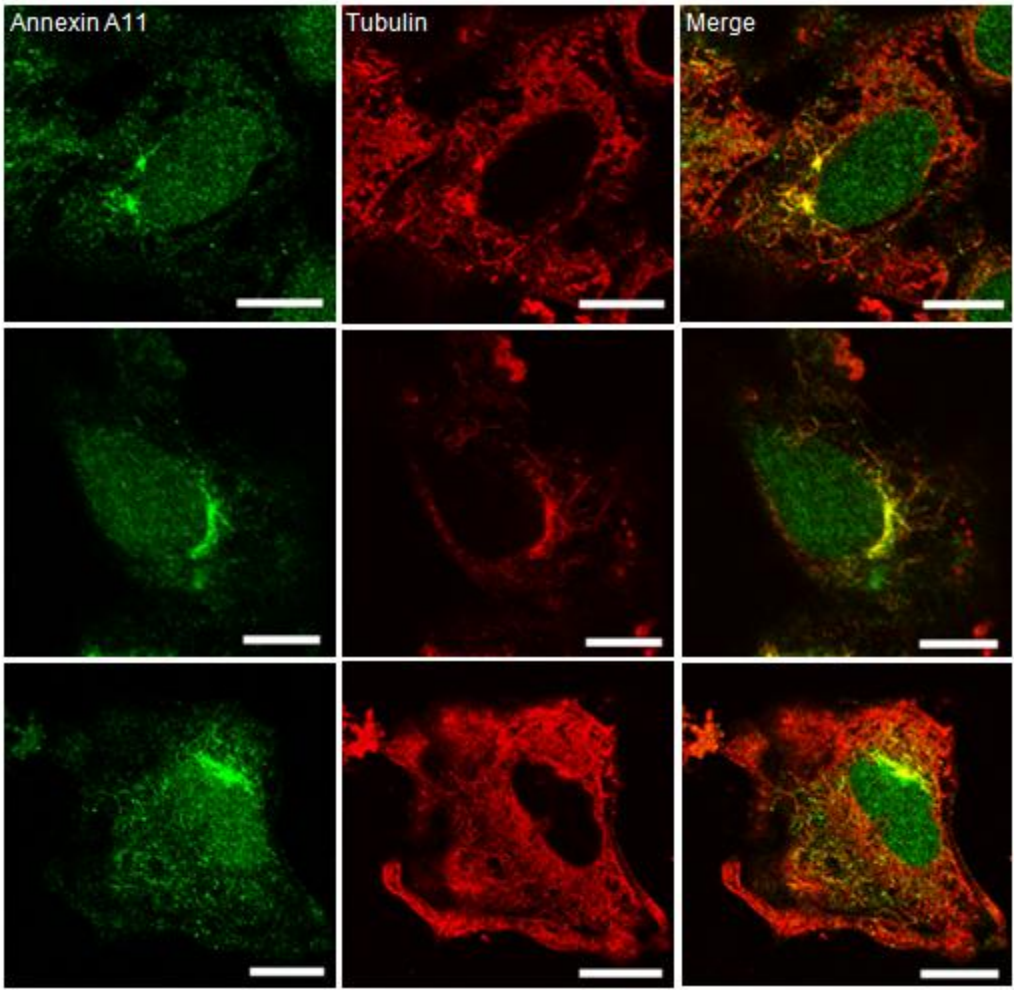

Figure 39 Annexin A11 Localisation Along Microtubules upon Nocadazole Treatment

HeLa cells were incubated for 90min in media containing 100ng/ml nocodazole, prior to fixation in methanol. Cells were then stained for annexin A11 using a polyclonal goat anti-annexin A11 antibody (1/50 dilution) and tubulin using a monoclonal mouse anti-alpha tubulin antibody (1/100 dilution). (Scale bars 10μm)

5.4 Discussion

The intracellular localisation of annexin A11 in this study has been investigated during the cell cycle, under both methanol and PFA fixation conditions (as discussed in 4.5 Discussion of Annexin A11 and CHO1). Methanol fixation was adopted as this is known to better preserve the integrity of the microtubule network, as fixation occurs faster than with PFA. This is due to the mechanism of action employed by each fixative, as explained previously in 4.5 Discussion of Annexin A11 and CHO1. The speed at which methanol fixes the cells provides less time for the highly dynamic microtubule filaments to depolymerise. In addition to the preservation of the microtubules, methanol fixation results in the loss of some of the cytoplasmic staining of annexin A11. This allowed a clearer visualisation of annexin A11 puncta in interphase cells.

These puncta of annexin A11 appeared to line up along microtubule filaments. The microtubule network traffics a large number of vesicles to different cellular domains through the use of the motor proteins, kinesin and dynein, which link microtubules to vesicles [276]. The puncta of annexin A11 may represent such vesicles. It has been shown that a population of these puncta are also COPII (Coat Protein Complex II) positive [personal communication, Dr Hideki Shibata, University of Nagoya, Japan]. COPII is comprised of three main subunits; Sar1p, Sec13/31p and Sec23/24p, which act together to bud off vesicles from the endoplasmic reticulum for transport to the Golgi apparatus [277]. COPII vesicles have been shown to associate with the microtubule network [278] through an interaction between the human COPII component, Sec23p, and dynactin, an accessory protein of the dynein complex. Furthermore the human COPII component Sec31A has been shown to directly interact with ALG2 (Apoptosis-Linked Gene 2) in a calcium dependent manner [279]. ALG2 was also shown to partially colocalise with Sec31A at endoplasmic reticulum (ER) exit sites, again in a calcium dependent manner, as a calcium binding mutant of ALG2 no longer interacted with Sec31A or localised to ER exit sites. In line with these data, knock down of Sec31A also prevented ALG2 localisation at ER exit sites. Equally, knock down of ALG2 perturbed the localisation of Sec31A at these sites, with diminished levels detected here [279].

These observations suggest that ALG2 has a role in ER to Golgi trafficking and its calcium dependent regulation. The partial co-localisation of annexin A11 and COPII vesicles,

alongside the known interaction between annexin A11 and ALG2 [68], tentatively suggests a role for annexin A11 in this process. Furthermore, given that COPII vesicles have been shown to associate with microtubules [278] and a subpopulation of annexin A11 puncta have been shown in this study to localise along these structures, it is possible that annexin A11 is specifically trafficked from the ER to the Golgi along the microtubules. This transport could be mediated by a protein complex involving annexin A11, ALG2, COPII components and the dynactin-dynein complex or some other motor protein such as CHO1 (Figure 41). Work is currently underway to determine whether annexin A11 interacts with the COPII component Sec31 [personal communication, Dr Hideki Shibata, University of Nagoya, Japan]. It would also be of interest to investigate the effect of depletion of the proteins within this hypothetical complex on the distribution of annexin A11.

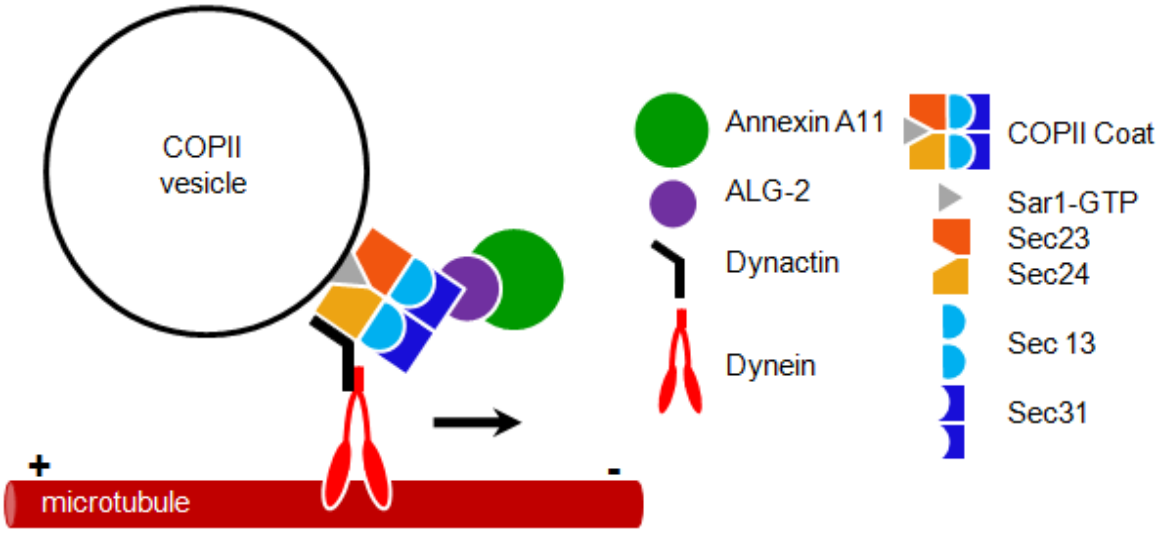

Figure 40 Hypothetical Model for Annexin A11 Trafficking Along Microtubules

Annexin A11 may be transported along microtubules via its known direct interaction with ALG2. ALG2 has been shown to interact with Sec31, a component of the COPII vesicle coat with which annexin A11 has been shown to partially co-localise. COPII vesicles are capable of associating with microtubules through the interaction of Sec24 with the dynactin-dynein motor protein complex, which directly binds microtubules and directs cargo to the microtubule minus end.

The pool of annexin A11 observed in this study to be associated with the microtubule network appears to represent a small proportion of the total annexin present in the cell, as judged by immunofluorescence. This may account for the lack of any visible co-sedimentation of annexin A11 with tubulin. However this could also be due to limitations of the microtubule co-sedimentation procedure. More specifically, the microtubule network is first depolymerised during lysis and clarification, and is only then subjected to treatment

with GTP and magnesium ions to re-polymerise the network. This network is then stabilised through the addition of taxol. Therefore the interaction with annexin A11 may be lost upon depolymerisation and not easily regained once the cellular architecture is disrupted and potentially essential proteins required for this interaction are diluted. None of the other vertebrate annexins have been shown to directly interact with tubulin, although annexin A1 has been shown to co-localise with tubulin-rich focal patches at the plasma membrane of A549 human lung adenocarcinoma cells [280]. Annexin A2 is also suggested to co-immunoprecipitate with beta and gamma tubulin from rod photoreceptor outer segments [281], although this interaction was not confirmed through immunofluorescence analysis or co-sedimentation assays. The only other annexin known to associate with tubulin is annexin E1 of the flagellated protozoan *Giardia lamblia* [282], as shown via co-localisation from immunocytochemical analysis and affinity chromatography.

In order to determine whether annexin A11 has a role in the regulation of the microtubule network, aside from being transported along it, annexin A11 was knocked down in several cell lines. Subsequent immunofluorescence analysis of the microtubule network showed no apparent, defects in knock down cells as compared to control cells. The overexpression of annexin A11 also did not affect the microtubule network. Therefore annexin A11 does not appear to regulate this network, but is tightly associated with it during both the cell cycle and in interphase cells. The association with microtubules can be more strikingly seen upon treatment of cells with nocodazole. Nocodazole causes the net depolymerisation of the microtubule network [269], however more stable tubulin structures tend to be more resistant to nocodazole treatment [283]. The resistance to nocodazole and enhanced stability can be mediated by the post-translational acetylation of alpha tubulin at lysine 40 [283]. Microtubule structures such as the centrosome are known to be acetylated and therefore are inherently more stable [284]. This is in line with the data presented in this study showing nocodazole-resistant structures present in a perinuclear region, upon which annexin A11 accumulates. Acetylated tubulin has been shown to promote the binding of microtubule motors [285,286] and enhance protein trafficking [287]. The enrichment of annexin A11 on nocodazole-resistant structures may therefore reflect a specific association of annexin A11 on stable, acetylated microtubules. The depolymerisation of the rest of the microtubule network could result in a block in the transport of annexin A11 positive vesicles, resulting in their accumulation perinuclearly. It would be of interest to investigate the effect of other microtubule depolymerising agents on

the distribution of annexin A11, such as colchicine which acts in a similar manner to nocodazole [270]. Furthermore one could also determine the effect of hyper- or de-acetylation of tubulin on the localisation of annexin A11 to microtubules, through the inhibition or overexpression of known tubulin deacetylases such as SIRT2 [287,288] and HDAC6 [289].

Chapter Six:
Study of Annexin A11 and the Centrosome

6. Results: Study of Annexin A11 and the Centrosome

The centrosome is also known as the primary microtubule organising centre (MTOC) in animal cells, and as the name suggests it coordinates microtubule nucleation throughout the cell. It comprises two centrioles, arranged at right angles to each other, surrounded by electron dense pericentriolar material (PCM). This structure was initially discovered over 130 years ago by Flemming [290] and later named by Boveri [291]. Since then the centrosome has been implicated in a wide range of processes during both interphase and mitosis; including cell motility, cytokinesis and vesicle trafficking [292].

At interphase the centrosome is in close apposition to the nucleus, where it serves as the MTOC. Core centrosomal components particularly required for this function, include γ tubulin, γTuRC (γ tubulin ring complex) and pericentrin. γ tubulin is a member of the tubulin family present at far lower levels than α and β, which make up the microtubule filaments, but with a vital role in the assembly of these filaments. Purification of γ tubulin from Xenopus egg extracts showed it to be part of a large complex of at least seven different proteins [293]. Electron micrography showed this complex to have a ring structure and it was accordingly coined the γ tubulin ring complex (γTuRC). *In vitro* experiments went on to show that this complex could nucleate microtubules from one end of the filament, namely the minus end where it was shown to bind.

Pericentrin is known to form a complex with γ tubulin [294] and has also been shown to anchor γTuRC to the centrosome via its interaction with γ tubulin complex proteins 2 and 3 (GCP2/3) [295]. It is believed that there may be up to ten different isoforms of this coiled-coil domain protein, however the two major isoforms are pericentrin A and pericentrin B/kendrin [296]. Depletion of both isoforms resulted in defects in mitotic cells, including the loss of γ tubulin at the centrosome and the formation of monopolar spindles. This highlights the importance of the centrosome, not just as an MTOC in interphase cells, but as a regulator of the cell cycle.

During mitosis, chromosome duplication is tightly coupled to the centrosome cycle (Figure 41). At G1 the two parent centrioles separate slightly and lose their orthogonal orientation, before budding off a daughter centriole each. During S phase centrosome duplication

completes, as each daughter centriole has grown to full length, and DNA replication ends. By G2 the cell now contains two parent centrioles and two full length daughter centrioles, bound within the same PCM. At the onset of mitosis, as the chromosomes begin to condense, the new centrosomes, consisting of one parent centriole and one daughter centriole, migrate to opposite poles of the cell [236].

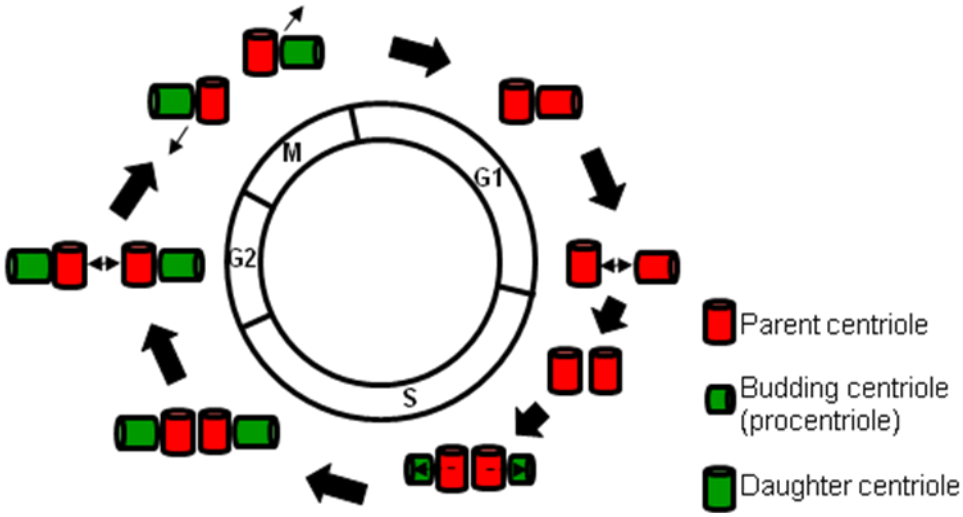

Figure 41 The Centrosome Cycle in Relation to the Stages of the Cell Cycle

The centrosome cell cycle progresses in line with the cell cycle. At G1 (growth phase 1) the parent centrioles separate just enough to allow for their duplication during S phase. At S phase as the DNA replicates the parent centrioles each bud off a daughter centriole. At G2 (growth phase 2) the two new centrosomes separate and during the beginning of mitosis migrate to opposite poles of the dividing cell.

During prometaphase the centrosomes organise three distinct sets of microtubules, all of which serve different purposes during the cell cycle (Figure 42). Polar microtubules radiate out from the centrosome towards the cell equator where they overlap with each other and define the spindle midzone. Astral microtubules radiate out towards the cell cortex, where some will attach to help position the mitotic spindle. Kinetochore microtubules attach to kinetochores at centromeres on the sister chromatids and are responsible for physically pulling apart the chromatids to form their respective chromosomes. This organisation of microtubules allows alignment of the chromatids along the cell equator at metaphase, separation of the chromatids at anaphase and ultimately cell cleavage at the furrow at telophase and cytokinesis. This results in two daughter cells, each containing a centrosome of two centrioles encased in PCM [236].

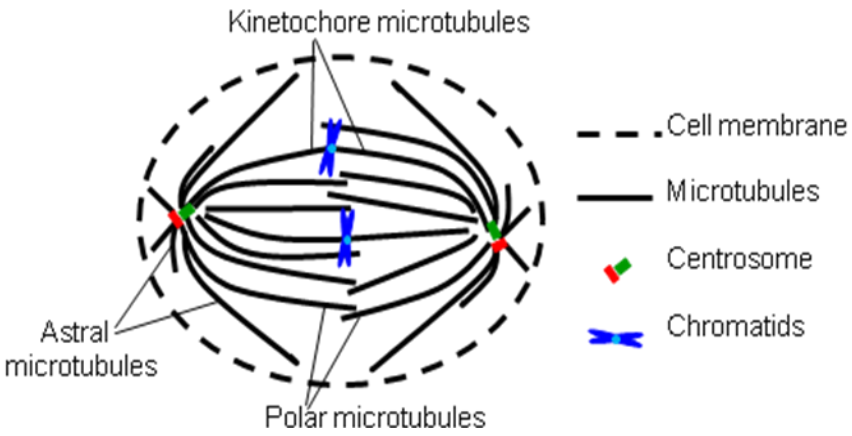

Figure 42 The Three Groups of Microtubules That Comprise The Mitotic Spindle

During mitosis the microtubule network undergoes massive changes in structure in order to accommodate the new functions it must perform. The production of the mitotic spindle results in the formation of three distinct groups of microtubules called kinetochore, astral and polar microtubules. Kinetochore microtubules bind to the chromatids at their centromeres. Astral microtubules extend cortically to anchor the mitotic spindle. Polar microtubules extend towards the cell equator and set the location of the spindle midzone.

It should be noted that during the centrosome cycle, mitotic centrosomes mature and accumulate an array of different centrosome associated proteins that interphase centrosomes lack. Maturation begins at prometaphase when, for example NuMA (Nuclear Mitotic Apparatus Protein) is acquired, as it translocates from the nucleus to the centrosome. Other cell cycle dependent centrosome associated proteins include Plk1 [297], Cdk1 (Cyclin dependent kinase 1) [298] and AurA (Aurora A kinase) [263]. These proteins have also been implicated in cascades controlling cytokinesis [299-301]. The link between the centrosome and cytokinesis has been further strengthened by the discovery of a centriole protein, centriolin, which also localises to the midbody – a protein dense structure at the cleavage furrow crucial for cytokinesis [302]. The knock down of this protein resulted in the failure of cytokinesis, with cells remaining connected by a long intracellular bridge of membrane. This phenotype is also seen with the knockdown of annexin A11 [146]. Further investigation has shown centriolin to interact with exocyst and SNARE complex proteins and to recruit these to the midbody [303], therefore strengthening ideas of the centrosome influencing cytokinesis, perhaps via membrane trafficking.

6.1 Annexin A11 Localises to the Centrosome

The distribution of annexin A11 in PFA fixed cells is both nuclear and cytoplasmic in several cultured lines, including HeLa and A431 [146,147,150]. Methanol fixation retains the nuclear and cytoplasmic distribution of annexin A11 (Figure 43A), however the signal is diminished and exposes more distinct puncta within the cytoplasm that would otherwise be obscured. It is in this manner that the co-localisation of annexin A11 with the centrosome can be observed. HeLa cells were fixed in methanol and stained for annexin A11 using a polyclonal goat antibody against annexin A11, and pericentrin, a known component of the centrosome [294,304], using a polyclonal rabbit antibody against pericentrin. The cells were then imaged on an inverted confocal microscope. Annexin A11 and pericentrin co-localised at the centrosome (Figure 43A).

In order to confirm that this co-localisation was not due to cross talk between the two fluorescent channels used to visualise annexin A11 and pericentrin (FITC and Cy5 respectively), secondary antibody controls were carried out. Cells were stained with both primary antibodies and then incubated with either FITC conjugated donkey anti-goat antibody or Cy5 conjugated donkey anti-rabbit antibody. Images were taken in both FITC and Cy5 channels. No bleed through between the channels was detected (Figure 43B). Primary antibody controls were also carried out to confirm that the staining was not due to non-specific binding to the centrosome. Normal immunoglobulin G (IgG) corresponding to the species in which the primary antibodies were raised in, was used instead of the antigen specific primary antibodies. Cells were then incubated with the appropriate secondary antibody. No non-specific staining was seen for the rabbit IgG. Although there was some faint background in the goat IgG contol, there were no discrete puncta as detected when the polyclonal goat anti-annexin A11 antibody was used.

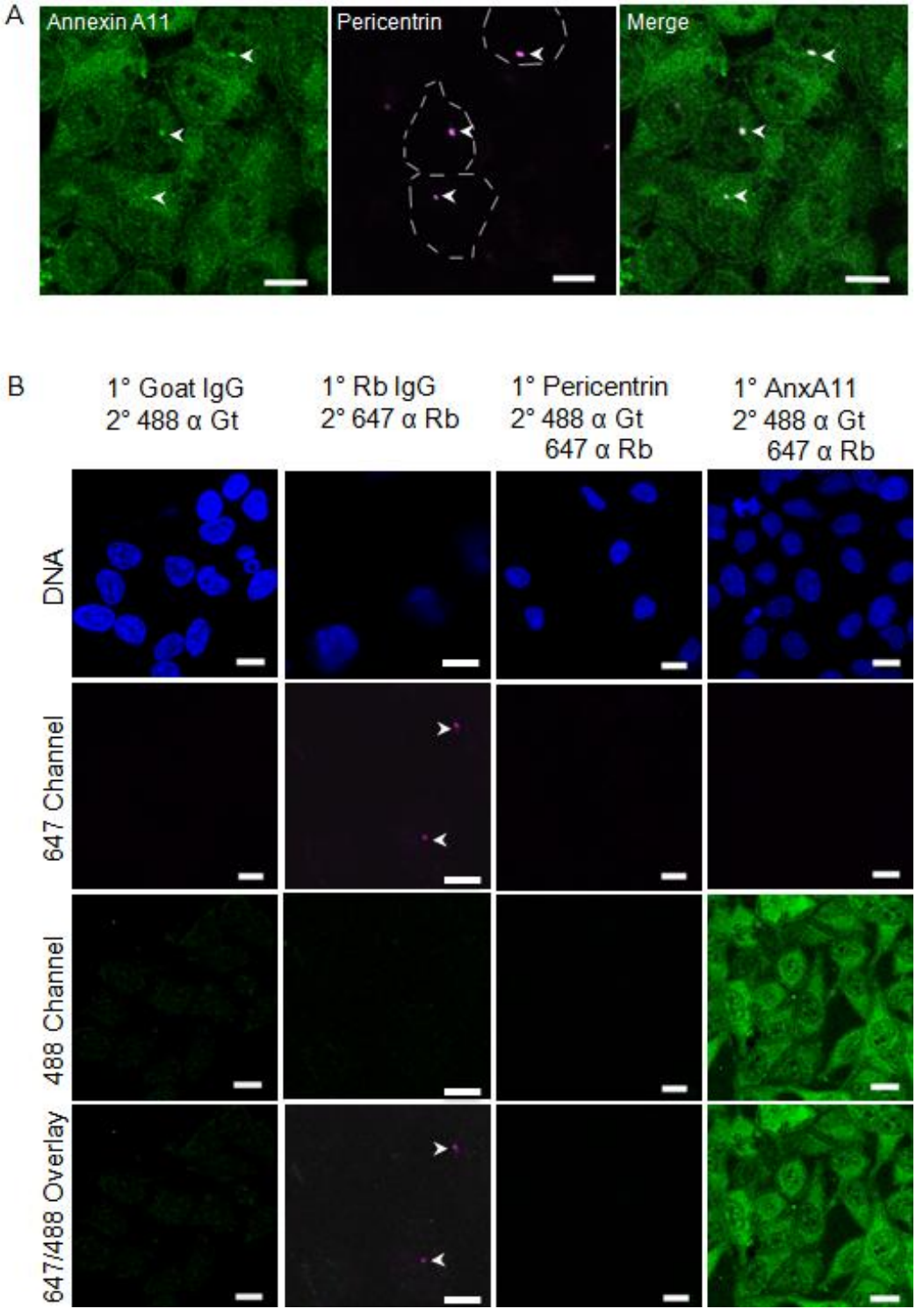

Figure 43 Annexin A11 Colocalises with Pericentrin

(A) HeLa cells were fixed in methanol and stained for annexin A11 using a polyclonal goat anti annexin A11 antibody (1/50 dilution), pericentrin using a polyclonal rabbit anti pericentrin antibody (1/1000 dilution) and DNA using DAPI (1/500 dilution). **(B)** HeLa cells were fixed in methanol and subjected to primary and secondary antibody controls. Centrosomes (arrowheads) (Scale Bar 10μm)

The co-localisation of pericentrin and annexin A11 was quantified in 20 cells using line scan analysis (Figure 44A). Line scans were taken across the cells and passed through the centrosome, as determined by pericentrin staining. The signals for both annexin A11 and pericentrin were plotted against the position along the line scan. Pericentrin is represented by a singular, sharp peak. Annexin A11 is represented by several small peaks corresponding to the diffuse, cytoplasmic distribution. In addition, there is a large, sharp peak which overlaps with the peak in pericentrin staining – this overlap corresponds to the co-localisation of these two proteins (Figure 44A, Graph (a)). An average graph was plotted from 20 such line scans, where the maximal pericentrin signal was used as a standard point against which all the line scans were set. The signals for annexin A11 and pericentrin were therefore plotted against the position relative to the peak pericentrin signal. Pericentrin is represented by a singular peak, slightly broader than that seen in individual traces due to the variation in the length of the pericentrin signal between cells. Annexin A11 is also represented by a singular, broad peak. The smaller peaks seen in individual traces representing the diffuse, cytoplasmic staining are no longer visible due to averaging. The broad annexin A11 and pericentrin peaks clearly overlap, again illustrating the co-localisation of these two proteins (Figure 44A, Graph (b)). Pericentrin however does not co-localise with annexin A2 or annexin A7, which has the highest degree of homology with annexin A11 (Figure 44B). The co-localisation between annexin A11 and pericentrin occurs throughout the cell cycle (Figure 45) at metaphase, anaphase, telophase and cytokinesis. At metaphase and anaphase pericentrin and annexin A11 are localised at both centrosomes of the dividing cell at opposite poles. At telophase and cytokinesis the extreme, polarised localisation of the centrosomes is lost and the two centrosomes are each clearly localised within each of the two prospective daughter cells. In both instances pericentrin and annexin A11 co-localise.

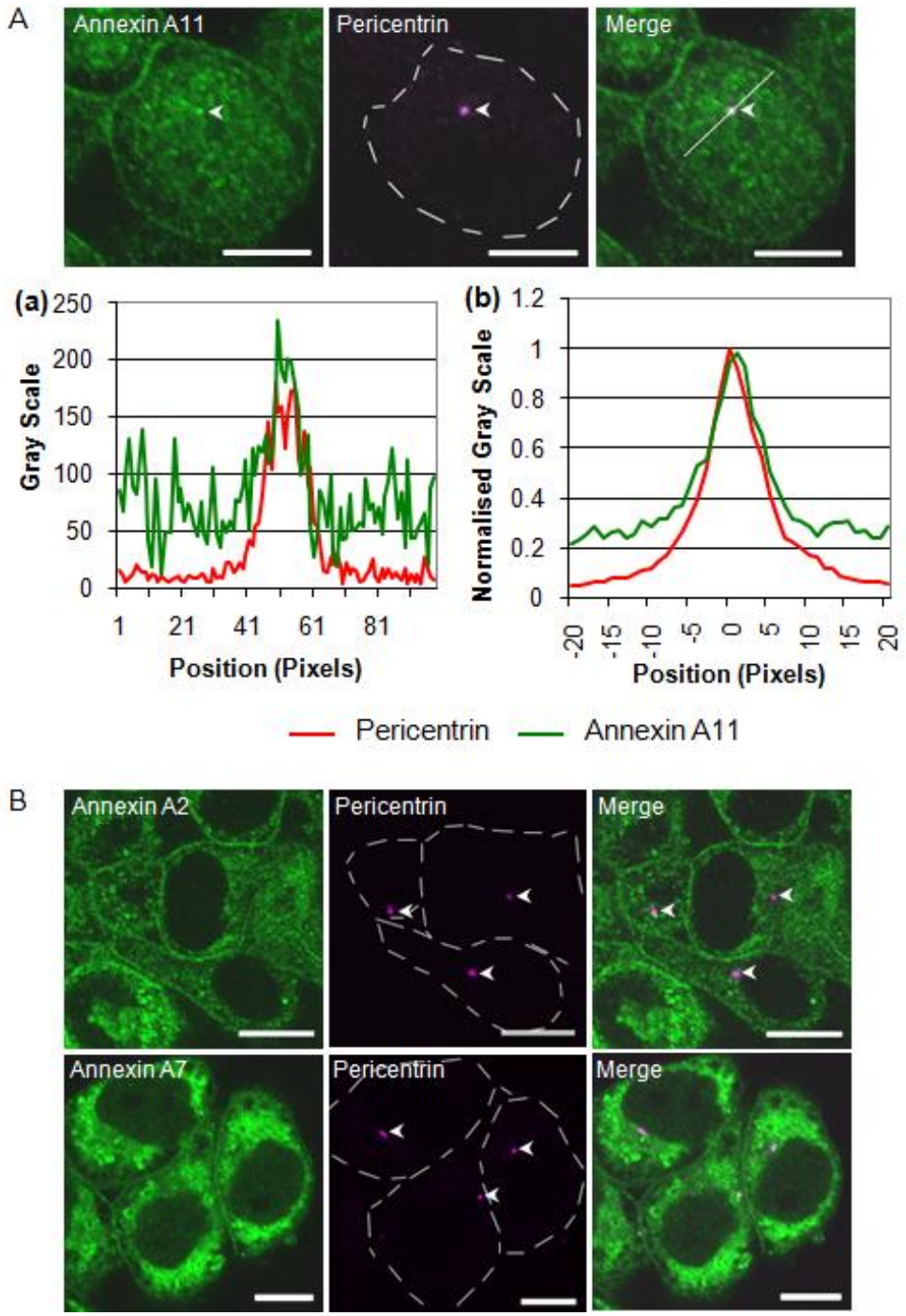

Figure 44 Annexin A11, but not A2 or A7, Colocalises with Pericentrin

HeLa cells were fixed in methanol and stained for pericentrin using a polyclonal rabbit anti-pericentrin antibody (1/1000 dilution), DNA using DAPI (1/500 dilution) and either annexin A11 using a polyclonal goat anti-annexin A11 antibody (1/50 dilution) or annexin A7 using a polyclonal goat anti-annexin A11 antibody (1/50 dilution) or annexin A2 using a polyclonal rabbit anti-annexin A2 antibody (1/60 dilution). **(A)** Line scan through the point of co-localisation (line in merge) between annexin A11 and pericentrin plotted in graph (a). Average of 20 such line scans shown in graph (b). Gray scale normalised to the maximal pericentrin value. Position denoted as plus or minus pixels from the pericentrin peak. **(B)** Absence of co-localisation between pericentrin and annexins A2 and A7. Centrosomes (arrowheads) (Scale Bar 10µm)

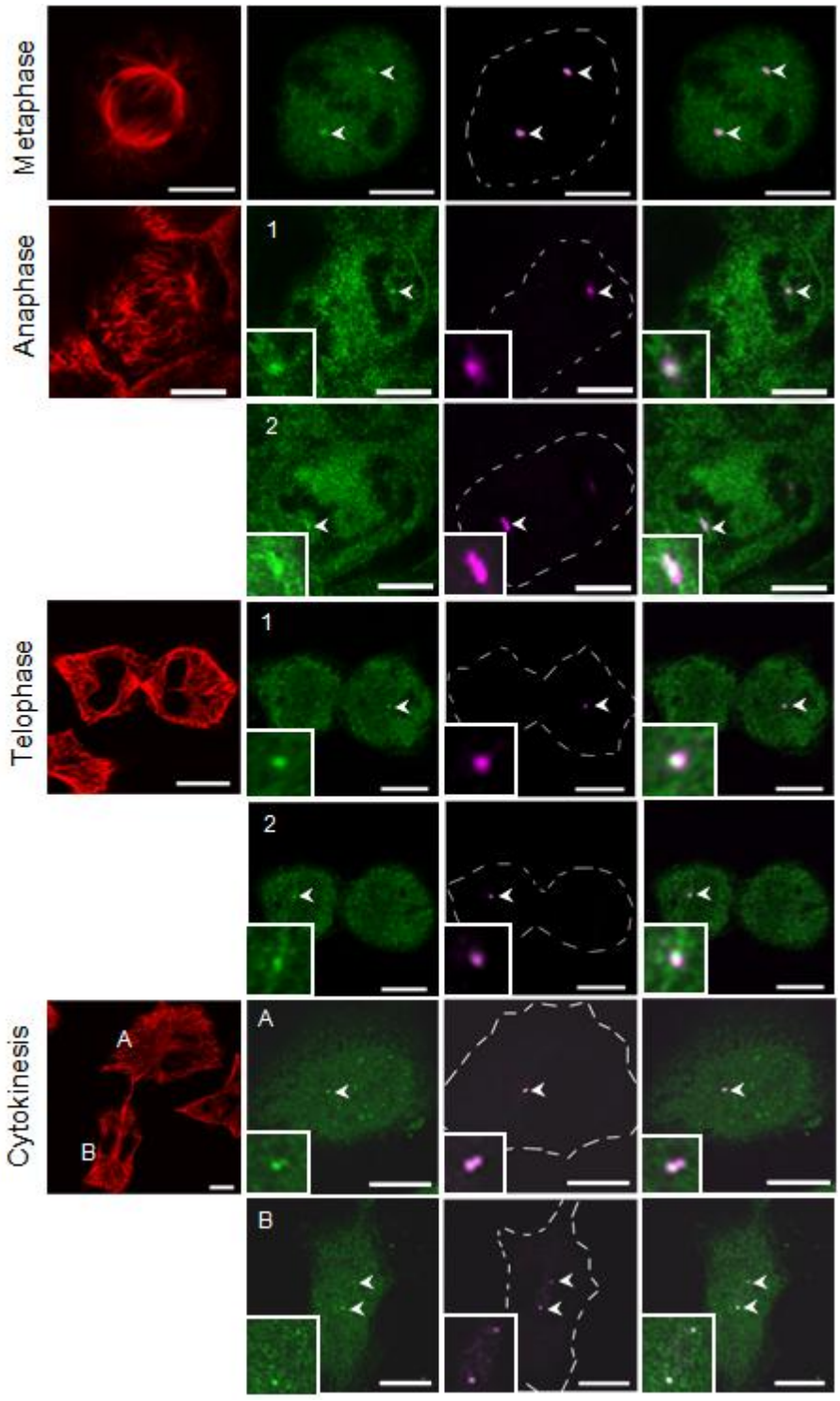

Figure 45 Annexin A11 Co-localises with Pericentrin During the Cell Cycle

HeLa cells were fixed in methanol and stained for annexin A11 using a polyclonal goat-anti annexin A11 antibody (1/50 dilution), pericentrin using a polyclonal rabbit anti-pericentrin antibody (1/1000 dilution) and tubulin using a monoclonal mouse anti-alpha tubulin antibody (1/100 dilution). At anaphase and telophase two focal planes (1, 2) are depicted per cell in order to show both centrosomes. At telophase each daughter cell is shown in a zoom (A, B). Centrosomes (arrowheads) (Scale Bar 10µm)

The co-localisation of annexin A11 and the centrosome was confirmed with a second centrosomal marker, γ tubulin (Figure 46A). Primary and secondary antibody controls again showed that this co-localisation was not due to either non-specific centrosomal binding or cross talk between the fluorescent channels, respectively (Figure 46B). Line scans were taken across cells passing through the centrosome, in this case as defined by γ tubulin staining (Figure 47A). Individual line scans showed a singular, sharp peak representing γ tubulin and a series of smaller peaks as well as a large, sharp peak representing annexin A11. The two large, sharp peaks overlapped (Figure 47A, Graph (a)). This was recapitulated in an average of 20 such line scans, which show a clear overlap between the peak in annexin A11 signal and the peak in γ tubulin signal (Figure 47A, Graph (b)), indicating the co-localisation of these two proteins. However γ tubulin did not co-localise with annexin A2 or annexin A7 (Figure 47B), demonstrating that this is not simply a generic property of annexins. The co-localisation between annexin A11 and γ tubulin also occurs throughout the cell cycle, from metaphase through to cytokinesis in the same manner as pericentrin and annexin A11 (Figure 48A).

The centrosome is known to expand at metaphase due to an increase in the distribution of the pericentriolar matrix. The distribution of annexin A11 at the centrosome also appears to expand at metaphase. The increase in size of the centrosome between interphase and metaphase was quantified using Image J, as determined by the area of γ tubulin staining (Figure 48B). The area of γ tubulin at the centrosome increased from 0.63 μm^2 (+/- 0.18 μm^2) at interphase to 1.29 μm^2 (+/- 0.15 μm^2) at metaphase i.e. the centrosome roughly doubles in size (P=0.00052, two tailed student t-test). The area of annexin A11 at the centrosome was also measured and increased from 0.45 μm^2 (+/- 0.18 μm^2) at interphase to 0.86 μm^2 (+/- 0.15 μm^2) at metaphase – again showing an approximate doubling in size (P=0.0015, two tailed students t-test), though remaining smaller than the total area of the centrosome itself.

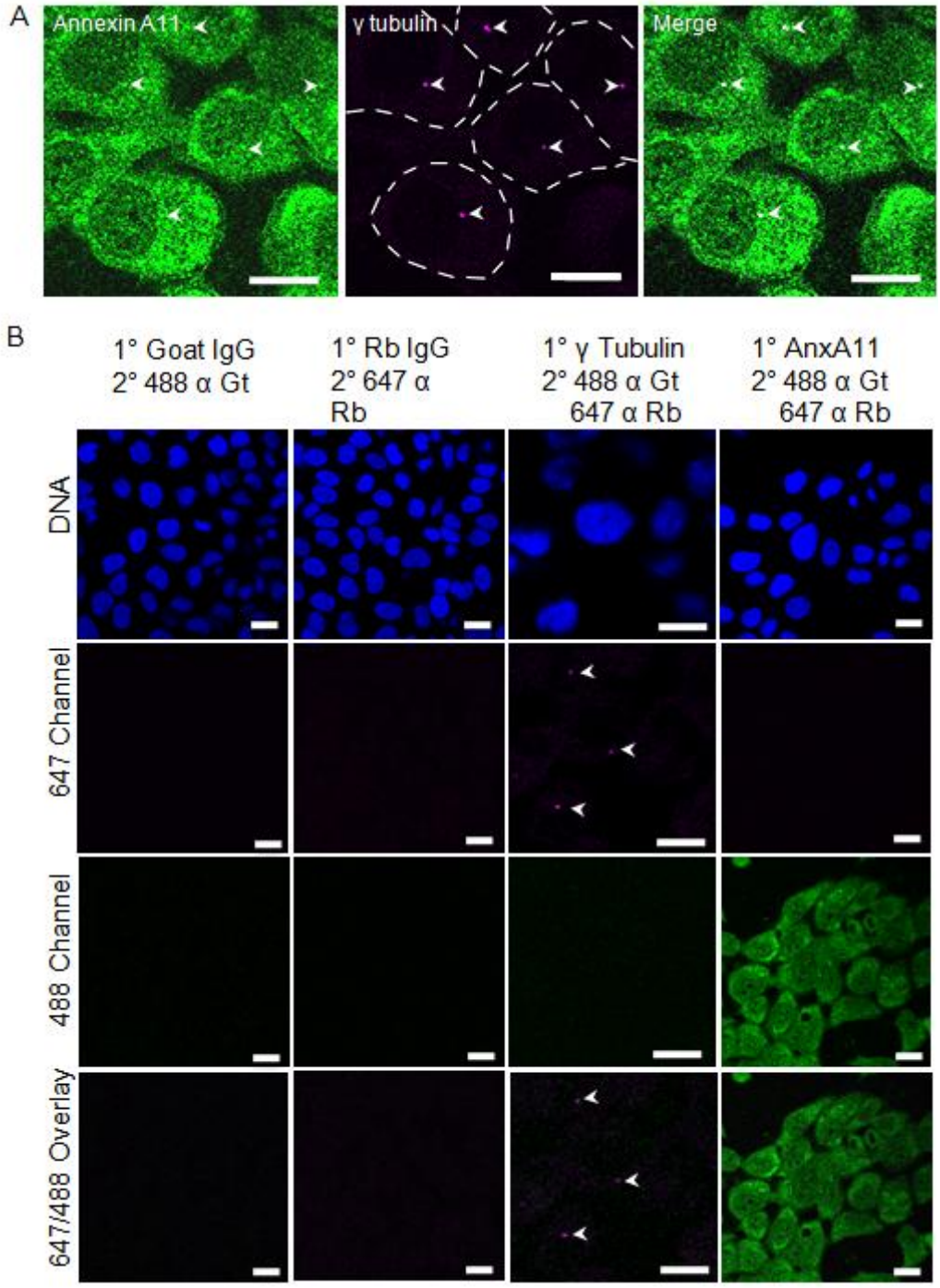

Figure 46 Annexin A11 Colocalises with γ Tubulin

(A) HeLa cells were fixed in methanol and stained for annexin A11 using a polyclonal goat anti-annexin A11 antibody (1/50 dilution), γ tubulin using a polyclonal rabbit anti-γ tubulin antibody (1/1000 dilution) and DNA using DAPI (1/500 dilution). **(B)** HeLa cells were fixed in methanol and subjected to primary and secondary antibody controls. Centrosomes (arrowheads) (Scale Bar 10μm)

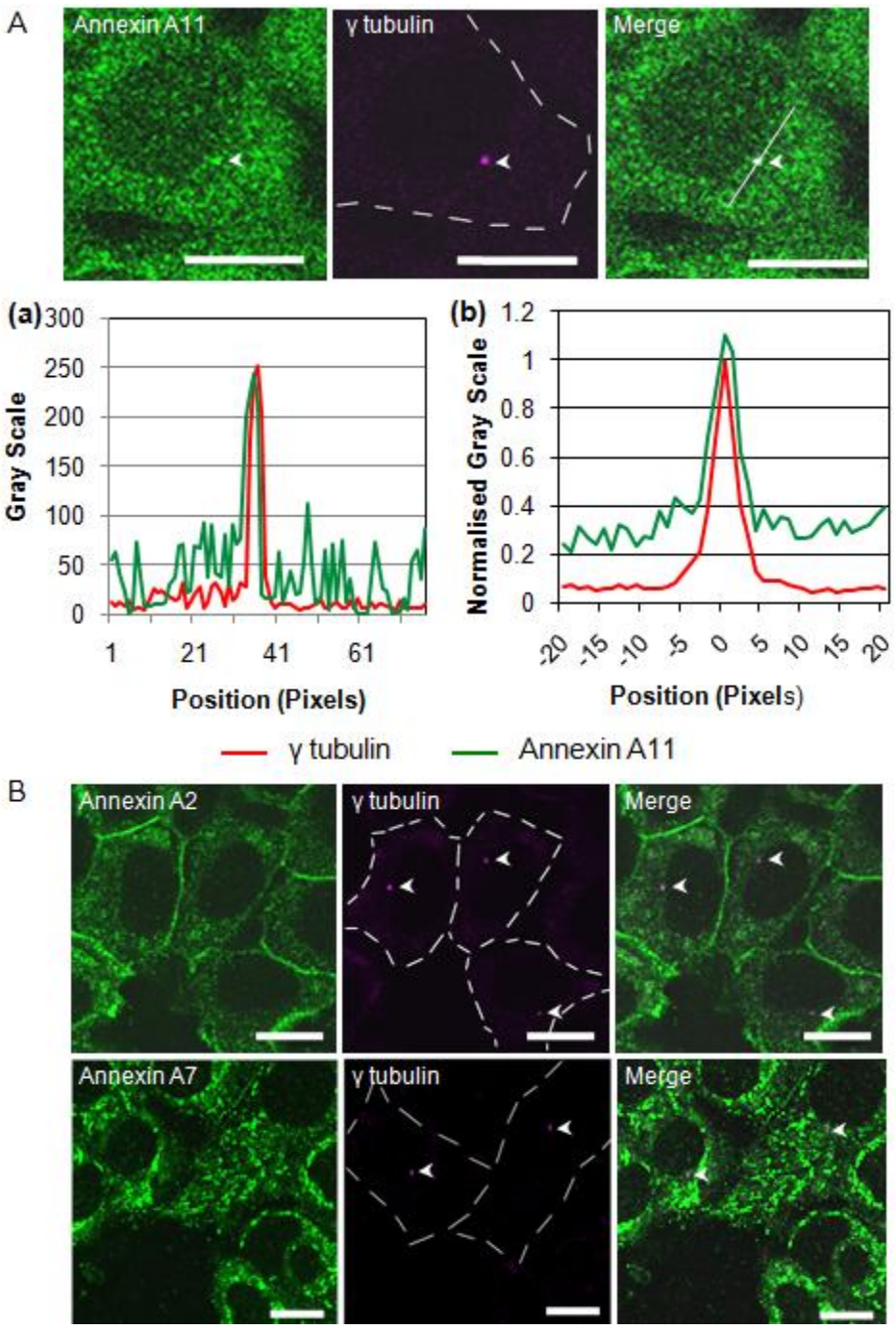

Figure 47 Annexin A11, but not A2 or A7, Colocalises with γ Tubulin

HeLa cells were fixed in methanol and stained for γ tubulin using a polyclonal rabbit anti-γ tubulin antibody (1/1000 dilution), DNA using DAPI (1/500 dilution) and either annexin A11 using a polyclonal goat anti-annexin A11 antibody (1/50 dilution) or annexin A7 using a polyclonal goat anti-annexin A11 antibody (1/50 dilution) or annexin A2 using a polyclonal rabbit anti-annexin A2 antibody (1/60 dilution). **(A)** Line scan through the point of co-localisation (line in merge) between annexin A11 and γ tubulin plotted in graph (a). Average of 20 such line scans shown in graph (b). Gray scale normalised to the maximal γ tubulin value. Position denoted as plus or minus pixels from the γ tubulin peak. **(B)** Absence of co-localisation between γ tubulin and annexins A2 and A7. Centrosomes (arrowheads) (Scale Bar 10μm)

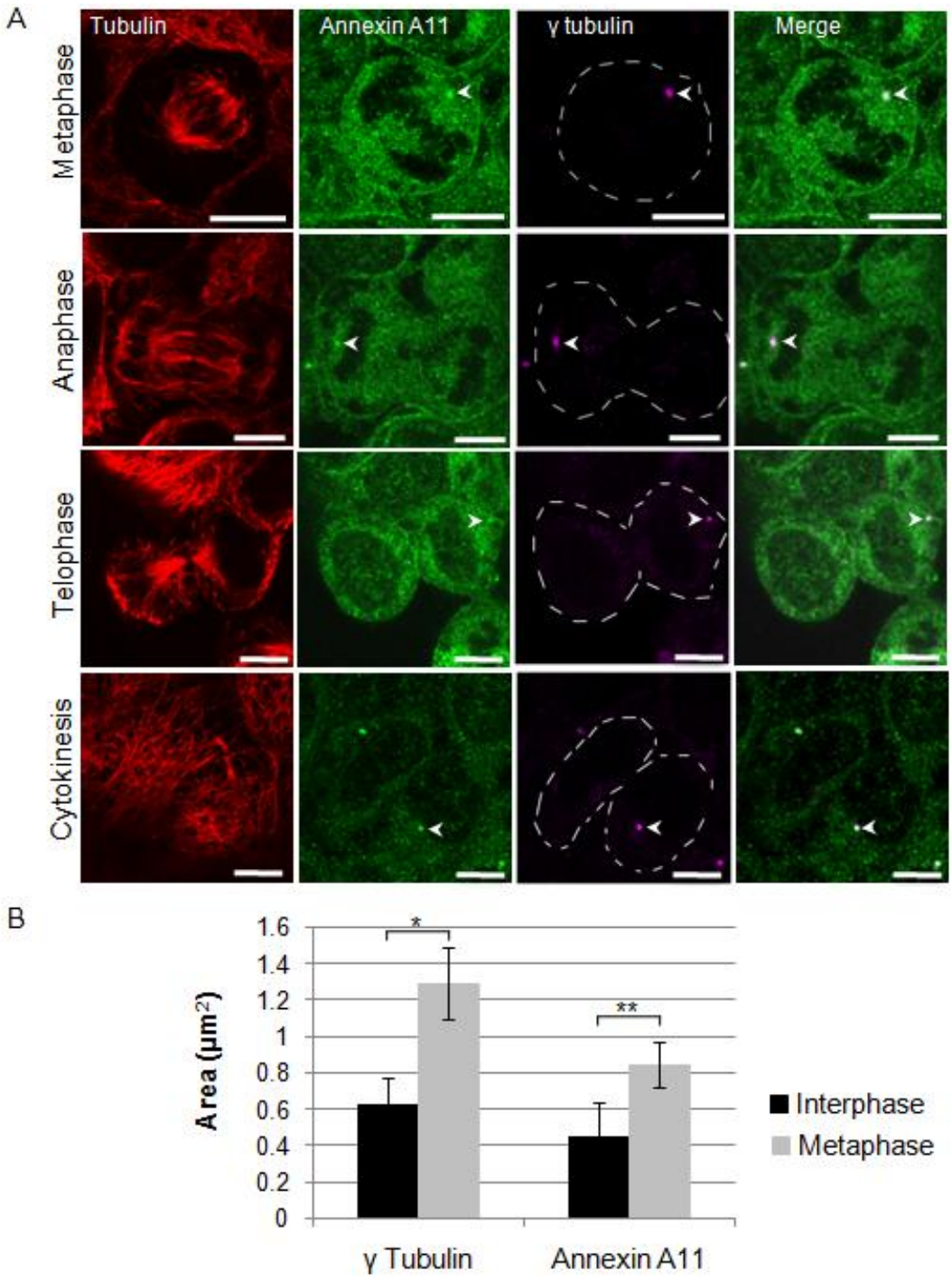

Figure 48 Annexin A11 Co-localises with γ Tubulin During the Cell Cycle

(A) HeLa cells were fixed in methanol and stained for annexin A11 using a polyclonal goat anti-annexin A11 antibody (1/50 dilution), γ tubulin using a polyclonal rabbit anti-γ tubulin antibody (1/1000 dilution) and tubulin using a monoclonal mouse anti-alpha tubulin antibody (1/100 dilution). Centrosomes (arrowheads). A single focal plane is shown per cell depicting one of the two centrosomes within the dividing cell. (Scale Bar 10μm) **(B)** The area of the centrosome, as detected by γ tubulin staining was measured using Image J (1.40g) in cells at interphase (n=21) and metaphase (n=4). The same was done for the annexin A11 puncta that colocalised here with γ tubulin. Error bars are standard deviations. * P=0.00052 ** P=0.0015

6.2 Annexin A11 Knock Down and the Centrosome

In order to determine whether the localisation of annexin A11 at the centrosome had an effect on the centrosome itself, annexin A11 was depleted using siRNA. Cells were plated at 30% confluency and transfected the next day with 20µM annexin A11 siRNA or 20µM negative control siRNA. Cells were transfected with siRNA again three days after plating. Cells were lysed on 2, 3 and 6 days after plating and subjected to SDS-PAGE and Western blotting. The knock down of annexin A11 was carried out in A431, HeLa and CaCo-2 cells and in all three cases significant knock down of annexin A11 was achieved, as detected by Western blotting against annexin A11 and tubulin (Figure 35A). Annexin A11 proteins levels were normalised to tubulin in three independent knock down experiments for each cell line. By day 6 annexin A11 levels had decreased by 95% in A431 cells, 82% in HeLa cells and 89% in CaCo-2 cells (Figure 35B).

The knockdown of annexin A11 was confirmed by immunofluorescence of annexin A11 in A431 cells. Cells were methanol fixed on day 6, following two rounds of transfection with siRNA, and stained for annexin A11, alpha tubulin, DNA and γ tubulin. Cells were imaged at different stages of the cell cycle on an inverted confocal microscope. At metaphase (Figure 49) and anaphase (Figure 50) in both control and annexin A11 depleted cells, γ tubulin is located at both the poles of the mitotic spindle marking out each of the two centrosomes. At telophase, following mitotic spindle disassembly, the centrosomes are no longer localised at the extreme opposite ends of the cell. The two centrosomes, as detected by γ tubulin staining, can clearly be seen to localise within each of the two prospective daughter cells in both control and annexin A11 depleted cells (Figure 51). Therefore the centrosome is present in annexin A11 depleted cells and its localisation throughout the cell cycle appears unchanged relative to control cells.

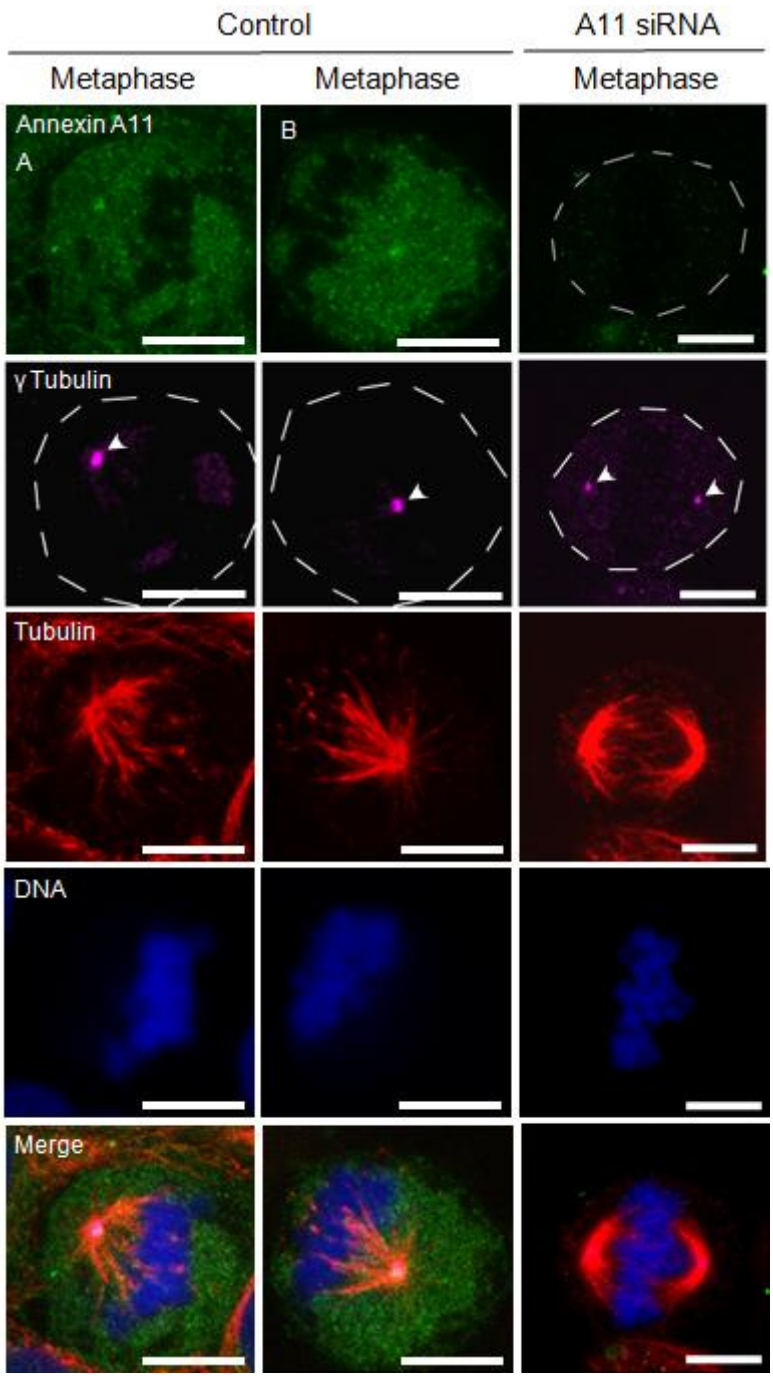

Figure 49 Annexin A11 Knock Down Does Not Affect the Distribution of γ Tubulin at Metaphase

A431 cells were treated with 20µM annexin A11 siRNA or 20µM scrambled control siRNA for 6 days, with two treatments administered on day 1 and day 3. Cells were then methanol fixed on day 6 and stained for annexin A11 using a polyclonal goat anti-annexin A11 antibody (1/50 dilution), γ tubulin using a polyclonal rabbit anti-γ tubulin antibody (1/1000 dilution), tubulin using a monoclonal mouse anti-alpha tubulin antibody (1/100 dilution) and DNA using DAPI (1/500 dilution). In instances where the two centosomes of a dividing cell could not be seen in one focal plane, two focal planes (A, B) are shown at the level of each centrosome. Centrosomes (arrowheads) (Scale bars 10µm)

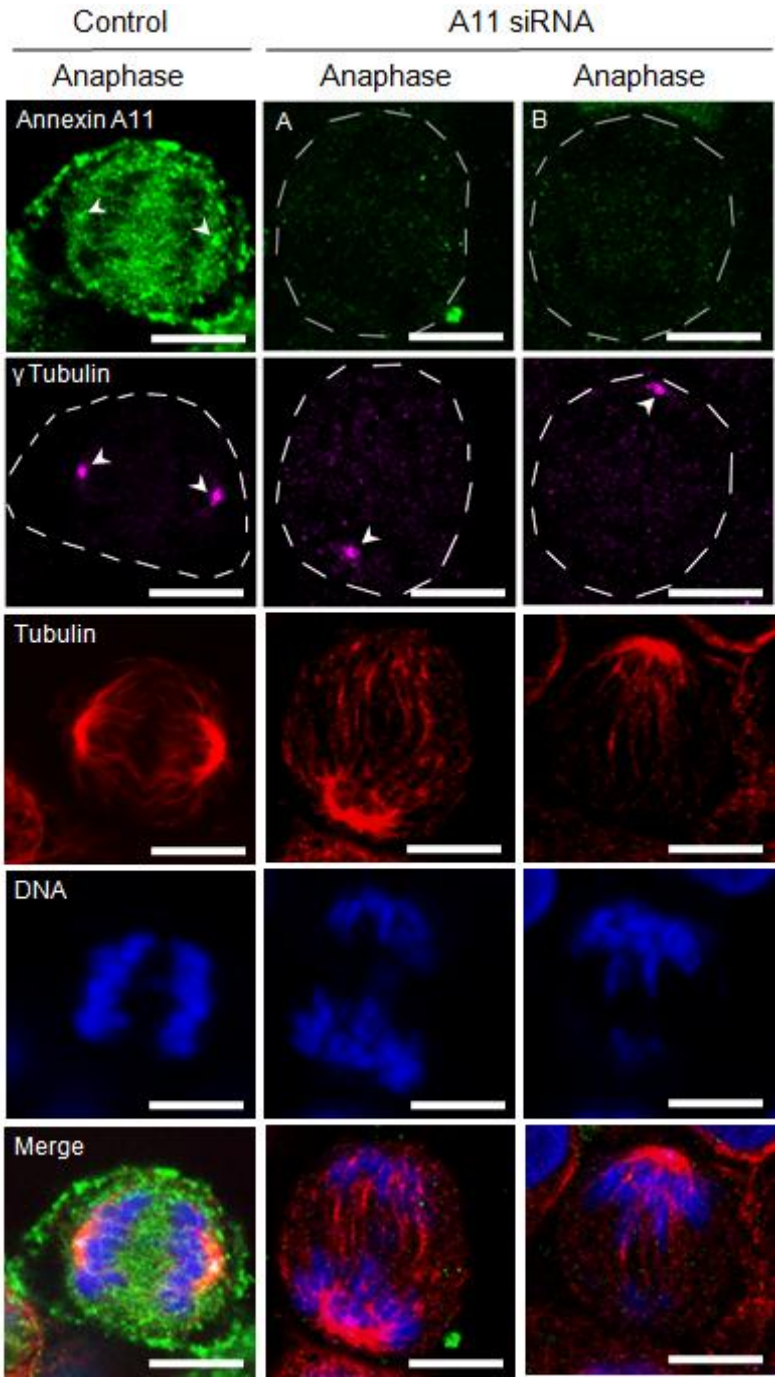

Figure 49 Annexin A11 Knock Down Does Not Affect the Distribution of γ Tubulin at Anaphase

A431 cells were treated with 20µM annexin A11 siRNA or 20µM scrambled control siRNA for 6 days, with two treatments administered on day 1 and day 3. Cells were then methanol fixed on day 6 and stained for annexin A11 using a polyclonal goat anti-annexin A11 antibody (1/50 dilution), γ tubulin using a polyclonal rabbit anti-γ tubulin antibody (1/1000 dilution), tubulin using a monoclonal mouse anti-alpha tubulin antibody (1/100 dilution) and DNA using DAPI (1/500 dilution). In instances where the two centosomes of a dividing cell could not be seen in one focal plane, two focal planes (A, B) are shown at the level of each centrosome. Centrosomes (arrowheads) (Scale bars 10µm)

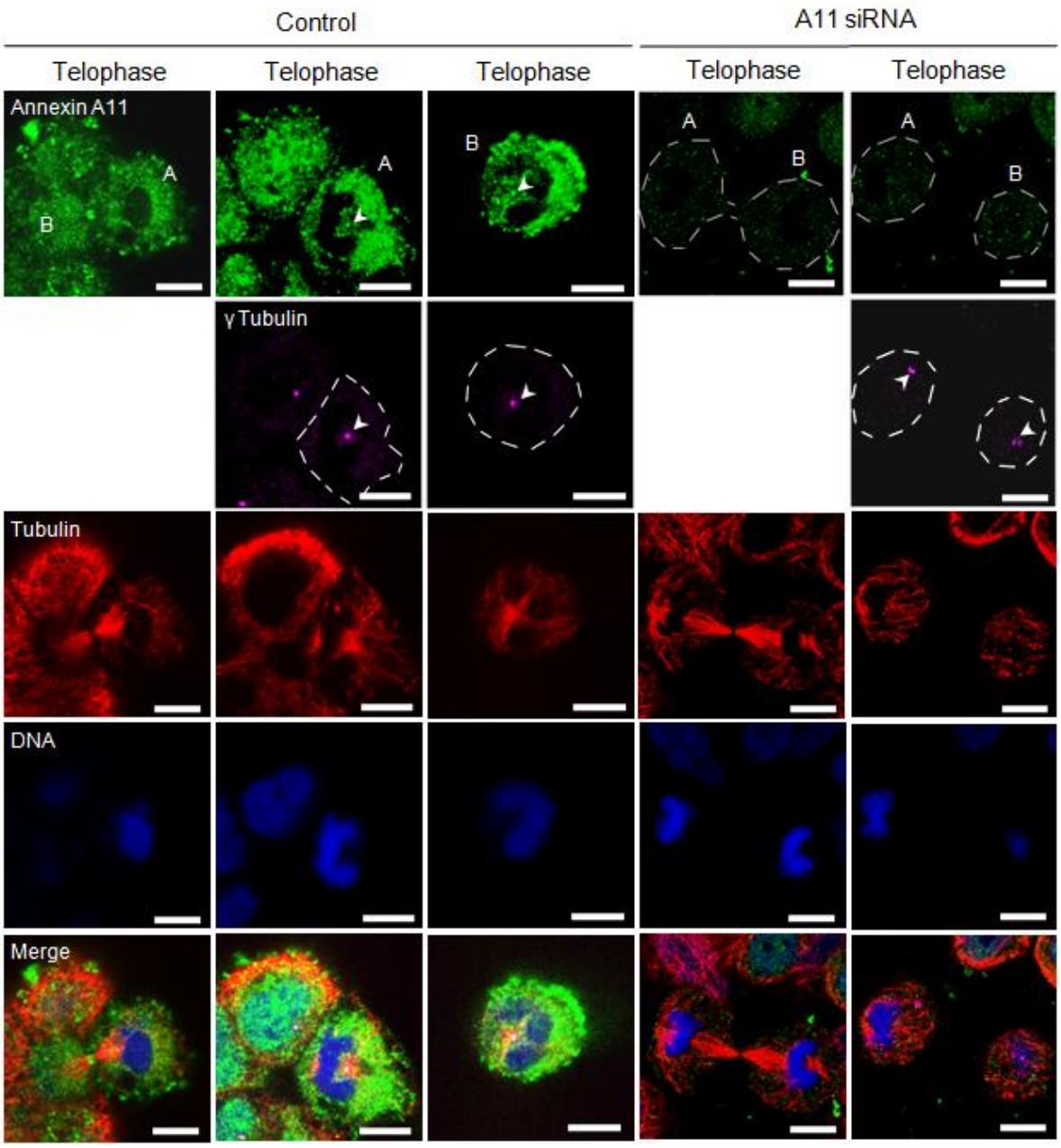

Figure 50 Annexin A11 Knock Down Does Not Affect the Distribution of γ Tubulin at Telophase

A431 cells were treated with 20μM annexin A11 siRNA or 20μM scrambled control siRNA for 6 days, with two treatments administered on day 1 and day 3. Cells were then methanol fixed on day 6 and stained for annexin A11 using a polyclonal goat anti-annexin A11 antibody (1/50 dilution), γ tubulin using a polyclonal rabbit anti-γ tubulin antibody (1/1000 dilution), tubulin using a monoclonal mouse anti-alpha tubulin antibody (1/100 dilution) and DNA using DAPI (1/500 dilution). In instances where the two centosomes of a dividing cell could not be seen in one focal plane, two focal planes (A, B) are shown at the level of each centrosome. Centrosomes (arrowheads) (Scale bars 10μm)

6.3 Annexin A11 Knock Down and Cell Cycle Markers

The depletion of annexin A11 had no detectable effect on the localisation of the centrosome, as detected by γ tubulin staining. In order to determine whether there were effects on other proteins involved in the cell cycle, several cell cycle markers were stained for in A431 cells depleted of annexin A11 for 6 days. Cells were PFA fixed and stained for annexin A11, alpha tubulin, DNA and either Plk1 (polo-like kinase 1), aurora B (aurora B kinase) or INCENP (Inner Centromere protein). Cells were then imaged on an inverted confocal microscope at different stages of the cell cycle.

In control cells Plk1 localised to the centrosomes at the spindle poles at metaphase (Figure 52). At anaphase Plk1 localised to the spindle midzone (Figure 53) and at telophase to the cleavage furrow, either side of the midbody (Figure 53). These localisations were unchanged in annexin A11 depleted cells. In control cells at metaphase aurora B was localised to puncta on the condensed chromosomes (Figure 54). At anaphase aurora B localised to the spindle midzone (Figure 54) and at telophase to the cleavage furrow, either side of the midbody (Figure 55). These localisations were also unchanged in annexin A11 depleted cells. INCENP also localised to the condensed chromosomes as metaphase (Figure 56), the spindle midzone at anaphase (Figure 56) and the cleavage furrow, either side of the midbody, at telophase (Figure 57). These localisations were the same in both control and annexin A11 depleted cells. The knockdown of annexin A11 therefore does not alter the distribution of a range of cell cycle markers.

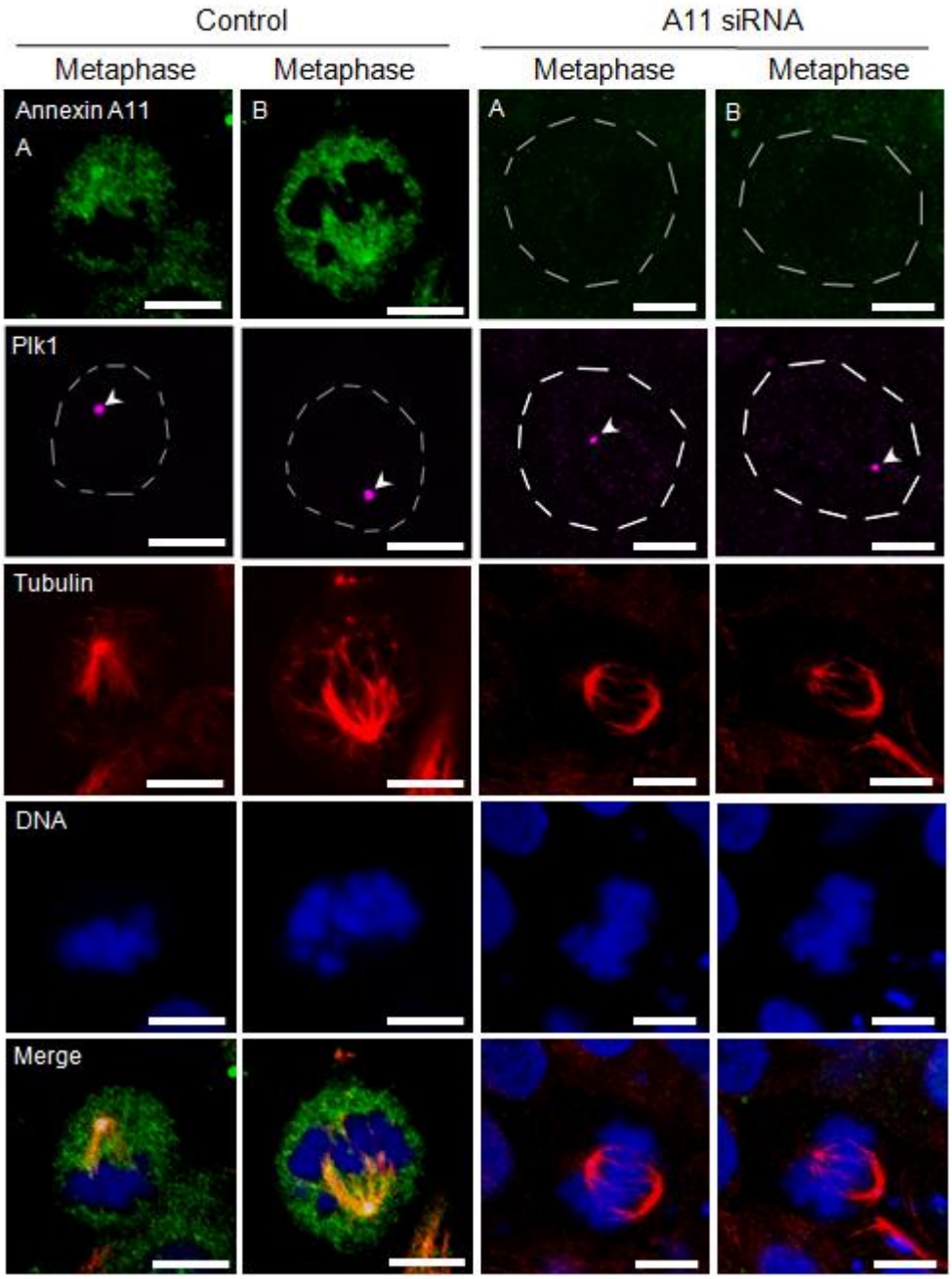

Figure 51 Annexin A11 Knock Down Does Not Affect the Distribution of Polo-like Kinase 1 at Metaphase

A431 cells were treated with 20µM annexin A11 siRNA or 20µM scrambled control siRNA for 6 days, with two treatments administered on day 1 and day 3. Cells were then PFA fixed on day 6 and stained for annexin A11 using a polyclonal goat anti-annexin A11 antibody (1/50 dilution), Plk1 using a polyclonal rabbit anti-Plk1 antibody (1/1000 dilution), tubulin using a monoclonal mouse anti-alpha tubulin antibody (1/100 dilution) and DNA using DAPI (1/500 dilution). In instances where the localisations of Plk1 cannot be seen in one focal plane, two focal planes (A, B) within the same cell are shown. Centrosomes (arrowheads) (Scale bars 10µm)

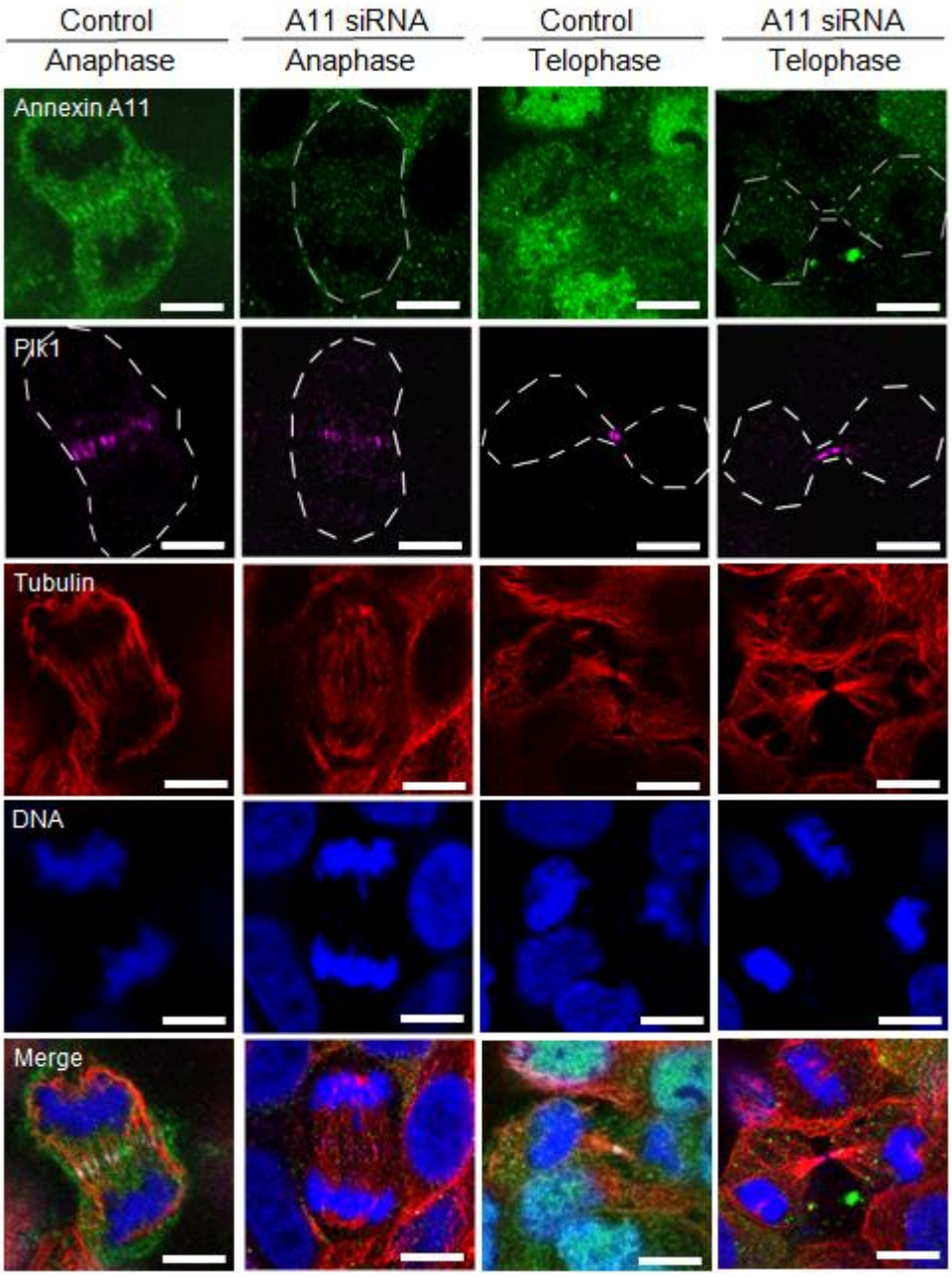

Figure 52 Annexin A11 Knock Down Does Not Affect the Distribution of Polo-like Kinase 1 at Anaphase or Telophase

A431 cells were treated with 20µM annexin A11 siRNA or 20µM scrambled control siRNA for 6 days, with two treatments administered on day 1 and day 3. Cells were then PFA fixed on day 6 and stained for annexin A11 using a polyclonal goat anti-annexin A11 antibody (1/50 dilution), Plk1 using a polyclonal rabbit anti-Plk1 antibody (1/1000 dilution), tubulin using a monoclonal mouse anti-alpha tubulin antibody (1/100 dilution) and DNA using DAPI (1/500 dilution). (Scale bars 10µm)

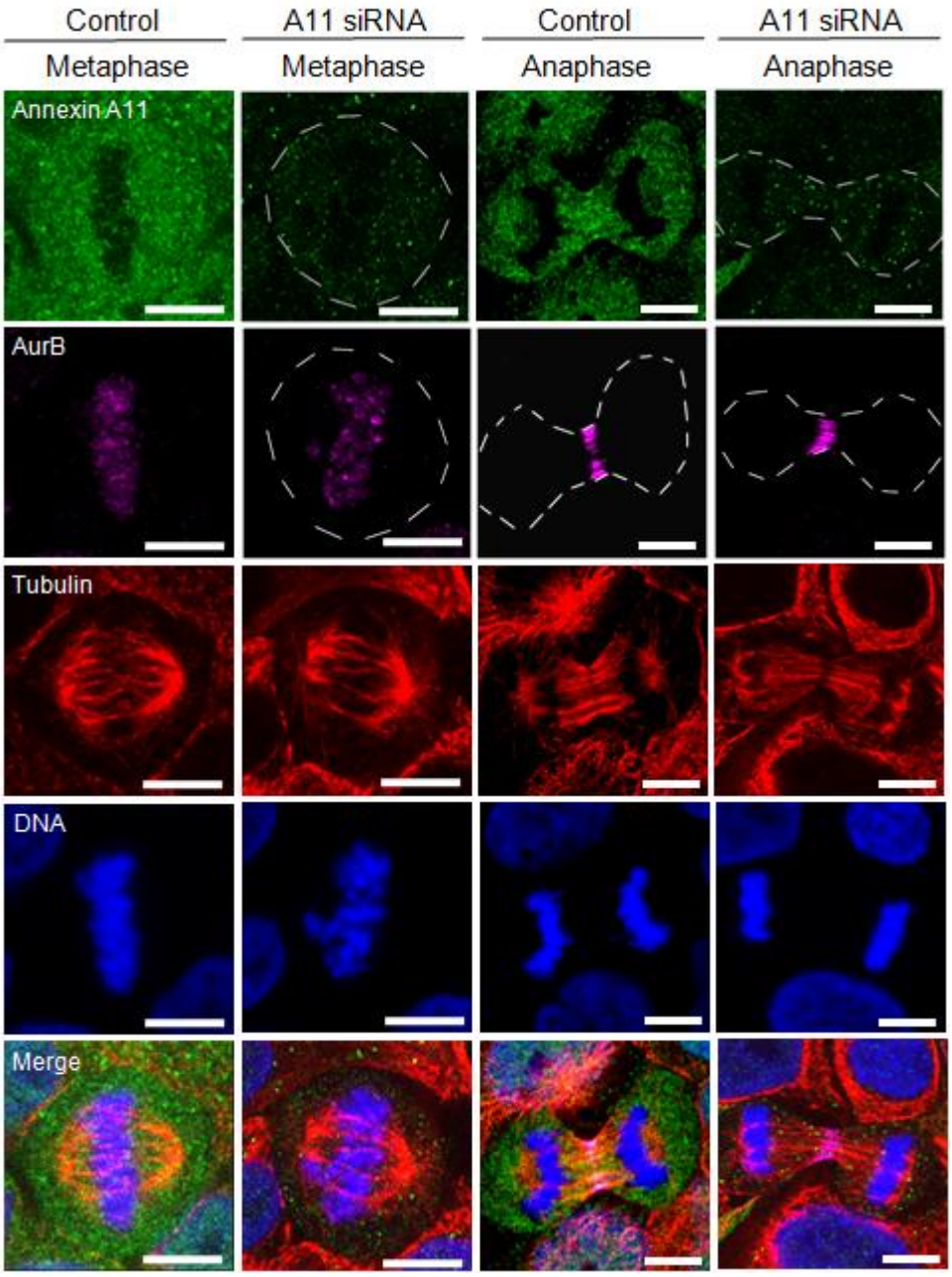

Figure 53 Annexin A11 Knock Down Does Not Affect the Distribution of Aurora B Kinase at Metaphase or Anaphase

A431 cells were treated with 20µM annexin A11 siRNA or 20µM scrambled control siRNA for 6 days, with two treatments administered on day 1 and day 3. Cells were then PFA fixed on day 6 and stained for annexin A11 using a polyclonal goat anti-annexin A11 antibody (1/50 dilution), Aurora B kinase using a polyclonal rabbit anti-Aurora B kinase antibody (1/1000 dilution), tubulin using a monoclonal mouse anti-alpha tubulin antibody (1/100 dilution) and DNA using DAPI (1/500 dilution). (Scale bars 10µm)

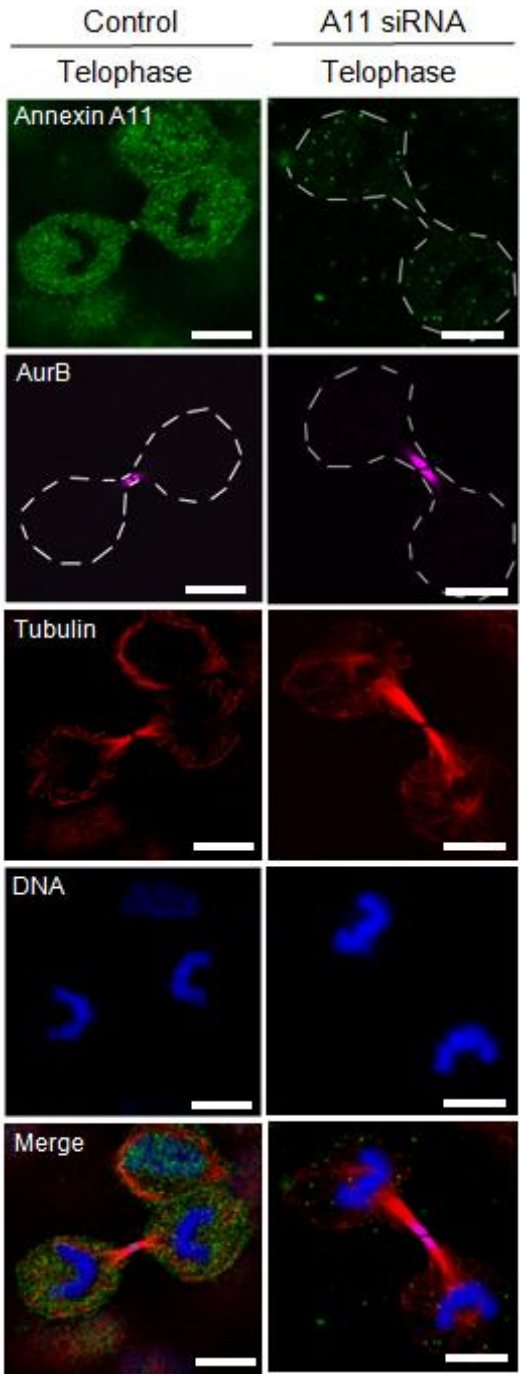

Figure 54 Annexin A11 Knock Down Does Not Affect the Distribution of Aurora B Kinase at Telophase

A431 cells were treated with 20µM annexin A11 siRNA or 20µM scrambled control siRNA for 6 days, with two treatments administered on day 1 and day 3. Cells were then PFA fixed on day 6 and stained for annexin A11 using a polyclonal goat anti-annexin A11 antibody (1/50 dilution), Aurora B kinase using a polyclonal rabbit anti-Aurora B kinase antibody (1/1000 dilution), tubulin using a monoclonal mouse anti-alpha tubulin antibody (1/100 dilution) and DNA using DAPI (1/500 dilution). (Scale bars 10µm)

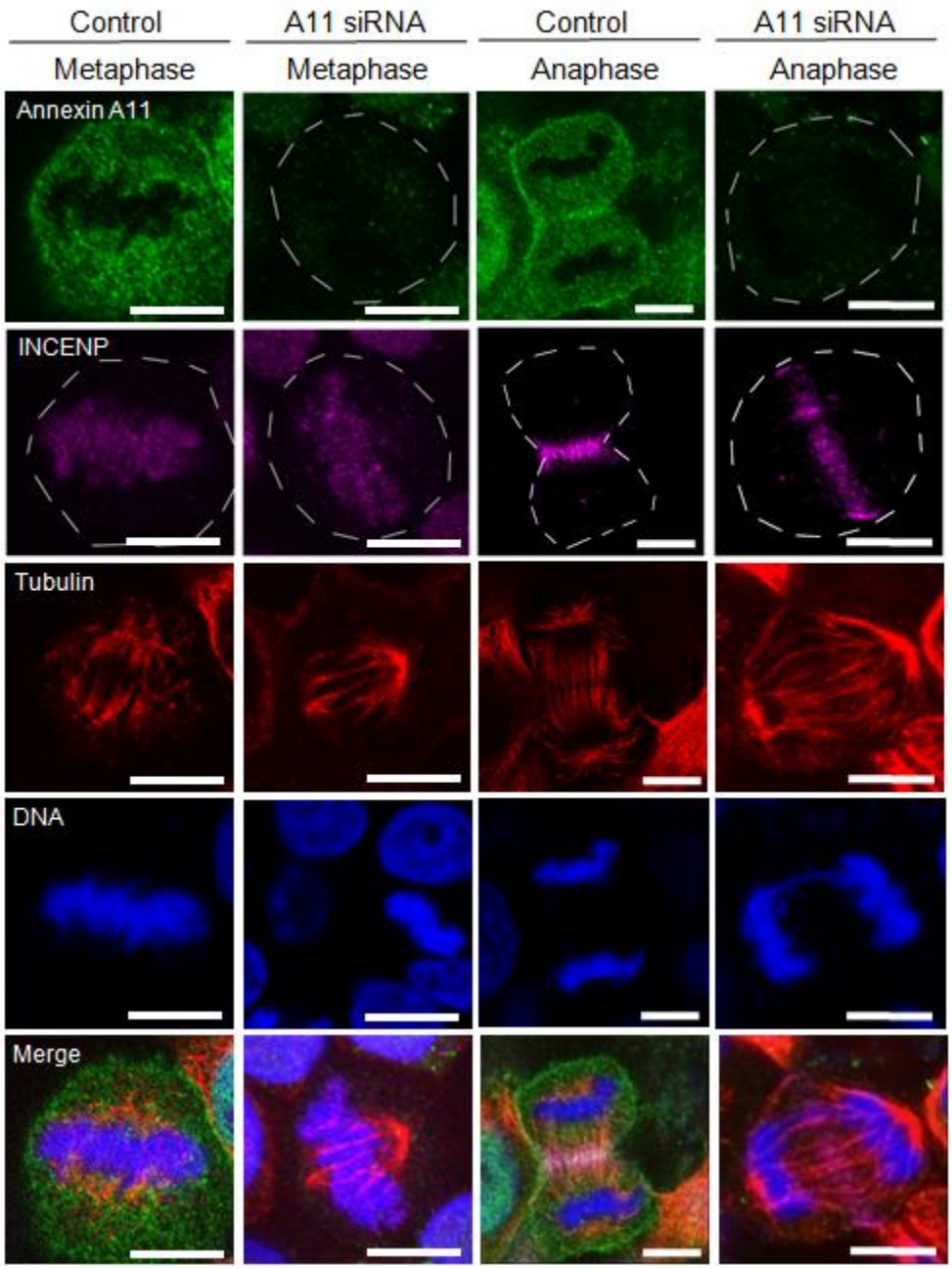

Figure 55 Annexin A11 Knock Down Does Not Affect the Distribution of INCENP at Metaphase or Anaphase

A431 cells were treated with 20µM annexin A11 siRNA or 20µM scrambled control siRNA for 6 days, with two treatments administered on day 1 and day 3. Cells were then PFA fixed on day 6 and stained for annexin A11 using a polyclonal goat anti-annexin A11 antibody (1/50 dilution), INCENP using a polyclonal rabbit anti-INCENP antibody (1/1000 dilution), tubulin using a monoclonal mouse anti-alpha tubulin antibody (1/100 dilution) and DNA using DAPI (1/500 dilution). (Scale bars 10µm)

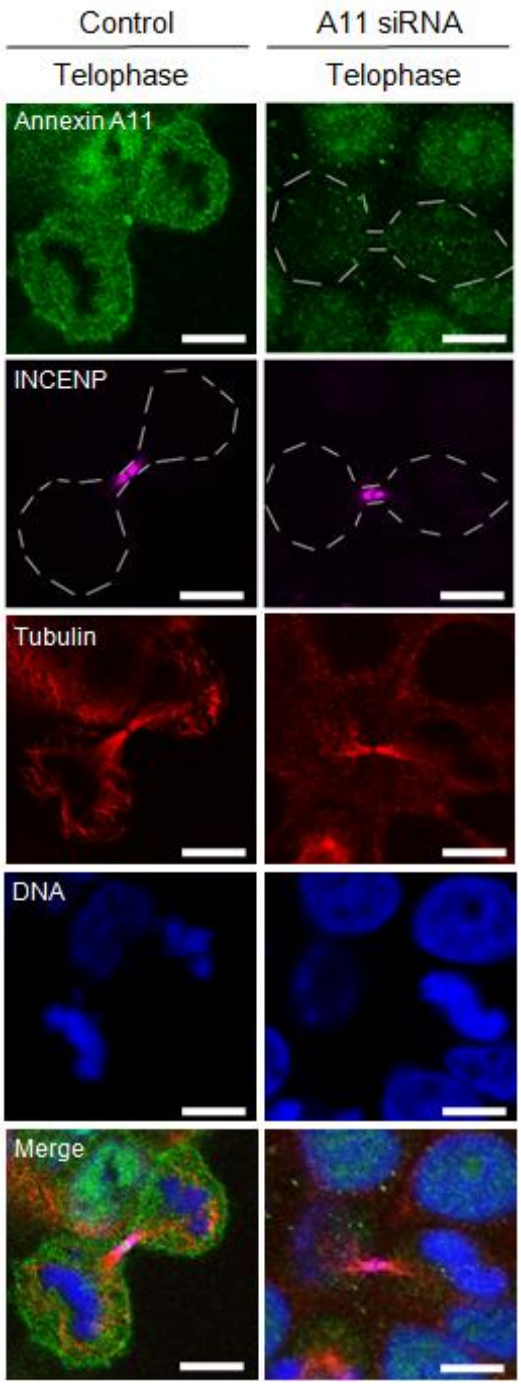

Figure 56 Annexin A11 Knock Down Does Not Affect the Distribution of INCENP at Telophase

A431 cells were treated with 20µM annexin A11 siRNA or 20µM scrambled control siRNA for 6 days, with two treatments administered on day 1 and day 3. Cells were then PFA fixed on day 6 and stained for annexin A11 using a polyclonal goat anti-annexin A11 antibody (1/50 dilution), INCENP using a polyclonal rabbit anti-INCENP antibody (1/1000 dilution), tubulin using a monoclonal mouse anti-alpha tubulin antibody (1/100 dilution) and DNA using DAPI (1/500 dilution). (Scale bars 10µm)

In accordance with the normal distribution of cell cycle markers in the annexin A11 knock down cells, as well as the detection of these cells throughout the different stages of the cell cycle, cell proliferation also appeared unchanged from that of control cells. A431 cells were treated with either annexin A11 siRNA or control siRNA four times over the course of two weeks. At the end of two weeks, strong knock down of annexin A11 was achieved with a decrease of 90% on average when compared to control cells, from three independent experiments (Figure 58A). The cells were counted on days 1, 3, 7, 9 and 14 and a graph plotted of their growth over time. No difference can be seen between the control and knock down cells (Figure 58B). In addition the distribution of cells within mitosis was also investigated. A431 cells were treated with control or annexin A11 siRNA for six days prior to fixation in PFA. The cells were then stained for annexin A11, tubulin and DNA. For each dish of treated cells, five fields of view were randomly chosen and the number of cells in mitosis counted, including the phase of the cell cycle they were in (Figure 58C). No significant difference in the proportion of cells in each phase of mitosis was seen between control and knock down cells (Prophase $P=0.68$, metaphase $P=1$, anaphase $P=1$, telophase $P=0.30$, cytokinesis $P=0.15$).

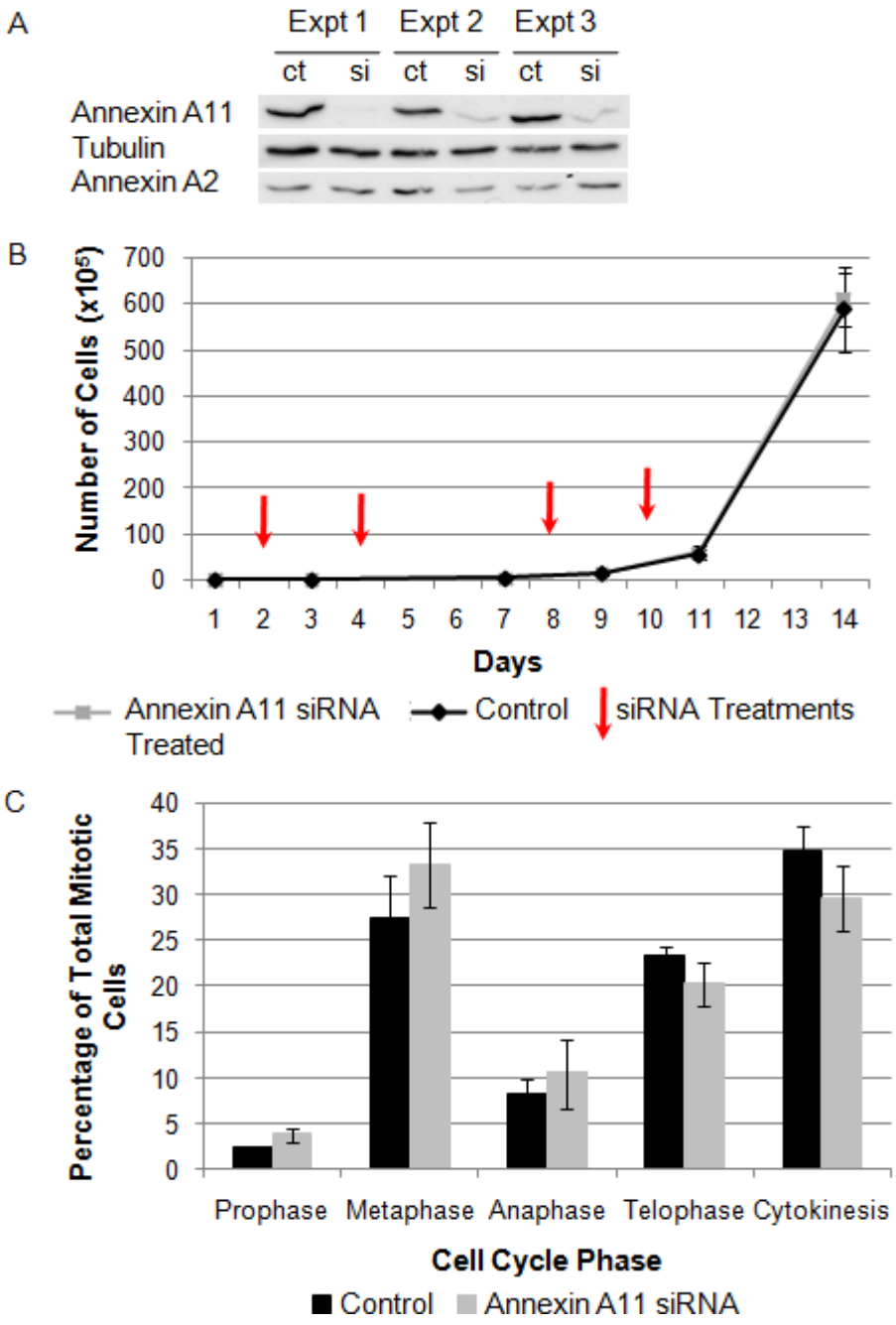

Figure 57 Annexin A11 Knock Down Does Not Affect Proliferation or Cell Cycle Distribution

(A) Western blot of whole cell lysates from A431 cells treated with 20µM annexin A11 siRNA or 20µM scrambled control siRNA for two weeks, in three independent experiments. Four treatments were administered on days 2, 4, 8 and 10. Cell lysates were then collected on day 14. Annexin A11 was blotted for using a polyclonal goat anti-annexin A11 antibody (1/200 dilution) and tubulin using a monoclonal mouse anti-alpha tubulin antibody (1/1000 dilution) **(B)** A graph of the number of A431 cells counted on days 1, 3, 7, 9, 11 and 14 in annexin A11 siRNA treated samples and control samples. Cells were treated with 20µM annexin A11 siRNA or 20µM scrambled control siRNA for two weeks. Four treatments were administered on days 2, 4, 8 and 10. **(C)** Bar chart of the cell cycle distribution of A431 cells treated with 20µM annexin A11 siRNA or 20µM scrambled control siRNA for six days, with two treatments administered on days 1 and 3. n = 3 experiments, with five fields of view for each experiment. Error bars are standard errors of the mean. Prophase P=0.68, metaphase P=1, anaphase P=1, telophase P=0.30, cytokinesis P=0.15.

6.4 Discussion

Work in this study has revealed a novel localisation of annexin A11 to the centrosome, through the application of immunostaining against annexin A11 alongside pericentrin or γ tubulin – two markers of the centrosome. The localisation of annexin A11 to the centrosome appears to be specific to this particular annexin, as this was not observed for annexin A2 or annexin A7, with annexin A7 sharing the highest degree of homology to annexin A11. Annexin A11 is therefore likely to be unique amongst the annexins in its ability to target to both the centrosome and the midbody. Annexin A11 has previously been shown to have a role at cytokinesis, such that the loss of annexin A11 results in the loss of the midbody and the failure of daughter cells to abscise from each other [150]. Interestingly a strong link has emerged for the role of the centrosome in cytokinesis.

Initial studies demonstrated that the centrosome was not essential for mitotic spindle formation. This was shown through both laser ablation [305] and micro-surgical removal [306] of the centrosome. The subsequent recruitment of centrosomal-associated proteins, such as γ tubulin and pericentrin, to mitotic spindle poles varied between these studies. However the acentrosomal cells consistently entered metaphase and progressed through to anaphase, demonstrating the ability of cells to form a mitotic spindle and initiate mitosis in a centrosome-independent manner. In a significant proportion of acentrosomal cells, although the cells were able to initiate cytokinesis, the cleavage furrows regressed [306]. This is suggested to be due to the inability of these cells to re-position the mitotic spindle along the appropriate axis for division [305], as this process requires astral microtubules which ordinarily extend towards the cell cortex from the centrosome [307]. This highlights the essential role of the centrosome in the later stages of mitosis.

Further studies uncovered the localisation of known centrosome proteins, such as γ tubulin and centriolin, targeting to the midbody [302]. Interestingly the knock down of centriolin resulted in a cytokinesis defect [302] similar to that described for the knock down of annexin A11 [150], whereby the daughter cells remain connected by a long, intercellular bridge of membrane and the midbody is lost. It is therefore not wholly surprising that a protein such as annexin A11, which localises to the midbody and is implicated in the final stages of cytokinesis, should also localise to the centrosome.

The localisation of annexin A11 to the centrosome was shown in this study to be consistent throughout the life cycle of a cell i.e. from interphase through to mitosis. Although annexin A11 appears to be intimately involved in the cell cycle, the knock down of annexin A11 did not perturb the centrosome or present any other obvious cell cycle phenotype. Previous studies however have shown the knock down of annexin A11 to cause either a complete failure in the completion of cytokinesis leading to apoptosis [150] or a general decrease in cell proliferation though the population is still maintained [196]. It is therefore likely that although the knock down achieved in this study is considerable, a small but significant amount of annexin A11 is still translated. This appears to be enough for the cells to remain viable and continue through the cell cycle without any detectable defects. Therefore one cannot rule out an essential role for annexin A11 at the centrosome during either interphase or mitosis.

Interestingly during mitosis, the distribution of annexin A11 at metaphase centrosomes in particular appears to change, such that it expands in area. The centrosome is known to expand in area at metaphase during a process called centrosome maturation. This process of maturation is said to represent an increase in the ability of the centrosome to nucleate microtubules, but is increasingly thought to also involve the gain of other non-nucleating abilities [308]. Maturation during mitosis involves the loss of certain proteins such as C-Nap1 and Nlp, and the gain of others such as Plk1 and NuMA [292]. Annexin A11 however is present on both interphase and mitotic centrosomes, but appears to be additionally recruited during maturation. This mimics more the behaviour of γ tubulin [309] which is present on interphase centrosomes but has also been shown to accumulate at the centrosome during mitosis. This accumulation was shown to be microtubule independent. The function of γ tubulin here revolves around its ability to nucleate microtubules [294], enhancing the most noted function of the centrosome. Other proteins, including the centrosomal marker pericentrin, are known to be trafficked to the centrosome in a microtubule-dependent manner involving the movement of granules along microtubules via dynactin, an accessory protein of the motor protein dynein [310]. This is perhaps a more likely pathway for the transport of annexin A11 to the centrosome, given its previously noted localisation along microtubules.

The role of pericentrin at the centrosome is to anchor the γ TuRC (γ tubulin ring complex), which is responsible for microtubule nucleation at this site [294]. More recent studies of the

centrosome have extended its founding function as a nucleating site, to that of a docking station for a range of protein complexes involved in different cell signalling pathways [292]. This emphasises the new functions being uncovered for the centrosome, such as its involvement in nuclear envelope breakdown through the release of a diffusible factor, speculated to be Aurora A kinase, which like Plk1 and NuMA also accumulates at the centrosome during mitosis [311]. Therefore annexin A11 may also be involved in a more unconventional centrosomal function.

Defects in the centrosome cycle, such as centriole separation, duplication and migration can result in unequal segregation of chromosomes and therefore poly- or aneuploidy. Such an unstable situation is often present in malignant tumours and it is suggested therefore that centrosomal defects may be important in oncogenesis [312]. Annexin A11 has recently been identified as being down-regulated in a range of cancers, including kidney, colon, lung and ovarian cancer [194]. Further investigation into the role of annexin A11 in ovarian cancer demonstrated that knock down of annexin A11 decreased cell proliferation, colony formation and increased resistance to the anti-cancer drug cisplatin [196]. The increase in non-proliferating, quiescent cells was suggested to be a mechanism by which cells may become more resistant to drug treatment and apoptosis. The mechanism by which annexin A11 mediates this change in cell cycling is as yet unclear. Although it is unlikely that annexin A11 is capable of nucleating microtubules at the centrosome, its localisation to this organelle may still be of some significance, particularly during cell cycle regulation (Figure 59).

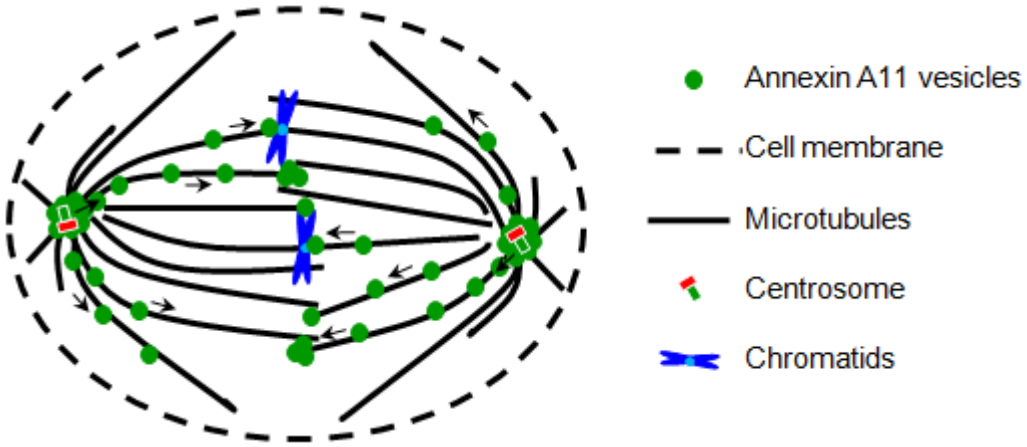

Figure 59 Model of Annexin A11 Redistribution During the Cell Cycle

Annexin A11 may accumulate at the centrosome in order to more easily facilitate its dynamic redistribution during the cell cycle, exemplified here at metaphase. Annexin A11 vesicles could be transported along microtubules emanating from the centrosome, which form the mitotic spindle. This would allow annexin A11 to target to the spindle midzone at anaphase and the midbody at telophase and cytokinesis, where it can then carry out its function.

It is plausible that annexin A11 may utilise the centrosome as a docking station for accumulation, before redistribution along the mitotic spindle where it carries out its designated function – perhaps in regulating the cell cycle (Figure 59). Further investigation of annexin A11 trafficking during the cell cycle, both to and from the centrosome, would therefore be of great interest.

Chapter Seven:
Conclusions and Summary

7. Conclusions and Summary

Annexin A11 is the common ancestor of nine of the eleven vertebrate annexins [144]. Although it is one of the oldest vertebrate annexins in terms of evolution, far less is known about its physiological functions compared to the other annexins. However it has been strongly implicated in the cell cycle [150]. Work carried out in this study confirms the highly dynamic localisation of annexin A11 during the cell cycle and further elucidates this through different fixation methods. The use of methanol fixation has uncovered several novel localisations of this protein, all of which point towards annexin A11 being tightly coupled to the cell cycle in a microtubule dependent manner.

In this study puncta of annexin A11 were observed along microtubules in interphase cells, and upon depolymerisation of the microtubule network annexin A11 appeared to accumulate perinuclearly on more stable microtubule structures. The perinuclear localisation of annexin A11 has been further characterised in both interphase and mitotic cells and been shown to specifically localise to the centrosome. Taken together, it is plausible that annexin A11 is trafficked to and from the centrosome via microtubules, a process which when interrupted through microtubule depolymerisation results in the accumulation of annexin A11 in this region. During the cell cycle, at the onset of metaphase, annexin A11 further accumulates at the centrosome during centrosome maturation. Annexin A11 is also seen along the length of metaphase and anaphase mitotic spindles. It is therefore possible that the accumulation of annexin A11 at mitotic centrosomes primes the cell for the redistribution of annexin A11 along the mitotic apparatus. Live imaging of GFP-tagged annexin A11 would help uncover the dynamic trafficking of this protein during the cell cycle. However careful attention would need to be paid to the GFP controls, as GFP alone targets to both the centrosome and midbody, though the same trafficking pathway may not be utilised.

The trafficking of annexin A11 positive vesicles from the centrosome (as modelled in Figure 59) would require the involvement of a protein complex which directly binds microtubules. A potential protein complex was previously suggested (see Figure 40) in the context of ER to Golgi trafficking of COPII positive vesicles. This involved dynein, a minus end directed motor protein. However trafficking away from the centrosome, towards the

spindle midzone or midbody, would require the use of a plus end directed motor protein. Annexin A11 has been shown to interact with the plus end directed motor protein CHO1 at cytokinesis [146]. CHO1 belongs to the kinesin-6 family of kinesins - a superfamily of plus end directed motor proteins, that provide potential candidates for the transport of annexin A11 away from the centrosome. The kinesin-6 family currently comprises two members; KIF20 and KIF23, also known as Rab6-KIFL (Rab6 binding kinesin) and MKLP1/CHO1, respectively. MKLP1/CHO1 has been shown in this study to co-localise with annexin A11 during the cell cycle. Rab6-KIFL has also been shown to localise to similar domains during the cell cycle, specifically the spindle midzone at anaphase and the midbody at telophase and cytokinesis [313]. The knock down of CHO1 [238], MKLP1 [176] or Rab6-KIFL [313], all cause defects in cytokinesis resulting in the formation of binucleate cells. These motor proteins therefore all appear to have crucial roles in regulating the cell cycle, perhaps in part due to their role in delivering cargo to target destinations such as the midbody. For example MKLP1 is known to be required for the targeting of centriolin to the midbody [303]. Therefore it would be of interest to investigate the targeting of annexin A11 throughout the cell cycle in cells depleted of MKLP1/CHO1 and Rab6-KIFL.

The potential delivery of annexin A11 positive vesicles to the midbody, via the microtubule network, is supported by the observation that under methanol fixation conditions annexin A11 strongly co-localises with the densely packed microtubules of the cleavage furrow. Membrane delivery to the cleavage furrow is now well-established to be required for the completion of abscission (reviewed in [314]). A substantial body of evidence exists for the involvement of exocyst components in cytokinesis, specifically the ESCRT machinery (Endosomal Sorting Complex Required for Transport). Cep55, a centrosomal and midbody protein, has been shown to recruit the ESCRTI component, Tsg101 and the ESCRT associated protein, Alix (ALG2 Interacting Protein X) to the midbody [157-159]. The knock down of either Alix or Tsg101 resulted in cytokinesis defects and multinucleated cells. It has been suggested that midbody targeted ESCRTI machinery goes on to recruit ESCRTIII, which is thought to be able to mediate abscission and sever the link between the two daughter cells [158].

Targeted membrane delivery to the cleavage furrow is also believed to involve the SNARE complexes (SNAP (Soluble NSF Attachment Protein) Receptors). The midbody protein centriolin has been shown to interact with exocyst proteins Sec5, Sec8 and Sec15 and to

directly bind the SNARE associated protein snapin [303]. The knock down of centriolin, which results in cytokinesis defects and subsequent multicellular syncitia [302], also caused the loss of exocyst and SNARE proteins from the midbody [303]. Furthermore the knock down of the SNARE component snapin also resulted in cytokinesis defects and multicellular syncitia. Interestingly the knock down of the exocyst component Sec5 resulted in the accumulation of v-SNARE positive secretory vesicles at the midbody, suggesting that vesicle fusion was delayed or inhibited.

Studies carried out into both the SNARE and ESCRT complexes clearly demonstrate the involvement of post-Golgi secretory vesicle trafficking in cytokinesis. In accordance with this the inhibition of post-Golgi trafficking, through the use of Brefeldin A (BFA), has been demonstrated to delay the completion of cytokinesis [150,303]. Under these circumstances however, annexin A11 was still shown to target to the midbody [150]. It is important to note that while cytokinesis is delayed upon BFA treatment, it is not completely blocked, suggesting the presence of alternative membrane delivery pathways which allow cytokinesis to complete even when one pathway is disrupted. Given the persistent targeting of annexin A11 to the midbody upon BFA treatment, it is likely that annexin A11 is involved in these alternative pathways, which include the trafficking of recycling endosomes.

Rab11 GTPase-positive recycling endosomes have been shown to accumulate in the cleavage furrow. Over-expression of a Rab11 dominant negative mutant or knock down of Rab11 resulted in increased numbers of binucleate cells. The Rab11 interacting proteins, FIP3 and FIP4 (Family of Rab11 Interacting Proteins 3 and 4), both target to the cleavage furrow and midbody. The interaction between FIP3 and Rab11 was shown to be necessary for the completion of cytokinesis, as the over-expression of a Rab11 binding deficient FIP3 resulted in binucleate cells. This study [315] illustrates the possible contribution of recycling endosomes to the cleavage furrow. An interesting point to note is the cell cycle dependent localisations of FIP3. During interphase, metaphase and early anaphase FIP3 localises to endosomes. However as anaphase proceeds FIP3 translocates to the centrosome, then during cytokinesis it is trafficked to the cleavage furrow and midbody [315]. It is proposed that the Rab11-FIP3 complex may regulate this dynamic distribution, through the trafficking of endosomes from the centrosome to the cleavage furrow. It is further speculated that this pathway may utilise the midzone microtubules. A similar route

may be taken by annexin A11 which also localises to the centrosome and cleavage furrow and in addition is present along the length of the midzone microtubules. The link between recycling endosomes, the centrosome and the microtubule network was further strengthened through experiments on the Rab11 effector Nuf (Nuclear-fallout protein) in *Drosophila* [316]. Nuf and Rab11 both localise to the centrosome, but Nuf only does so during cleavage furrow formation. Depolymerisation of the microtubule network, using colchicine, prevents Nuf accumulation at the centrosome in the following round of the cell cycle. Similarly Rab11 was diminished at the centrosome following treatment with colchicine. Nuf was shown to interact with the motor protein dynein and its localisation to the centrosome to be dependent on this interaction. This supports the role of the microtubule network in the delivery of recycling endosome-derived vesicles to the centrosome.

Several of the annexins have previously been associated with endosomal trafficking. Most notably annexin A1, which regulates EGF-stimulated multivesicular body (MVB) inward vesiculation [24] and annexin A2, which regulates early to late endosome trafficking [89]. More recently annexin A8 has been shown to regulate the late endocytic pathway. The knock down of annexin A8 resulted in a delay in the transport of late endosome cargo, thought to be due to the dispersal of these endosomes and their diminished association to the actin network [317]. It is clear from these studies that the loss of annexins can impair endosomal trafficking. It would be interesting to investigate the kinetics of endosomal trafficking upon knock down of annexin A11 and to investigate the kinetics of the cell cycle in cells where annexins known to regulate endosomal trafficking have been knocked down.

Beyond the role of annexin A11 in the cell cycle, this study has also focused on the affect of a recently identified single nucleotide polymorphism (SNP) [193] within annexin A11 in the context of sarcoidosis. This SNP, namely the R230C mutation, was identified as the most highly associated SNP with a subpopulation of German sarcoidosis patients. Although no difference was detected between annexin $A11^{WT}$ and annexin $A11^{R230C}$ in response to calcium, much is still left to be investigated. Most importantly it would be of interest to investigate annexin $A11^{R230C}$ in more disease relevant cells such as T cells. This is of particular note given the high expression of annexin A11 in T cells [148] which contribute greatly to the hyper-inflammatory environment present in sarcoidosis.

Annexin A11 is notably down-regulated in CD8 and CD19 positive lymphocytes [193], with the greatest decrease in mRNA expression in CD8 positive T cells. It is not yet known if this drop is also seen at the protein level and whether it also occurs in sarcoidosis patients expressing annexin $A11^{R230C}$. It has however been shown that CD8 positive T cells, harvested from a population of American sarcoidosis patients, behave normally. This is in regards to their ability to suppress the proliferation of activated CD4 positive T cells, which are expanded in sarcoidosis patients, and to proliferate normally [318]. It is not known whether annexin A11 in this subpopulation of patients also contains the R230C mutation. Given the association between annexin A11 and the cell cycle, it would be important to determine whether the CD8 positive T cells in the German population expressing the R230C mutation also proliferate normally, as in the American population. In addition it would be interesting to examine the protein expression of annexin A11 in CD4 positive T cells from control and sarcoidosis patients, in order to determine whether there is a correlation between annexin A11 expression and cell proliferation, particularly as activated CD4 positive T cells are significantly increased in number in sarcoidosis patients [231].

A role for annexin A11 in sarcoidosis, separate to its function during mitosis, may focus on its effect extracellularly especially given that autoantibodies against annexin A11 have been detected in a range of autoimmune diseases, including rheumatoid arthritis, systemic lupus erythrematosus and Raynauds disease [319]. A number of the annexins are known to be secreted [228,229], including annexin A11 [227] which was shown to be secreted by activated neutrophils. Annexin A1, which is also secreted [228,229], has been shown to exert extracellular affects through binding members of the formyl peptide receptor family on neutrophils [320]. This results in the inhibition of neutrophil transendothelial migration and desensitisation to chemoattractant. It would therefore be interesting to investigate whether extracellular annexin A11 exerts similar effects on leukocytes.

7.1 Future Perspectives

In summary, this study supports a role for annexin A11 in the cell cycle, potentially through an association with the microtubule network. In order to further elucidate the role of annexin A11 during mitosis, live imaging of GFP tagged annexin A11 in conjunction with RFP tagged tubulin would be useful in determining how annexin A11 is trafficked to the discrete localisations observed in this study. Furthermore the use of GFP tagged tyrosine phosphorylation mutants of annexin A11 would be of interest, given the cytokinesis-

specific tyrosine phosphorylation of annexin A11 [146]. In more general terms, the trafficking of annexin A11 in interphase cells could also be investigated, initially through the knock down of ALG-2 and COPII components speculated to be part of the protein complex required for its transport.

Future studies of the role of annexin A11 in interphase cells would also involve further work on the sarcoidosis-associated variant of annexin A11, annexin A11^{R230C}. Although the calcium-dependent translocations of this variant were shown in this study to not differ spatially or temporally from wild type annexin A11, the extracellular role of this protein has yet to be investigated. Initial studies would require the determination of secretion of endogenous annexin A11 from disease-relevant cell types, such as macrophages and monocytes [206], as well as subsets of B and T cells [193]. It would be particularly interesting to determine whether the role of annexin A11 in sarcoidosis relates to its function in the cell cycle, and as such an initial characterisation of the cell cycle distribution of annexin A11 in these cells would be important, particularly in cells harbouring the R230C mutation.

Reference List

1. Creutz C.E., Pazoles C.J., and Pollard H.B. (1978). Identification and purification of an adrenal medullary protein (synexin) that causes calcium-dependent aggregation of isolated chromaffin granules**.** J. Biol. Chem. *253***:** 2858-2866.

2. Buday L., Farkas G., and Farago A. (1989). The dominant substrate of protein kinase C in the extracts of pig granulocytes is a 38 kDa Ca2+/membrane binding protein**.** Acta Biochim. Biophys. Hung. *24***:** 101-106.

3. Human Genome Organisation. (2009). HUGO Gene Nomenclature Committee**.**).

4. Morgan R.O. and Fernandez M.P. (1997). Annexin gene structures and molecular evolutionary genetics**.** Cell Mol. Life Sci. *53***:** 508-515.

5. Moss S.E. and Morgan R.O. (2004). The annexins**.** Genome Biol *5***:** 219.

6. Crompton M.R., Moss S.E., and Crumpton M.J. (1988). Diversity in the lipocortin/calpactin family**.** Cell *55***:** 1-3.

7. Morgan R.O., Jenkins N.A., Gilbert D.J., Copeland N.G., Balsara B.R., Testa J.R., and Fernandez M.P. (1999). Novel human and mouse annexin A10 are linked to the genome duplications during early chordate evolution**.** Genomics *60***:** 40-49.

8. Benz J., Bergner A., Hofmann A., Demange P., Gottig P., Liemann S., Huber R., and Voges D. (1996). The structure of recombinant human annexin VI in crystals and membrane-bound**.** J Mol Biol *260***:** 638-643.

9. Clark G.B., Thompson G., Jr., and Roux S.J. (2001). Signal transduction mechanisms in plants: an overview**.** Curr. Sci. *80***:** 170-177.

10. Huber R., Romisch J., and Paques E.P. (1990). The crystal and molecular structure of human annexin V, an anticoagulant protein that binds to calcium and membranes**.** EMBO J. *9***:** 3867-3874.

11. Weng X., Luecke H., Song I.S., Kang D.S., Kim S.H., and Huber R. (1993). Crystal structure of human annexin I at 2.5 A resolution**.** Protein Sci. *2***:** 448-458.

12. Huber R., Schneider M., Mayr I., Romisch J., and Paques E.P. (1990). The calcium binding sites in human annexin V by crystal structure analysis at 2.0 A resolution. Implications for

membrane binding and calcium channel activity**.** FEBS Lett. *275***:** 15-21.

13. Liemann S., Benz J., Burger A., Voges D., Hofmann A., Huber R., and Gottig P. (1996). Structural and functional characterisation of the voltage sensor in the ion channel human annexin V**.** J. Mol. Biol. *258***:** 555-561.

14. Lambert O., Gerke V., Bader M.F., Porte F., and Brisson A. (1997). Structural analysis of junctions formed between lipid membranes and several annexins by cryo-electron microscopy**.** J. Mol. Biol. *272***:** 42-55.

15. Lambert O., Cavusoglu N., Gallay J., Vincent M., Rigaud J.L., Henry J.P., and yala-Sanmartin J. (2004). Novel organization and properties of annexin 2-membrane complexes**.** J. Biol. Chem. *279***:** 10872-10882.

16. Huber R., Berendes R., Burger A., Schneider M., Karshikov A., Luecke H., Romisch J., and Paques E. (1992). Crystal and molecular structure of human annexin V after refinement. Implications for structure, membrane binding and ion channel formation of the annexin family of proteins**.** J. Mol. Biol. *223***:** 683-704.

17. Kawasaki H., vila-Sakar A., Creutz C.E., and Kretsinger R.H. (1996). The crystal structure of annexin VI indicates relative rotation of the two lobes upon membrane binding**.** Biochim. Biophys. Acta *1313***:** 277-282.

18. Rosengarth A., Gerke V., and Luecke H. (2001). X-ray structure of full-length annexin 1 and implications for membrane aggregation**.** J. Mol. Biol. *306***:** 489-498.

19. Favier-Perron B., Lewit-Bentley A., and Russo-Marie F. (1996). The high-resolution crystal structure of human annexin III shows subtle differences with annexin V**.** Biochemistry *35***:** 1740-1744.

20. Sudo T. and Hidaka H. (1998). Regulation of calcyclin (S100A6) binding by alternative splicing in the N-terminal regulatory domain of annexin XI isoforms**.** J Biol Chem *273***:** 6351-6357.

21. Rety S., Sopkova J., Renouard M., Osterloh D., Gerke V., Tabaries S., Russo-Marie F., and Lewit-Bentley A. (1999). The crystal structure of a complex of p11 with the annexin II N-terminal peptide**.** Nat. Struct. Biol. *6***:** 89-95.

22. Oudinet J.P., Russo-Marie F., Cavadore J.C., and Rothhut B. (1993). Protein kinase C-dependent phosphorylation of annexins I and II in mesangial cells**.** Biochem. J. *292 (Pt 1)***:**

63-68.

23. Futter C.E., Felder S., Schlessinger J., Ullrich A., and Hopkins C.R. (1993). Annexin I is phosphorylated in the multivesicular body during the processing of the epidermal growth factor receptor**.** J. Cell Biol. *120***:** 77-83.

24. White I.J., Bailey L.M., Aghakhani M.R., Moss S.E., and Futter C.E. (2006). EGF stimulates annexin 1-dependent inward vesiculation in a multivesicular endosome subpopulation**.** EMBO J. *25***:** 1-12.

25. Solito E., Christian H.C., Festa M., Mulla A., Tierney T., Flower R.J., and Buckingham J.C. (2006). Post-translational modification plays an essential role in the translocation of annexin A1 from the cytoplasm to the cell surface**.** FASEB J. *20***:** 1498-1500.

26. Barnes J.A. and Gomes A.V. (2002). Proteolytic signals in the primary structure of annexins**.** Mol. Cell Biochem. *231***:** 1-7.

27. Mizutani A., Watanabe N., Kitao T., Tokumitsu H., and Hidaka H. (1995). The long amino-terminal tail domain of annexin XI is necessary for its nuclear localization**.** Arch Biochem Biophys *318***:** 157-165.

28. Turnay J., Lecona E., Fernandez-Lizarbe S., Guzman-Aranguez A., Fernandez M.P., Olmo N., and Lizarbe M.A. (2005). Structure-function relationship in annexin A13, the founder member of the vertebrate family of annexins**.** Biochem. J. *389***:** 899-911.

29. Ando Y., Imamura S., Owada M.K., and Kannagi R. (1991). Calcium-induced intracellular cross-linking of lipocortin I by tissue transglutaminase in A431 cells. Augmentation by membrane phospholipids**.** J. Biol. Chem. *266***:** 1101-1108.

30. Santamaria-Kisiel L., Rintala-Dempsey A.C., and Shaw G.S. (2006). Calcium-dependent and -independent interactions of the S100 protein family**.** Biochem. J. *396***:** 201-214.

31. Sopkova-de Oliveira S.J., Oling F.K., Rety S., Brisson A., Smith J.C., and Lewit-Bentley A. (2000). S100 protein-annexin interactions: a model of the (Anx2-p11)(2) heterotetramer complex**.** Biochim. Biophys. Acta *1498***:** 181-191.

32. Becker T., Weber K., and Johnsson N. (1990). Protein-protein recognition via short amphiphilic helices; a mutational analysis of the binding site of annexin II for p11**.** EMBO J. *9***:** 4207-4213.

33. van de Graaf S.F., Hoenderop J.G., Gkika D., Lamers D., Prenen J., Rescher U., Gerke V.,

Staub O., Nilius B., and Bindels R.J. (2003). Functional expression of the epithelial Ca(2+) channels (TRPV5 and TRPV6) requires association of the S100A10-annexin 2 complex**.** EMBO J. *22***:** 1478-1487.

34. Borthwick L.A., McGaw J., Conner G., Taylor C.J., Gerke V., Mehta A., Robson L., and Muimo R. (2007). The formation of the cAMP/protein kinase A-dependent annexin 2-S100A10 complex with cystic fibrosis conductance regulator protein (CFTR) regulates CFTR channel function**.** Mol. Biol. Cell *18***:** 3388-3397.

35. Knop M., Aareskjold E., Bode G., and Gerke V. (2004). Rab3D and annexin A2 play a role in regulated secretion of vWF, but not tPA, from endothelial cells**.** EMBO J. *23***:** 2982-2992.

36. Jacob R., Heine M., Eikemeyer J., Frerker N., Zimmer K.P., Rescher U., Gerke V., and Naim H.Y. (2004). Annexin II is required for apical transport in polarized epithelial cells**.** J. Biol. Chem. *279***:** 3680-3684.

37. Yamada A., Irie K., Hirota T., Ooshio T., Fukuhara A., and Takai Y. (2005). Involvement of the annexin II-S100A10 complex in the formation of E-cadherin-based adherens junctions in Madin-Darby canine kidney cells**.** J. Biol. Chem. *280***:** 6016-6027.

38. Lee D.B., Jamgotchian N., Allen S.G., Kan F.W., and Hale I.L. (2004). Annexin A2 heterotetramer: role in tight junction assembly**.** Am. J. Physiol Renal Physiol *287***:** F481-F491.

39. Mailliard W.S., Haigler H.T., and Schlaepfer D.D. (1996). Calcium-dependent binding of S100C to the N-terminal domain of annexin I**.** J. Biol. Chem. *271***:** 719-725.

40. Chang N., Sutherland C., Hesse E., Winkfein R., Wiehler W.B., Pho M., Veillette C., Li S., Wilson D.P., Kiss E. et al. (2007). Identification of a novel interaction between the Ca(2+)-binding protein S100A11 and the Ca(2+)- and phospholipid-binding protein annexin A6**.** Am. J. Physiol Cell Physiol *292***:** C1417-C1430.

41. Robinson N.A., Lapic S., Welter J.F., and Eckert R.L. (1997). S100A11, S100A10, annexin I, desmosomal proteins, small proline-rich proteins, plasminogen activator inhibitor-2, and involucrin are components of the cornified envelope of cultured human epidermal keratinocytes**.** J. Biol. Chem. *272***:** 12035-12046.

42. Johnstone S.A., Hubaishy I., and Waisman D.M. (1993). Regulation of annexin I-dependent aggregation of phospholipid vesicles by protein kinase C**.** Biochem. J. *294 (Pt 3)***:** 801-807.

43. Garbuglia M., Verzini M., and Donato R. (1998). Annexin VI binds S100A1 and S100B and blocks the ability of S100A1 and S100B to inhibit desmin and GFAP assemblies into intermediate filaments**.** Cell Calcium *24***:** 177-191.

44. Khanna N.C., Helwig E.D., Ikebuchi N.W., Fitzpatrick S., Bajwa R., and Waisman D.M. (1990). Purification and characterization of annexin proteins from bovine lung**.** Biochemistry *29***:** 4852-4862.

45. Ma A.S., Bystol M.E., and Tranvan A. (1994). In vitro modulation of filament bundling in F-actin and keratins by annexin II and calcium**.** In Vitro Cell Dev. Biol. Anim *30A***:** 329-335.

46. Tzima E., Trotter P.J., Orchard M.A., and Walker J.H. (2000). Annexin V relocates to the platelet cytoskeleton upon activation and binds to a specific isoform of actin**.** Eur. J. Biochem. *267***:** 4720-4730.

47. Babiychuk E.B., Palstra R.J., Schaller J., Kampfer U., and Draeger A. (1999). Annexin VI participates in the formation of a reversible, membrane-cytoskeleton complex in smooth muscle cells**.** J. Biol. Chem. *274***:** 35191-35195.

48. Filipenko N.R. and Waisman D.M. (2001). The C terminus of annexin II mediates binding to F-actin**.** J. Biol. Chem. *276***:** 5310-5315.

49. de G.M., Tijdens I., Smeets M.B., Hensbergen P.J., Deelder A.M., and van de W.B. (2008). Annexin A2 phosphorylation mediates cell scattering and branching morphogenesis via cofilin Activation**.** Mol. Cell Biol. *28***:** 1029-1040.

50. Rescher U., Ludwig C., Konietzko V., Kharitonenkov A., and Gerke V. (2008). Tyrosine phosphorylation of annexin A2 regulates Rho-mediated actin rearrangement and cell adhesion**.** J. Cell Sci. *121***:** 2177-2185.

51. Hayes M.J., Shao D.M., Grieve A., Levine T., Bailly M., and Moss S.E. (2008). Annexin A2 at the interface between F-actin and membranes enriched in phosphatidylinositol 4,5,-bisphosphate**.** Biochim. Biophys. Acta.

52. Rescher U., Ruhe D., Ludwig C., Zobiack N., and Gerke V. (2004). Annexin 2 is a phosphatidylinositol (4,5)-bisphosphate binding protein recruited to actin assembly sites at cellular membranes**.** J. Cell Sci. *117***:** 3473-3480.

53. Hayes M.J., Shao D., Bailly M., and Moss S.E. (2006). Regulation of actin dynamics by annexin 2**.** EMBO J. *25***:** 1816-1826.

54. Babbin B.A., Parkos C.A., Mandell K.J., Winfree L.M., Laur O., Ivanov A.I., and Nusrat A. (2007). Annexin 2 regulates intestinal epithelial cell spreading and wound closure through Rho-related signaling**.** Am. J. Pathol. *170***:** 951-966.

55. Falsey R.R., Marron M.T., Gunaherath G.M., Shirahatti N., Mahadevan D., Gunatilaka A.A., and Whitesell L. (2006). Actin microfilament aggregation induced by withaferin A is mediated by annexin II**.** Nat. Chem. Biol. *2***:** 33-38.

56. Tatenhorst L., Rescher U., Gerke V., and Paulus W. (2006). Knockdown of annexin 2 decreases migration of human glioma cells in vitro**.** Neuropathol. Appl. Neurobiol. *32***:** 271-277.

57. Lu Q.Y., Jin Y.S., Zhang Z.F., Le A.D., Heber D., Li F.P., Dubinett S.M., and Rao J.Y. (2007). Green tea induces annexin-I expression in human lung adenocarcinoma A549 cells: involvement of annexin-I in actin remodeling**.** Lab Invest *87***:** 456-465.

58. Xiao G.S., Jin Y.S., Lu Q.Y., Zhang Z.F., Belldegrun A., Figlin R., Pantuck A., Yen Y., Li F., and Rao J. (2007). Annexin-I as a potential target for green tea extract induced actin remodeling**.** Int. J. Cancer *120***:** 111-120.

59. Ikebuchi N.W. and Waisman D.M. (1990). Calcium-dependent regulation of actin filament bundling by lipocortin-85**.** J. Biol. Chem. *265***:** 3392-3400.

60. varez-Martinez M.T., Mani J.C., Porte F., Faivre-Sarrailh C., Liautard J.P., and Sri W.J. (1996). Characterization of the interaction between annexin I and profilin**.** Eur. J. Biochem. *238***:** 777-784.

61. Locate S., Colyer J., Gawler D.J., and Walker J.H. (2008). Annexin A6 at the cardiac myocyte sarcolemma--evidence for self-association and binding to actin**.** Cell Biol. Int. *32***:** 1388-1396.

62. Monastyrskaya K., Babiychuk E.B., Hostettler A., Wood P., Grewal T., and Draeger A. (2009). Plasma membrane-associated annexin A6 reduces CA2+ entry by stabilizing the cortical actin cytoskeleton**.** J. Biol. Chem.

63. Davis A.J., Butt J.T., Walker J.H., Moss S.E., and Gawler D.J. (1996). The Ca2+-dependent lipid binding domain of P120GAP mediates protein-protein interactions with Ca2+-dependent membrane-binding proteins. Evidence for a direct interaction between annexin VI and P120GAP**.** J. Biol. Chem. *271***:** 24333-24336.

64. Chow A. and Gawler D. (1999). Mapping the site of interaction between annexin VI and the p120GAP C2 domain**.** FEBS Lett. *460***:** 166-172.

65. Grewal T., Evans R., Rentero C., Tebar F., Cubells L., de D., I, Kirchhoff M.F., Hughes W.E., Heeren J., Rye K.A. et al. (2005). Annexin A6 stimulates the membrane recruitment of p120GAP to modulate Ras and Raf-1 activity**.** Oncogene *24***:** 5809-5820.

66. Brownawell A.M. and Creutz C.E. (1997). Calcium-dependent binding of sorcin to the N-terminal domain of synexin (annexin VII)**.** J. Biol. Chem. *272***:** 22182-22190.

67. Verzili D., Zamparelli C., Mattei B., Noegel A.A., and Chiancone E. (2000). The sorcin-annexin VII calcium-dependent interaction requires the sorcin N-terminal domain**.** FEBS Lett. *471***:** 197-200.

68. Satoh H., Shibata H., Nakano Y., Kitaura Y., and Maki M. (2002). ALG-2 interacts with the amino-terminal domain of annexin XI in a Ca(2+)-dependent manner**.** Biochem. Biophys. Res. Commun. *291***:** 1166-1172.

69. Filipenko N.R., MacLeod T.J., Yoon C.S., and Waisman D.M. (2004). Annexin A2 is a novel RNA-binding protein**.** J. Biol. Chem. *279***:** 8723-8731.

70. Hirata A. and Hirata F. (1999). Lipocortin (Annexin) I heterotetramer binds to purine RNA and pyrimidine DNA**.** Biochem. Biophys. Res. Commun. *265***:** 200-204.

71. Hirata A. and Hirata F. (2002). DNA chain unwinding and annealing reactions of lipocortin (annexin) I heterotetramer: regulation by Ca(2+) and Mg(2+)**.** Biochem. Biophys. Res. Commun. *291***:** 205-209.

72. Haigler H.T., Schlaepfer D.D., and Burgess W.H. (1987). Characterization of lipocortin I and an immunologically unrelated 33-kDa protein as epidermal growth factor receptor/kinase substrates and phospholipase A2 inhibitors**.** J. Biol. Chem. *262***:** 6921-6930.

73. Koster J.J., Boustead C.M., Middleton C.A., and Walker J.H. (1993). The sub-cellular localization of annexin V in cultured chick-embryo fibroblasts**.** Biochem. J. *291 (Pt 2)***:** 595-600.

74. Creutz C.E. (1981). cis-Unsaturated fatty acids induce the fusion of chromaffin granules aggregated by synexin**.** J. Cell Biol. *91***:** 247-256.

75. Drust D.S. and Creutz C.E. (1988). Aggregation of chromaffin granules by calpactin at micromolar levels of calcium**.** Nature *331***:** 88-91.

76. Ali S.M., Geisow M.J., and Burgoyne R.D. (1989). A role for calpactin in calcium-dependent exocytosis in adrenal chromaffin cells. Nature *340*: 313-315.

77. Sarafian T., Pradel L.A., Henry J.P., Aunis D., and Bader M.F. (1991). The participation of annexin II (calpactin I) in calcium-evoked exocytosis requires protein kinase C. J. Cell Biol. *114*: 1135-1147.

78. Graham M.E., Gerke V., and Burgoyne R.D. (1997). Modification of annexin II expression in PC12 cell lines does not affect Ca(2+)-dependent exocytosis. Mol. Biol. Cell *8*: 431-442.

79. Lorusso A., Covino C., Priori G., Bachi A., Meldolesi J., and Chieregatti E. (2006). Annexin2 coating the surface of enlargeosomes is needed for their regulated exocytosis. EMBO J. *25*: 5443-5456.

80. Fiedler K., Lafont F., Parton R.G., and Simons K. (1995). Annexin XIIIb: a novel epithelial specific annexin is implicated in vesicular traffic to the apical plasma membrane. J. Cell Biol. *128*: 1043-1053.

81. Lafont F., Lecat S., Verkade P., and Simons K. (1998). Annexin XIIIb associates with lipid microdomains to function in apical delivery. J. Cell Biol. *142*: 1413-1427.

82. Lecat S., Verkade P., Thiele C., Fiedler K., Simons K., and Lafont F. (2000). Different properties of two isoforms of annexin XIII in MDCK cells. J. Cell Sci. *113 (Pt 14)*: 2607-2618.

83. Sudhof T.C. and Rothman J.E. (2009). Membrane fusion: grappling with SNARE and SM proteins. Science *323*: 474-477.

84. Damer C.K. and Creutz C.E. (1994). Synergistic membrane interactions of the two C2 domains of synaptotagmin. J. Biol. Chem. *269*: 31115-31123.

85. Tucker W.C., Weber T., and Chapman E.R. (2004). Reconstitution of Ca2+-regulated membrane fusion by synaptotagmin and SNAREs. Science *304*: 435-438.

86. Emans N., Gorvel J.P., Walter C., Gerke V., Kellner R., Griffiths G., and Gruenberg J. (1993). Annexin II is a major component of fusogenic endosomal vesicles. J. Cell Biol. *120*: 1357-1369.

87. Jackle S., Beisiegel U., Rinninger F., Buck F., Grigoleit A., Block A., Groger I., Greten H., and Windler E. (1994). Annexin VI, a marker protein of hepatocytic endosomes. J. Biol. Chem. *269*: 1026-1032.

88. Mayran N., Parton R.G., and Gruenberg J. (2003). Annexin II regulates multivesicular endosome biogenesis in the degradation pathway of animal cells**.** EMBO J. *22***:** 3242-3253.

89. Morel E., Parton R.G., and Gruenberg J. (2009). Annexin A2-dependent polymerization of actin mediates endosome biogenesis**.** Dev. Cell *16***:** 445-457.

90. Watanabe T., Inui M., Chen B.Y., Iga M., and Sobue K. (1994). Annexin VI-binding proteins in brain. Interaction of annexin VI with a membrane skeletal protein, calspectin (brain spectrin or fodrin)**.** J. Biol. Chem. *269***:** 17656-17662.

91. Kamal A., Ying Y., and Anderson R.G. (1998). Annexin VI-mediated loss of spectrin during coated pit budding is coupled to delivery of LDL to lysosomes**.** J. Cell Biol. *142***:** 937-947.

92. Smythe E., Smith P.D., Jacob S.M., Theobald J., and Moss S.E. (1994). Endocytosis occurs independently of annexin VI in human A431 cells**.** J. Cell Biol. *124***:** 301-306.

93. Pons M., Ihrke G., Koch S., Biermer M., Pol A., Grewal T., Jackle S., and Enrich C. (2000). Late endocytic compartments are major sites of annexin VI localization in NRK fibroblasts and polarized WIF-B hepatoma cells**.** Exp. Cell Res. *257***:** 33-47.

94. Grewal T., Heeren J., Mewawala D., Schnitgerhans T., Wendt D., Salomon G., Enrich C., Beisiegel U., and Jackle S. (2000). Annexin VI stimulates endocytosis and is involved in the trafficking of low density lipoprotein to the prelysosomal compartment**.** J. Biol. Chem. *275***:** 33806-33813.

95. Pons M., Grewal T., Rius E., Schnitgerhans T., Jackle S., and Enrich C. (2001). Evidence for the Involvement of annexin 6 in the trafficking between the endocytic compartment and lysosomes**.** Exp. Cell Res. *269***:** 13-22.

96. Gerke V. and Moss S.E. (2002). Annexins: from structure to function**.** Physiol Rev. *82***:** 331-371.

97. Menke M., Gerke V., and Steinem C. (2005). Phosphatidylserine membrane domain clustering induced by annexin A2/S100A10 heterotetramer**.** Biochemistry *44***:** 15296-15303.

98. Junker M. and Creutz C.E. (1993). Endonexin (annexin IV)-mediated lateral segregation of phosphatidylglycerol in phosphatidylglycerol/phosphatidylcholine membranes**.** Biochemistry *32***:** 9968-9974.

99. Gokhale N.A., Abraham A., Digman M.A., Gratton E., and Cho W. (2005). Phosphoinositide specificity of and mechanism of lipid domain formation by annexin A2-p11 heterotetramer**.**

J. Biol. Chem. *280*: 42831-42840.

100. Babiychuk V.S., Draeger A., and Babiychuk E.B. (2000). Smooth muscle actomyosin promotes Ca2+-dependent interactions between annexin VI and detergent-insoluble glycosphingolipid-enriched membrane domains. Acta Biochim. Pol. *47*: 579-589.

101. Babiychuk E.B., Monastyrskaya K., Burkhard F.C., Wray S., and Draeger A. (2002). Modulating signaling events in smooth muscle: cleavage of annexin 2 abolishes its binding to lipid rafts. FASEB J. *16*: 1177-1184.

102. az-Munoz M., Hamilton S.L., Kaetzel M.A., Hazarika P., and Dedman J.R. (1990). Modulation of Ca2+ release channel activity from sarcoplasmic reticulum by annexin VI (67-kDa calcimedin). J. Biol. Chem. *265*: 15894-15899.

103. Naciff J.M., Behbehani M.M., Kaetzel M.A., and Dedman J.R. (1996). Annexin VI modulates Ca2+ and K+ conductances of spinal cord and dorsal root ganglion neurons. Am. J. Physiol *271*: C2004-C2015.

104. Berendes R., Burger A., Voges D., Demange P., and Huber R. (1993). Calcium influx through annexin V ion channels into large unilamellar vesicles measured with fura-2. FEBS Lett. *317*: 131-134.

105. Berendes R., Voges D., Demange P., Huber R., and Burger A. (1993). Structure-function analysis of the ion channel selectivity filter in human annexin V. Science *262*: 427-430.

106. Burger A., Voges D., Demange P., Perez C.R., Huber R., and Berendes R. (1994). Structural and electrophysiological analysis of annexin V mutants. Mutagenesis of human annexin V, an in vitro voltage-gated calcium channel, provides information about the structural features of the ion pathway, the voltage sensor and the ion selectivity filter. J. Mol. Biol. *237*: 479-499.

107. Nilius B., Gerke V., Prenen J., Szucs G., Heinke S., Weber K., and Droogmans G. (1996). Annexin II modulates volume-activated chloride currents in vascular endothelial cells. J. Biol. Chem. *271*: 30631-30636.

108. Okuse K., Malik-Hall M., Baker M.D., Poon W.Y., Kong H., Chao M.V., and Wood J.N. (2002). Annexin II light chain regulates sensory neuron-specific sodium channel expression. Nature *417*: 653-656.

109. Girard C., Tinel N., Terrenoire C., Romey G., Lazdunski M., and Borsotto M. (2002). p11,

an annexin II subunit, an auxiliary protein associated with the background K+ channel, TASK-1**.** EMBO J. *21***:** 4439-4448.

110. Donier E., Rugiero F., Okuse K., and Wood J.N. (2005). Annexin II light chain p11 promotes functional expression of acid-sensing ion channel ASIC1a**.** J. Biol. Chem. *280***:** 38666-38672.

111. Boersma H.H., Kietselaer B.L., Stolk L.M., Bennaghmouch A., Hofstra L., Narula J., Heidendal G.A., and Reutelingsperger C.P. (2005). Past, present, and future of annexin A5: from protein discovery to clinical applications**.** J. Nucl. Med. *46***:** 2035-2050.

112. Olofsson A., Mallouh V., and Brisson A. (1994). Two-dimensional structure of membrane-bound annexin V at 8 A resolution**.** J. Struct. Biol. *113***:** 199-205.

113. Andree H.A., Reutelingsperger C.P., Hauptmann R., Hemker H.C., Hermens W.T., and Willems G.M. (1990). Binding of vascular anticoagulant alpha (VAC alpha) to planar phospholipid bilayers**.** J. Biol. Chem. *265***:** 4923-4928.

114. Masuda J., Takayama E., Satoh A., Ida M., Shinohara T., Kojima-Aikawa K., Ohsuzu F., Nakanishi K., Kuroda K., Murakami M. et al. (2004). Levels of annexin IV and V in the plasma of pregnant and postpartum women**.** Thromb. Haemost. *91***:** 1129-1136.

115. Zammiti W., Mtiraoui N., Hidar S., Fekih M., Almawi W.Y., and Mahjoub T. (2006). Antibodies to beta2-glycoprotein I and annexin V in women with early and late idiopathic recurrent spontaneous abortions**.** Arch. Gynecol. Obstet. *274***:** 261-265.

116. Rand J., Eerden P.V., Wu X.X., and Chazotte C. (2005). Defective annexin A5 crystallization: a mechanism for pregnancy losses in the antiphospholipid syndrome**.** Thromb. Res. *115 Suppl 1***:** 77-81.

117. Thiagarajan P. and Tait J.F. (1990). Binding of annexin V/placental anticoagulant protein I to platelets. Evidence for phosphatidylserine exposure in the procoagulant response of activated platelets**.** J. Biol. Chem. *265***:** 17420-17423.

118. Perretti M., Croxtall J.D., Wheller S.K., Goulding N.J., Hannon R., and Flower R.J. (1996). Mobilizing lipocortin 1 in adherent human leukocytes downregulates their transmigration**.** Nat. Med. *2***:** 1259-1262.

119. Hayhoe R.P., Kamal A.M., Solito E., Flower R.J., Cooper D., and Perretti M. (2006). Annexin 1 and its bioactive peptide inhibit neutrophil-endothelium interactions under flow:

indication of distinct receptor involvement. Blood *107*: 2123-2130.

120. Chatterjee B.E., Yona S., Rosignoli G., Young R.E., Nourshargh S., Flower R.J., and Perretti M. (2005). Annexin 1-deficient neutrophils exhibit enhanced transmigration in vivo and increased responsiveness in vitro. J. Leukoc. Biol. *78*: 639-646.

121. Mancuso F., Flower R.J., and Perretti M. (1995). Leukocyte transmigration, but not rolling or adhesion, is selectively inhibited by dexamethasone in the hamster post-capillary venule. Involvement of endogenous lipocortin 1. J. Immunol. *155*: 377-386.

122. Perretti M. and D'Acquisto F. (2009). Annexin A1 and glucocorticoids as effectors of the resolution of inflammation. Nat. Rev. Immunol. *9*: 62-70.

123. Xin W., Rhodes D.R., Ingold C., Chinnaiyan A.M., and Rubin M.A. (2003). Dysregulation of the annexin family protein family is associated with prostate cancer progression. Am. J. Pathol. *162*: 255-261.

124. Kang J.S., Calvo B.F., Maygarden S.J., Caskey L.S., Mohler J.L., and Ornstein D.K. (2002). Dysregulation of annexin I protein expression in high-grade prostatic intraepithelial neoplasia and prostate cancer. Clin. Cancer Res. *8*: 117-123.

125. Chetcuti A., Margan S.H., Russell P., Mann S., Millar D.S., Clark S.J., Rogers J., Handelsman D.J., and Dong Q. (2001). Loss of annexin II heavy and light chains in prostate cancer and its precursors. Cancer Res. *61*: 6331-6334.

126. Srivastava M., Bubendorf L., Srikantan V., Fossom L., Nolan L., Glasman M., Leighton X., Fehrle W., Pittaluga S., Raffeld M. et al. (2001). ANX7, a candidate tumor suppressor gene for prostate cancer. Proc. Natl. Acad. Sci. U. S. A *98*: 4575-4580.

127. Srivastava M., Torosyan Y., Raffeld M., Eidelman O., Pollard H.B., and Bubendorf L. (2007). ANXA7 expression represents hormone-relevant tumor suppression in different cancers. Int. J. Cancer *121*: 2628-2636.

128. Leighton X., Srikantan V., Pollard H.B., Sukumar S., and Srivastava M. (2004). Significant allelic loss of ANX7region (10q21) in hormone receptor negative breast carcinomas. Cancer Lett. *210*: 239-244.

129. Srivastava M., Montagna C., Leighton X., Glasman M., Naga S., Eidelman O., Ried T., and Pollard H.B. (2003). Haploinsufficiency of Anx7 tumor suppressor gene and consequent genomic instability promotes tumorigenesis in the Anx7(+/-) mouse. Proc. Natl. Acad. Sci.

U. S. A *100*: 14287-14292.

130. Sharma M.R., Koltowski L., Ownbey R.T., Tuszynski G.P., and Sharma M.C. (2006). Angiogenesis-associated protein annexin II in breast cancer: selective expression in invasive breast cancer and contribution to tumor invasion and progression. Exp. Mol. Pathol. *81*: 146-156.

131. Hajjar K.A., Jacovina A.T., and Chacko J. (1994). An endothelial cell receptor for plasminogen/tissue plasminogen activator. I. Identity with annexin II. J. Biol. Chem. *269*: 21191-21197.

132. Ishii H., Yoshida M., Hiraoka M., Hajjar K.A., Tanaka A., Yasukochi Y., and Numano F. (2001). Recombinant annexin II modulates impaired fibrinolytic activity in vitro and in rat carotid artery. Circ. Res. *89*: 1240-1245.

133. Ishii H., Hiraoka M., Tanaka A., Shimokado K., and Yoshida M. (2007). Recombinant annexin-2 inhibits the progress of diabetic nephropathy in a diabetic mouse model via recovery of hypercoagulability. Thromb. Haemost. *97*: 124-128.

134. Gugliucci A. and Ghitescu L. (2002). Is diabetic hypercoagulability an acquired annexinopathy? Glycation of annexin II as a putative mechanism for impaired fibrinolysis in diabetic patients. Med. Hypotheses *59*: 247-251.

135. Cesarman-Maus G., Rios-Luna N.P., Deora A.B., Huang B., Villa R., Cravioto M.C., arcon-Segovia D., Sanchez-Guerrero J., and Hajjar K.A. (2006). Autoantibodies against the fibrinolytic receptor, annexin 2, in antiphospholipid syndrome. Blood *107*: 4375-4382.

136. Rand J.H., Wu X.X., Quinn A.S., and Taatjes D.J. (2008). Resistance to annexin A5 anticoagulant activity: a thrombogenic mechanism for the antiphospholipid syndrome. Lupus *17*: 922-930.

137. Odenwald W.F. and Morris S.J. (1983). Identification of a second synexin-like adrenal medullary and liver protein that enhances calcium-induced membrane aggregation. Biochem. Biophys. Res. Commun. *112*: 147-154.

138. Zhuang Q. and Stracher A. (1989). Purification and characterization of a calcium binding protein with "synexin-like" activity from human blood platelets. Biochem. Biophys. Res. Commun. *159*: 236-241.

139. Tokumitsu H., Mizutani A., Minami H., Kobayashi R., and Hidaka H. (1992). A calcyclin-

associated protein is a newly identified member of the Ca2+/phospholipid-binding proteins, annexin family**.** J Biol Chem *267***:** 8919-8924.

140. Mizutani A., Usuda N., Tokumitsu H., Minami H., Yasui K., Kobayashi R., and Hidaka H. (1992). CAP-50, a newly identified annexin, localizes in nuclei of cultured fibroblast 3Y1 cells**.** J Biol Chem *267***:** 13498-13504.

141. Towle C.A. and Treadwell B.V. (1992). Identification of a novel mammalian annexin. cDNA cloning, sequence analysis, and ubiquitous expression of the annexin XI gene**.** J Biol Chem *267***:** 5416-5423.

142. Tokumitsu H., Mizutani A., Muramatsu M., Yokota T., Arai K., and Hidaka H. (1992). Molecular cloning of rabbit CAP-50, a calcyclin-associated annexin protein**.** Biochem. Biophys. Res. Commun. *186***:** 1227-1235.

143. Towle C.A., Weissbach L., and Treadwell B.V. (1992). Alternatively spliced annexin XI transcripts encode proteins that differ near the amino-terminus**.** Biochim. Biophys. Acta *1131***:** 223-226.

144. Bances P., Fernandez M.R., Rodriguez-Garcia M.I., Morgan R.O., and Fernandez M.P. (2000). Annexin A11 (ANXA11) gene structure as the progenitor of paralogous annexins and source of orthologous cDNA isoforms**.** Genomics *69***:** 95-103.

145. Lecona E., Turnay J., Olmo N., Guzman-Aranguez A., Morgan R.O., Fernandez M.P., and Lizarbe M.A. (2003). Structural and functional characterization of recombinant mouse annexin A11: influence of calcium binding**.** Biochem. J. *373***:** 437-449.

146. Tomas A.An Investigation into the Physiological Role of Annexin 11*.* London: University College London, Division of Cell Biology, Institute of Ophthalmology; 2003.

147. Tomas A. and Moss S.E. (2003). Calcium- and cell cycle-dependent association of annexin 11 with the nuclear envelope**.** J Biol Chem *278***:** 20210-20216.

148. (2009). BioGPS**.**).

149. Mamiya N., Iino S., Mizutani A., Kobayashi S., and Hidaka H. (1994). Development-related and cell-type specific nuclear localization of annexin XI: immunolocalization analysis in rat tissues**.** Biochem Biophys Res Commun *202***:** 403-409.

150. Tomas A., Futter C., and Moss S.E. (2004). Annexin 11 is required for midbody formation and completion of the terminal phase of cytokinesis**.** J Cell Biol *165***:** 813-822.

151. Skop A.R., Bergmann D., Mohler W.A., and White J.G. (2001). Completion of cytokinesis in C. elegans requires a brefeldin A-sensitive membrane accumulation at the cleavage furrow apex**.** Curr Biol *11***:** 735-746.

152. Furge L.L., Chen K., and Cohen S. (1999). Annexin VII and annexin XI are tyrosine phosphorylated in peroxovanadate-treated dogs and in platelet-derived growth factor-treated rat vascular smooth muscle cells**.** J. Biol. Chem. *274***:** 33504-33509.

153. Mizutani A., Tokumitsu H., Kobayashi R., and Hidaka H. (1993). Phosphorylation of annexin XI (CAP-50) in SR-3Y1 cells**.** J. Biol. Chem. *268***:** 15517-15522.

154. Ohkouchi S., Nishio K., Maeda M., Hitomi K., Adachi H., and Maki M. (2001). Identification and characterization of two penta-EF-hand Ca(2+)-binding proteins in Dictyostelium discoideum**.** J. Biochem. *130***:** 207-215.

155. Vito P., Lacana E., and D'Adamio L. (1996). Interfering with apoptosis: Ca(2+)-binding protein ALG-2 and Alzheimer's disease gene ALG-3**.** Science *271***:** 521-525.

156. Shibata H., Yamada K., Mizuno T., Yorikawa C., Takahashi H., Satoh H., Kitaura Y., and Maki M. (2004). The penta-EF-hand protein ALG-2 interacts with a region containing PxY repeats in Alix/AIP1, which is required for the subcellular punctate distribution of the amino-terminal truncation form of Alix/AIP1**.** J. Biochem. *135***:** 117-128.

157. Carlton J.G. and Martin-Serrano J. (2007). Parallels between cytokinesis and retroviral budding: a role for the ESCRT machinery**.** Science *316***:** 1908-1912.

158. Carlton J.G., Agromayor M., and Martin-Serrano J. (2008). Differential requirements for Alix and ESCRT-III in cytokinesis and HIV-1 release**.** Proc. Natl. Acad. Sci. U. S. A *105***:** 10541-10546.

159. Katoh K., Shibata H., Hatta K., and Maki M. (2004). CHMP4b is a major binding partner of the ALG-2-interacting protein Alix among the three CHMP4 isoforms**.** Arch. Biochem. Biophys. *421***:** 159-165.

160. Katoh K., Suzuki H., Terasawa Y., Mizuno T., Yasuda J., Shibata H., and Maki M. (2005). The penta-EF-hand protein ALG-2 interacts directly with the ESCRT-I component TSG101, and Ca2+-dependently co-localizes to aberrant endosomes with dominant-negative AAA ATPase SKD1/Vps4B**.** Biochem. J. *391***:** 677-685.

161. Shibata H., Suzuki H., Yoshida H., and Maki M. (2007). ALG-2 directly binds Sec31A and

localizes at endoplasmic reticulum exit sites in a Ca2+-dependent manner. Biochem. Biophys. Res. Commun. *353*: 756-763.

162. Filipek A., Michowski W., and Kuznicki J. (2008). Involvement of S100A6 (calcyclin) and its binding partners in intracellular signaling pathways. Adv. Enzyme Regul. *48*: 225-239.

163. Zeng F.Y., Gerke V., and Gabius H.J. (1993). Identification of annexin II, annexin VI and glyceraldehyde-3-phosphate dehydrogenase as calcyclin-binding proteins in bovine heart. Int. J. Biochem. *25*: 1019-1027.

164. Williams L.H., McClive P.J., Van Den Bergen J.A., and Sinclair A.H. (2005). Annexin XI co-localises with calcyclin in proliferating cells of the embryonic mouse testis. Dev Dyn *234*: 432-437.

165. Kindy M.S., Brown K.E., and Sonenshein G.E. (1991). Regulation of expression of the growth-state-related genes 2F1 and 2A9 during entry of quiescent smooth muscle cells into the cell cycle. J Cell Biochem *46*: 345-350.

166. Kim J., Kim J., Yoon S., Joo J., Lee Y., Lee K., Chung J., and Choe I. (2002). S100A6 protein as a marker for differential diagnosis of cholangiocarcinoma from hepatocellular carcinoma. Hepatol Res *23*: 274.

167. Vimalachandran D., Greenhalf W., Thompson C., Luttges J., Prime W., Campbell F., Dodson A., Watson R., Crnogorac-Jurcevic T., Lemoine N. et al. (2005). High nuclear S100A6 (Calcyclin) is significantly associated with poor survival in pancreatic cancer patients. Cancer Res *65*: 3218-3225.

168. Lawrence C.J., Dawe R.K., Christie K.R., Cleveland D.W., Dawson S.C., Endow S.A., Goldstein L.S., Goodson H.V., Hirokawa N., Howard J. et al. (2004). A standardized kinesin nomenclature. J. Cell Biol. *167*: 19-22.

169. Adams R.R., Tavares A.A., Salzberg A., Bellen H.J., and Glover D.M. (1998). pavarotti encodes a kinesin-like protein required to organize the central spindle and contractile ring for cytokinesis. Genes Dev *12*: 1483-1494.

170. Raich W.B., Moran A.N., Rothman J.H., and Hardin J. (1998). Cytokinesis and midzone microtubule organization in Caenorhabditis elegans require the kinesin-like protein ZEN-4. Mol Biol Cell *9*: 2037-2049.

171. Nislow C., Lombillo V.A., Kuriyama R., and McIntosh J.R. (1992). A plus-end-directed motor

enzyme that moves antiparallel microtubules in vitro localizes to the interzone of mitotic spindles. Nature *359*: 543-547.

172. Minestrini G., Mathe E., and Glover D.M. (2002). Domains of the Pavarotti kinesin-like protein that direct its subcellular distribution: effects of mislocalisation on the tubulin and actin cytoskeleton during Drosophila oogenesis. J Cell Sci *115*: 725-736.

173. Chen M.C., Zhou Y., and Detrich H.W., III (2002). Zebrafish mitotic kinesin-like protein 1 (Mklp1) functions in embryonic cytokinesis. Physiol Genomics *8*: 51-66.

174. Gruneberg U., Neef R., Honda R., Nigg E.A., and Barr F.A. (2004). Relocation of Aurora B from centromeres to the central spindle at the metaphase to anaphase transition requires MKlp2. J Cell Biol *166*: 167-172.

175. Neef R., Preisinger C., Sutcliffe J., Kopajtich R., Nigg E.A., Mayer T.U., and Barr F.A. (2003). Phosphorylation of mitotic kinesin-like protein 2 by polo-like kinase 1 is required for cytokinesis. J Cell Biol *162*: 863-875.

176. Zhu C., Zhao J., Bibikova M., Leverson J.D., Bossy-Wetzel E., Fan J.B., Abraham R.T., and Jiang W. (2005). Functional analysis of human microtubule-based motor proteins, the kinesins and dyneins, in mitosis/cytokinesis using RNA interference. Mol Biol Cell *16*: 3187-3199.

177. Kuriyama R., Gustus C., Terada Y., Uetake Y., and Matuliene J. (2002). CHO1, a mammalian kinesin-like protein, interacts with F-actin and is involved in the terminal phase of cytokinesis. J Cell Biol *156*: 783-790.

178. Matuliene J. and Kuriyama R. (2002). Kinesin-like protein CHO1 is required for the formation of midbody matrix and the completion of cytokinesis in mammalian cells. Mol Biol Cell *13*: 1832-1845.

179. Janetopoulos C., Borleis J., Vazquez F., Iijima M., and Devreotes P. (2005). Temporal and spatial regulation of phosphoinositide signaling mediates cytokinesis. Dev Cell *8*: 467-477.

180. Emoto K., Inadome H., Kanaho Y., Narumiya S., and Umeda M. (2005). Local change in phospholipid composition at the cleavage furrow is essential for completion of cytokinesis. J Biol Chem *280*: 37901-37907.

181. Naito Y., Okada M., and Yagisawa H. (2006). Phospholipase C Isoforms Are Localized at the Cleavage Furrow during Cytokinesis. J Biochem (Tokyo).

182. Field S.J., Madson N., Kerr M.L., Galbraith K.A., Kennedy C.E., Tahiliani M., Wilkins A., and Cantley L.C. (2005). PtdIns(4,5)P2 functions at the cleavage furrow during cytokinesis**.** Curr Biol *15***:** 1407-1412.

183. Kramer P.R. and Wray S. (2002). 17-Beta-estradiol regulates expression of genes that function in macrophage activation and cholesterol homeostasis**.** J. Steroid Biochem. Mol. Biol. *81***:** 203-216.

184. Pittis M.G. and Garcia R.C. (1999). Annexins VII and XI are present in a human macrophage-like cell line. Differential translocation on FcR-mediated phagocytosis**.** J. Leukoc. Biol. *66***:** 845-850.

185. Sjolin C. and Dahlgren C. (1996). Isolation by calcium-dependent translation to neutrophil-specific granules of a 42-kD cytosolic protein, identified as being a fragment of annexin XI**.** Blood *87***:** 4817-4823.

186. Hofmann S., Franke A., Fischer A., Jacobs G., Nothnagel M., Gaede K.I., Schurmann M., Muller-Quernheim J., Krawczak M., Rosenstiel P. et al. (2008). Genome-wide association study identifies ANXA11 as a new susceptibility locus for sarcoidosis**.** Nat. Genet.

187. Sjolin C., Movitz C., Lundqvist H., and Dahlgren C. (1997). Translocation of annexin XI to neutrophil subcellular organelles**.** Biochim. Biophys. Acta *1326***:** 149-156.

188. Pittis M.G. and Garcia R.C. (1999). Annexins VII and XI are present in a human macrophage-like cell line. Differential translocation on FcR-mediated phagocytosis**.** J. Leukoc. Biol. *66***:** 845-850.

189. Misaki Y., Pruijn G.J., van der Kemp A.W., and Van Venrooij W.J. (1994). The 56K autoantigen is identical to human annexin XI**.** J. Biol. Chem. *269***:** 4240-4246.

190. Kramer P.R. and Wray S. (2002). 17-Beta-estradiol regulates expression of genes that function in macrophage activation and cholesterol homeostasis**.** J. Steroid Biochem. Mol. Biol. *81***:** 203-216.

191. Umeda S., Suzuki M.T., Okamoto H., Ono F., Mizota A., Terao K., Yoshikawa Y., Tanaka Y., and Iwata T. (2005). Molecular composition of drusen and possible involvement of anti-retinal autoimmunity in two different forms of macular degeneration in cynomolgus monkey (Macaca fascicularis)**.** Faseb J *19***:** 1683-1685.

192. Alge C.S., Suppmann S., Priglinger S.G., Neubauer A.S., May C.A., Hauck S., Welge-

Lussen U., Ueffing M., and Kampik A. (2003). Comparative proteome analysis of native differentiated and cultured dedifferentiated human RPE cells**.** Invest Ophthalmol Vis Sci *44***:** 3629-3641.

193. Hofmann S., Franke A., Fischer A., Jacobs G., Nothnagel M., Gaede K.I., Schurmann M., Muller-Quernheim J., Krawczak M., Rosenstiel P. et al. (2008). Genome-wide association study identifies ANXA11 as a new susceptibility locus for sarcoidosis**.** Nat Genet.

194. Song J., Shih I., Salani R., Chan D.W., and Zhang Z. (2007). Annexin XI is associated with cisplatin resistance and related to tumor recurrence in ovarian cancer patients**.** Clin. Cancer Res. *13***:** 6842-6849.

195. Song J S.X.S.L.M.M.T.Y.C.D.Z.Z. (2009). Detection of Autoantibodies to Annexin A11 in Different Types of Human Cancer**.** Clinical Proteomics.

196. Song J., Shih I., Chan D.W., and Zhang Z. (2009). Suppression of annexin A11 in ovarian cancer: implications in chemoresistance**.** Neoplasia. *11***:** 605-14, 1.

197. Sukardi S., Elliott R.M., Withers J.O., Fontaine U., Millar J.D., Curry M.R., and Watson P.F. (2001). Calcium-binding proteins from the outer acrosomal membrane of ram spermatozoa: potential candidates for involvement in the acrosome reaction**.** Reproduction. *122***:** 939-946.

198. Iino S., Sudo T., Niwa T., Fukasawa T., Hidaka H., and Niki I. (2000). Annexin XI may be involved in Ca2+ - or GTP-gammaS-induced insulin secretion in the pancreatic beta-cell**.** FEBS Lett. *479***:** 46-50.

199. Chiou J.F., Woon M.D., Cheng S.N., Hsu C.H., Cherng S.C., Hsieh F.K., Lin S.M., and Shiau C.Y. (2007). Staphylokinase-annexin XI chimera exhibited efficient in vitro thrombolytic activities**.** Biosci. Biotechnol. Biochem. *71***:** 1122-1129.

200. Reverse Complimentation of DNA Sequences**.**).

201. GeneWalker Primer Design Testing (Cybergene)**.**).

202. Sharma O.P. (2007). Sarcoidosis: a historical perspective**.** Clin. Dermatol. *25***:** 232-241.

203. Pinkston P., Bitterman P.B., and Crystal R.G. (1983). Spontaneous release of interleukin-2 by lung T lymphocytes in active pulmonary sarcoidosis**.** N. Engl. J. Med. *308***:** 793-800.

204. Robinson B.W., McLemore T.L., and Crystal R.G. (1985). Gamma interferon is spontaneously released by alveolar macrophages and lung T lymphocytes in patients with

pulmonary sarcoidosis. J. Clin. Invest *75*: 1488-1495.

205. Monsuez J.J., Carcelain G., Charniot J.C., Barriere J., Duclos-Vallee J.C., Parent F., and Autran B. (2009). T Cells Subtypes in a Patient With Interferon-alpha Induced Sarcoidosis. Am. J. Med. Sci. *337*: 60-62.

206. Baughman R.P (2006). Lung Biology in Health and Disease: Sarcoidosis. Taylor & Francis).

207. Toussirot E., Pertuiset E., Kantelip B., and Wendling D. (2008). Sarcoidosis occuring during anti-TNF-alpha treatment for inflammatory rheumatic diseases: report of two cases. Clin. Exp. Rheumatol. *26*: 471-475.

208. Agostini C., Trentin L., Facco M., Sancetta R., Cerutti A., Tassinari C., Cimarosto L., Adami F., Cipriani A., Zambello R. et al. (1996). Role of IL-15, IL-2, and their receptors in the development of T cell alveolitis in pulmonary sarcoidosis. J. Immunol. *157*: 910-918.

209. Noor A. and Knox K.S. (2007). Immunopathogenesis of sarcoidosis. Clin. Dermatol. *25*: 250-258.

210. Ezzie M.E. and Crouser E.D. (2007). Considering an infectious etiology of sarcoidosis. Clin. Dermatol. *25*: 259-266.

211. Valentonyte R., Hampe J., Huse K., Rosenstiel P., Albrecht M., Stenzel A., Nagy M., Gaede K.I., Franke A., Haesler R. et al. (2005). Sarcoidosis is associated with a truncating splice site mutation in BTNL2. Nat. Genet. *37*: 357-364.

212. Spagnolo P. and du Bois R.M. (2007). Genetics of sarcoidosis. Clin. Dermatol. *25*: 242-249.

213. Burke D.F., Worth C.L., Priego E.M., Cheng T., Smink L.J., Todd J.A., and Blundell T.L. (2007). Genome bioinformatic analysis of nonsynonymous SNPs. BMC. Bioinformatics. *8*: 301.

214. Leclerc E., Fritz G., Weibel M., Heizmann C.W., and Galichet A. (2007). S100B and S100A6 differentially modulate cell survival by interacting with distinct RAGE (receptor for advanced glycation end products) immunoglobulin domains. J. Biol. Chem. *282*: 31317-31331.

215. Ullrich A., Coussens L., Hayflick J.S., Dull T.J., Gray A., Tam A.W., Lee J., Yarden Y., Libermann T.A., Schlessinger J. et al. (1984). Human epidermal growth factor receptor cDNA sequence and aberrant expression of the amplified gene in A431 epidermoid carcinoma cells. Nature *309*: 418-425.

216. Misaki Y., Pruijn G.J., van der Kemp A.W., and Van Venrooij W.J. (1994). The 56K autoantigen is identical to human annexin XI**.** J. Biol. Chem. *269***:** 4240-4246.

217. Rodriguez-Garcia M.I., Fernandez J.A., Rodriguez A., Fernandez M.P., Gutierrez C., and Torre-Alonso J.C. (1996). Annexin V autoantibodies in rheumatoid arthritis**.** Ann. Rheum. Dis. *55***:** 895-900.

218. Salle V., Maziere J.C., Smail A., Cevallos R., Maziere C., Fuentes V., Tramier B., Makdassi R., Choukroun G., Vittecoq O. et al. (2008). Anti-annexin II antibodies in systemic autoimmune diseases and antiphospholipid syndrome**.** J. Clin. Immunol. *28***:** 291-297.

219. Badminton M.N., Kendall J.M., Rembold C.M., and Campbell A.K. (1998). Current evidence suggests independent regulation of nuclear calcium**.** Cell Calcium *23***:** 79-86.

220. Raynal P., Kuijpers G., Rojas E., and Pollard H.B. (1996). A rise in nuclear calcium translocates annexins IV and V to the nuclear envelope**.** FEBS Lett. *392***:** 263-268.

221. Barwise J.L. and Walker J.H. (1996). Subcellular localization of annexin V in human foreskin fibroblasts: nuclear localization depends on growth state**.** FEBS Lett. *394***:** 213-216.

222. Podszywalow-Bartnicka P., Strzelecka-Kiliszek A., Bandorowicz-Pikula J., and Pikula S. (2007). Calcium- and proton-dependent relocation of annexin A6 in Jurkat T cells stimulated for interleukin-2 secretion**.** Acta Biochim. Pol. *54***:** 261-271.

223. Clemen C.S., Herr C., Hovelmeyer N., and Noegel A.A. (2003). The lack of annexin A7 affects functions of primary astrocytes**.** Exp. Cell Res. *291***:** 406-414.

224. Moolenaar W.H., Aerts R.J., Tertoolen L.G., and de Laat S.W. (1986). The epidermal growth factor-induced calcium signal in A431 cells**.** J. Biol. Chem. *261***:** 279-284.

225. Lecona E., Turnay J., Olmo N., Guzman-Aranguez A., Morgan R.O., Fernandez M.P., and Lizarbe M.A. (2003). Structural and functional characterization of recombinant mouse annexin A11: influence of calcium binding**.** Biochem. J. *373***:** 437-449.

226. Rikova K., Guo A., Zeng Q., Possemato A., Yu J., Haack H., Nardone J., Lee K., Reeves C., Li Y. et al. (2007). Global survey of phosphotyrosine signaling identifies oncogenic kinases in lung cancer**.** Cell *131***:** 1190-1203.

227. Boussac M. and Garin J. (2000). Calcium-dependent secretion in human neutrophils: a proteomic approach**.** Electrophoresis *21***:** 665-672.

228. Christmas P., Callaway J., Fallon J., Jones J., and Haigler H.T. (1991). Selective secretion of annexin 1, a protein without a signal sequence, by the human prostate gland. J. Biol. Chem. *266*: 2499-2507.

229. Zhao W.Q., Chen G.H., Chen H., Pascale A., Ravindranath L., Quon M.J., and Alkon D.L. (2003). Secretion of Annexin II via activation of insulin receptor and insulin-like growth factor receptor. J. Biol. Chem. *278*: 4205-4215.

230. (2009). The SWISS-MODEL Workspace.).

231. Grunewald J. and Eklund A. (2007). Role of CD4+ T cells in sarcoidosis. Proc. Am. Thorac. Soc. *4*: 461-464.

232. Lee K.S., Yuan Y.L., Kuriyama R., and Erikson R.L. (1995). Plk is an M-phase-specific protein kinase and interacts with a kinesin-like protein, CHO1/MKLP-1. Mol Cell Biol *15*: 7143-7151.

233. Severson A.F., Hamill D.R., Carter J.C., Schumacher J., and Bowerman B. (2000). The aurora-related kinase AIR-2 recruits ZEN-4/CeMKLP1 to the mitotic spindle at metaphase and is required for cytokinesis. Curr Biol *10*: 1162-1171.

234. Jantsch-Plunger V., Gonczy P., Romano A., Schnabel H., Hamill D., Schnabel R., Hyman A.A., and Glotzer M. (2000). CYK-4: A Rho family gtpase activating protein (GAP) required for central spindle formation and cytokinesis. J Cell Biol *149*: 1391-1404.

235. Sellitto C. and Kuriyama R. (1988). Distribution of a matrix component of the midbody during the cell cycle in Chinese hamster ovary cells. J Cell Biol *106*: 431-439.

236. Lodish B.M.K.K.S.Z.D. (2009). Microtubules. In Molecular Cell Biology, Freeman), pp. 779-852.

237. Kuriyama R., Dragas-Granoic S., Maekawa T., Vassilev A., Khodjakov A., and Kobayashi H. (1994). Heterogeneity and microtubule interaction of the CHO1 antigen, a mitosis-specific kinesin-like protein. Analysis of subdomains expressed in insect sf9 cells. J Cell Sci *107 (Pt 12)*: 3485-3499.

238. Matuliene J. and Kuriyama R. (2004). Role of the midbody matrix in cytokinesis: RNAi and genetic rescue analysis of the mammalian motor protein CHO1. Mol Biol Cell *15*: 3083-3094.

239. Zhu C., Bossy-Wetzel E., and Jiang W. (2005). Recruitment of MKLP1 to the spindle

midzone/midbody by INCENP is essential for midbody formation and completion of cytokinesis in human cells. Biochem J *389*: 373-381.

240. Maliga Z. and Mitchison T.J. (2006). Small-molecule and mutational analysis of allosteric Eg5 inhibition by monastrol. BMC. Chem Biol *6*: 2.

241. DeBonis S., Simorre J.P., Crevel I., Lebeau L., Skoufias D.A., Blangy A., Ebel C., Gans P., Cross R., Hackney D.D. et al. (2003). Interaction of the mitotic inhibitor monastrol with human kinesin Eg5. Biochemistry *42*: 338-349.

242. Parry H., McDougall A., and Whitaker M. (2005). Microdomains bounded by endoplasmic reticulum segregate cell cycle calcium transients in syncytial Drosophila embryos. J. Cell Biol. *171*: 47-59.

243. Beaudouin J., Gerlich D., Daigle N., Eils R., and Ellenberg J. (2002). Nuclear envelope breakdown proceeds by microtubule-induced tearing of the lamina. Cell *108*: 83-96.

244. Busson S., Dujardin D., Moreau A., Dompierre J., and De M., Jr. (1998). Dynein and dynactin are localized to astral microtubules and at cortical sites in mitotic epithelial cells. Curr. Biol. *8*: 541-544.

245. Piehl M. and Cassimeris L. (2003). Organization and dynamics of growing microtubule plus ends during early mitosis. Mol. Biol. Cell *14*: 916-925.

246. Mishima M., Pavicic V., Gruneberg U., Nigg E.A., and Glotzer M. (2004). Cell cycle regulation of central spindle assembly. Nature *430*: 908-913.

247. Neef R., Klein U.R., Kopajtich R., and Barr F.A. (2006). Cooperation between mitotic kinesins controls the late stages of cytokinesis. Curr. Biol. *16*: 301-307.

248. Cao L.G. and Wang Y.L. (1996). Signals from the spindle midzone are required for the stimulation of cytokinesis in cultured epithelial cells. Mol. Biol. Cell *7*: 225-232.

249. Foe V.E. and von D.G. (2008). Stable and dynamic microtubules coordinately shape the myosin activation zone during cytokinetic furrow formation. J. Cell Biol. *183*: 457-470.

250. Odell G.M. and Foe V.E. (2008). An agent-based model contrasts opposite effects of dynamic and stable microtubules on cleavage furrow positioning. J. Cell Biol. *183*: 471-483.

251. Skop A.R., Liu H., Yates J., III, Meyer B.J., and Heald R. (2004). Dissection of the mammalian midbody proteome reveals conserved cytokinesis mechanisms. Science *305*:

61-66.

252. Fox C.H., Johnson F.B., Whiting J., and Roller P.P. (1985). Formaldehyde fixation**.** J. Histochem. Cytochem. *33***:** 845-853.

253. Miller S.G., Carnell L., and Moore H.H. (1992). Post-Golgi membrane traffic: brefeldin A inhibits export from distal Golgi compartments to the cell surface but not recycling**.** J. Cell Biol. *118***:** 267-283.

254. Jackson C.L. and Casanova J.E. (2000). Turning on ARF: the Sec7 family of guanine-nucleotide-exchange factors**.** Trends Cell Biol. *10***:** 60-67.

255. Yang F., Camp D.G., Gritsenko M.A., Luo Q., Kelly R.T., Clauss T.R., Brinkley W.R., Smith R.D., and Stenoien D.L. (2007). Identification of a novel mitotic phosphorylation motif associated with protein localization to the mitotic apparatus**.** J. Cell Sci. *120***:** 4060-4070.

256. Kasahara K., Nakayama Y., Nakazato Y., Ikeda K., Kuga T., and Yamaguchi N. (2007). Src signaling regulates completion of abscission in cytokinesis through ERK/MAPK activation at the midbody**.** J Biol Chem *282***:** 5327-5339.

257. Herrmann L., Dittmar T., and Erdmann K.S. (2003). The protein tyrosine phosphatase PTP-BL associates with the midbody and is involved in the regulation of cytokinesis**.** Mol. Biol. Cell *14***:** 230-240.

258. ngers-Loustau A., Cote J.F., Charest A., Dowbenko D., Spencer S., Lasky L.A., and Tremblay M.L. (1999). Protein tyrosine phosphatase-PEST regulates focal adhesion disassembly, migration, and cytokinesis in fibroblasts**.** J. Cell Biol. *144***:** 1019-1031.

259. Spencer S., Dowbenko D., Cheng J., Li W., Brush J., Utzig S., Simanis V., and Lasky L.A. (1997). PSTPIP: a tyrosine phosphorylated cleavage furrow-associated protein that is a substrate for a PEST tyrosine phosphatase**.** J. Cell Biol. *138***:** 845-860.

260. Weisenberg R.C., Borisy G.G., and Taylor E.W. (1968). The colchicine-binding protein of mammalian brain and its relation to microtubules**.** Biochemistry *7***:** 4466-4479.

261. Weisenberg R.C., Deery W.J., and Dickinson P.J. (1976). Tubulin-nucleotide interactions during the polymerization and depolymerization of microtubules**.** Biochemistry *15***:** 4248-4254.

262. Desai A. and Mitchison T.J. (1997). Microtubule polymerization dynamics**.** Annu. Rev Cell Dev Biol *13***:** 83-117.

263. Hannak E., Kirkham M., Hyman A.A., and Oegema K. (2001). Aurora-A kinase is required for centrosome maturation in Caenorhabditis elegans**.** J. Cell Biol. *155***:** 1109-1116.

264. Walker R.A., O'Brien E.T., Pryer N.K., Soboeiro M.F., Voter W.A., Erickson H.P., and Salmon E.D. (1988). Dynamic instability of individual microtubules analyzed by video light microscopy: rate constants and transition frequencies**.** J. Cell Biol. *107***:** 1437-1448.

265. Zhang C., Hughes M., and Clarke P.R. (1999). Ran-GTP stabilises microtubule asters and inhibits nuclear assembly in Xenopus egg extracts**.** J. Cell Sci. *112 (Pt 14)***:** 2453-2461.

266. Denarier E., Fourest-Lieuvin A., Bosc C., Pirollet F., Chapel A., Margolis R.L., and Job D. (1998). Nonneuronal isoforms of STOP protein are responsible for microtubule cold stability in mammalian fibroblasts**.** Proc. Natl. Acad. Sci. U. S. A *95***:** 6055-6060.

267. Vale R.D. (1991). Severing of stable microtubules by a mitotically activated protein in Xenopus egg extracts**.** Cell *64***:** 827-839.

268. McNally F.J. and Thomas S. (1998). Katanin is responsible for the M-phase microtubule-severing activity in Xenopus eggs**.** Mol. Biol. Cell *9***:** 1847-1861.

269. Xu K S.P.L.R. (2002). Interaction of Nocodazole With Tubulin Isotypes**.** DRUG DEVELOPMENT RESEARCH *55***:** 91-96.

270. Hoebeke J., Van N.G., and De B.M. (1976). Interaction of oncodazole (R 17934), a new antitumoral drug, with rat brain tubulin**.** Biochem. Biophys. Res. Commun. *69***:** 319-324.

271. Horwitz S.B. (1994). Taxol (paclitaxel): mechanisms of action**.** Ann. Oncol. *5 Suppl 6***:** S3-S6.

272. Kumar N. (1981). Taxol-induced polymerization of purified tubulin. Mechanism of action**.** J. Biol. Chem. *256***:** 10435-10441.

273. De B.M., Geuens G., Nuydens R., Willebrords R., and De M.J. (1981). Taxol induces the assembly of free microtubules in living cells and blocks the organizing capacity of the centrosomes and kinetochores**.** Proc. Natl. Acad. Sci. U. S. A *78***:** 5608-5612.

274. Dutcher S.K. (2001). The tubulin fraternity: alpha to eta**.** Curr. Opin. Cell Biol. *13***:** 49-54.

275. Hammond J.W., Cai D., and Verhey K.J. (2008). Tubulin modifications and their cellular functions**.** Curr. Opin. Cell Biol. *20***:** 71-76.

276. Caviston J.P. and Holzbaur E.L. (2006). Microtubule motors at the intersection of trafficking and transport**.** Trends Cell Biol. *16***:** 530-537.

277. Matsuoka K., Orci L., Amherdt M., Bednarek S.Y., Hamamoto S., Schekman R., and Yeung T. (1998). COPII-coated vesicle formation reconstituted with purified coat proteins and chemically defined liposomes**.** Cell *93***:** 263-275.

278. Watson P., Forster R., Palmer K.J., Pepperkok R., and Stephens D.J. (2005). Coupling of ER exit to microtubules through direct interaction of COPII with dynactin**.** Nat. Cell Biol. *7***:** 48-55.

279. Yamasaki A., Tani K., Yamamoto A., Kitamura N., and Komada M. (2006). The Ca2+-binding protein ALG-2 is recruited to endoplasmic reticulum exit sites by Sec31A and stabilizes the localization of Sec31A**.** Mol. Biol. Cell *17***:** 4876-4887.

280. Traverso V., Morris J.F., Flower R.J., and Buckingham J. (1998). Lipocortin 1 (annexin 1) in patches associated with the membrane of a lung adenocarcinoma cell line and in the cell cytoplasm**.** J. Cell Sci. *111 (Pt 10)***:** 1405-1418.

281. Nishizawa Y Y.A.U.J. (2003). Identification of Tubulin Subunits Specific Binding Proteins in Rod Outer Segments**.** Investigative Ophthalmology & Visual Science *44***:** 2866.

282. Vahrmann A., Saric M., Koebsch I., and Scholze H. (2008). alpha14-Giardin (annexin E1) is associated with tubulin in trophozoites of Giardia lamblia and forms local slubs in the flagella**.** Parasitol. Res. *102***:** 321-326.

283. Takemura R., Okabe S., Umeyama T., Kanai Y., Cowan N.J., and Hirokawa N. (1992). Increased microtubule stability and alpha tubulin acetylation in cells transfected with microtubule-associated proteins MAP1B, MAP2 or tau**.** J. Cell Sci. *103 (Pt 4)***:** 953-964.

284. Poole C.A., Zhang Z.J., and Ross J.M. (2001). The differential distribution of acetylated and detyrosinated alpha-tubulin in the microtubular cytoskeleton and primary cilia of hyaline cartilage chondrocytes**.** J. Anat. *199***:** 393-405.

285. Dompierre J.P., Godin J.D., Charrin B.C., Cordelieres F.P., King S.J., Humbert S., and Saudou F. (2007). Histone deacetylase 6 inhibition compensates for the transport deficit in Huntington's disease by increasing tubulin acetylation**.** J. Neurosci. *27***:** 3571-3583.

286. Reed N.A., Cai D., Blasius T.L., Jih G.T., Meyhofer E., Gaertig J., and Verhey K.J. (2006). Microtubule acetylation promotes kinesin-1 binding and transport**.** Curr. Biol. *16***:** 2166-

2172.

287. Bulinski J.C. (2007). Microtubule modification: acetylation speeds anterograde traffic flow**.** Curr. Biol. *17***:** R18-R20.

288. North B.J., Marshall B.L., Borra M.T., Denu J.M., and Verdin E. (2003). The human Sir2 ortholog, SIRT2, is an NAD+-dependent tubulin deacetylase**.** Mol. Cell *11***:** 437-444.

289. Hubbert C., Guardiola A., Shao R., Kawaguchi Y., Ito A., Nixon A., Yoshida M., Wang X.F., and Yao T.P. (2002). HDAC6 is a microtubule-associated deacetylase**.** Nature *417***:** 455-458.

290. Flemming W (1875). Studien über die Entwicklungsgeschichte der Najaden **.** Sitzungsber. Akad. Wissensch. Wien *71***:** 81-147.

291. Boveri T (2009). Zellenstudien II: Die Befruchtung und Teilung des Eies von Ascaris megalocephala**.** Jena. Zeit. Naturwiss *22***:** 685-882.

292. Schatten H. (2008). The mammalian centrosome and its functional significance**.** Histochem. Cell Biol. *129***:** 667-686.

293. Zheng Y., Wong M.L., Alberts B., and Mitchison T. (1995). Nucleation of microtubule assembly by a gamma-tubulin-containing ring complex**.** Nature *378***:** 578-583.

294. Dictenberg J.B., Zimmerman W., Sparks C.A., Young A., Vidair C., Zheng Y., Carrington W., Fay F.S., and Doxsey S.J. (1998). Pericentrin and gamma-tubulin form a protein complex and are organized into a novel lattice at the centrosome**.** J. Cell Biol. *141***:** 163-174.

295. Zimmerman W.C., Sillibourne J., Rosa J., and Doxsey S.J. (2004). Mitosis-specific anchoring of gamma tubulin complexes by pericentrin controls spindle organization and mitotic entry**.** Mol. Biol. Cell *15***:** 3642-3657.

296. Flory M.R. and Davis T.N. (2003). The centrosomal proteins pericentrin and kendrin are encoded by alternatively spliced products of one gene**.** Genomics *82***:** 401-405.

297. Tsvetkov L., Xu X., Li J., and Stern D.F. (2003). Polo-like kinase 1 and Chk2 interact and co-localize to centrosomes and the midbody**.** J. Biol. Chem. *278***:** 8468-8475.

298. Jackman M., Lindon C., Nigg E.A., and Pines J. (2003). Active cyclin B1-Cdk1 first appears on centrosomes in prophase**.** Nat. Cell Biol. *5***:** 143-148.

299. Birkenfeld J., Nalbant P., Bohl B.P., Pertz O., Hahn K.M., and Bokoch G.M. (2007). GEF-H1 modulates localized RhoA activation during cytokinesis under the control of mitotic kinases**.** Dev Cell *12***:** 699-712.

300. Dai B.N., Yang Y., Chau Z., and Jhanwar-Uniyal M. (2007). Polo-like kinase 1 regulates RhoA during cytokinesis exit in human cells**.** Cell Prolif. *40***:** 550-557.

301. Pohl C. and Jentsch S. (2008). Final stages of cytokinesis and midbody ring formation are controlled by BRUCE**.** Cell *132***:** 832-845.

302. Gromley A., Jurczyk A., Sillibourne J., Halilovic E., Mogensen M., Groisman I., Blomberg M., and Doxsey S. (2003). A novel human protein of the maternal centriole is required for the final stages of cytokinesis and entry into S phase**.** J. Cell Biol. *161***:** 535-545.

303. Gromley A., Yeaman C., Rosa J., Redick S., Chen C.T., Mirabelle S., Guha M., Sillibourne J., and Doxsey S.J. (2005). Centriolin anchoring of exocyst and SNARE complexes at the midbody is required for secretory-vesicle-mediated abscission**.** Cell *123***:** 75-87.

304. Zimmerman W.C., Sillibourne J., Rosa J., and Doxsey S.J. (2004). Mitosis-specific anchoring of gamma tubulin complexes by pericentrin controls spindle organization and mitotic entry**.** Mol Biol Cell *15***:** 3642-3657.

305. Khodjakov A., Cole R.W., Oakley B.R., and Rieder C.L. (2000). Centrosome-independent mitotic spindle formation in vertebrates**.** Curr. Biol. *10***:** 59-67.

306. Hinchcliffe E.H. and Sluder G. (2001). "It takes two to tango": understanding how centrosome duplication is regulated throughout the cell cycle**.** Genes Dev. *15***:** 1167-1181.

307. Devore J.J., Conrad G.W., and Rappaport R. (1989). A model for astral stimulation of cytokinesis in animal cells**.** J. Cell Biol. *109***:** 2225-2232.

308. Palazzo R.E., Vogel J.M., Schnackenberg B.J., Hull D.R., and Wu X. (2000). Centrosome maturation**.** Curr. Top. Dev. Biol. *49***:** 449-470.

309. Khodjakov A. and Rieder C.L. (1999). The sudden recruitment of gamma-tubulin to the centrosome at the onset of mitosis and its dynamic exchange throughout the cell cycle, do not require microtubules**.** J. Cell Biol. *146***:** 585-596.

310. Dammermann A. and Merdes A. (2002). Assembly of centrosomal proteins and microtubule organization depends on PCM-1**.** J. Cell Biol. *159***:** 255-266.

311. Portier N., Audhya A., Maddox P.S., Green R.A., Dammermann A., Desai A., and Oegema K. (2007). A microtubule-independent role for centrosomes and aurora a in nuclear envelope breakdown**.** Dev. Cell *12***:** 515-529.

312. Whitehead C.M. and Salisbury J.L. (1999). Regulation and regulatory activities of centrosomes**.** J. Cell Biochem. *Suppl 32-33***:** 192-199.

313. Hill E., Clarke M., and Barr F.A. (2000). The Rab6-binding kinesin, Rab6-KIFL, is required for cytokinesis**.** EMBO J. *19***:** 5711-5719.

314. Montagnac G., Echard A., and Chavrier P. (2008). Endocytic traffic in animal cell cytokinesis**.** Curr Opin. Cell Biol *20***:** 454-461.

315. Wilson G.M., Fielding A.B., Simon G.C., Yu X., Andrews P.D., Hames R.S., Frey A.M., Peden A.A., Gould G.W., and Prekeris R. (2005). The FIP3-Rab11 protein complex regulates recycling endosome targeting to the cleavage furrow during late cytokinesis**.** Mol. Biol. Cell *16***:** 849-860.

316. Riggs B., Fasulo B., Royou A., Mische S., Cao J., Hays T.S., and Sullivan W. (2007). The concentration of Nuf, a Rab11 effector, at the microtubule-organizing center is cell cycle regulated, dynein-dependent, and coincides with furrow formation**.** Mol. Biol. Cell *18***:** 3313-3322.

317. Goebeler V., Poeter M., Zeuschner D., Gerke V., and Rescher U. (2008). Annexin A8 regulates late endosome organization and function**.** Mol. Biol. Cell *19***:** 5267-5278.

318. Saltini C., Spurzem J.R., Kirby M.R., and Crystal R.G. (1988). Sarcoidosis is not associated with a generalized defect in T cell suppressor function**.** J. Immunol. *140***:** 1854-1860.

319. Misaki Y., Pruijn G.J., van der Kemp A.W., and Van Venrooij W.J. (1994). The 56K autoantigen is identical to human annexin XI**.** J. Biol. Chem. *269***:** 4240-4246.

320. Walther A., Riehemann K., and Gerke V. (2000). A novel ligand of the formyl peptide receptor: annexin I regulates neutrophil extravasation by interacting with the FPR**.** Mol. Cell *5***:** 831-840.